ALTHAGAFY, HANAN SAAD, Ph.D. Milk Thistle Flavonolignans: Biomimetic Synthesis, Synthesis of Analogues and Biological Evaluation of Synthetic Products. (2013)
Directed by Dr. Nicholas H. Oberlies and Mitchell P. Croatt. 199pp.

7-*O*-methylflavonolignans from milk thistle were synthesized by first isolating the seven primary components of silymarin and individually methylating them. Optimization of conditions allowed for each of these seven compounds to be selectively methylated at the phenol in the 7-position in the presence of each metabolite's 4-5 other alcoholic positions without the use of protecting groups. These site-selectively methylated compounds were then evaluated for their cytotoxic and antiviral actions in the hepatoma cell line HuH7; in all cases the monomethylated analogues were more cytotoxic than the parent compounds. Moreover, parent compounds that were relatively non-toxic and inactive or weak inhibitors of hepatitis C virus infection had enhanced toxicity and anti-HCV activity upon 7-*O*-methylation. Also, the compounds were tested for inhibition of major drug metabolizing enzymes in pooled human liver and intestinal microsomes. Methylation of flavonolignans differentially modified inhibitory potency, with compounds demonstrating both increased and decreased potency depending upon the compound tested and the drug metabolizing enzyme system investigated. In total, these data indicated that monomethylation modulates the cytotoxic, antiviral, and drug interaction potential of silymarin flavonolignans.

A biomimetic synthesis of flavonolignans was also accomplished. Coniferyl alcohol was oxidized using silver oxide in the presence of taxifolin to form four of the major components of silymarin, silibinin (silybin A and silybin B), and isosilibinin

(isosilybin A and isosilybin B). The mechanism of this transformation was probed and it appears to undergo two sequential single electron oxidations with coupling of coniferyl alcohol to taxifolin between the two oxidations. Synthetic flavolignans were confirmed to be identical to natural compounds by NMR, HPLC, UPLC and HRMS. This results in a good yield of some of the minor natural compounds, such as isosilybin B. Moreover, it provides a means to generate structural analogues.

MILK THISTLE FLAVONOLIGNANS: BIOMIMETIC SYNTHESIS, SYNTHESIS OF ANALOGOUS AND BIOLOGICAL EVALUATION OF SYNTHETIC PRODUCTS

by

Hanan Saad Althagafy

A Dissertation Submitted to
the Faculty of The Graduate School at
The University of North Carolina at Greensboro
in Pratrial Fulfillment
of the Requirements for the Degree
Doctor of Philosophy

Greensboro
2013

Approved by

_____
Committee Co-Chair

_____
Committee Co-Chair

To

My parents for their love, prayer and encourgement;
I think my father would have been proud of me.

"My Lord, have mercy upon my parents as they brought me up when I was small."

APPROVAL PAGE

This dissertation has been approved by the following committee of the Faculty of The Graduate School at The University of North Carolina at Greensboro.

Committee Co-Chair _____
Nicholas H. Oberlies

Committee Co-Chair _____
Mitchell P. Croatt

Committee Members _____
Patricia H. Reggio

_____
Nadja B. Cech

3/19/2013
Date of Acceptance by Committee

3/19/2013
Date of Final Oral Examination

ACKNOWLEDGMENTS

In the name of Allah, the Entirely Merciful, the Especially Merciful.
"All praise is due to Allah, Lord of the worlds"

I would like to express my sincere gratitude to Professor Nicholas H. Oberlies, for giving me the opportunity to join your research group in spring 2010. I am very grateful for your patience, encouragement, invaluable guidance, and giving me the opportunity for performing independent research, which has greatly helped me in developing useful skills in problem solving. The successful completion of my study was made possible through your efforts. These years will shape my future and I will always be grateful for your support during this time.

I would also like to thank Professor Mitchell P. Croatt for his continuous support, helpful discussions, guidance, and encouragement. You are an excellent mentor and have been a great source of motivation. Thank you for teaching me and I would not be in the place I am now without your help. Thank you for providing me with the opportunity to work with you through biomimetic research.

My special thanks to my committee members Professors Patricia Reggio and Nadja Cech, for their support and helpful suggestions.

I would like to thank Professor Stephen J. Polyak from Laboratory Medicine and Global Health, University of Washington, Seattle, for biological evaluations of our compounds, as well as, Professor Mary F. Paine from Pharmacotherapy and Experimental Therapeutics, UNC at Chapel Hill.

I would specially like to thank Tyler Graf, for teaching me various separation and instrumentation techniques. Thanks to Dr. Arlene Sy-Coredero for NMR training in the earlier stages of my research. I would also like to thank all past and present members of Dr. Oberlies research group: Dr. Sloan Ayers, Dr. Mario Figueroa, Dr. Huzefa Raja, Dr. Amninder Kaur, Tamam El-Elimat, Rabia Bukhari, Vincent Sica, Danielle Hayes, Noemi Paguigan, Karen VanderMolen, Thomas Johnston, Cherilyn Strader, Sarah Winters, Ericca Smith and Robin Tate Uhl. I would like to thank members of Dr. Croatt's research group. My special thanks to Dr. Maria Elena Meza-Aviña, for helping me with synthetic chemistry. I also express my gratitude to Dr. I. F. Dempsey Hyatt and Emma Nagy.

I would like to thank the Department of Chemistry and Biochemistry for excellent NMR and MS facilities. I would like to thank Mary Katsikas. You are an extremely nice person.

I would also like to acknowledge the Saudi Arabia ministry of higher education and King Abdullah Scholarships Program for financial support. I would like to thank my academic advisor at Saudi Cultural Mission, WDC, Dr. Abdulaziz Rabatchi for all his help and support during my graduate study.

Finally and most of all, I wish to express my appreciation for my family: parents, my sisters and brothers, life-long friends in Saudi Arabia, specialy Dr. Huda Al Doghaither and her family for your care, unconditional love, prayers, and encouragement. You always made me feel close to home. I believe that all of you never gave up on me and for that I will forever be indebted to you.

TABLE OF CONTENTS

Page

LIST OF TABLES

Page

LIST OF FIGURES

Page

LIST OF SCHEMES

Page

LIST OF ABBREVIATIONS

$[\alpha]_D^{20}$	specific optical rotation at 20 °C
°C	degrees centigrade
δ	NMR chemical shift
ε	extinction coefficient
22Rv1	human prostate carcinoma epithelial cell line
4-MU	4-methylumbelliferone
A431	epidermoid carcinoma
A549	human lung adenocarcinoma epithelial cell line
ANOVA	statistical method that stands for analysis of variance
br	broad
calcd	calculated
CD	circular dichroism spectroscopy
CDK	cyclin-dependent kinase
^{13}C NMR	carbon-13 nuclear magnetic resonance
Cs_2CO_3	cesium carbonate
CYP2A6	a member of the cytochrome P450 mixed-function oxidase system
CYP3A4	isozymes cytochrome P-450 present in all livers and small intestines
CYP2B6	a member of the Cytochrome P450 group of enzymes
CYP2C9	isozymes cytochrome P-450
CYP2D6	a member of the cytochrome P450 mixed-function oxidase system

CYP2E1	a member of the cytochrome P450 mixed-function oxidase system
d	doublet
DBU	diazabicycloundecene
DMSO	dimethylsulfoxide
DNA	deoxyribonucleic acid
DU145	human prostate cancer cells
ED_{50}	the dose that is effective for 50% of exposed population
ERK1/2	extracellular-signal-regulated kinases
ESI	electrospray ionization
EtOAc	ethyl acetate
g	gram(s)
G1-phase	the first of four phases of the cell cycle prior to the synthesis of DNA
G2-M phase	is the last phase of the interphase part of the cell cycle
^{1}H NMR	proton nuclear magnetic resonance
h	hour(s)
HCl	hydrochloride
HCV	hepatitis C virus
HT29	human colorectal cancer cells
HPLC	high performance liquid chromatography
HMBC	heteronuclear multiple-bond correlation
HSS T3	high-strength silica bonding to trifunctional C18 alkyl phase bonded

HSQC	heteronuclear single-quantum coherence
Hz	hertz
Huh 7.5.1	human hepatoma cells
IC_{50}	50% inhibitory concentrations
J	NMR coupling constant
JFH-1	hepatitis C virus strain
JNK	c-Jun N-terminal kinases
K_2CO_3	potassium carbonate
K562	human myeloid leukemia cells
LNCaP	androgen -sensitive human prostate adenocarcinoma cells
LoVo	colon cancer cell line
m/z	mass to charge ratio (in mass spectrometry)
m	multiplet
M^-	negative charged molecular ion
M^+	positive charged molecular ion
MCF-7	human breast adenocarcinoma cell line
Me	methyl
mg	milligram(s)
mL	milliliter(s)
mmol	millimole
Na_2SO_4	sodium sulfate

CHAPTER I

SEMISYNTHESIS, CYTOTOXICITY, ANTIVIRAL ACTIVITY, AND DRUG INTERACTION LIABILITY OF 7-*O*-METHYLATED ANALOGUES OF FLAVONOLIGNANS FROM MILK THISTLE

This chapter has been accepted by the Journal, Bioorganic and Medicinal Chemistry.

1.1. Introduction

1.1.1. Milk thistle: flavonolignans nomenclature and stereochemistry

Milk thistle (*Silybum marianum*) (L.) Gaertner (Asteraceae) is a biennial plant native to Mediterranean regions and has been used for several liver diseases. Milk thisle derives its name from the milky veins leaves.[1,2] This plant can rich in height of 2-3 meters and has purple flowers with green spiky leaves (Fig. 1.1), in 1970s a new white-flowered variety was found.[1,3] The flowers of milk thistle hold seeds that contain a primary active extract compound called silymarin which was isolated in 1968 by Wagner.[4, 5]

Figure1.1. Milk thistle flower. These photos were taken at UNCG, Dr. Oberlies lab, 3/10/2013 (Hanan Althagafy)

Silymarin was considered as a one compound with the structure of 7-chromanol-3-methyl-taxifolin, but separation method was shown that silymarin consists of a mixture of seven diastereoisomers flavonolignans, include: silybin A (**1**), silybin B (**2**), isosilybin A (**3**), isosilybin B (**4**), silychristin (**5**), isosilychristin (**6**), and silydianin (**7**; Fig. 1.2).[6-10]

The structures and stereochemistry of flavonolignans were extensively studied between 1960 and the mid-1980s by Hänsel and Wagner independently.[11-18] Silybin A and B were initially isolated and characterized as a mixture. Besides silybin, two other compounds silychristin and silydianin were isolated.[19,12] However, in 1974 Wagner reported other constituent, isosilibinin also as one compound.[14] Silibinin and isosilibinin structures were determined based on degradative work and the synthesis and characterization of the dehydrosilybinin pentamethyl ether.[12,13,15]

In 1979, Arnone *et al.*,[14] determined the structure of the two individual diastereoisomers of silybinin and isosilibinin based on their comparison study of biomimetic synthesis products.

Separation of both diastereoisomers and the absolute configuration of silybin A, B and isosilybin A, B were complicated in 2003 as: silybin A, 2R, 3R, 7″R, 8″R; silybin B, 2R, 3R, 7″S, 8″S; isosilybin A, 2R, 3R, 7″R, 8″R; and isosilybin B, 2R, 3R, 7″S, 8″S, using 2D NMR, X-ray crystallographic analysis and CD.[20,21]

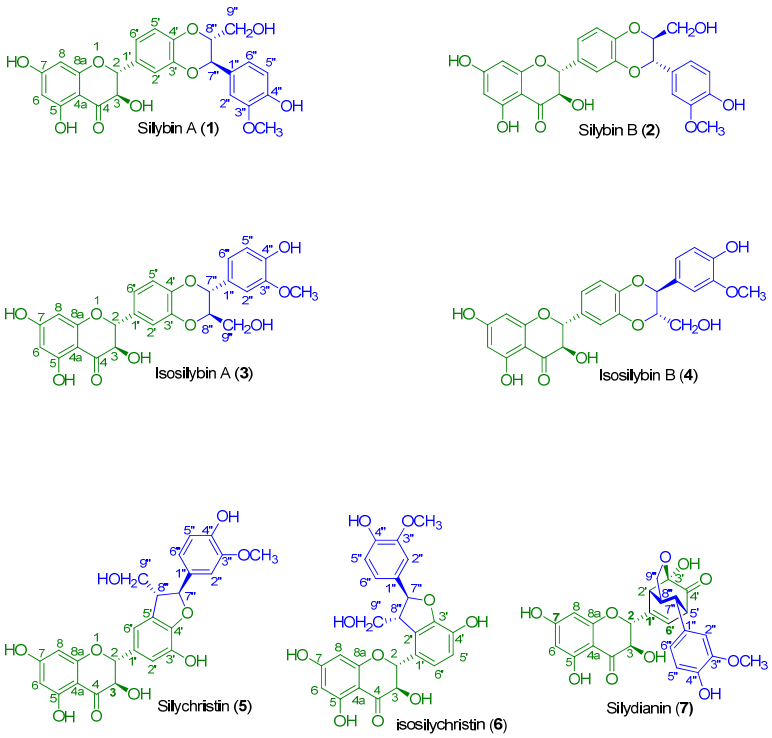

Figure 1.2. Structures for the seven major flavonolignans from silymarin

1.1.2. Hepatoprotactive activity of flavonolignans

Initially, flavonolignans were isolated and used in clinical research as a hepatoprotective agents;[22-24] hepatitis[25], cirrhosis, alcoholic liver diseases[26], poisoning by phalloidin,[27,28] chemicals[29] and toxin drug-induced.[30,31] In animal experiments, silymarin and silibinin have been shown to prevent the cirrhotic changes in rat against hepatotoxicity induced by some chemical such as carbon tetrachloride and against amanita phalloides.[32-34] Silymarin regulates inflammatory mediators such an interleukins,[35] tumor necrosis factor (TNF)[36] and inhibits NF-κB activation.[37,38]

Also silymarin components modulate protein kinases and suppress cellular proliferation.[39,40] The influence of the flavonolignane on the rate of RNA synthesis was studied in rat livers. ~60% increase in nuclear RNA synthesis was observed.[41,42] Experimental studies showed that silymarin can promote DNA polymerase and enhance hepatocyte regeneration.[42,43]

Studies showed that silymarin increase the anti-oxidants levels; stabilize the plasma membrane by reducing lipid peroxidation and free radical production.[44-46] The effect of silymarin on phospholipid in rat liver and brain microsomal membranes was studied. Resultes showed that silymarin effective the lipoxygenase and cyclooxygenase pathways.[47,48] Therefore, flavonolignans may be useful to inhibit the fatty acid peroxidation and control the prostaglandin formation.[49,50]

1.1.3 Anti-cancer activity of flavonolignans

Flavonolignans have been demonstrated to have strong anti-tumor, chemoprevention and anti-proliferative activities.[51-54] More recent studies have shown that flavonolignans **1-4** are selective inhibitors against large types of cancer cell lines. [55] There are several studies in an animal and cell culture that show selective inhibitor of silibinin and isosilibinin against large types of cancer cell lines such as, SHP-77 and A549 lung cancer cells,[54,56,57] K562 human leukemia,[58] renal cell carcinoma (RCC) metastasis,[59,60] human breast cancer MCF-7 cells,[61,62] colorectal cancer LoVo cells,[63,64] colon carcinoma HT-29 cells[65] and human prostate carcinoma PC-3.[66,67]

In a xenograft mice model using a DU145 human prostate cancer cells, dietary silibinin significantly reduced the xenograft tumor growth.[68,69] In addition silibinin has shown strong anticancer efficacy against both androgen-dependent and androgen-independent prostate cancer cells.[70,71] Silymarin and silybin were shown to suppress the activity of the DNA topoisomerase II alpha gene promoter in DU145 cells.[72]

Silibinin strongly inhibit cell proliferation at the G1-phase of the cell cycle and inhibit angiogenesis, and enhanced apoptosis in the prostate tumor cells.[39,73] Molecular studies showed that silymarin caused p21/Cip 1, p27/Kip1, G1 and G2-M cell cycle arrest associated with decrease in dependent kinase CDK4, CDK6 and CDK2 protein levels.[74-76] Animal study showed that silybin also increased activated caspase-3- positive cells and decreased vascular endothelial growth factor (VEGF) expression in tumors.[73,77] At low doses silymarin was shown to inhibit ERK1/2 activation, and at higher doses

silymarin stimulated JNK activation in A431 cells. [39,59,78] Silibinin has shown synergic anti-cancer activity in prostate cancer models when combined with doxorubicin[37]. Moreover, isosilybin B, which is no more than 5% of silymarin, has been shown to have significant antiproliferative activity against human prostate cell lines (PCA DU145, PCA LNCaP and 22Rv1).[72,79,80]

1.1.4 Metabolism and pharmacokinetic of flavonolignans

Metabolism of silymarin components are started early and referred to study on silibinin.[81-83] Silibinin has been shown to undergo sulfates and glucuronides conjugation (phase II) reactions and are excreted into bile and urine.[81,84-86] The hydroxylation (CYP2E1), oxidation (CYP3A4) and demethylation metabolism (phase I) of silibinin by CYP450 enzymes have been also observed (Fig. 1.3).[87,88]

Silibinin in vitro and in vivo has been shown prominent inhibition and alter the activities of a variety of cytochrome P450 isoenzymes, such as; CYP3A4[88] and CYP2C9 isoforms[89,90] (IC_{50} < 50 mu M), UDP glucuronosyltransferase isoform1A1 (UGT1A1) and P-glycoprotein (P-gp)mediated efflux transporters.[91-93] A weak interaction with human microsomal CYP2E1, 2A6, 2B6, 2C19, and 2D6 (IC_{50} > 250 mμ M) was found; a moderate inhibition was observed for CYP1A2 and 2C8.[94]

It is important to mention that the flavonolignans cytochrome P450 interaction is dose dependent. This modulation may interact with metabolism of therapeutic drugs or reduce the activity of carcinogenic compounds.

Silibinin absorption and bioavailability are low due to extensive multiple conjugation reactions.[10,81,86] In general hydroxyl of phenolic group at C-7 and C-4″ are the major sites for glucuronidation. Studies in the glucuronidation process showed that these are a significant chemoselective. The glucuronidation of silybin B was more efficient rate than silybin A. Glucuronidation at the C-4″ position was much preferred in silybin B. However, in case of silybin A glucuronidation was similar at the C-7 and C-4″.[81,95] In sulfation reactions there is a similarity in reaction rate in case of silybin A and silybin B.[81] The conjugation metabolites such as mono-methylated at C-7 and di-methylated at C-7 and C-4″ have been shown to have a biological activity.[66,96]

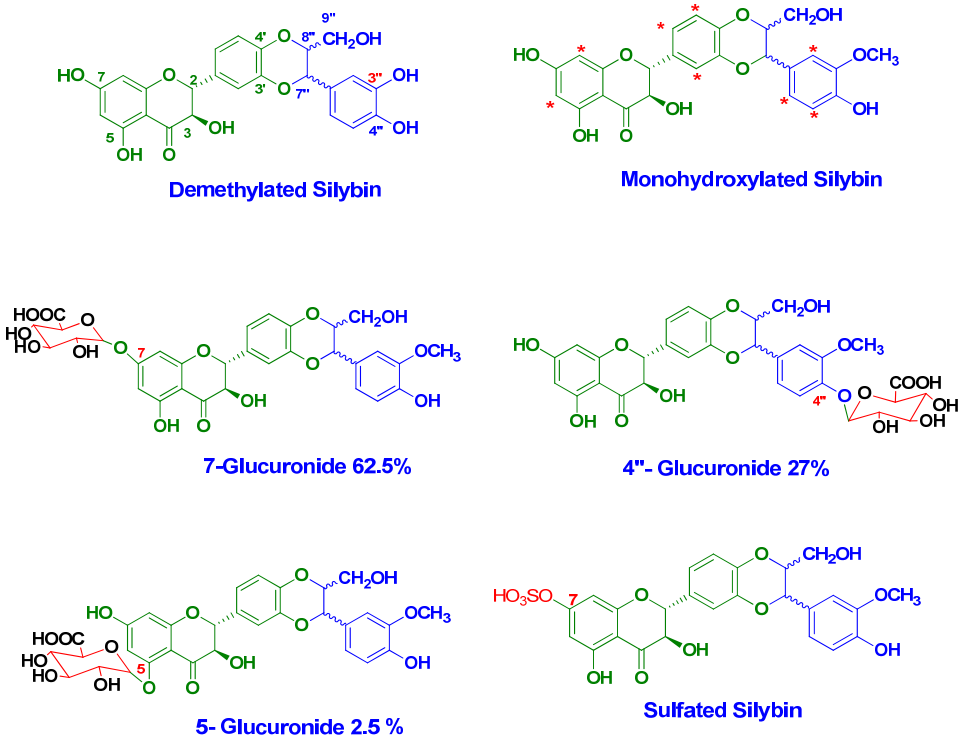

Figure 1.3 Oxidative, demethylenation and subsequent glucuronidation are the major flavonolignans metabolic products

1.1.5 History of flavonolignans derivatives

Several analogues of silibinin were synthesized from beginning of 1970s with better bioavailability, solubility and activities. Synthesis of the 3, 4″-O-bis-hemisuccinate silybin, was the first example of a water-soluble analogue silybin.[97,98] Glycosides semisynthetic derivatives also enhanced water-soluble and the antioxidant property.[10,99] Silibinin in a complex with phosphatidylcholine has been developed to increase its bioavailability and absorption.[100-102] In animal models phosphatidylcholine shows greater oral bioavailability as indicated by higher plasma silybin levels and greater activity compared with with pure silybin. Complexes of flavanolignans (silybin, silidianin, and

silicristin) with phospholipids are prepared to enhance absorption in the gastrointestinal tract. This flavonolignans-lipophilic complex was used orally administered to carbon tetrachloride-treated rats to inhibit the liver toxicity.[98]

Silybin esterification with long-chain fatty acids were tested as anti-influenza virus activities and for their antioxidant (inhibition of lipid peroxidation and it found that the activity improved with increasing length of the acyl moiety.[103,104]

It also found that carboxylic acid derivatives of silybin and 2,3-dehydrosilybin improved the antioxidant effectiveness.[105,106] *O*-alkyl derivatives (methyl and benzyl) of silibinin and 2,3-dehydrosilibinin enhanced the cytotoxicity in multidrug resistant cell lines.[96] The 7-*O*-monomethyl and 7, 4″-*O*-dimethyl analogues were shown to have enhanced cytotoxicity, antiviral activity (up to 6-fold increased potency) compared to the parent compound (Figure 1.4). [66] Gažák and his co-workers synthesized *O*-galloylsilybin for pure silybin A and silybin B and for the mixture (silibinin) and the derivitives showed good antiangiogenic activity [108]

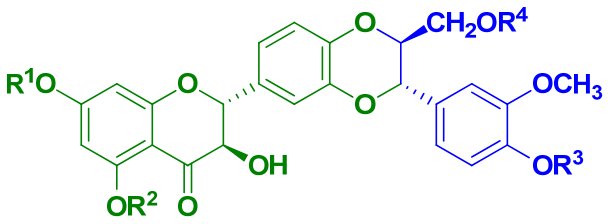

(1) R^1, R^2, R^3, R^4 = H (IC_{50} = 60.5 ± 4.3)

(2) R^1, R^2, R^3 = CH_3; R^4 = H (IC_{50} = 36.3 ± 3.7)

(3) R^1 = CH_3, R^2, R^3, R^4 = H (IC_{50} = 16.9 ± 3.6)

(4) R^1, R^3 = CH_3; R^2, R^4 = H(IC_{50} = 8.1 ± 3.5)

(5) R^1, R^2, R^3, R^4 = CH_3 (IC_{50} = 14.4 ± 4.4)

(6) R^1, R^3, R^4 = CH_3, R^2 = H (IC_{50} = 21.9 ± 4.1)

Figure 1.4 Silybin B and the methylated analogues 2-6 and IC_{50} values[66]

1.1.6 Aim of the work

The goal of the present study was to expand upon that initial SAR by selectively synthesizing 7-*O*-methyl analogues of the seven major flavonolignans. However, rather than relying upon protecting groups, which require two additional synthetic steps for installation and removal, it was hypothesized that the inherent reactivity of the molecule could be harnessed to guide the selectivity. By judicious choice of reaction conditions, a single position, the C-7-phenol, was methylated selectively in the presence of multiple centers with similar reactivity, including two or three other phenolic positions, a similarly acidic secondary alcohol, and a primary alcohol. This chemoselectivity was comparable for all seven flavonolignans, which enabled the site-specific analysis of the importance of the methylated phenol for each compounds activity in a suite of bioassays that probed cytotoxicity, anti-hepatitis C virus (HCV) activity, and inhibition of prominent drug metabolizing enzymes.

1.2 Result and Discussion

1.2.1 Chemistry

The synthesis of 7-*O*-methyl analogues of the natural flavonolignans was challenging due to the possibility of alkylation at more than one hydroxyl group. Therefore, a variety of bases [Cs_2CO_3, K_2CO_3, and Diazabicycloundecene (DBU)], electrophilic methylating agents (dimethyl carbonate, methyl iodide), solvents (acetone, THF, acetonitrile), temperatures (rt to 75 °C under standard heating or up to 130 °C

using microwave heating), and times (2 h to 2 days) were examined, all with the goal of minimizing the formation of polymethylated side products. Selective monomethylation of the phenolic group at C-7 was possible for all seven major flavonolignans over a temperature range of 30–60 °C using methyl iodide in dry acetone in the presence of K_2CO_3. The 7-position was the most reactive for methylation, presumably due to both acidity, being an arylogous carboxylic acid, and steric accessibility. While the yields were moderate to low, ranging from approximately 20 to 40%, the reaction conditions were optimized for selective monomethylation rather than yield.

1.2.2 Purification

Published methods were utilized to isolate the individual flavonolignans as starting materials for the methylation reactions.[108] To purify the reaction mixtures, two different reverse-phase columns [ODS-A C18 (5 μm; 250 × 20 mm) and PFP (5 μm; 250 × 21 mm)] were examined. ODS-A C18 gave a good result in separation of disterioesomers and PFP gave a good result in separation of other anpurities that not separated in C18 column. PFP gave the best results according to peak symmetry and resolution when using acetonitrile as the organic modifier (data not shown). Accordingly, each 7-*O*-methylated flavonolignan analogue was purified until >98% pure, as measured by analytical HPLC (see the experiment section). 7-*O*-methylsilybin A (**2**) and 7-*O*-methylisosilybin A (**6**) were purified using a gradient of 30:70 to 50:50 CH_3CN:H_2O (0.1% formic acid) over 30 min. 7-*O*-methylsilybin B (**4**) was purified using a gradient of 20:80 to 40:60 CH_3CN:H_2O (0.1 % formic acid) over 30 min. 7-*O*-methylisosilybin B (**8**)

was purified using 20:80 to 60:40 $CH_3CN:H_2O$ (0.1 % formic acid) over 40 min. 7-*O*-methylsilychristin (**10**) and 7-*O*-methylsilydianin (**12**) were purified using a gradient of 20:80 to 36:64 $CH_3CN:H_2O$ (0.1% formic acid) over 24 min. 7-*O*-methylisosilychristin (**14**) was purified using a gradient of 15:80 to 36:64 $CH_3CN:H_2O$ (0.1 % formic acid) over 26 min.

1.2.3 Structure determination

Structures of the 7-*O*-methylated analogues were determined using a suite of NMR spectroscopy and mass spectrometry experiments (see Tables 1, 2 and 3). Using the data for 7-*O*-methylsilybin A (**2**) as a representative example, two methoxy singlets were apparent at δH 3.78 (3H) and 3.77 (3H), due to the introduced methoxy group at C-7 and the natural one at C-3″, respectively. In contrast, the parent flavonolignan silybin A (**1**) displayed a sharp singlet at δH 10.86 for the C-7 phenolic proton signal. Further evidence for the methoxy group on C-7 in analogue 2 was observed in the meta-coupled protons at H-6 and H-8 (δH 6.12 and 6.10, respectively), which were shifted downfield slightly compared to **1** (Table 1.1 and 1.2). The ^{13}C NMR data (Table 1.2) of each methylated analogue displayed 26 distinct signals, which was one more than the non-methylated starting materials, including resonances at δC 56.0 and 55.7 due to the two methoxy moieties at C-7 and C-3″, respectively; these assignments were supported by HSQC correlations. Moreover, data from the HMBC experiment demonstrated the connectivity of the methoxy moieties, where correlations were observed between the protons at δH 3.78 to C-7 (δC 167.6) and δH 3.77 to C-3″ (δC 147.6), respectively, verifying that the

introduced methoxy moiety was at the C-7 position in 2. For each of the analogues, a similar set of NMR experiments and data, coupled with comparisons to the data for the natural flavonolignans, were utilized to establish that the methoxy moiety was connected at the 7 position in all of the analogues. Finally, HRMS data supported the introduction of a single methyl moiety, where the $[M-H]^-$ ion peak for all of the analogues was fourteen mass units greater than that of the parent flavonolignans (see experimental).

Table 1.1. ^{1}H NMR data of flavonolignans (**1, 3, 5, 7**) and 7-*O*-methylflavonolignans (**2, 4, 6, 8**) in DMSO-d_6 (500 MHz, 30 °C)

position	**1**	**2**	**3**	**4**	**5**	**6**	**7**	**8**
2	5.08, d (11.5)	5.14, d (11.5)	5.08, d (11.5)	5.14, d (11.5)	5.11, d (10.9)	5.16, d (10.9)	5.11, d (11.5)	5.16, d (11.5)
3	4.63, dd (11.5, 6.3)	4.69, dd (11.5, 6.3)	4.61, dd (11.5, 6.3)	4.67, dd (11.5, 6.3)	4.60, dd (10.9, 6.3)	4.66, dd (10.9, 6.3)	4.61, dd (11.5, 5.9)	4.67, dd (11.5, 6.3)
6	5.91, d (1.7)	6.12, d (1.7)	5.91, d (2.3)	6.12, d (2.3)	5.92, d (2.3)	6.13, d (2.3)	5.92, d (2.0)	6.13, d (2.3)
8	5.86, d (1.7)	6.10, d (1.7)	5.87, d (2.3)	6.10, d (2.3)	5.89, d (2.3)	6.12, d (2.3)	5.89, d (2.0)	6.12, d (2.3)
2'	7.09, d (1.7)	7.10, d (1.7)	7.08, d (1.8)	7.10, d (2.3)	7.09, d (2.3)	7.11, d (2.3)	7.10, d (1.8)	7.11, d (1.7)
5'	6.97, d (8.0)	6.98, d (8.6)	6.97, d (8.1)	6.98, d (8.0)	6.93, d (8.6)	6.94, d (8.6)	6.93, d (8.0)	6.94, d (8.0)
6'	7.00, dd (8.0, 1.7)	7.01, dd (8.6, 1.7)	7.02, dd (8.1, 1.8)	7.02, dd (8.0, 2.3)	6.98, dd (8.6, 2.3)	6.99, dd (8.6, 2.3)	6.98, dd (8.0, 1.8)	7.00, dd (8.0, 1.7)
2"	7.01, d (1.8)	7.03, d (1.8)	7.02, d (1.7)	7.04, d (1.7)	7.00, d (1.7)	7.00, d (1.7)	7.00, d (2.3)	7.01, d (1.8)

chemical shifts in δ, coupling constants in Hz

Table 1.1. ^{1}H NMR (continued)

position	**1**	**2**	**3**	**4**	**5**	**6**	**7**	**8**
5"	6.80, d (8.6)	6.80, d (8.6)	6.79, d (8.6)	6.80, d (8.0)	6.80, d (8.6)	6.80, d (8.0)	6.80, d (8.6)	6.80, d (8.2)
6"	6.86, dd (8.6, 1.8)	6.86, dd (8.6, 1.8)	6.86, dd (8.6, 1.7)	6.86, dd (8.0, 1.7)	6.86, dd (8.6, 1.7)	6.85, dd (8.0, 1.7)	6.86, dd (8.6, 2.3)	6.85, dd (8.2, 1.8)
7"	4.90, d (7.5)	4.91, d (7.5)	4.90, d (7.5)	4.91, d (7.5)	4.91, d (8.1)	4.91, d (7.5)	4.91, d (7.5)	4.92, d (7.5)
8"	4.17, ddd (7.5, 4.6, 2.3)	4.18, ddd (7.5, 4.6, 2.3)	4.16, ddd (7.5, 4.1, 2.3)	4.17, ddd (7.5, 4.6, 2.3)	4.16, ddd (8.1, 4.6, 2.3)	4.17, ddd (7.5, 4.0, 2.3)	4.17, ddd (7.5, 4.6, 2.3)	4.17, ddd (7.5, 4.6, 1.7)
9"a	3.53, ddd (10.3, 5.2, 2.3)	3.53, ddd (10.3, 5.2, 2.3)	3.53, ddd (9.8, 4.6, 2.3)	3.54, ddd (12.0, 5.2, 2.3)	3.53, ddd (12, 4.6, 2.3)	3.53, ddd (12.0, 4.6, 2.3)	3.54, ddd (11.9, 5.2, 2.3)	3.53, ddd (10, 5.2, 1.7)
9"b	3.33, m	3.34, m	3.33, m	3.33, m	3.33, m	3.33, m	3.33, m	3.33, m
7-OCH_3	-	3.78, s	-	3.78, s	-	3.79, s	-	3.79, s

chemical shifts in δ, coupling constants in Hz

Table 1.1. ^{1}H NMR (continued)

position	**1**	**2**	**3**	**4**	**5**	**6**	**7**	**8**
3"-OCH_3	3.77, s	3.77, s	3.77, s	3.77, s	3.78, s	3.77, s	3.77, s	3.77, s
3-OH	5.83, d (6.3)	5.90, d (6.3)	5.83, d (6.3)	5.89, d (6.3)	5.83, d (6.3)	5.91, d (6.3)	5.84, d (5.9)	5.91, d (6.3)
5-OH	11.90, s	11.86, s	11.90, s	11.87, s	11.90, s	11.87, s	11.90, s	11.87, s
7-OH	10.86, s	-	10.86, s	-	10.85, s	-	10.86 s	-
4"-OH	9.18, s	9.19, s	9.17, s	9.18, s	9.15, s	9.18, s	9.16, s	9.18, s
9"-OH	4.97, dd	4.98, dd	4.98, dd	4.98, dd	4.95, dd	4.97, dd	4.96, dd	4.97, dd
	(5.7, 5.2)	(5.7, 5.2)	(5.7, 4.6)	(5.7, 5.2)	(5.7, 4.6)	(5.7, 4.6)	(5.5, 5.0)	(5.2, 4.6)

chemical shifts in δ, coupling constants in Hz

Table 1.2. ^{1}H NMR data of flavonolignans (**9, 11, 13**) and 7-*O*-methylflavonolignans (**10, 12, 14**) in DMSO-d_6 (500 MHz, 30 °C)

position	**9**	**10**	**11**	**12**	**13**	**14**
2	5.02, d (11.4)	5.05, d (11.4)	5.17, d (11.9)	5.22, d (11.4)	4.86, dd (10.4)	4.91, dd (10.4)
3	4.52, dd (11.4, 6.4)	4.58, dd (11.4, 6.3)	4.64, dd (11.9, 6.5)	4.67, dd (11.4, 6.9)	4.44, dd (10.4, 5.4)	4.48, dd (10.4, 5.4)
6	5.91, d (2.0)	6.12, d (2.3)	5.93, d (1.9)	6.13, d (2.0)	5.91, d (2.5)	6.12, d (1.9)
8	5.86, d (2.0)	6.09, d (2.3)	5.88, d (1.9)	6.11, d (2.0)	5.88, d (2.5)	6.11, d (1.9)
2'	6.82, d (1. 5)	6.84, d (1.2)	-	-	3.44, dd (4.0, 2.0)	3.45, dd (4.0, 2.0)
5'	-	-	6.75, d (8.1)	6.74, d (8.1)	3.17, dd (8.9, 3.0)	3.19, dd (6.9, 3.0)
6'	6.87, br s	6.88, br s	6.96, d (8.1)	6.97, d (8.1)	5.92, d (8.9)	6.01, d (6.9)
2"	6.96, d (2.0)	6.96, d (1.8)	6.86, d (1.5)	6.86, d (2.0)	6.75, d (2.0)	6.76, d (1.9)
5"	6.76, d (8.4)	6.76, d (8.1)	6.70, d (7.9)	6.69, d (8.5)	6.63, d (8.5)	6.64, d (8.4)

chemical shifts in δ, coupling constants in Hz

Table 1.2. ^{1}H NMR (continued)

position	**9**	**10**	**11**	**12**	**13**	**14**
6"	6.80, dd (8.4, 2.0)	6.81, dd (8.1, 1.8)	6.76, dd (7.9, 1.5)	6.76, dd (8.5, 2.0)	6.55, dd (8.5, 2.0)	6.56, dd (8.4, 1.9)
7"	5.46, d (7.0)	5.46, d (6.9)	5.58, d (2.5)	5.57, d (2.5)	3.31, b s	3.31, b s
8"	3.47, ddd (12.6, 12.0, 7.0)	3.47, ddd (12.6, 12.0, 6.9)	3.67, m	3.67, m	2.72, b s	2.73, br s
9"a	3.72, ddd (12.6, 10.9, 5.0)	3.72, ddd (12.6, 10.9, 5.2)	3.68, m	3.68, m	4.12, dd (8.0, 3.0)	4.13, dd (8.0, 3.0)
9"b	3.63, ddd (12.6, 10.9, 5.6)	3.63, ddd (12.6, 10.9, 5.7)	3.45, m	3.44, m	3.78, d (8.0)	3.78, d (8.0)

chemical shifts in δ, coupling constants in Hz

Table 1.2. ^{1}H NMR (continued)

position	**9**	**10**	**11**	**12**	**13**	**14**
7-OCH_3	-	3.78, s	-	3.80, s	-	3.79, s
3"-OCH_3	3.76, s	3.76, s	3.70, s	3.69, s	3.73, s	3.74, s
3-OH	5.77, d (6.4)	5.81, d (6.3)	5.76, d (6.5)	5.81, d (6.9)	6.02, d (6.3)	6.04, d (6.3)
5-OH	11.91, s	11.87, s	11.93, s	11.90, s	11.81, s	11.77, s
7-OH	10.84, s	-	10.98, s	-	10.9, s	-
4"-OH	9.03, s	9.02, s	9.00, s	8.99, s	8.79, s	8.79, s
9"-OH	5.01, dd (5.6, 5.0)	5.01, dd (5.7, 5.2)	5.07, br dd (4.5, 2.0)	5.06, dd (6.5, 4.5)		
3'-OH					7.19, s	7.17, s

chemical shifts in δ, coupling constants in Hz

Table 1.3. ^{13}C NMR data of flavonolignans and 7-*O*-methylated analogues in DMSO-d_6 (125 MHz, 30 °C).

position	**type**	**1**	**2**	**3**	**4**	**5**	**6**	**7**	**8**	**9**	**10**	**11**	**12**	**13**	**14**
2	CH	82.6	82.7	82.5	82.7	82.5	82.7	82. 5	82.7	83.3	83.4	79.9	80.0	81.7	81.8
3	CH	71.4	71.5	71.4	71.5	71.5	71.6	71.5	71.6	71.7	71.8	71.5	71.7	70.8	71.0
4	C	197.8	198.5	197.7	198.5	197.8	198.5	197.8	198.4	197.8	198.4	198.2	198.7	196.5	197.6
4a	C	100.4	101.4	100.4	101.4	100.5	101.4	100.5	101.4	100.5	101.4	100.6	101.5	100.3	101.2
5	C	163.3	163.0	163.3	163.0	163.3	163.0	163.3	163.0	163.3	163.0	163.4	163.1	163.4	163.0
6	CH	96.1	95.0	96.1	94.9	96.1	95.0	96.1	95.0	96.0	94.9	96.1	95.0	96.2	95.2
7	C	167.1	167.6	166.9	167.6	166.9	167.6	166.9	167.6	166.8	167.5	166.8	167.6	166.9	167.6
8	CH	95.1	93.9	95.0	93.9	95.1	93.9	95.1	93.9	95.0	93.8	95.1	93.9	95.0	93.8
8a	C	162.5	162.4	162.4	162.4	162.5	162.4	162.5	162.4	162.6	162.5	162.6	162.5	162.0	162.0
1'	C	130.1	129.9	130.1	130.0	130.3	130.2	130.3	130.2	130.0	129.8	124.5	124.4	139.5	139.4
2'	CH	116.6	116.7	116.6	116.7	116.5	116.6	116.5	116.5	115.6	115.7	128.9	128.9	48.6	48.7
3'	C	143.3	143.3	143.2	143.2	142.9	142.9	142.9	142.9	146.4	146.4	141.6	141.6	96.7	96.7

chemical shifts in δ

Table 1.3. ^{13}C NMR (continued)

position	type	1	2	3	4	5	6	7	8	9	10	11	12	13	14
4'	C	143.7	143.7	143.6	143.7	143.9	143.9	143.9	143.9	140.7	140.7	145.9	145.8	201.9	201.9
5'	CH	116.3	116.4	116.3	116.4	116.4	116.5	116.5	116.4	129.1	129.1	116.1	116.1	53.4	53.3
6'	CH	121.4	121.5	121.1	121.2	120.9	121.0	120.9	121.0	115.4	115.4	119.5	119.4	124.0	124.0
1"	C	127.5	127.5	127.5	127.5	127.5	127.5	127.5	127.5	132.4	132.4	132.8	132.8	133.0	133.0
2"	CH	111.6	111.6	111.6	111.6	111.7	111.7	111.7	111.7	110.4	110.9	110.2	110.3	112.4	112.4
3"	C	147.6	147.6	147.6	147.6	147.6	147.6	147.6	147.6	147.5	148.1	147.5	147.5	147.1	147.2
4"	C	147.0	147.0	147.0	147.0	147.0	147.0	147.0	147.0	147.1	147.7	146.3	146.3	145.1	145.1
5"	CH	115.3	115.3	115.3	115.3	115.3	115.3	115.3	115.3	115.3	115.3	115.1	115.1	114.9	115.0
6"	CH	120.5	120.6	120.5	120.5	120.5	120.5	120.5	120.4	118.7	118.7	118.5	118.6	120.3	120.3
7"	CH	75.9	75.9	75.8	75.9	75.9	75.9	75.9	75.9	87.0	87.5	86.4	86.4	46.0	46.0
8"	CH	78.1	78.1	78.1	78.1	78.0	78.0	78.0	78.0	53.4	53.9	52.0	51.9	44.0	44.0
9"	CH_2	60.2	60.2	60.2	60.2	60.2	60.2	60.2	60.2	63.0	63.5	63.5	63.5	72.8	72.8

chemical shifts in δ

Table 1.3. ^{13}C NMR (continued)

position	**type**	**1**	**2**	**3**	**4**	**5**	**6**	**7**	**8**	**9**	**10**	**11**	**12**	**13**	**14**
3"-OCH_3	CH_3	55.7	55.7	55.7	55.7	55.7	55.7	55.7	55.7	55.6	55.6	55.6	55.6	55.4	55.4
7-OCH_3	CH_3	-	56.0	-	56.0	-	56.0	-	56.0		55.9	-	56.0	-	56.0

chemical shifts in δ

1.3. Biological Studies

1.3.1. Cytotoxicity and cell viability

In comparing the cytotoxicity profiles of 7-*O*-methylated analogues vs. parental counterparts (Table 1.4), addition of a single methyl group increased cytotoxicity against human hepatoma cells (Huh7.5.1). These findings were consistent with an earlier pilot study that examined a series of mono-, di-, tri- and tetra-methylated analogues of silybin B (**3**).[66] Silychristin (**9**), isosilychristin (**11**), and silydianin (**13**) have been reported to be relatively non-toxic compared to the other silymarin flavonolignans.[109] In the current study, marked increases in the cytotoxicity of silydianin (**13**), silybin A (**1**), and isosilybin A (**5**) were observed upon methylation (compounds **14**, **2**, and **6**, with 13.8, 8.4, and 6.1 fold, respectively). However, the 7-*O*-methylation of isosilybin B (**7**) did not produce a pronounced increase in cytotoxicity (i.e., compound **8**), which was interesting given that **7** has been shown to be the most cytotoxic of the parent flavonolignans, particularly in assays for prostate cancer chemoprevention.[80,109-113]

Table 1.4. Cytotoxic activity of flavonolignans and 7-*O*-methylated analogues against human hepatoma (Huh7.5.1) cells.

Compound	**IC_{50} Values (μM)**	**Fold Change [a,b]**
Silybin A (**1**)	80.0	
7-*O*-Methylsilybin A (**2**)	9.5	8.4
Silybin B (**3**)	68.7	
7-*O*-Methylsilybin B (**4**)	12.7	5.5
Isosilybin A (**5**)	80.0	
7-*O*-Methylisosilybin A (**6**)	13.2	6.1
Isosilybin B (**7**)	27.0	
7-*O*-Methylisosilybin B (**8**)	18.0	1.5
Silychristin (**9**)	>130	
7-*O*-Methylsilychristin (**10**)	66.4	>2
Isosilychristin (**11**)	>130	
7-*O*-Methylisosilychristin (**12**)	27.6	>4.7
Silydianin (**13**)	>130	
7-*O*-Methylsilydianin (**14**)	9.4	13.8
Resveratrol[c]	10.6	

[a] The fold change was calculated by dividing the IC_{50} value for the parent flavonolignan by the IC_{50} value for the corresponding 7-*O*-methylated analogue.
[b] The average fold change for all analogues was approximately 6.
[c] Typical average value as a positive control for the assay.

1.3.1.1. Anti-viral activity

In evaluating the anti-HCV profiles of these compounds (Fig. 1.5), some of the methylated flavonolignans displayed greater anti-HCV activity [i.e. 7-*O*-methylsilychristin (**10**), 7-*O*-methylisosilychristin (**12**)] than the corresponding parent compounds. In particular, silychristin (**9**), isosilychristin (**11**), and silydianin (**13**) did not show appreciable antiviral activity until they were methylated (i.e., **10**, **12**, and **14**).

On the other hand, if parent compounds were active in blocking HCV activity, such as silybin A (**1**), silybin B (**3**), and isosilybin A (**5**), the methylated counterparts either retained (**2**) or decreased (**4, 6**) activity. The most toxic parent compound, isosilybin B (**7**), had a slight enhancement of both antiviral activity and cytotoxicity (Table 1.4) by methylation (compound **8**). Thus, it appeared that HCV antiviral activity tracked with cytotoxicity. That is, as compounds became more toxic, the more likely antiviral activity was detected. However, that is not to say that antiviral activity coincided with cytotoxicity, as we were always able to detect anti-HCV activity that was independent of cytotoxicity.

We hypothesize that flavonolignans target shared cellular functions that confer both cytotoxic and antiviral activities. Huh7.5.1 cells were infected with JFH-1 at a multiplicity of infection of 0.05. Virus inoculum was removed after 5 h and compounds were added. Cultures were incubated for 72 h before protein lysates were analyzed for HCV core protein expression by Western blot analysis. Detection of actin protein served as a protein loading control. Panel A (Fig. 1.5). depicts an example of a parent compound that lacked anti-HCV activity (**9**) and acquired anti-HCV activity upon methylation (**10**).

Panel B (Fig. 1.5). depicts an example of a parent compound that had anti-HCV activity (**3**) and decreased anti-HCV activity upon methylation (**4**). The graphs below panels A and B present quantitation of HCV core pixel intensity following normalization to actin pixel intensity, expressed as percent inhibition relative to DMSO controls. Graphs below panel A depict parent compounds that lacked anti-HCV activity (**9**, **11**, **13**) and acquired anti-HCV activity upon methylation (**10**, **12**, **14**). Graphs below panel B depict parent compounds that had anti-HCV activity (**1**, **3**, **5**, **7**), and retained (**2**), decreased (**4**, **6**), or enhanced (**8**) anti-HCV activity upon methylation. Doses used were derived from toxicity data and were selected to be in the non-toxic range for each compound.

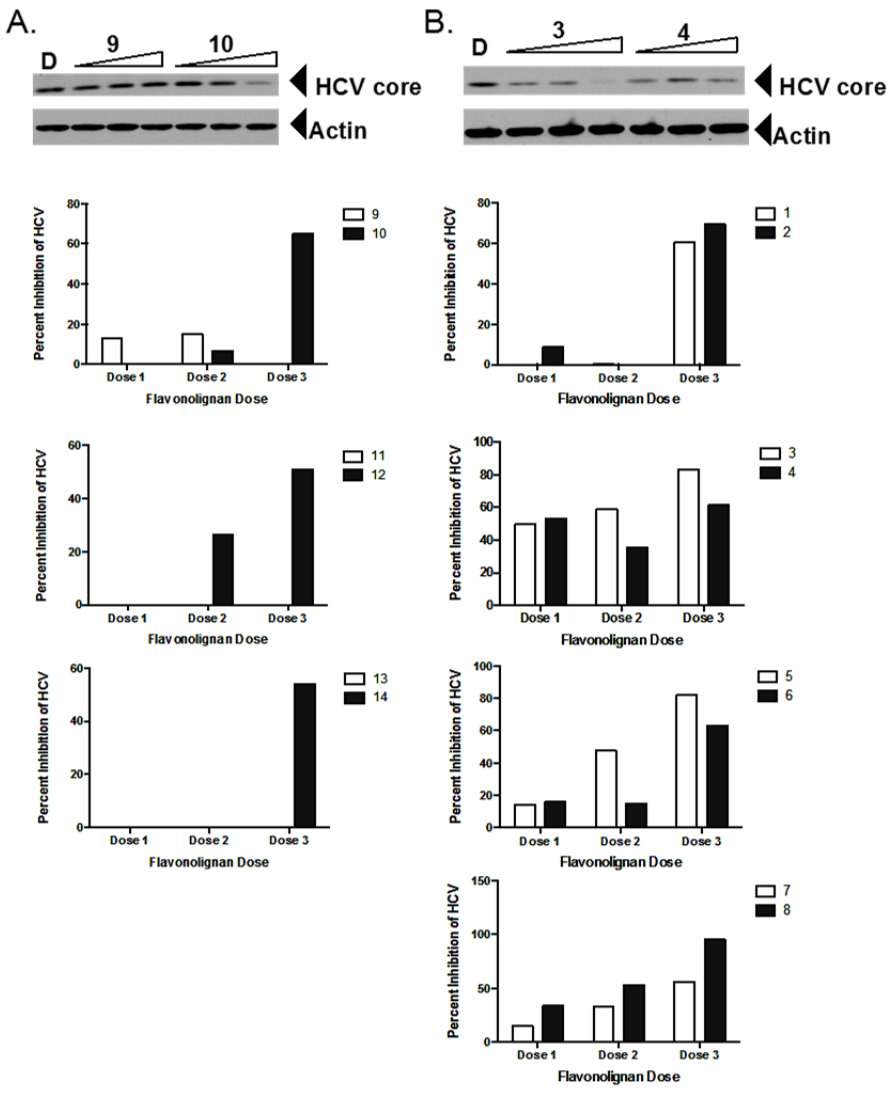

Figure 1.5. Antiviral profile of parent and 7-*O*-methyl flavonolignans.

Concentrations for compounds **1**, **3**, and **5**: 6.2, 20.7, 62.1 μM

Concentrations for compounds **2**, **4**, **6**, and **14**: 0.8, 2.7, 8.0 μM

Concentrations for compounds **7** and **8**: 1.6, 5.4, 16.1 μM

Concentrations for compounds **9**, **11**, **12** and **13**: 12.4, 41.4, 124.2 μM

Concentrations for compound **10**: 6.0, 20.1, 60.3 μM

1.3.2. Inhibition of drug metabolizing enzymes

The propensity of methylation at the 7-*O* position to alter drug interaction liability was evaluated by testing all compounds as inhibitors of drug metabolizing enzymes using the probe substrates (S)-warfarin (CYP2C9; Fig. 1.6), midazolam (CYP3A; Fig. 1.7), and 4-methylumbelliferone (UGT; Fig. 1.8) and human liver or intestinal microsomes (HLM or HIM, respectively). Although CYP2C9 and CYP3A are expressed in both the human intestine and liver,[114] intestinal CYP2C9 has not yet been shown to have clinical impact on drug disposition in vivo. As such, HLM were selected for (*S*)-warfarin 7-hydroxylation incubations, whereas HIM were selected for midazolam 1′-hydroxylation incubations.

All flavonolignans and 7-*O*-methylated analogues showed concentration-dependent inhibition (10 vs. 100 μM, $p<0.05$) of the tested enzymatic activities (Figs. 1.6-1.8), except for isosilybin A (**5**) against CYP2C9 activity (Fig. 1.6). The parent vs. methylated analogue pairs (at 100 μM) differed in inhibition potency ($p<0.05$) with the following exceptions: silybin B (3) vs. 7-*O*-methylsilybin B (**4**) (CYP2C9), silydianin (**13**) vs. 7-*O*-methylsilydianin (**14**) (CYP3A), silychristin (**9**) vs. 7-*O*-methylsilychristin (**10**) (CYP3A and UGT), and isosilybin B (**7**) vs. 7-*O*-methylisosilybin B (**8**) (UGT). Amongst the analogue series, compounds with an "iso" configuration inhibited the CYP enzymes (Figs. 1.6 and 1.7) to a greater extent. For example, relative to the control, 7-*O*-methylisosilybin A (**6**), 7-*O*-methylisosilybin B (**8**), and 7-*O*-methylisosilychristin (**12**) were more potent against CYP2C9 and CYP3A activities than 7-*O*-methylsilybin A (**2**), 7-*O*-methylsilybin B (**4**), and 7-*O*-methylsilychristin (**10**).

Compared to inhibition of the CYPs, inhibition of UGT was less extensive (Fig. 1.8). However, in general, the parent compounds were more potent than the analogues. For example, silybin A (**1**), silybin B (**3**), and silydianin (**13**) were more potent (maximum extent of inhibition, 44%) than the respective methylated analogues (i.e. **2**, **4**, and **14** with a maximum extent of inhibition, 23%), suggesting that methylation reduced activity against UGT. One exception was 7-*O*-methylisosilychristin (**12**), which was more potent than isosilychristin (**11**), which each inhibited by up to 41% and 24%, respectively ($p<0.05$). CYP2C9 activity was most sensitive to the compounds, both parent and analogues, followed by CYP3A and UGT activity (up to 91%, 72%, and 44% inhibition, respectively). In summary, 7-*O*-methylation of isolated flavonolignans from milk thistle modulated drug interaction potential in vitro, highlighting the importance of this metabolically labile site and providing mechanistic insight into the enzyme-ligand interaction.

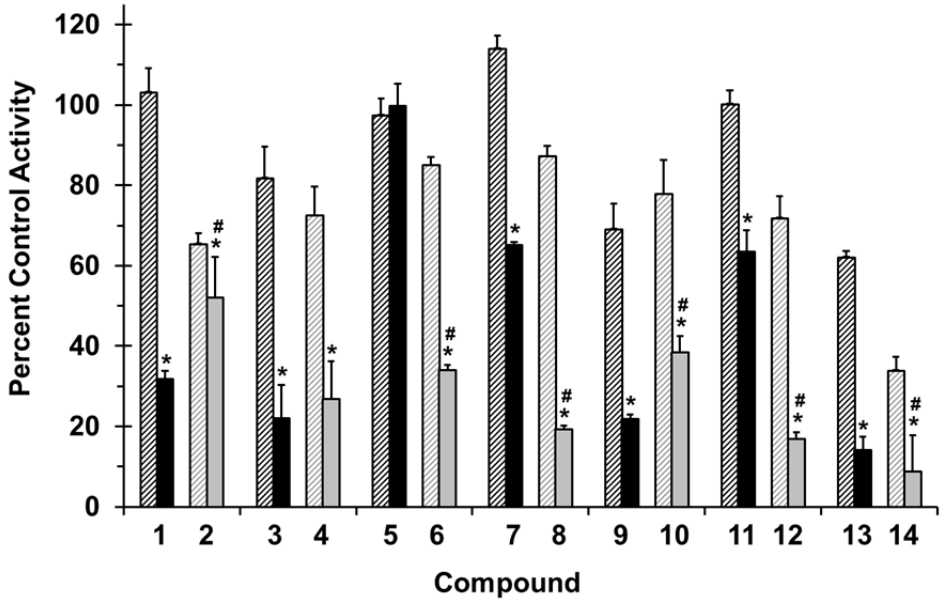

Figure 1.6. Effects of selected flavonolignans (black) and 7-*O*-methylated analogues (gray) on CYP2C9-mediated (*S*)-warfarin 7-hydroxylation in human liver microsomes (HLM). Bars and error bars denote means and SDs, respectively, of triplicate incubations. **p* < 0.05, 10 versus 100 μM; #*p* < 0.05, flavonolignan versus 7-*O*-methylated analogue at 100 μM (two-way ANOVA with Bonferroni adjustment).

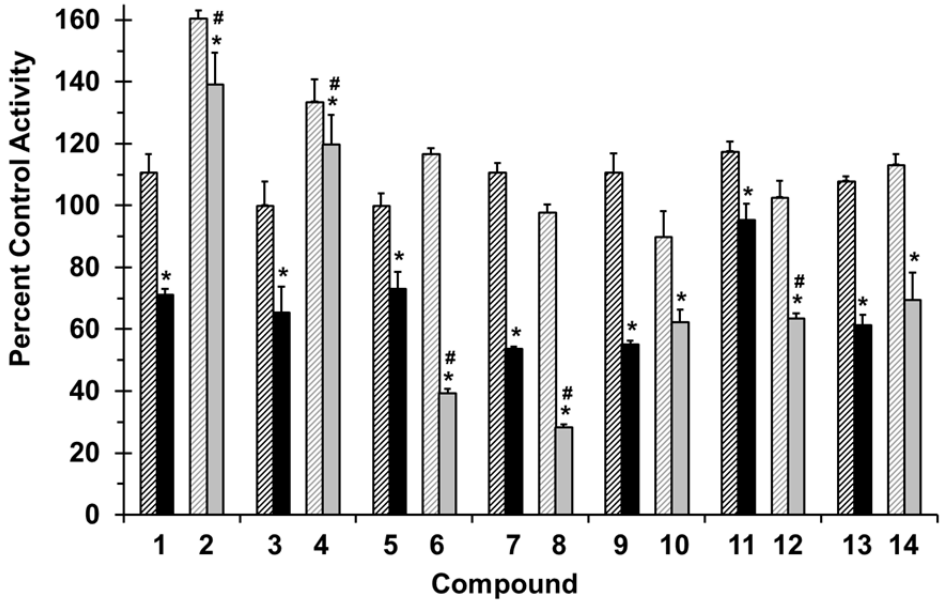

Figure 1.7. Effects of selected flavonolignans (black) and 7-*O*-methylated analogues (gray) on CYP3A-mediated midazolam 1′-hydroxylation in human intestinal microsomes (HIM). Bars and error bars denote means and SDs, respectively, of triplicate incubations. *$p < 0.05$, 10 versus 100 μM; #$p < 0.05$, flavonolignan versus 7-*O*-methylated analogue at 100 μM (two-way ANOVA with Bonferroni adjustment).

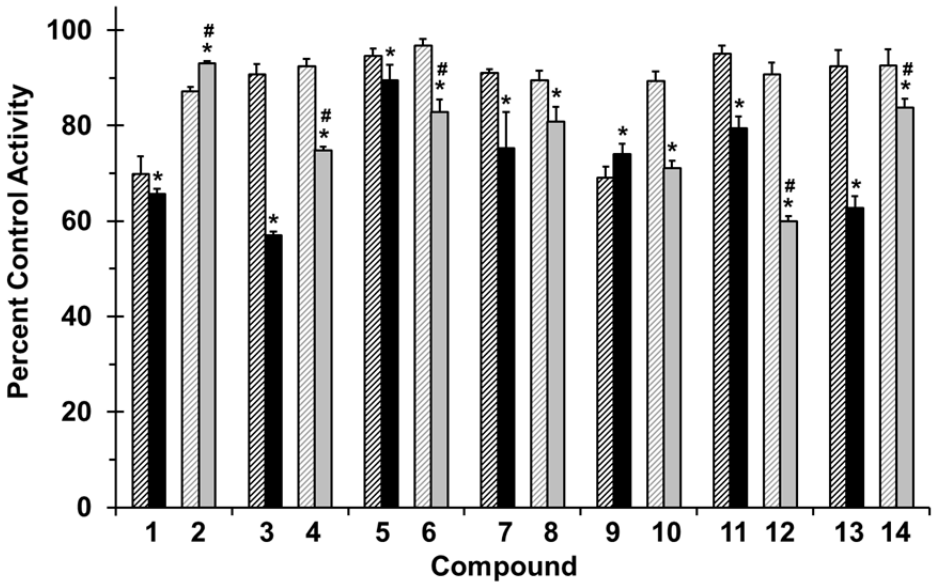

Figure 1.8. Effects of selected flavonolignans (black) and 7-*O*-methylated analogues (gray) on UGT-mediated 4-methylumbelliferone (4-MU) glucuronidation in human liver microsomes (HLM). Bars and error bars denote means and SDs, respectively, of triplicate incubations. *$p < 0.05$, 10 versus 100 μM; #$p < 0.05$, flavonolignan versus 7-*O*-methylated analogue at 100 μM (two-way ANOVA with Bonferroni adjustment).

1.4. Conclusions

In summary, a series of 7-*O*-methylflavonolignan derivatives have been synthesized selectively, and this study is the first to examine methylation of all seven of the major flavonolignans in silymarin. All the derivatives showed cytotoxic effects against human hepatoma cells. The most potent analogue was 7-*O*-methylsilybin A, which exhibited an IC_{50} value of 9.5 μM compared with natural silybin A with an IC_{50} value of 80 μM. In terms of anti-HCV activity, parent compounds with minimal to no antiviral activity (i.e., **9**, **11**, **13**) showed increased antiviral activity when converted to the 7-*O*-methyl derivatives. For these compounds, acquisition of antiviral activity by 7-*O*-methylation was associated with enhanced cytotoxicity. In contrast, parent compounds with anti-HCV activity either retained (**1**), decreased (**3**, **5**), or slightly increased (**7**) activity upon methylation.

7-*O*-Methylation differentially modified the inhibitory potency of flavonolignans towards drug metabolizing enzymes, with compounds demonstrating increased, decreased, or no change in inhibitory potency depending upon the enzyme system investigated. Although a consistent pattern was not observed regarding inhibition potency towards the various drug metabolizing enzymes, the differences observed between parent and analogue suggested the importance of the 7-position. Cumulatively, these data suggested that silymarin-derived compounds exert pleiotropic effects on cells. Ongoing efforts are focusing on how these compounds affect cellular metabolic processes that culminate in cytotoxicity, antiviral activity, and drug metabolism inhibition.

1.5. Experiments

1.5.1. General experimental procedures

1.5.1.1. Solvents and Reagents

All solvents and reagents were obtained from Sigma-Aldrich or Fisher Scientific and were used without further purification. All reactions were carried out in oven-dried glassware under N_2 atmosphere. Reactions temperature 0 °C was carried out on water-ice, rt refers to room temperature 20-25 °C and 40-80 °C was adjusted using oil bath control. DIBAL-H was transferred using oven-dried stainless steel cannulating needles through rubber septa.

1.5.1.2. Instruments

HPLC: analytical and preparative HPLC were carried out on Varian Prostar HPLC systems equipped with Prostar 210 pumps and a Prostar 335 photodiode array detector (PDA), with data collected and analyzed using Galaxie Chromatography Workstation software (version 1.9.3.2). For preparative HPLC, a YMC ODS-A (5 μm, 250 × 20 mm; Waters Corp.) column was used at a 7 mL/min flow rate and a Phenomenex PFP (pentafluorophenyl propyl; 5 μm; 250 × 21 mm) column was used at a 21.2 mL/min flow rate. For analytical HPLC, a YMC ODS-A (5 μm; 150 × 4.6 mm) column and a PFP (5 μm; 150 × 4.6 mm) column were used, both at a 1 mL/min flow rate.

UPLC: UPLC analysis was carried out on a Waters Acquity system with data collected and analyzed using Empower software (build 2154; Waters Corp., Milford, MA, USA).

Reversed-phase high-strength silica (HSS T3) trifunctional C_{18} alkyl phase bonded (1.8 μm; 2.1 x 100mm; Waters Corp.) column was used with a 0.60 ml/min flow rate at 50 °C.

Flash chromatography: Flash chromatography was performed on a Teledyne ISCO CombiFlash Rf (Teledyne-Isco, Lincoln, NE, USA) using a 40-g or 12-g Silica Gold column and monitored by UV and evaporative light-scattering detectors.

NMR spectrometry: All NMR experiments were conducted in DMSO- d_6 at 30 °C or Acetone-d_6 using a JEOL ECA-500 (JEOL Ltd., Tokyo, Japan) (operating at 500 MHz for ^{1}H and 125 MHz for ^{13}C).

HRESIMS data of compounds **2**, **4**, **6**, **8**, **10**, **12** and **14** were measured on a LTQ Orbitrap XL mass spectrometer (Thermo Scientific, Bremen, Germany) using an electrospray ionization (ESI) source coupled to a Q-TOF Premier mass spectrometer (Waters Corp., Milford, MA, USA) in negative ionization mode via a liquid chromatographic/autosampler system that consisted of an Acquity UPLC system (Waters Corp.). Compounds **1′**, **2′**, **3′** and **4′** were taken using electrospray ionization (ESI) source in negative ionization mode. HRMS of 4-(3-Hydroxyprop-1-ynyl)-2-methoxyphenol was measured using an atmospheric pressure chemical ionization source (APCI) under direct infusion flow conditions in positive mode ionization.

Optical rotation: was acquired on a Rudolph Research Autopol® III polarimeter.

UV: all data were acquired on and a Varian Cary 3 UV-Vis spectrophotometer.

Centrifuge: eppendorf centrifuge 5415 C, 14,000 rpm.

1.5.2. Chemistry and Synthesis

The individual flavonolignans were isolated from milk thistle extract (silymarin) in >98% purity as described in detail previously.[108]

1.5.2.1. 7-*O*-Methylsilybin A (2)

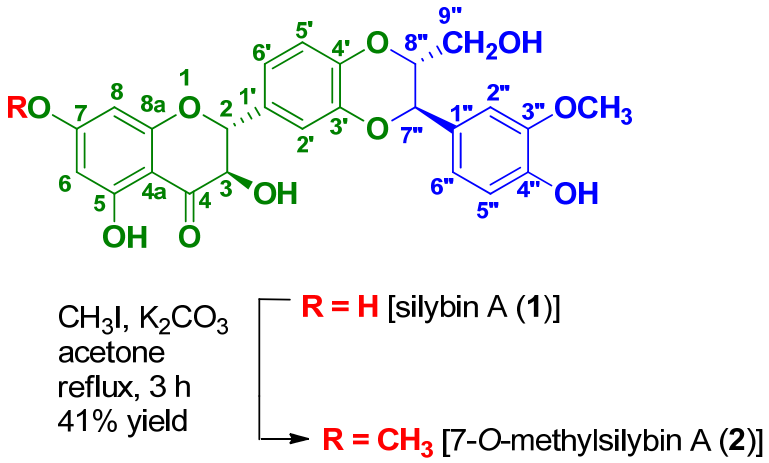

Scheme 1.1. Synthesis of 7-O-Methylsilybin A (2).

To a 150 mL three-neck round-bottom flask, silybin A (122 mg, 0.253 mmol) and K_2CO_3 (293 mg, 2.03 mmol) were dissolved in acetone (80 mL, 0.003 M). After stirring for 10 min, CH_3I (244 µL, 3.95 mmol) was added dropwise. The reaction mixture was heated at reflux under N_2 for 3 h and monitored by HPLC. After cooling to rt, the reaction was quenched by the addition of 2% aqueous HCl (pH 1.5) and diluted with H_2O (125 mL). The mixture was extracted with EtOAc (2 × 80 mL). The organic phases were combined and dried over Na_2SO_4, filtered, and then the solvent was removed under reduced pressure. The compounds were purified as described in Fig. 1.9. Yield: 51 mg, 41%; white solid;

$[\alpha]_D^{20}$ **:** + 20 (*c* 0.1, MeOH);

UV (MeOH) λ_{max} (log ε): 218 (4.2), 287 (4.1) nm;

CD (MeOH) λ_{ext} ($\Delta\varepsilon$): 237 (-3.3), 296 (-9.2), 330 (1.7) nm; see Fig. 1.58

^{1}H NMR (500 MHz, DMSO-d_6): δ = 3.34 (m, 1H, H-9"b), 3.53 (ddd, *J* = 10.3, 5.2, 2.3 Hz, 1H, H-9"a), 3.77 (s, 3H, 3"-OCH_3), 3.78 (s, 3H, 7-OCH_3), 4.18 (ddd, *J* = 7.5, 4.6, 2.3 Hz, 1H, H-8"), 4.69 (dd, *J* = 11.5, 6.3 Hz, 1H, 3-H), 4.91 (d, *J* = 7.5 Hz, 1H, H-7"), 4.98 (dd, *J* = 5.7, 5.2 Hz, OH-9"), 5.14 (d, *J* = 11.5 Hz, 1H, 2-H), 5.90 (d, *J* = 6.3 Hz, 3-OH), 6.10 (d, *J* = 1.7 Hz, 1H, H-8), 6.12 (d, *J* = 1.7 Hz, 1H, H-6), 6.80 (d, *J* = 8.6 Hz, 1H, H-5"), 6.86 (dd, *J* = 8.6, 1.8 Hz, 1H, H-6"), 6.98 (d, *J* = 8.6 Hz, 1H, H-5'), 7.01 (dd, *J* = 8.6, 1.7 Hz, 1H, H-6'), 7.03 (d, *J* = 1.8 Hz, 1H, H-2"), 7.10 (d, *J* = 1.7 Hz, 1H, H-2'), 9.19 (s, 4"-OH), 11.86 (s, 5-OH) (see, Tables 1.1 and Fig. 1.10).

^{13}C NMR (125 MHz, DMSO-d_6): δ 55.7 (3″-OCH_3), 60.2 (C-9″), 71.5 (C-3), 75.9 (C-7″), 78.1 (C-8″), 82.7 (C-2), 93.9 (C-8), 95.0 (C-6), 101.4 (C-4a), 111.6 (C-2″), 115.3 (C-5″), 116.4 (C-5′), 116.7 (C-2′), 120.6 (C-6″), 121.5 (C-6′), 127.5 (C-1″), 129.9 (C-1′), 143.3 (C-3′), 143.7 (C-4′), 147.0 (C-4″), 147.6 (C-3″), 162.4 (C-8a), 163.0 (C-5), 167.6 (C-7), 198.5 (C-4), see Tables 1.3 and Fig. 1.11;

HSQC data: H-2→C-2; H-3→C-3; H-6→C-6; H-8→C-8; H-2'→C-2'; H-5'→C-5'; H-6'→C-6'; H-2"→C-2"; H-5"→C-5"; H-6"→C-6"; H-7"→C-7"; H-8"→C-8"; H-9"a→C-9"; H-9"b→C-9"; OCH_3-7→C-7; OCH_3-3"→C-3" (see Fig.1.12).

HMBC data: HMBC data, H-3→C-2; OH-3→C-2, 3, 4; OH-5→C-5, 6, 4a; H-6→C-7,

8; OCH_3-7→C-7; H-8→C-8a, 4a; H-2'→C2, 1', 4'; H-6'→C-4'; H-5'→C-4'; H-8"→C-7"; H-7"→C-8"; H-9"→C-7"; H-2"→C-3", 6"; OCH_3-C3"→C3"; OH-4"→C-4", 5"; H-5"→C-1", 3"; H-6"→C-1" see Figs. 1.13 and 1.14;

HRESIMS m/z: 495.1281 $[M-H]^-$ (calcd for $C_{26}H_{23}O_{10}$ 495.1297; see Fig. 1.15).

Analytical method: 30:70 to 50:50 CH_3CN:H_2O (0.1% formic acid) over 30 min at a 1 mL/min flow rate (PFP column)

a

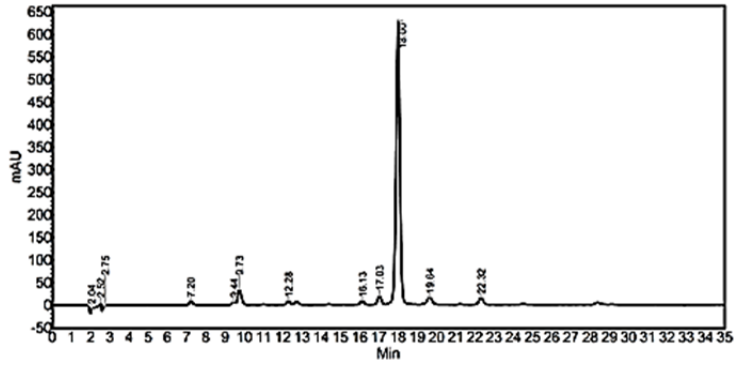

b

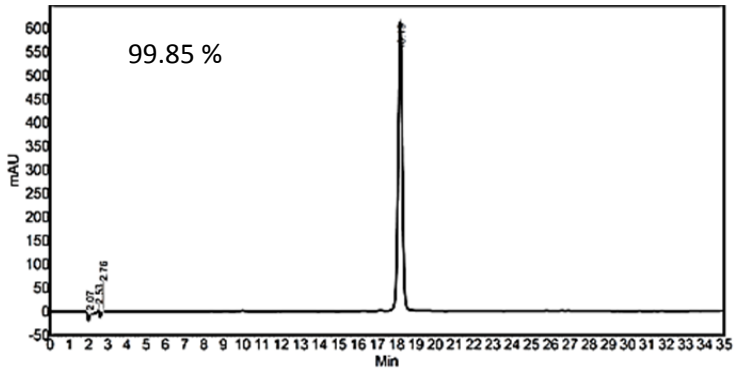

Separation method: PFP (5 µm; 250 × 21 mm) column was used at 30:70 to 50:50 CH_3CN:H_2O (0.1% formic acid) over 30 min at a 21.2 mL/min flow rate

c

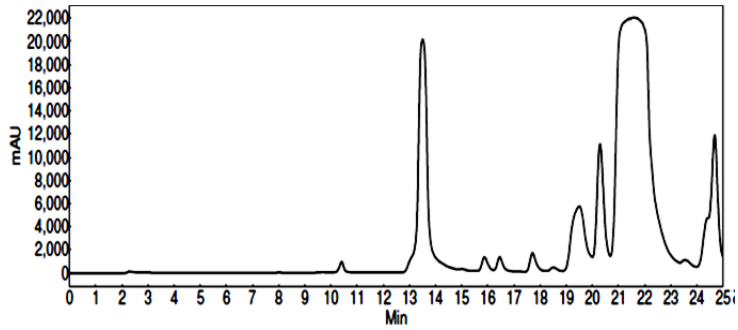

Figure 1.9. HPLC chromatograms of crude reaction mixtures (a), purified 7-*O*-methylsilybin A (b) at 288 nm and preparative HPLC (c)

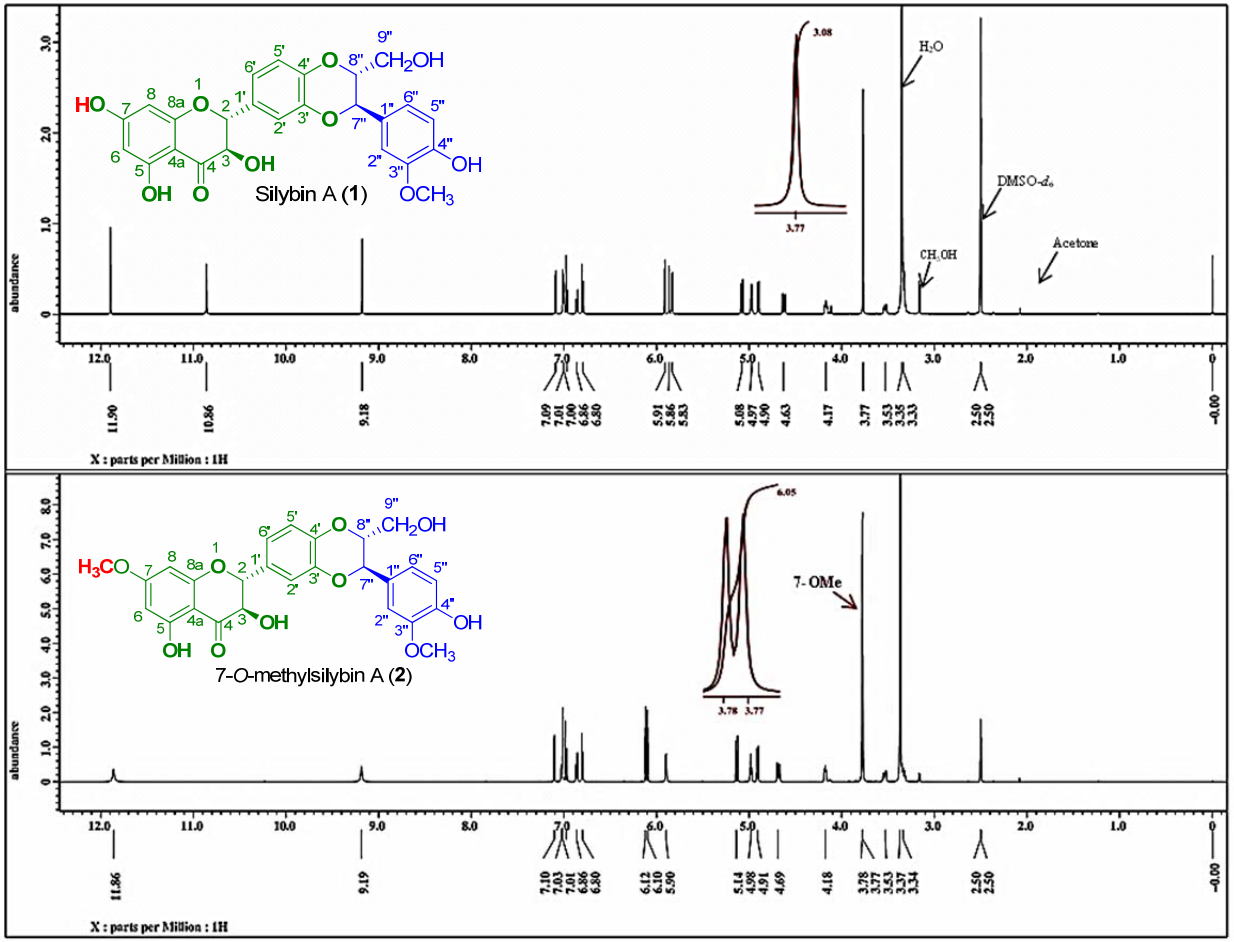

Figure 1.10. ^{1}H NMR spectra (500 MHz, 30 °C) of silybin A (**1**) and 7-*O*-methylsilybin A (**2**) in DMSO-d_6

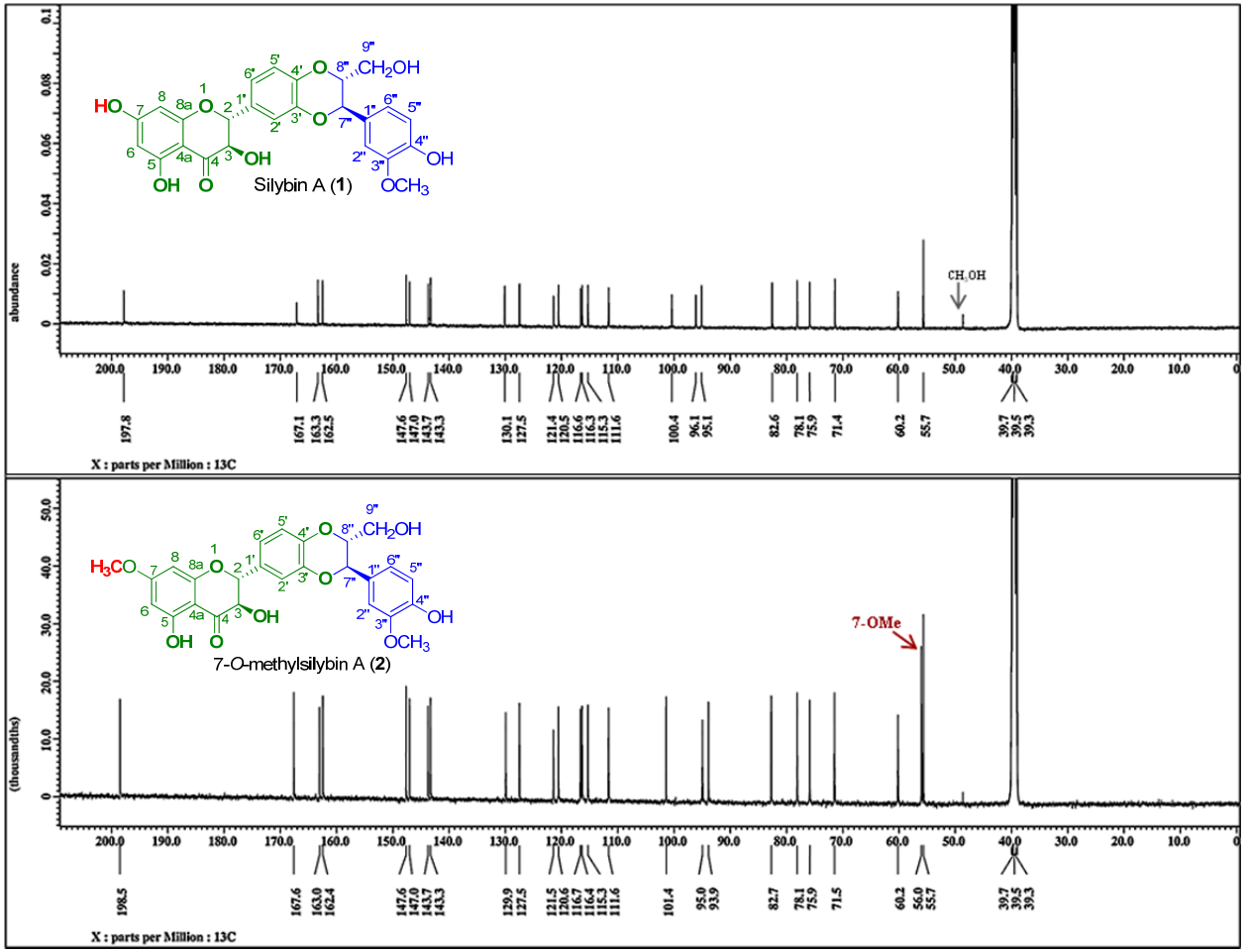

Figure 1.11. ^{13}C NMR spectra (125 MHz, 30 °C) of silybin A (**1**) and 7-*O*-methylsilybin A (**2**) in DMSO-d_6

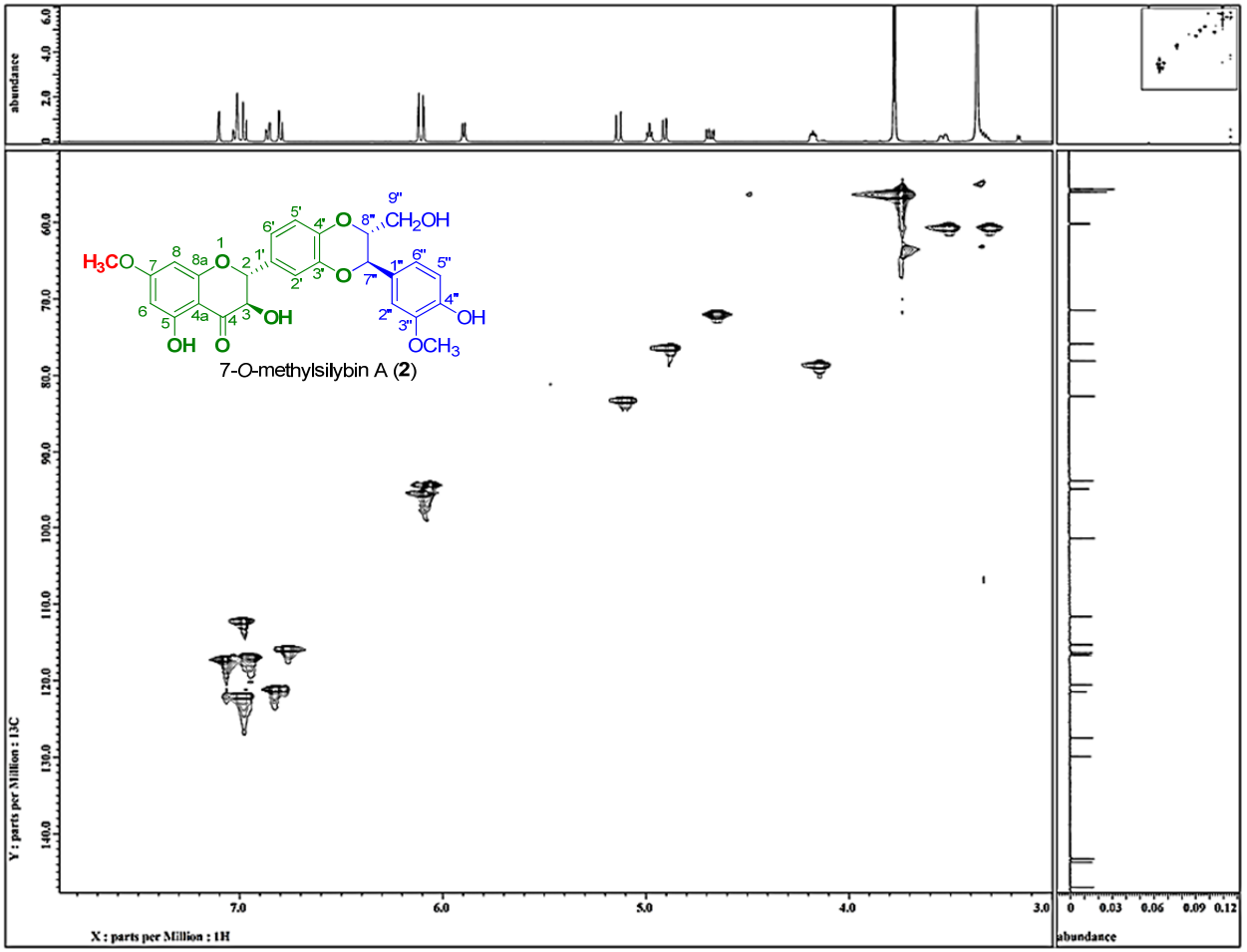

Figure 1.12. HSQC NMR spectrum (DMSO-d_6, 30 °C) of 7-*O*-methylsilybin A (**2**) showing the key correlation

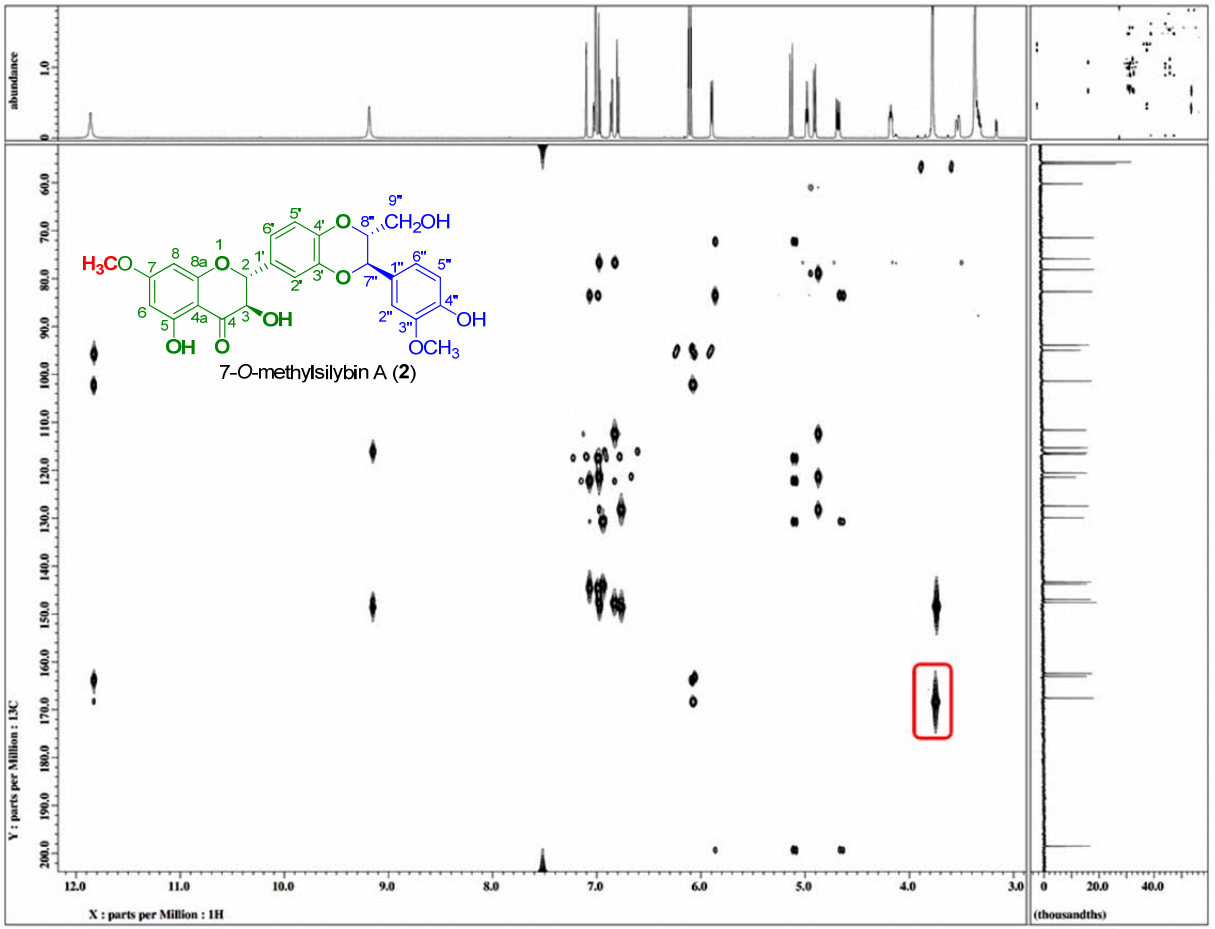

Figure 1.13. HMBC NMR spectrum (DMSO-d_6, 30 °C) of 7-*O*-methylsilybin A (**2**) showing the key correlation between the methoxy protons and C-7

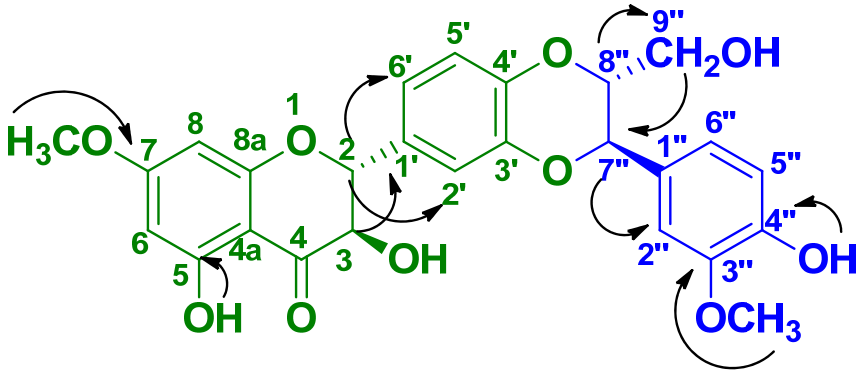

Figure 1.14. Key HMBC correlations of 7-*O*-methylsilybin A (**2**)

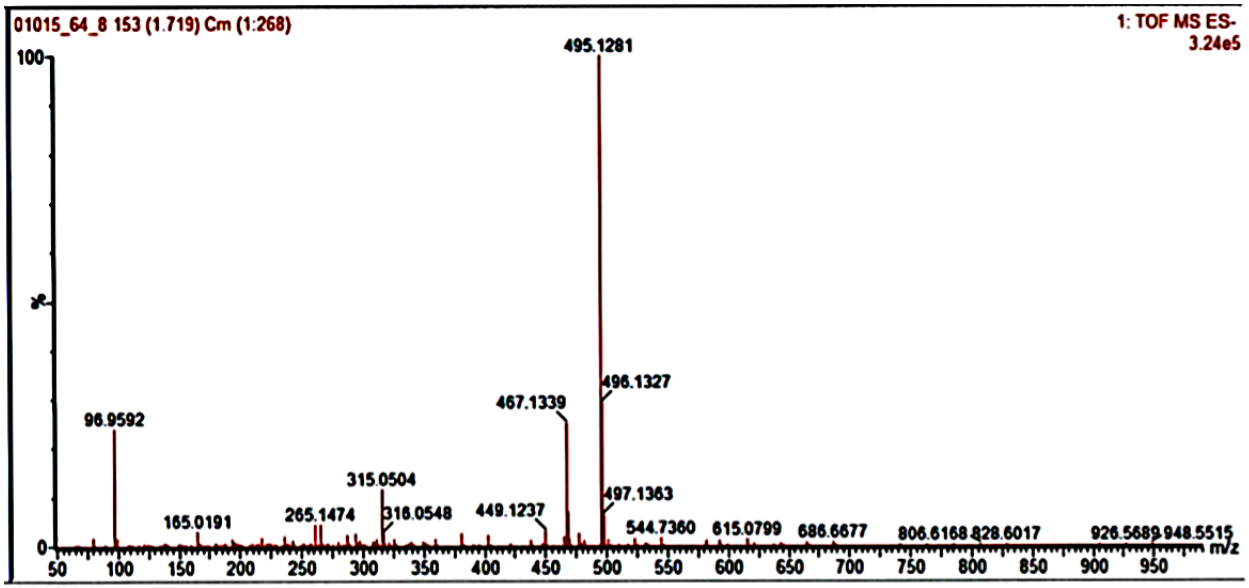

Figure 1.15. HRESIMS m/z 495.1281 $[M-H]^-$ of 7-*O*-methylsilybin A (**2**)

1.5.2.2. 7-*O*-Methylsilybin B (4)

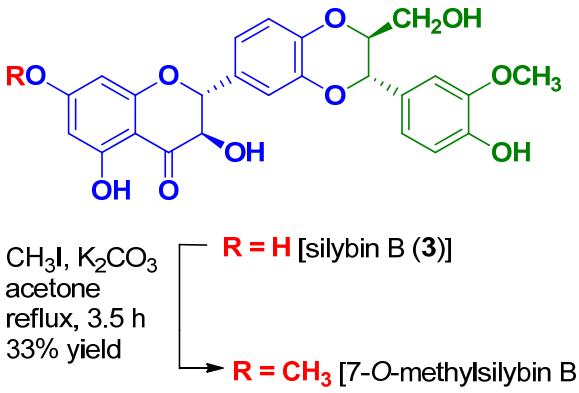

Scheme 1.2. Synthesis of 7-*O*-Methylsilybin A (**2**).

In a manner that was otherwise consistent with the preparation and purification of 2, compound 3 was reacted with 15 equivalents of CH_3I at reflux for 3.5 h to yield compound 4. The compounds were purified as described in Fig. 1.16. Yield: 10 mg, 33%; white solid;

$[\alpha]_D^{20}$**:** + 7.7 (*c* 0.2, MeOH);

UV (MeOH) λ_{max} **(log** ε**):** 230 (4.0) , 287 (4.0) nm;

CD (MeOH) λ_{ext} **(**$\Delta\varepsilon$**):** 230 (8.6), 296 (-9.2), 334 (1.3) nm; see Fig. 1.58.

^{1}H NMR (500 MHz, DMSO-d_6 at 30 °C): δ = 3.34 (m, 1H, H-9"b), 3.54 (ddd, *J* = 12.0, 5.2, 2.3 Hz, 1H, H-9"a), 3.77 (s, 3H, 3"-OCH_3), 3.78 (s, 3H, 7-OCH_3), 4.17 (ddd, *J* = 7.5, 4.6, 2.3 Hz, 1H, H-8"), 4.67 (dd, *J* = 11.5, 6.3 Hz, 1H, 3-H), 4.91 (d, *J* = 7.5 Hz, 1H, H-7"), 4.98 (dd, *J* = 5.7, 5.2 Hz, OH-9"), 5.14 (d, *J* = 11.5 Hz, 1H, 2-H), 5.89 (d, *J* = 6.3 Hz, 3-OH), 6.10 (d, *J* = 2.3 Hz, 1H, H-8), 6.12 (d, *J* = 2.3 Hz, 1H, H-6), 6.80 (d, *J* =

8.0 Hz, 1H, H-5"), 6.86 (dd, *J* = 8.0, 1.7 Hz, 1H, H-6"), 6.98 (d, *J* = 8.0 Hz, 1H, H-5'), 7.02 (dd, *J* = 8.0, 2.3 Hz, 1H, H-6'), 7.04 (d, *J* = 1.7 Hz, 1H, H-2"), 7.10 (d, *J* = 2.3 Hz, 1H, H-2'), 9.18 (s, 4"-OH), 11.87 (s, 5-OH) (see, Tables 1.1 and Fig. 1.17).

^{13}C NMR (125 MHz, DMSO-*d*$_6$): δ 55.7 (3″-OCH_3), 60.2 (C-9″), 71.5 (C-3), 75.9 (C-7″), 78.1 (C-8″), 82.7 (C-2), 93.9 (C-8), 94.9 (C-6), 101.4 (C-4a), 111.6 (C-2″), 115.3 (C-5″), 116.4 (C-5′), 116.7 (C-2′), 120.5 (C-6″), 121.2 (C-6′), 127.5 (C-1″), 130.0 (C-1′), 143.2 (C-3′), 143.7 (C-4′), 147.0 (C-4″), 147.6 (C-3″), 162.4 (C-8a), 163.0 (C-5), 167.6 (C-7), 198.5 (C-4). ^{1}H and ^{13}C NMR data, see Tables 1.3 and Fig. 1.18;

HSQC data: H-2→C-2; H-3→C-3; H-6→C-6; H-8→C-8; H-2'→C-2'; H-5'→C-5'; H-6'→C-6'; H-2"→C-2"; H-5"→C-5"; H-6"→C-6"; H-7"→C-7"; H-8"→C-8"; H-9"a→C-9"; H-9"b→C-9"; OCH_3-7→C-7; OCH_3-3"→C-3" (see, Fig. 1.19).

HMBC data: HMBC data, H-2→C-3, 4, 1', 2', 6'; H-3→C-2, 4, 1'; OH-3→C-2, 3 , 4; OH-5→C-5, 8, 4a; H-6→C-5, 7, 4a; H-8→C-5, 6; H-2'→C-2, 3', 6'; H-5'→C-1', 3'; H-6'→C-2, 2', 3', 4'; H-8"→C-7", 2", 6"; H-2"→C-8" , 3", 6"; H-5"→C-1", 3"; H-6"→C-2", 8", 4" see Figs. 1.20 and 1.21;

HRESIMS *m/z*: 495.1290 $[M-H]^-$ (calcd for $C_{26}H_{23}O_{10}$ 495.1297; see Fig. 1.22).

Analytical method: 30:70 to 50:50 $CH_3CN:H_2O$ (0.1% formic acid) over 30 min at a 1 mL/min flow rate (PFP column).

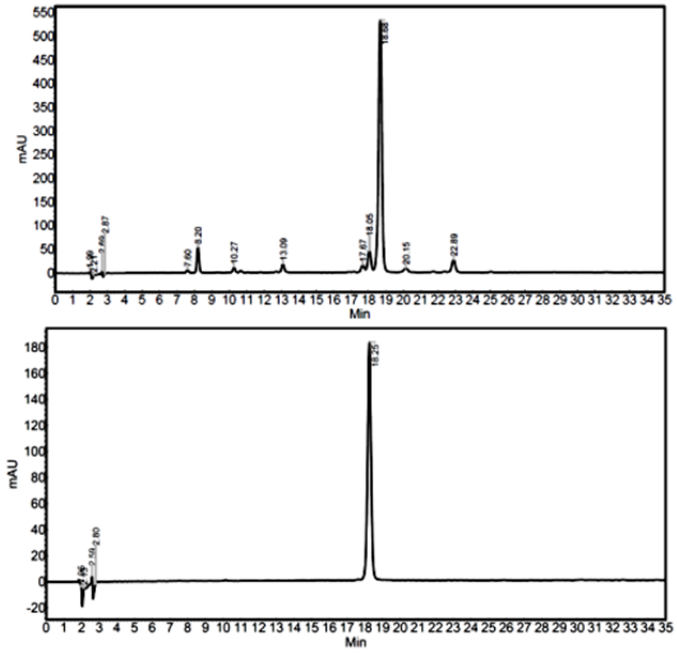

Separation method: PFP (5 µm; 250 × 21 mm) column was used at 20:80 to 40:60 $CH_3CN:H_2O$ (0.1 % formic acid) over 30 min at a 21.2 mL/min flow rate.

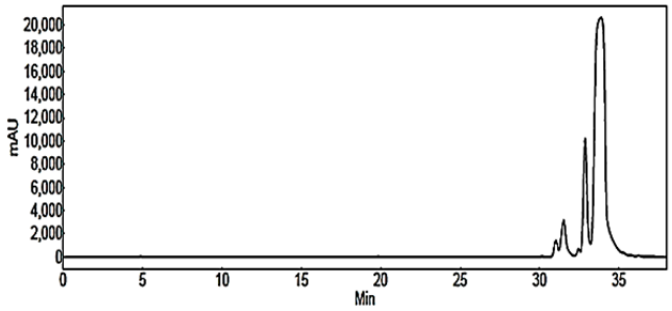

Figure 1.16. HPLC chromatograms of crude reaction mixtures (a), purified 7-*O*-methylsilybin B (b) at 288 nm and preparative HPLC (c).

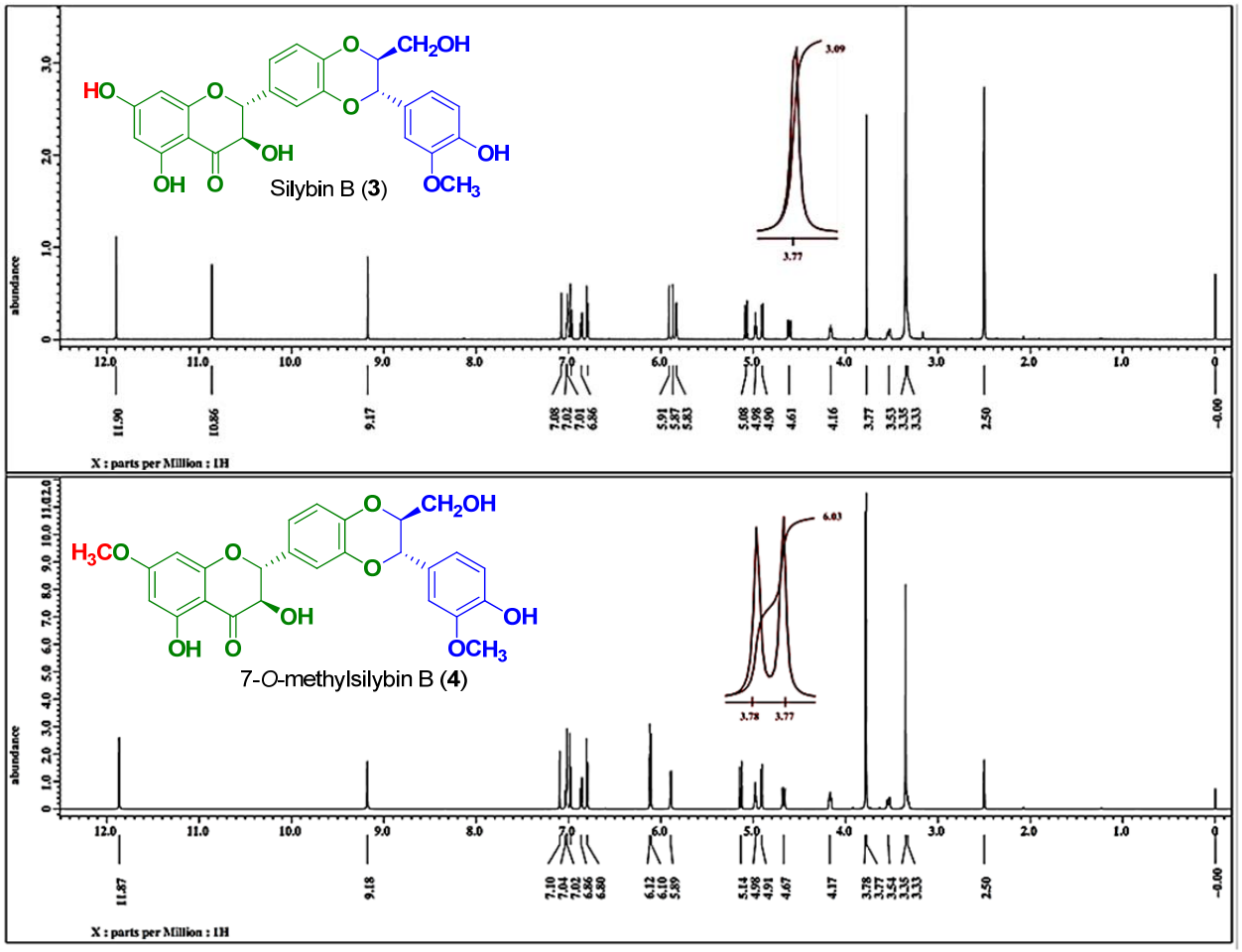

Figure 1.17. ^{1}H NMR spectra (500 MHz, 30 °C) of silybin B (**3**) and 7-*O*-methylsilybin B (**4**) in DMSO-d_6

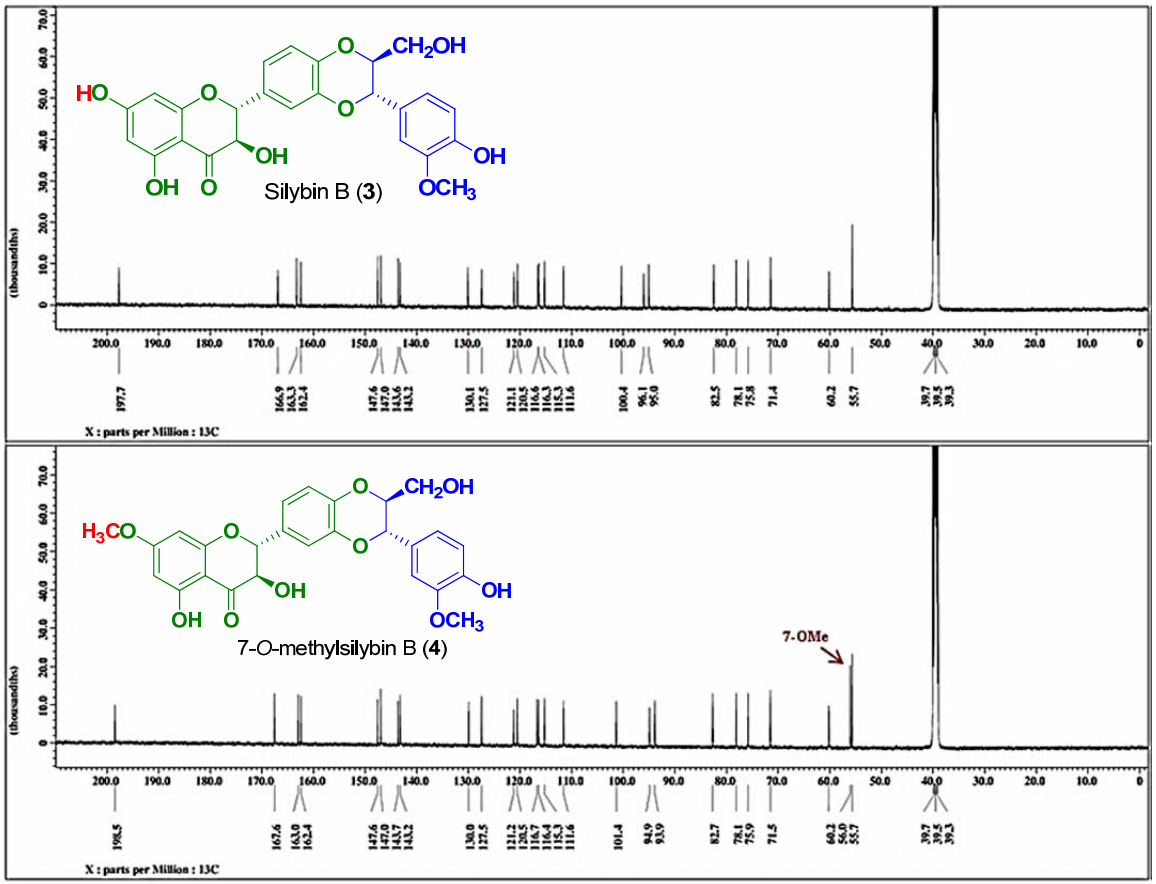

Figure 1.18. ^{13}C NMR spectra (125 MHz, 30 °C) of silybin B (**3**) and 7-*O*-methylsilybin B (**4**) in DMSO-d_6

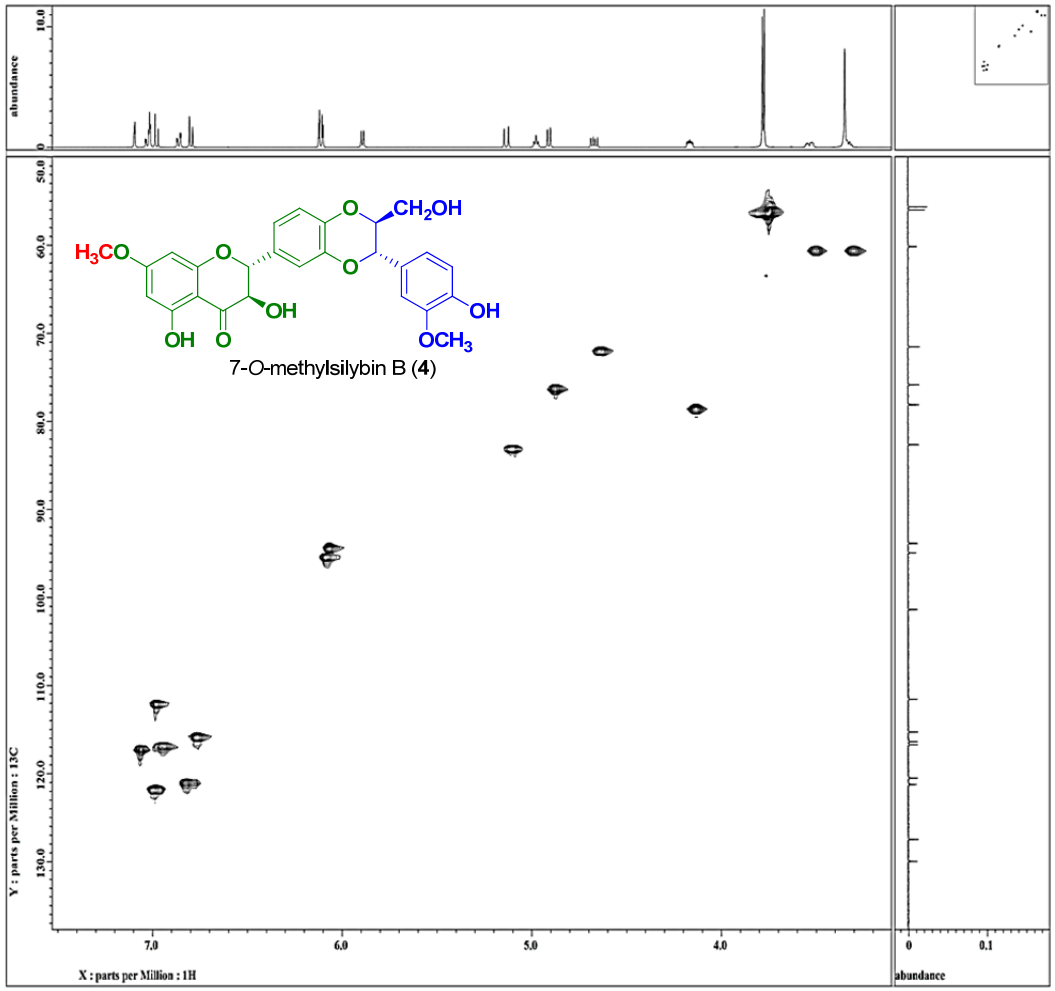

Figure 1.19. HSQC NMR spectrum (DMSO-d_6, 30 °C) of 7-*O*-methylsilybin B (**4**) showing the key correlation

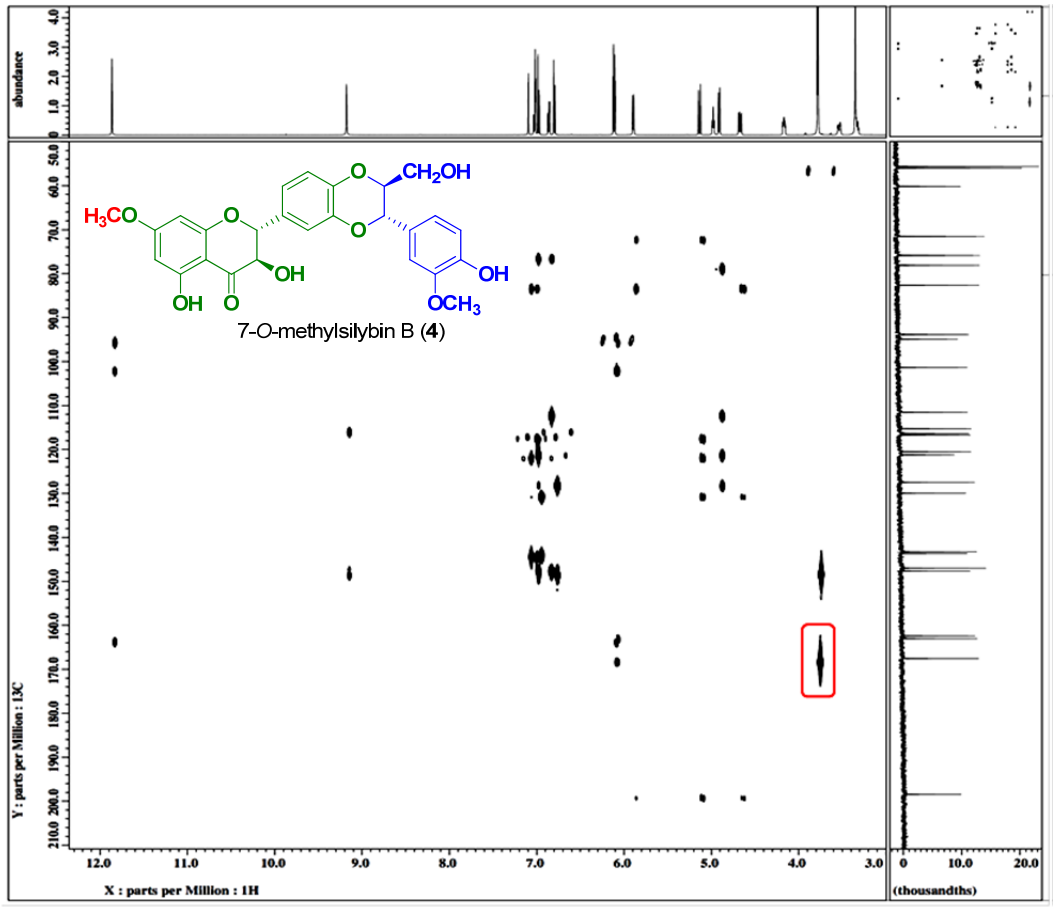

Figure 1.20. HMBC NMR spectrum (DMSO-d_6, 30 °C) of 7-*O*-methylsilybin B (**4**) showing the key correlation between the methoxy protons and C-7

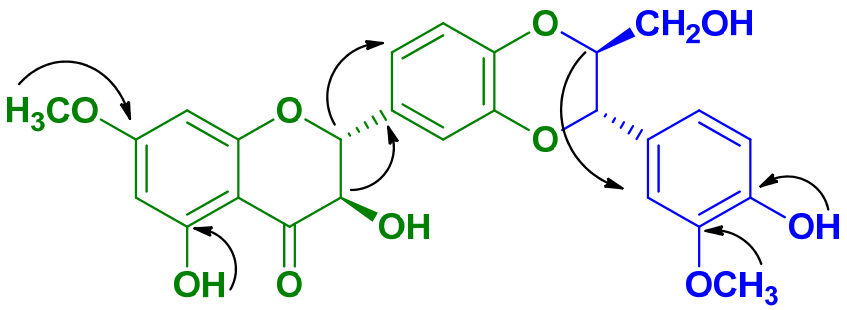

Figure 1.21. Key HMBC correlations of 7-*O*-methylsilybin B (**4**).

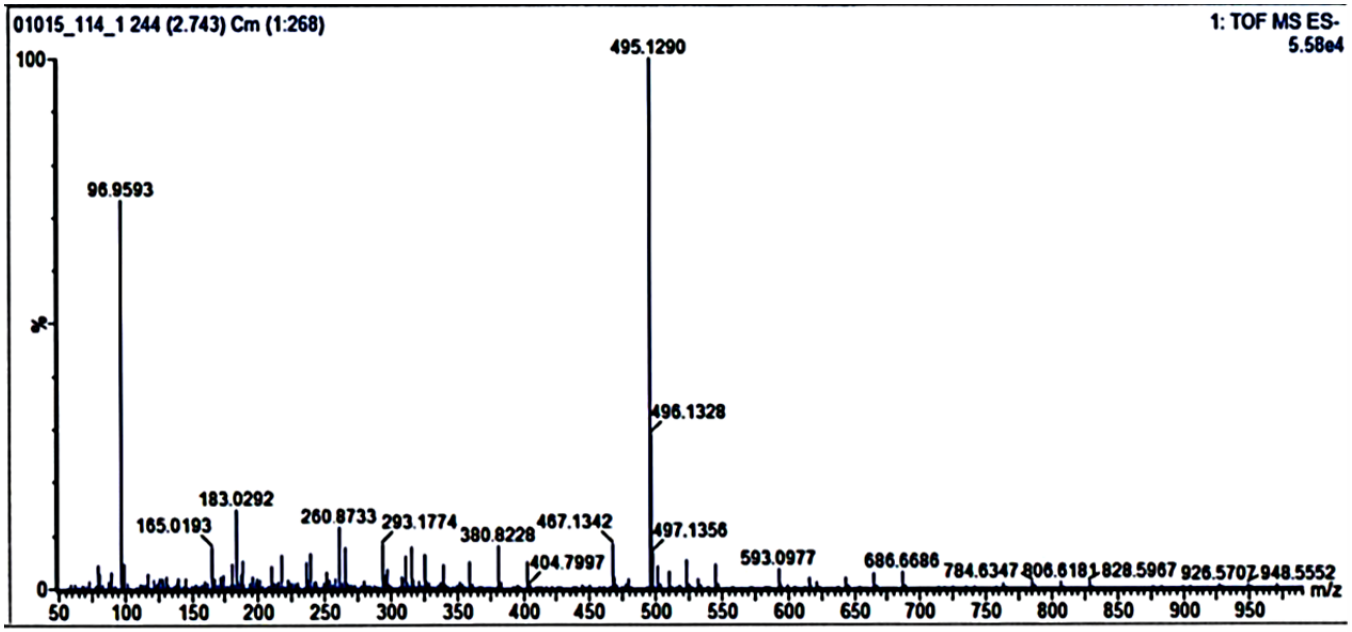

Figure 1.22. HRESIMS m/z 495.1290 $[M-H]^-$ of 7-*O*-methylsilybin B (**4**)

1.5.2.3. 7-*O*-Methylisosilybin A (6)

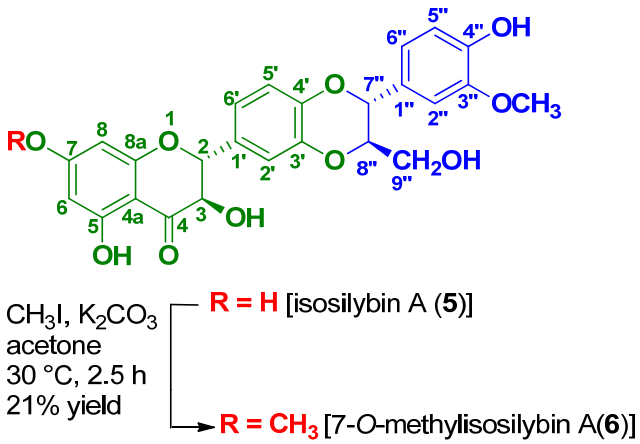

Scheme 1.3. Synthesis of 7-*O*-Methylisosilybin A (**6**).

In a manner that was otherwise consistent with the preparation and purification of 2, compound 5 was reacted with 2 equivalents of CH_3I at 30 °C for 2.5 h to yield compound 6. The compounds were purified as described in Fig. 1.23.

Yield: 22 mg, 21%; white solid;

$[\alpha]_D^{20}$: + 46 (*c* 0.1, MeOH);

UV (MeOH) λ_{max} (log ε): 214 (4.1), 287 (4.0) nm;

CD (MeOH) λ_{ext} ($\Delta\varepsilon$): 236 (-0.9), 296 (-5.7), 331 (0.7) nm; see Fig. 1.58

^{1}H NMR (500 MHz, DMSO-d_6): δ = 3.33 (m, 1H, H-9"b), 3.53 (ddd, *J* = 12.0, 5.2, 2.3 Hz, 1H, H-9"a), 3.77 (s, 3H, 3"-OCH_3), 3.79 (s, 3H, 7-OCH_3), 4.17 (ddd, *J* = 7.5, 4.0, 2.3 Hz, 1H, H-8"), 4.66 (dd, *J* = 10.9, 6.3 Hz, 1H, 3-H), 4.91 (d, *J* = 7.5 Hz, 1H, H-7"), 4.97 (dd, *J* = 5.7, 4.6 Hz, OH-9"), 5.16 (d, *J* = 11.5 Hz, 1H, 2-H), 5.91 (d, *J* = 6.3 Hz, 3-

OH), 6.12 (d, *J* = 2.3 Hz, 1H, H-8), 6.13 (d, *J* = 2.3 Hz, 1H, H-6), 6.80 (d, *J* = 8.0 Hz, 1H, H-5"), 6.85 (dd, *J* = 8.0, 1.7 Hz, 1H, H-6"), 6.94 (d, *J* = 8.6 Hz, 1H, H-5'), 6.99 (dd, *J* = 8.6, 2.3 Hz, 1H, H-6'), 7.00 (d, *J* = 1.7 Hz, 1H, H-2"), 7.11 (d, *J* = 2.3 Hz, 1H, H-2'), 9.18 (s, 4"-OH), 11.87 (s, 5-OH) ; (see, Tables 1.1 and Fig. 1.24).

^{13}C NMR (125 MHz, DMSO-d_6): δ 55.7 (3″-OCH_3), 60.2 (C-9″), 71.6 (C-3), 75.9 (C-7″), 78.0 (C-8″), 82.7 (C-2), 93.9 (C-8), 95.0 (C-6), 101.4 (C-4a), 111.7 (C-2″), 115.3 (C-5″), 116.5 (C-5′), 116.6 (C-2′), 120.5 (C-6″), 121.0 (C-6′), 127.5 (C-1″), 130.2 (C-1′), 142.9 (C-3′), 143.9 (C-4′), 147.0 (C-4″), 147.6 (C-3″), 162.4 (C-8a), 163.0 (C-5), 167.6 (C-7), 198.5 (C-4). ^{1}H and ^{13}C NMR data, see Tables 1.3 and Fig.1.25;

HSQC data : H-2→C-2; H-3→C-3; H-6→C-6; H-8→C-8; H-2'→C-2'; H-5'→C-5'; H-6'→C-6'; H-2"→C-2"; H-5"→C-5"; H-6"→C-6"; H-7"→C-7"; H-8"→C-8"; H-9"a→C-9"; H-9"b→C-9"; OCH_3-7→C-7; OCH_3-3"→C-3" (see Fig. 1.26).

HMBC data: HMBC data, H-2→C-4; H-3→C-2, 4; OH-3→C-2, 3 , OH-5→C-6, 4a; H-6→C-5 , OCH_3-7→C-7; H-8a →C-7, 4a; H-2'→C2; H-6'→C-2, H-7"→C- 8", 6", OCH_3-C3"→C3"; H-5"→C-1"; OH-4"→C-4", 5", 3". see Fig. 1.27 and 1.28;

HRESIMS *m/z*: 495.1292 $[M-H]^-$ (calcd for $C_{26}H_{23}O_{10}$ 495.1297; see Fig 1.29).

Analytical method: 30:70 to 50:50 $CH_3CN:H_2O$ (0.1% formic acid) over 30 min at a 1 mL/min flow rate (PFP column).

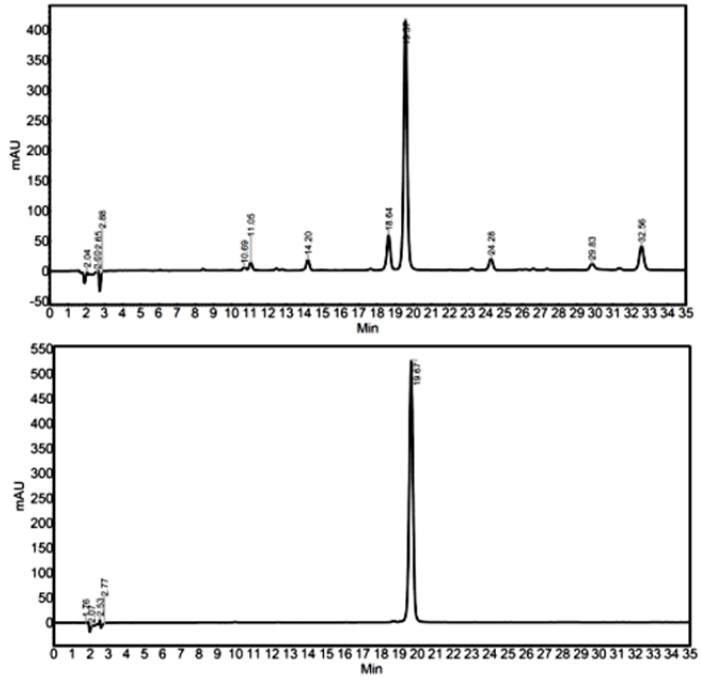

Separation method: PFP (5 µm; 250 × 21 mm) column was used at 30:70 to 50:50 $CH_3CN:H_2O$ (0.1% formic acid) over 30 min at a 21.2 mL/min flow rate.

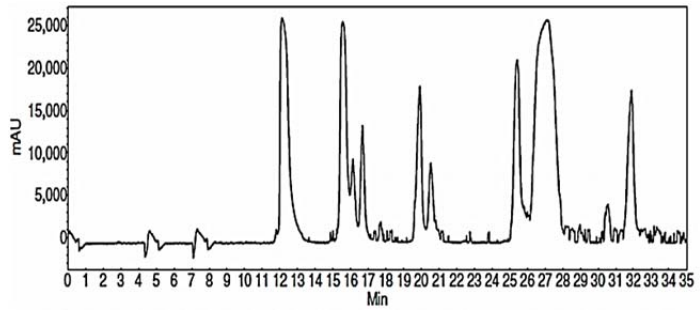

Figure 1.23. HPLC chromatograms of crude reaction mixtures (a), purified 7-*O*-methylisosilybin A (b) at 288 nm and preparative HPLC (c).

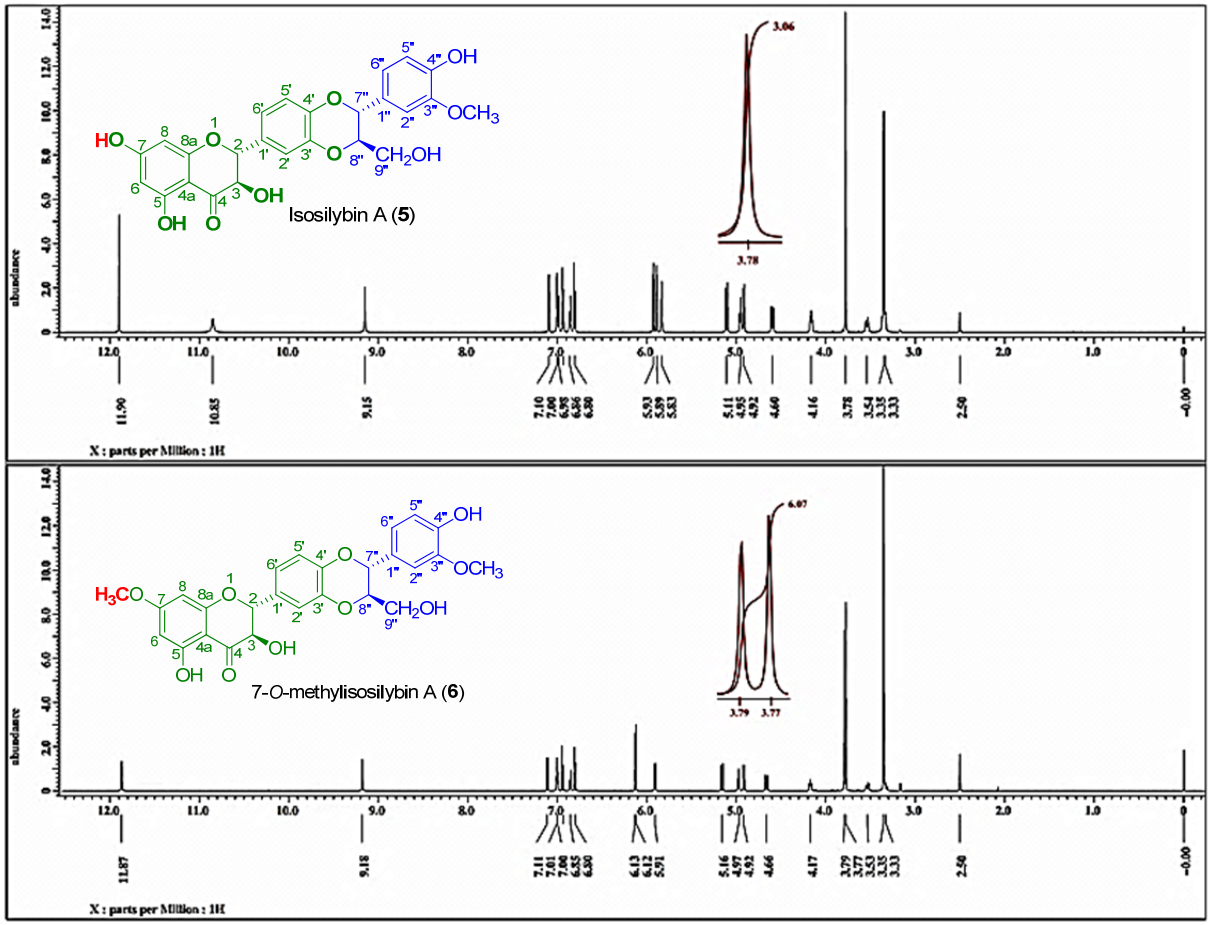

Figure 1.24. ^{1}H NMR spectra (500 MHz, 30 °C) of isosilybin A (**5**) and 7-*O*-methylisosilybin A (**6**) in DMSO-d_6

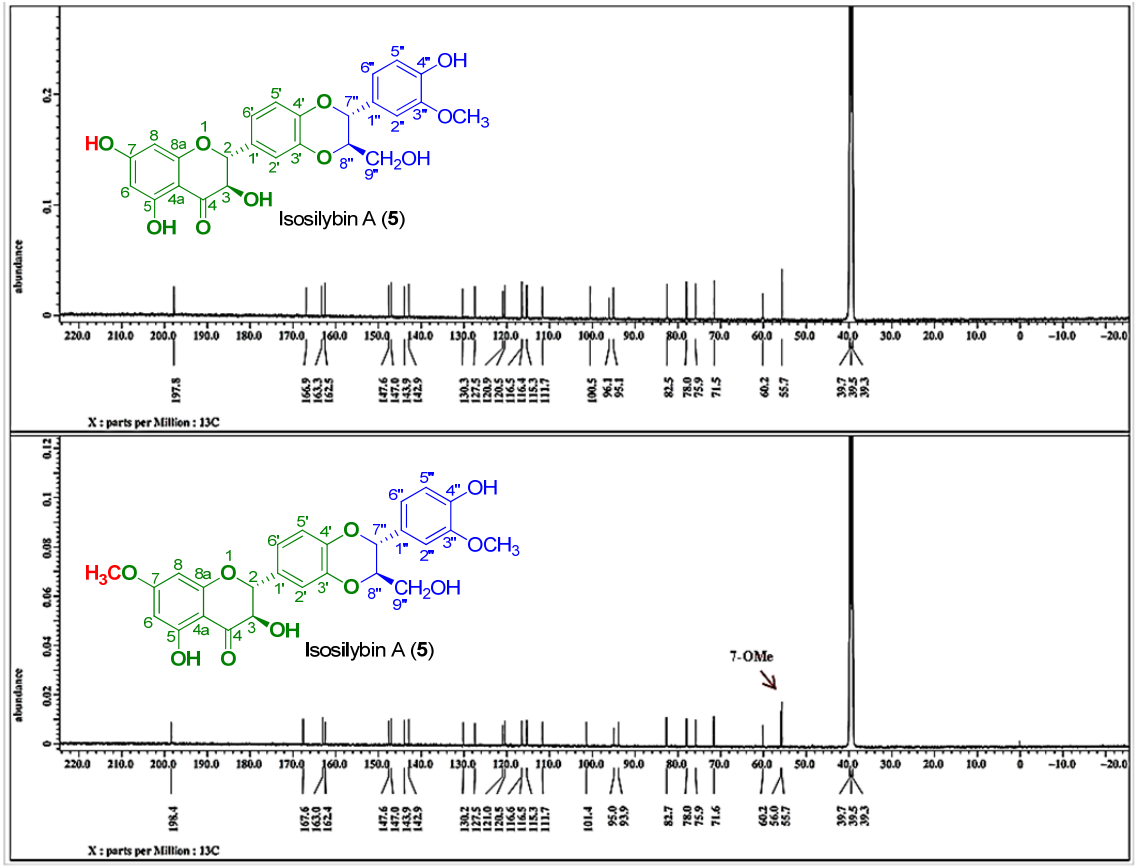

Figure 1.25. ^{13}C NMR spectra (125 MHz, 30°C) of isosilybin A (**5**) and 7-*O*-methylisosilybin A (**6**) in DMSO-d_6

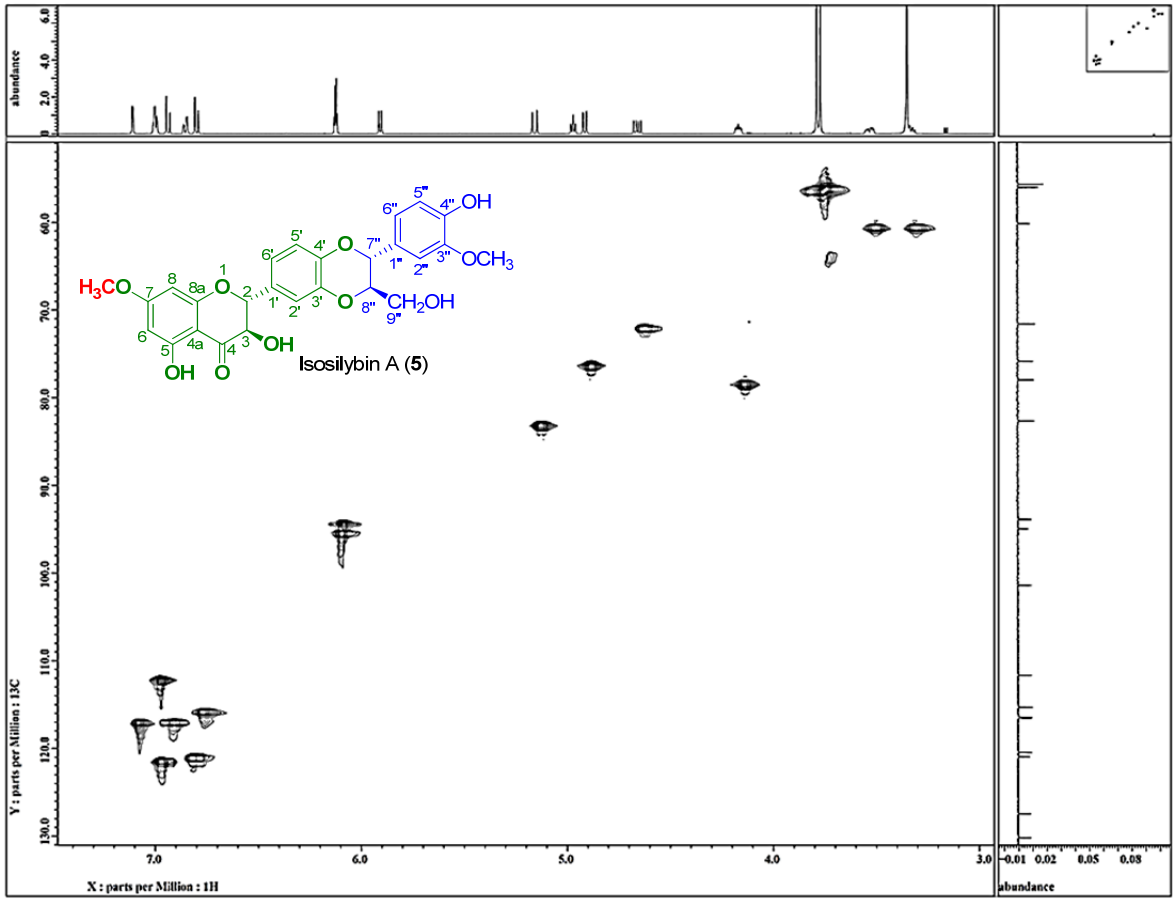

Figure 1.26. HMBC NMR spectrum (DMSO-d_6, 30 °C) of 7-*O*-methylisosilybin A (**6**) showing the key

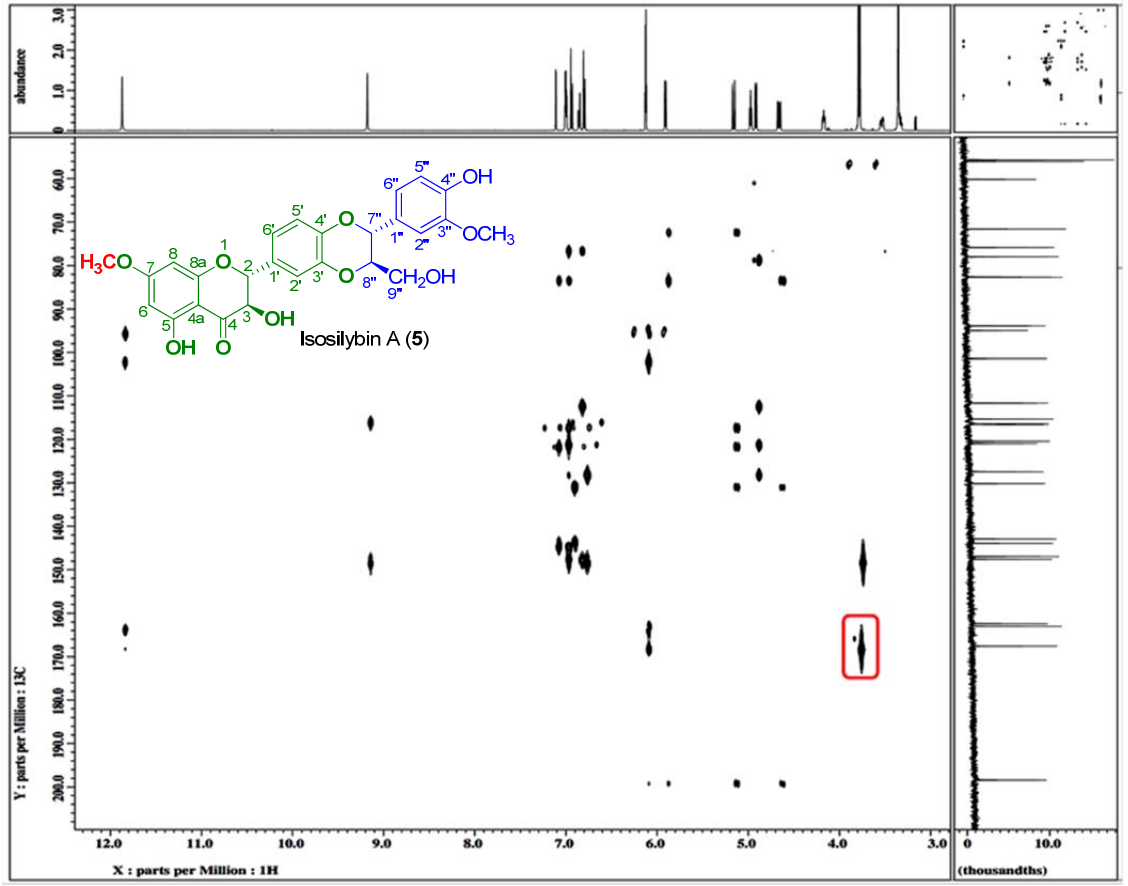

Figure 1.27. HMBC NMR spectrum (DMSO-d_6, 30 °C) of 7-*O*-methylisosilybin A (**6**) showing the key correlation between the methoxy protons and C-7

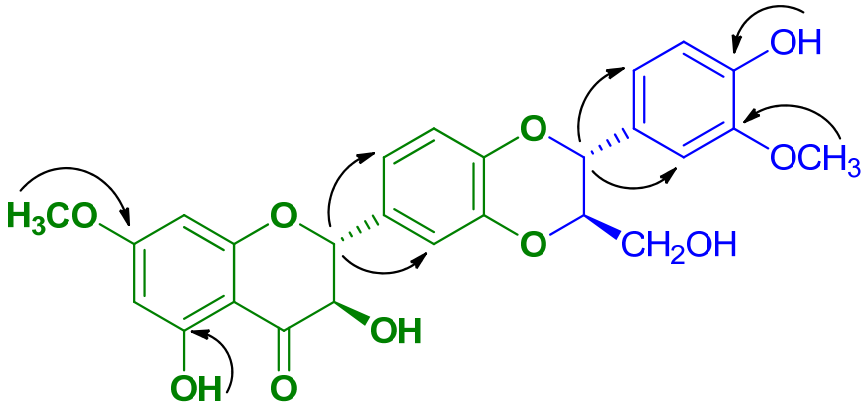

Figure 1.28. Key HMBC correlations of 7-*O*-methylisosilybin A (**6**)

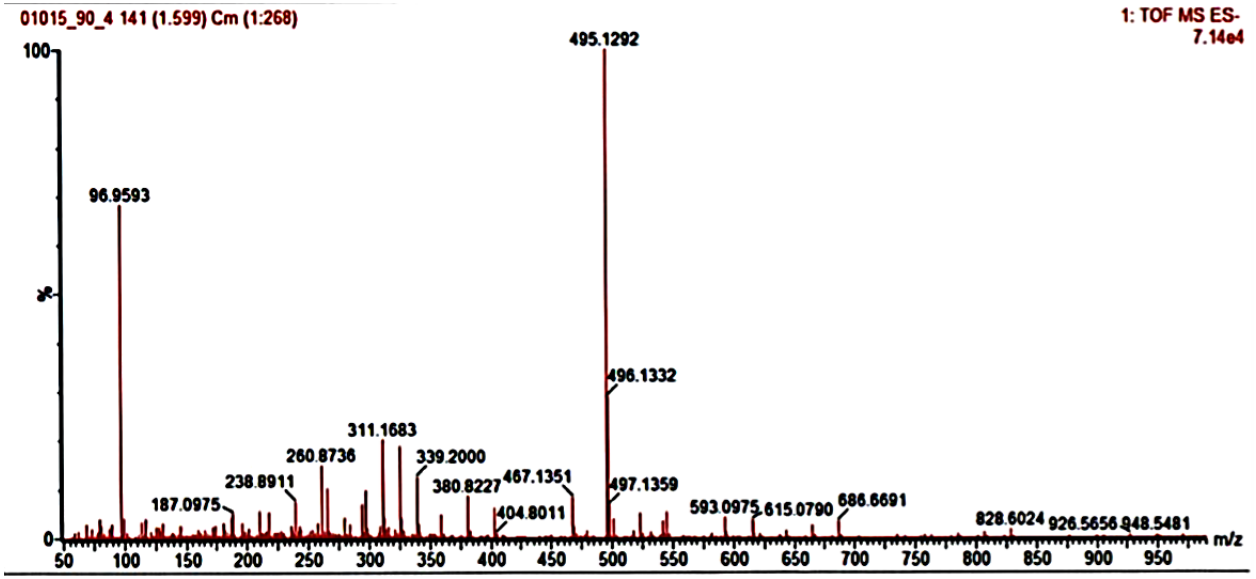

Figure 1.29. HRESIMS m/z 495.1292 $[M-H]^-$ of 7-*O*-methylisosilybin A (**6**)

1.5.2.4. 7-*O*-Methylisosilybin B (8)

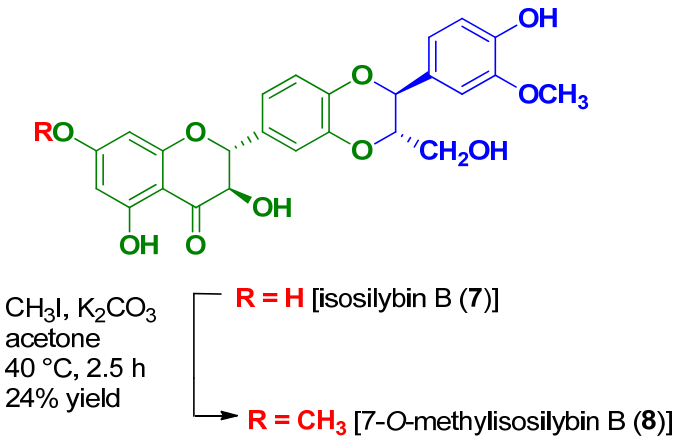

Scheme 1.4. Synthesis of 7-*O*-Methylisosilybin B (**8**).

In a manner that was otherwise consistent with the preparation and purification of 2, compound 7 was reacted with 4 equivalents of CH_3I at 40 °C for 2.5 h to yield compound 8. The compounds were purified as described in Fig. 1.30. Yield: 12 mg, 24%; white solid;

$[\alpha]_D^{20}$: -17.4 (*c* 0.09, MeOH);

UV (MeOH) λ_{max} (log ε): 211 (4.1), 287 (3.8) nm;

CD (MeOH) λ_{ext} ($\Delta\varepsilon$): 229 (1.8), 294 (-4.2), 331 (-0.1) nm; see Fig. 1.58

^{1}H NMR (500 MHz, DMSO-*d6*): δ = 3.33 (m, 1H, H-9"b), 3.53 (ddd, *J* = 10.0, 5.2, 1.7 Hz, 1H, H-9"a), 3.77 (s, 3H, 3"-OCH3), 3.79 (s, 3H, 7-*O*CH3), 4.17 (ddd, *J* = 7.5, 4.6, 1.7 Hz, 1H, H-8"), 4.67 (dd, *J* = 11.5, 6.3 Hz, 1H, 3-H), 4.92 (d, *J* = 7.5 Hz, 1H, H-7"), 4.97 (dd, *J* = 5.2, 4.6 Hz, OH-9"), 5.16 (d, *J* = 11.5 Hz, 1H, 2-H), 5.91 (d, *J* = 6.3 Hz, 3-OH), 6.12 (d, *J* = 2.3 Hz, 1H, H-8), 6.13 (d, *J* = 2.3 Hz, 1H, H-6), 6.80 (d, *J* = 8.0 Hz, 1H,

H-5"), 6.85 (dd, *J* = 8.2, 1.8 Hz, 1H, H-6"), 6.94 (d, J = 8.0 Hz, 1H, H-5'), 7.00 (dd, *J* = 8.0, 1.7 Hz, 1H, H-6'), 7.01 (d, *J* = 1.8 Hz, 1H, H-2"), 7.11 (d, *J* = 1.7 Hz, 1H, H-2'), 9.18 (s, 4"-OH), 11.87 (s, 5-OH); (see, Tables 1.1 and Fig. 1.31).

^{13}C NMR (125 MHz, DMSO-*d6*): δ 55.7 (3″-OCH3), 60.2 (C-9″), 71.6 (C-3), 75.9 (C-7″), 78.0 (C-8″), 82.7 (C-2), 93.9 (C-8), 95.0 (C-6), 101.4 (C-4a), 111.7 (C-2″), 115.3 (C-5″), 116.4 (C-5′), 116.5 (C-2′), 120.4 (C-6″), 121.0 (C-6′), 127.5 (C-1″), 130.2 (C-1′), 142.9 (C-3′), 143.9 (C-4′), 147.0 (C-4″), 147.6 (C-3″), 162.4 (C-8a), 163.0 (C-5), 167.6 (C-7), 198.4 (C-4). ^{1}H and ^{13}C NMR data, see Tables 1.3 and Fig. 1.32;

HSQC data: H-2→C-2; H-3→C-3; H-6→C-6; H-8→C-8; H-2'→C-2'; H-6'→C-6'; H-2"→C-2"; H-5"→C-5"; H-6"→C-6"; H-7"→C-7"; H-8"→C-8"; H-9"a→C-9"; H-9"b→C-9"; OCH_3-7→C-7; OCH_3-3"→C-3" (see Fig. 1.33).

HMBC data: HMBC data, H-2→C-3, 1', 6'; OH-5→C-5, 6; H-6→C-8, OCH_3-7→C-7; H-8→C-4a; H-2'→C-4'; H-5'→C-4'; H-7"→C-1", 6"; H-2"→C-3" ; OH-4"→C-6" ; H-5"→C-4"; OCH_3-C3"→C3"; H-6"→C-3". (see Figs. 1.34 and 1.35);

HRESIMS *m/z*: 495.1294 $[M-H]^-$ (calcd for $C_{26}H_{23}O_{10}$ 495.1297; see Fig 1.36).

Analytical method: 20:80 to 60:40 CH_3CN:H_2O (0.1 % formic acid) over 40 min.

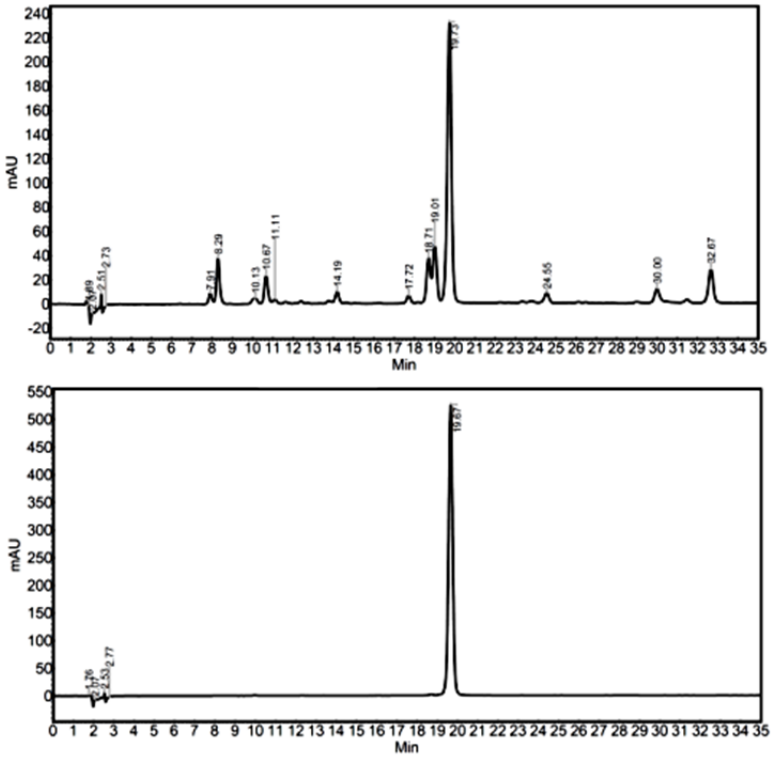

Separation method: gradient of 20:80 to 60:40 CH_3CN:H_2O (0.1 % formic acid) over 40 min 60: 40 hold for 5 min.

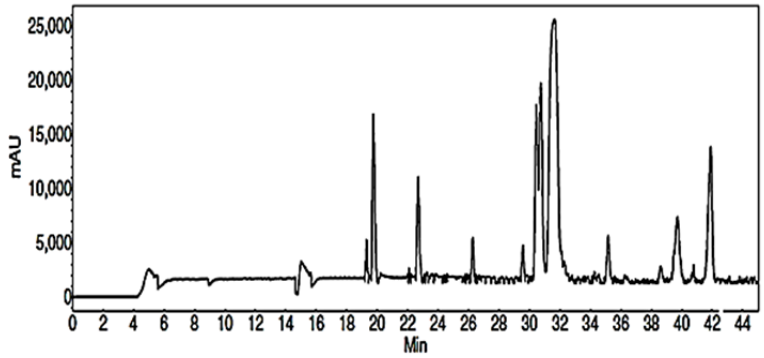

Figure 1.30. HPLC chromatograms of crude reaction mixtures (a), purified 7-*O*-methylisosilybin B (b) at 288 nm and preparative HPLC (c).

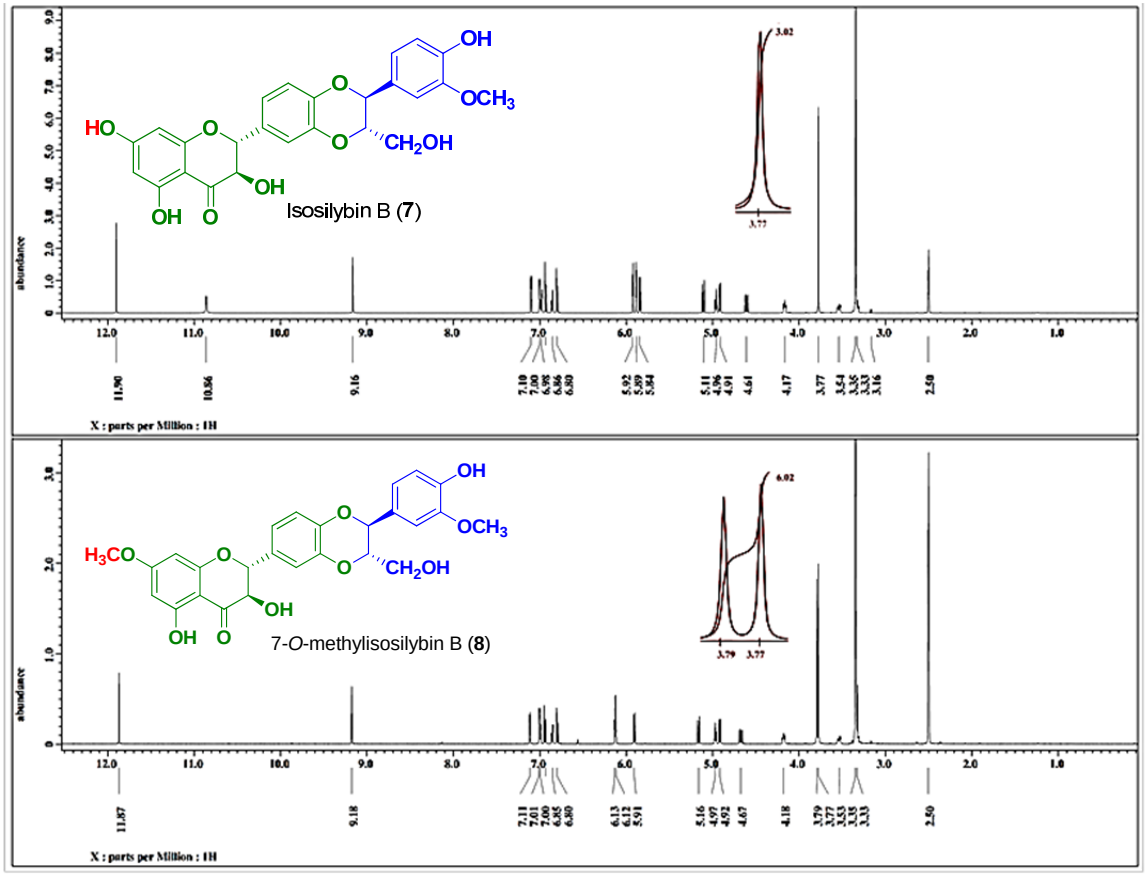

Figure 1.31. ^{1}H NMR spectra (500 MHz, 30 °C) of isosilybin B (**7**) and 7-*O*-methylisosilybin B (**8**) in DMSO-d_6

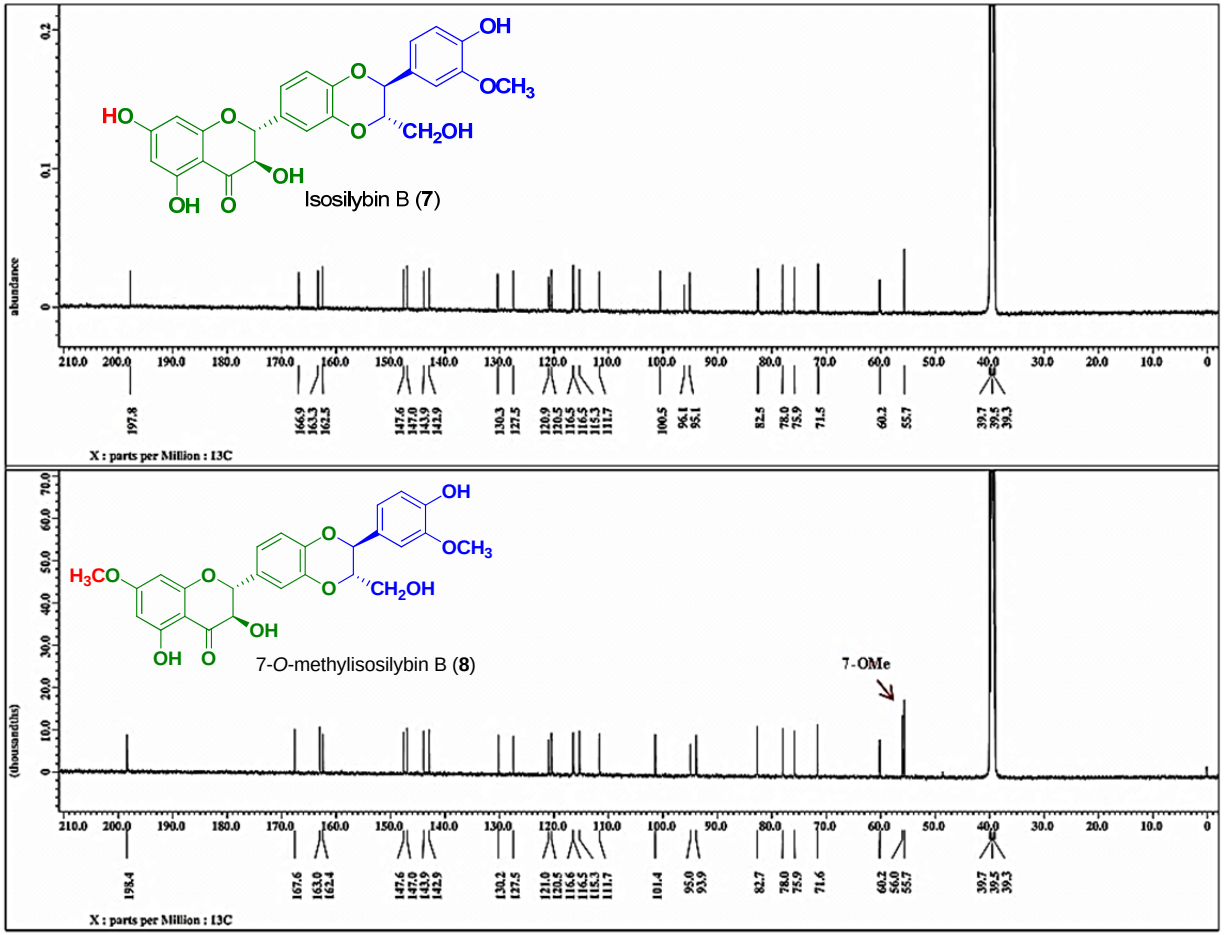

Figure 1.32 ^{13}C NMR spectra (125 MHz, 30 °C) of isosilybin B (**7**) and 7-*O*-methylisosilybin B (**8**) in DMSO-d_6

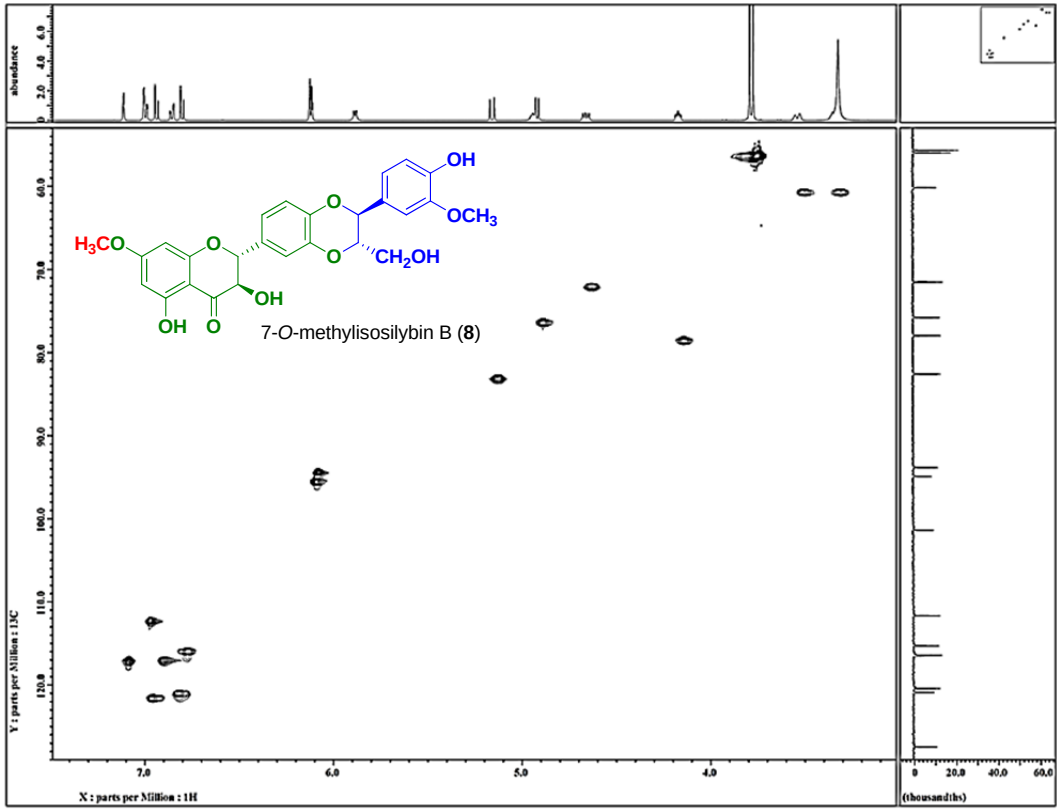

Figure 1.33. HSQC NMR spectrum (DMSO-d_6, 30 °C) of 7-*O*-methylisosilybin B (**8**) showing the key correlation

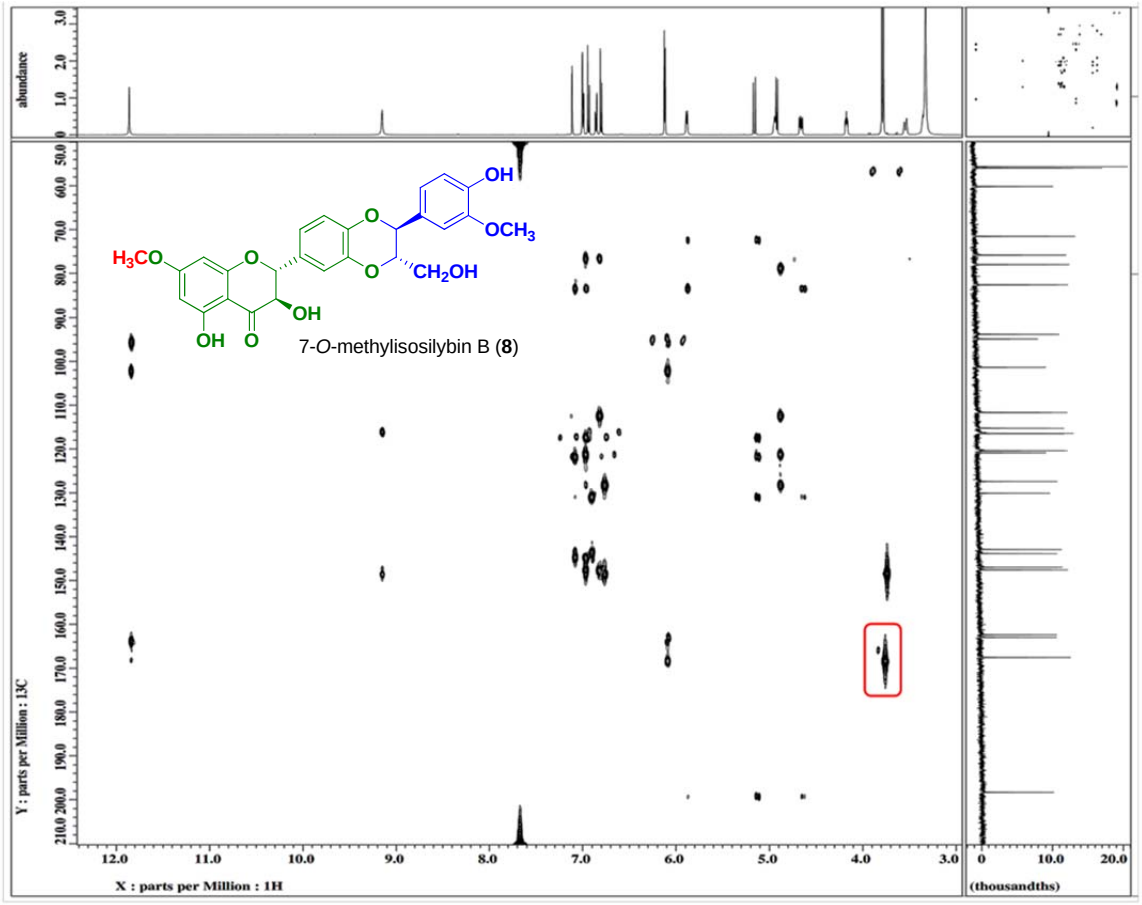

Figure 1.34. HMBC NMR spectrum (DMSO-d_6, 30 °C) of 7-*O*-methylisosilybin B (**8**) showing the key correlation between the methoxy protons and C-7

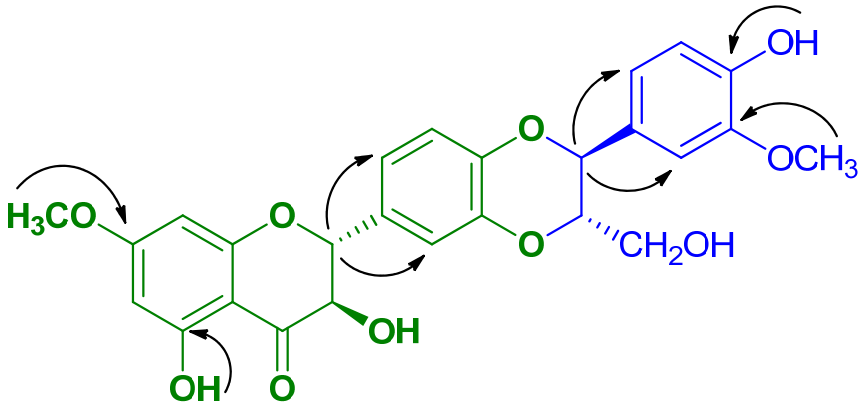

Figure 1.35. Key HMBC correlations of 7-*O*-methylisosilybin B (**8**)

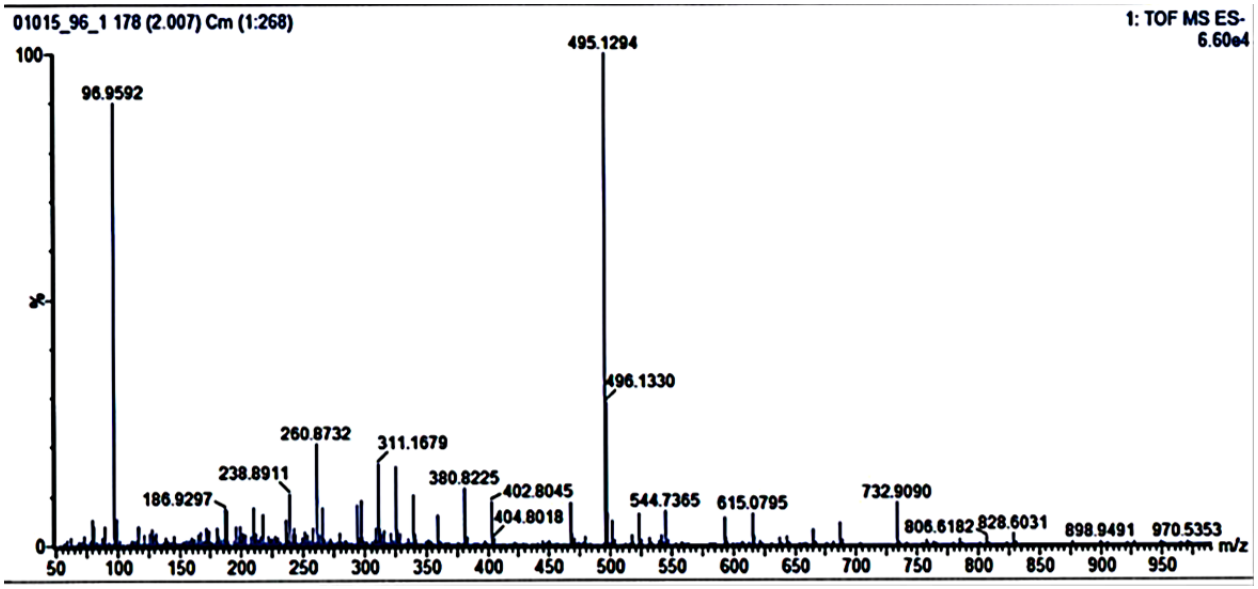

Figure 1.36. HRESIMS m/z 495.1294 $[M-H]^-$ of 7-*O*-methylisosilybin B (**8**)

1.5.2.5. 7-*O*-Methylsilychristin (10)

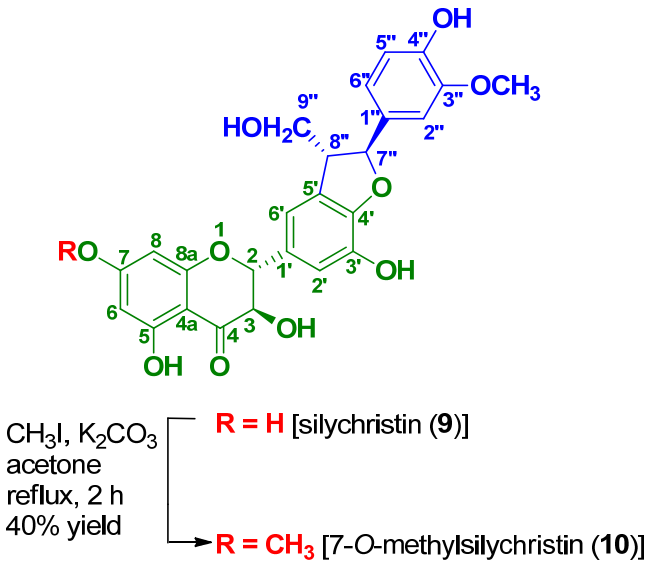

Scheme 1.5. Synthesis of 7-*O*-Methylsilychristin (**10**).

In a manner that was otherwise consistent with the preparation and purification of 2, compound 9 was reacted with 12 equivalents of CH_3I at reflux for 2 h to yield compound 10. The compounds were purified as described in Fig. 1.37 Yield: 41 mg, 40%; white solid;

$[\alpha]_D^{20}$: +56.6 (*c* 0.06, MeOH);

UV (MeOH) λ_{max} (log ε): 215 (4.0), 288 (3.8) nm;

^{1}H NMR (500 MHz, DMSO-d_6): δ = 3.47 (ddd, *J* = 12.6, 12.0, 6.9 Hz, 1H, H-8"), 3.63 (ddd, *J* = 12.6, 10.9, 6.9 Hz, 1H, H-9"b), 3.72 (ddd, *J* = 12.6, 10.9, 5.2 Hz, 1H, H-9"a), 3.76 (s, 3H, 3"-OCH_3), 3.78 (s, 3H, 7-OCH_3), 4.58 (dd, *J* = 11.4, 6.3 Hz, 1H, H-3), 5.01 (dd, *J* = 5.7, 5.2 Hz, OH-9"), 5.05 (d, J = 11.4 Hz, 1H, H-2), 5.46 (d, *J* = 6.9 Hz, 1H, H-

7''), 5.81 (d, *J* = 6.3 Hz, OH-3), 6.09 (d, *J* = 2.3 Hz, 1H, H-8), 6.12 (d, *J* = 2.3 Hz, 1H, H-6), 6.76 (d, *J* = 8.1 Hz, 1H, H-5''), 6.81 (dd, *J* = 8.1, 1.8 Hz, 1H, H-6''), 6.84 (d, *J* = 1.2 Hz, 1H, H-2'), 6.88 (br s, 1H, H-6'), 6.96 (d, *J* = 1.8 Hz, 1H, H-2''), 9.02 (s, 4''-OH), 11.87 (s, 5-OH) (see, Tables 1.2 and Fig. 1.38).

^{13}C NMR (125 MHz, DMSO-*d*$_6$): δ 53.9 (C-8″), 55.6 (3″-OCH_3), 63.5 (C-9″), 71.8 (C-3), 83.4 (C-2), 87.5 (C-7″), 93.8 (C-8), 94.9 (C-6), 101.4 (C-4a), 110.9 (C-2″), 115.3 (C-5″), 115.4 (C-6′), 115.7 (C-2′), 118.7 (C-6″), 129.1 (C-5′), 129.8 (C-1′), 132.4 (C-1″), 140.7 (C-4′), 162.4 (C-8a), 163.0 (C-5), 146.4 (C-3′), 147.7 (C-4″), 148.1 (C-3″), 167.5 (C-7), 198.4 (C-4). ^{1}H and ^{13}C NMR data, see Tables 1.3 and Fig. 1.39;

HSQC data: H-2→C-3, 4, 6'; H-3→C-2, 4; OH-5→C-6, 4a, 8a; H-6→C-7; OCH_3-7→C-7; H-8→C-6, 7; H-2'→C-3', 6'; OH-3'→C-2', 4'; H-7''→C-9''; H-9'' →C-8''; H-2''→C-7'', 6''; OCH_3-3''→C3''; OH-4''→C-4'', 5''; H-5''→C-1' '(see Fig. 1.40;

HMBC data: see Figs. 1.41 and 1.42;

HRESIMS *m/z*: 495.1284 $[M-H]^-$ (calcd for $C_{26}H_{23}O_{10}$ 495.1297; see Fig. 1.43).

Analytical method: 20:80 to 36:64 $CH_3CN:H_2O$ (0.1% formic acid) over 24 min.

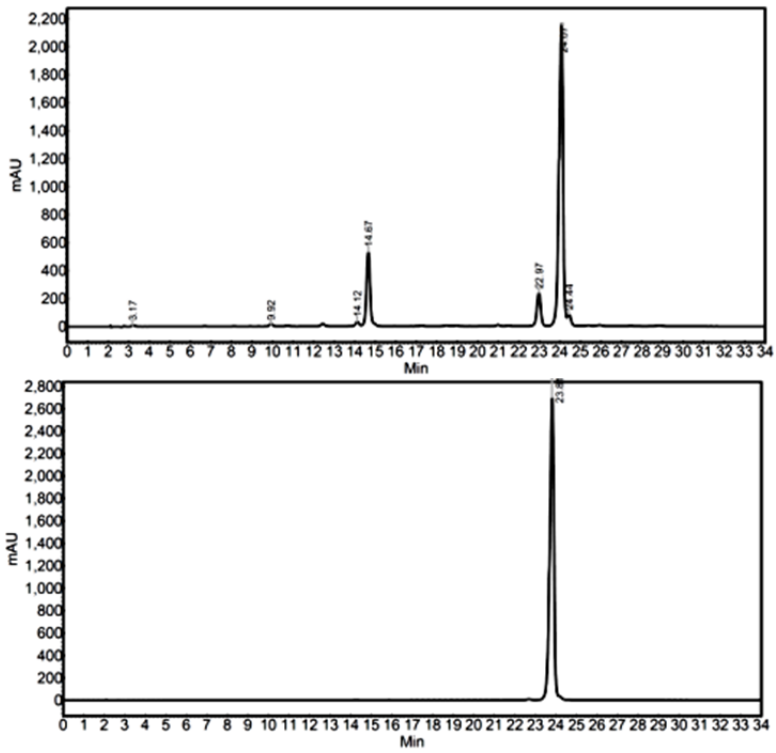

Separation method: gradient of 20:80 to 42:58 $CH_3CN:H_2O$ (0.1% formic acid) over 45 min hold 45:58 for 10 min.

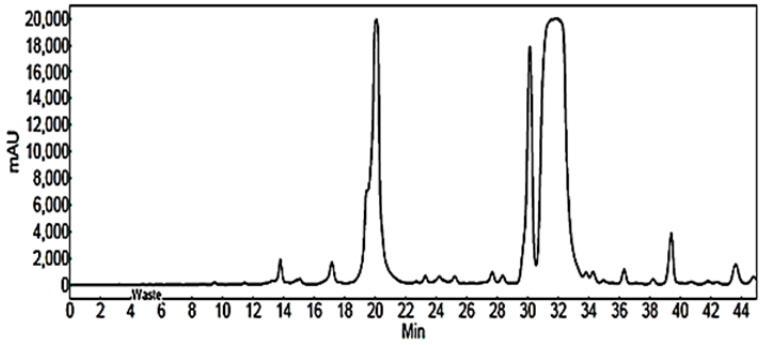

Figure 1.37. HPLC chromatograms of crude reaction mixtures (a), purified 7-*O*-methylsilychristin (b) at 288 nm and preparative HPLC (c).

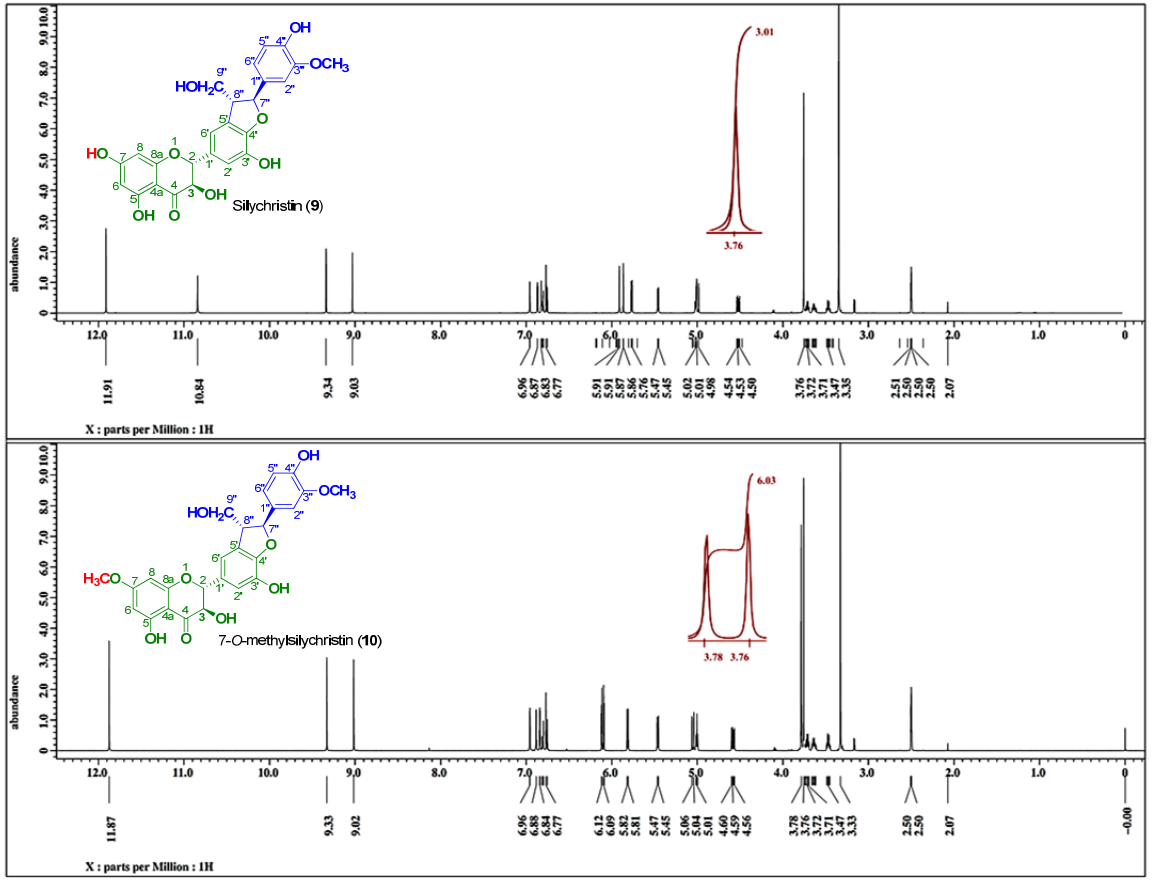

Figure 1.38. ^{1}H NMR spectra (500 MHz, 30 °C) of silychristin (**9**) and 7-*O*-methylsilychristin (**10**) in DMSO-d_6

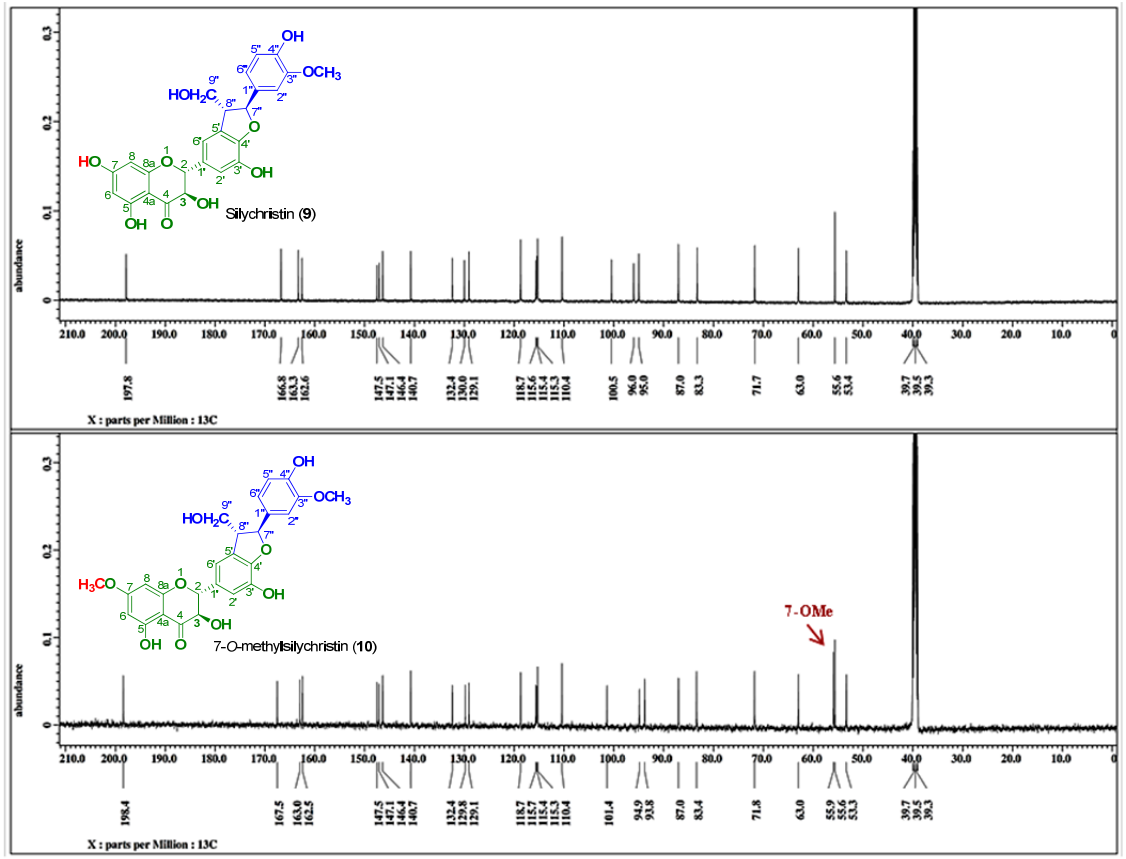

Figure 1.39. ^{13}C NMR spectra (125 MHz, 30 °C) of silychristin (**9**) and 7-*O*-methylsilychristin (**10**) in DMSO-d_6

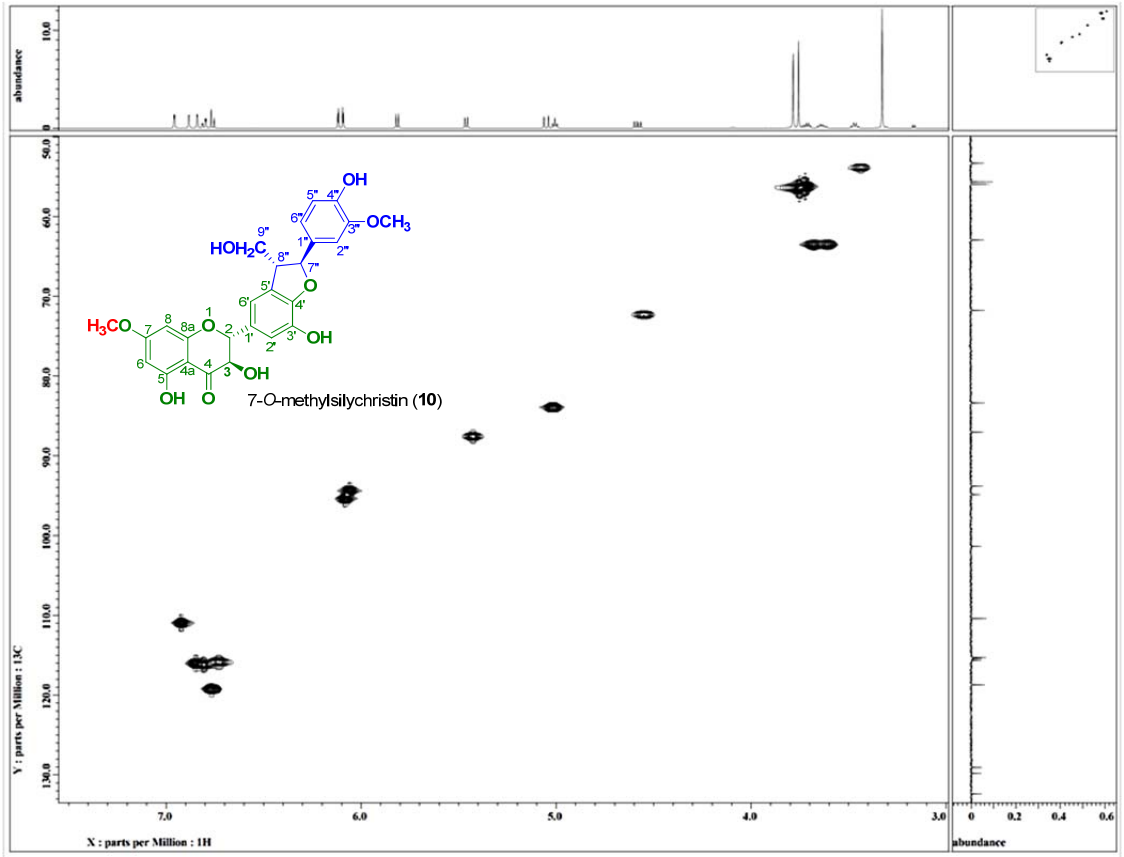

Figure 1.40. HSQC NMR spectrum (DMSO-d_6, 30 °C) of 7-*O*-methylsilychristin (**10**) showing the key

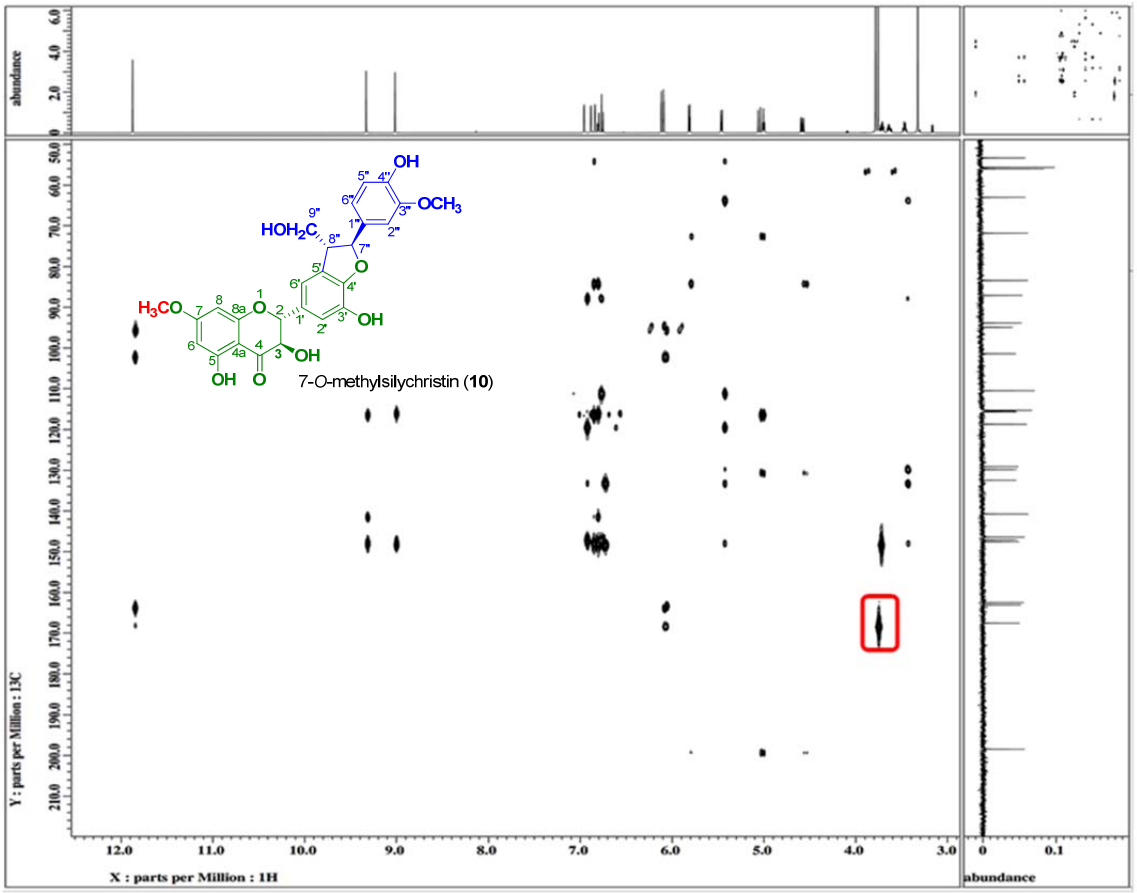

Figure 1.41. HMBC NMR spectrum (DMSO-d_6, 30 °C) of 7-*O*-methylsilychristin (**10**) showing the key correlation between the methoxy protons and C-7

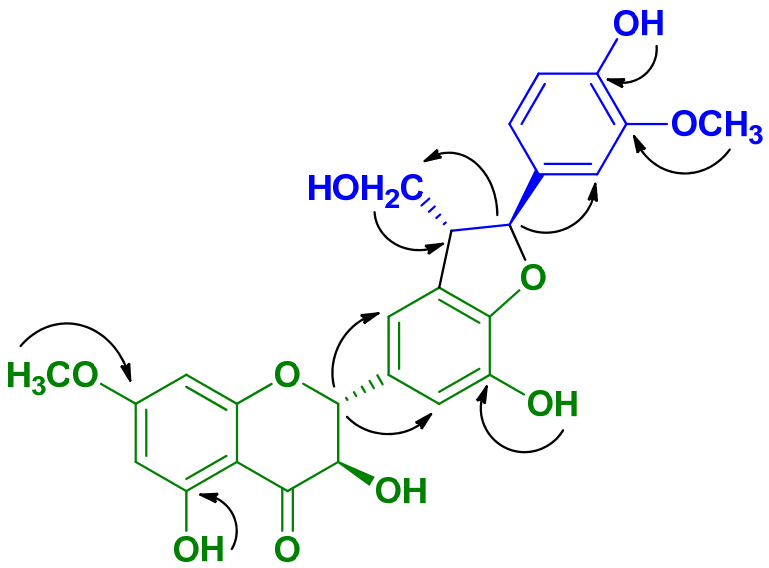

Figure 1.42. Key HMBC correlations of 7-*O*-methylsilychristin (**10**)

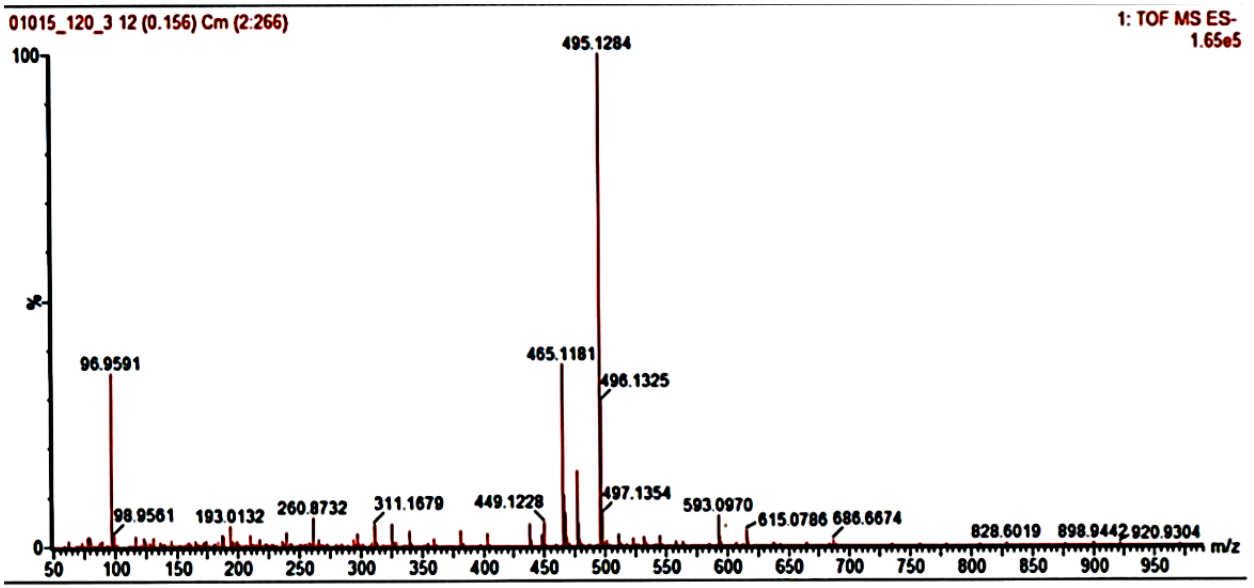

Figure 1.43. HRESIMS m/z 495.1284 $[M-H]^-$ of 7-*O*-methylsilychristin (**10**)

1.5.2.6. 7-*O*-Methylisosilychristin (12)

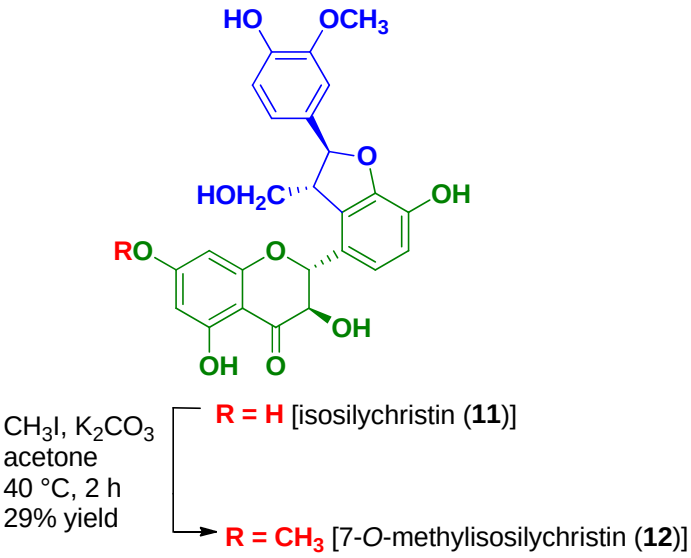

Scheme 1.6. Synthesis of 7-*O*-Methylisosilychristin (**12**).

In a manner that was otherwise consistent with the preparation and purification of 2, compound 11 was reacted with 24 equivalents of CH_3I at 40 °C for 2 h to yield compound 12. The compounds were purified as described in Fig. 1.44. Yield: 15 mg, 29%; white solid;

$[\alpha]_D^{20}$: +144.4 (*c* 0.05, MeOH);

UV (MeOH) λmax (log ε): 212 (4.1), 288 (3.7) nm.

^{1}H NMR (500 MHz, DMSO-d_6): δ = 3.44 (m, 1H, H-9"b), 3.67 (m, 1H, H-8"), 3.68 (m, 1H, H-9"a), 3.69 (s, 3H, 3"-OCH_3), 3.80 (s, 3H, 7-OCH_3), 4.67 (dd, J = 11.4, 6.9 Hz, 1H, H-3), 5.06 (dd, J = 6.5, 4.5 Hz, OH-9"), 5.22 (d, J = 11.4 Hz, 1H, H-2), 5.57 (d, J = 2.5 Hz, 1H, H-7"), 5.81 (d, *J* = 6.9 Hz, OH-3), 6.11 (d, *J* = 2.0 Hz, 1H, H-8), 6.13 (d, *J* = 2.0

Hz, 1H, H-6), 6.69 (d, *J* = 8.5 Hz, 1H, H-5″), 6.74 (d, *J* = 8.1 Hz, 1H, H-5'), 6.76 (d, *J* = 8.5 Hz, 1H, H-6"), 6.86 (d, *J* = 2.0 Hz, 1H, H-2"), 6.97 (d, *J* = 8.1 Hz, 1H, H-6'), 8.99 (s, 4"-OH), 11.90 (s, 5-OH) ; (see, Tables 1.2 and Fig. 1.45).

^{13}C NMR (125 MHz, DMSO-d_6) δ 53.9 (C-8″), 55.6 (3″-OCH_3), 63.5 (C-9″), 71.8 (C-3), 83.4 (C-2), 87.5 (C-7″), 93.8 (C-8), 94.9 (C-6), 101.4 (C-4a), 110.9 (C-2″), 115.3 (C-5″), 115.4 (C-6′), 115.7 (C-2′), 118.7 (C-6″), 129.1 (C-5′), 129.8 (C-1′), 132.4 (C-1″), 140.7 (C-4′), 162.4 (C-8a), 163.0 (C-5), 146.4 (C-3′), 147.7 (C-4″), 148.1 (C-3″), 167.5 (C-7), 198.4 (C-4). ^{1}H and ^{13}C NMR data, see Tables 1.2 and Figs. 1.46;

HSQC data: H-2→C-2; H-3→C-3; H-6→C-6; H-8→C-8; H-5'→C-5'; H-6'→C-6'; H-2"→C-2"; H-5"→C-5"; H-6"→C-6"; H-7"→C-7"; H-8"→C-8"; H-9"a→C-9"; H-9"b→C-9"; OCH_3-7→C-7; OCH_3-3"→C-3" (see, Fig. 1.47).

HMBC data: see Figs. 1.48 and 1.49;

HRESIMS m/z: 495.1284 [M-H]- (calcd for $C_{26}H_{23}O_{10}$ 495.1297; see Fig. 1.50).

Analytical method: 15:80 to 36:64 CH_3CN:H_2O (0.1 % formic acid) over 40 min.

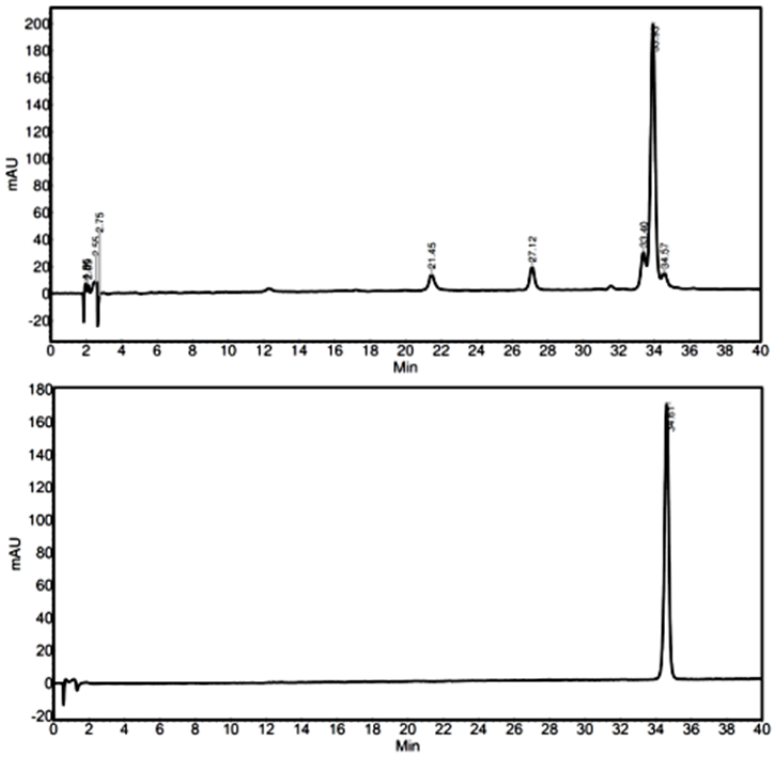

Separation method: gradient of 15: 85 to 36:64 over 50 min hold 36:64 for 10 min.

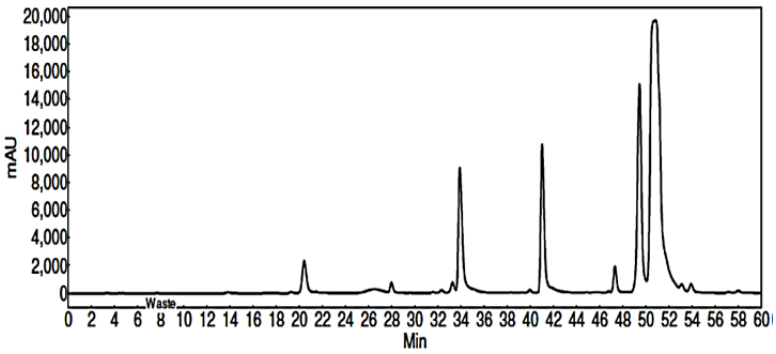

Figure 1.44. HPLC chromatograms of crude reaction mixtures (a), purified 7-*O*-methylisosilychristin (b) at 288 nm and preparative HPLC (c).

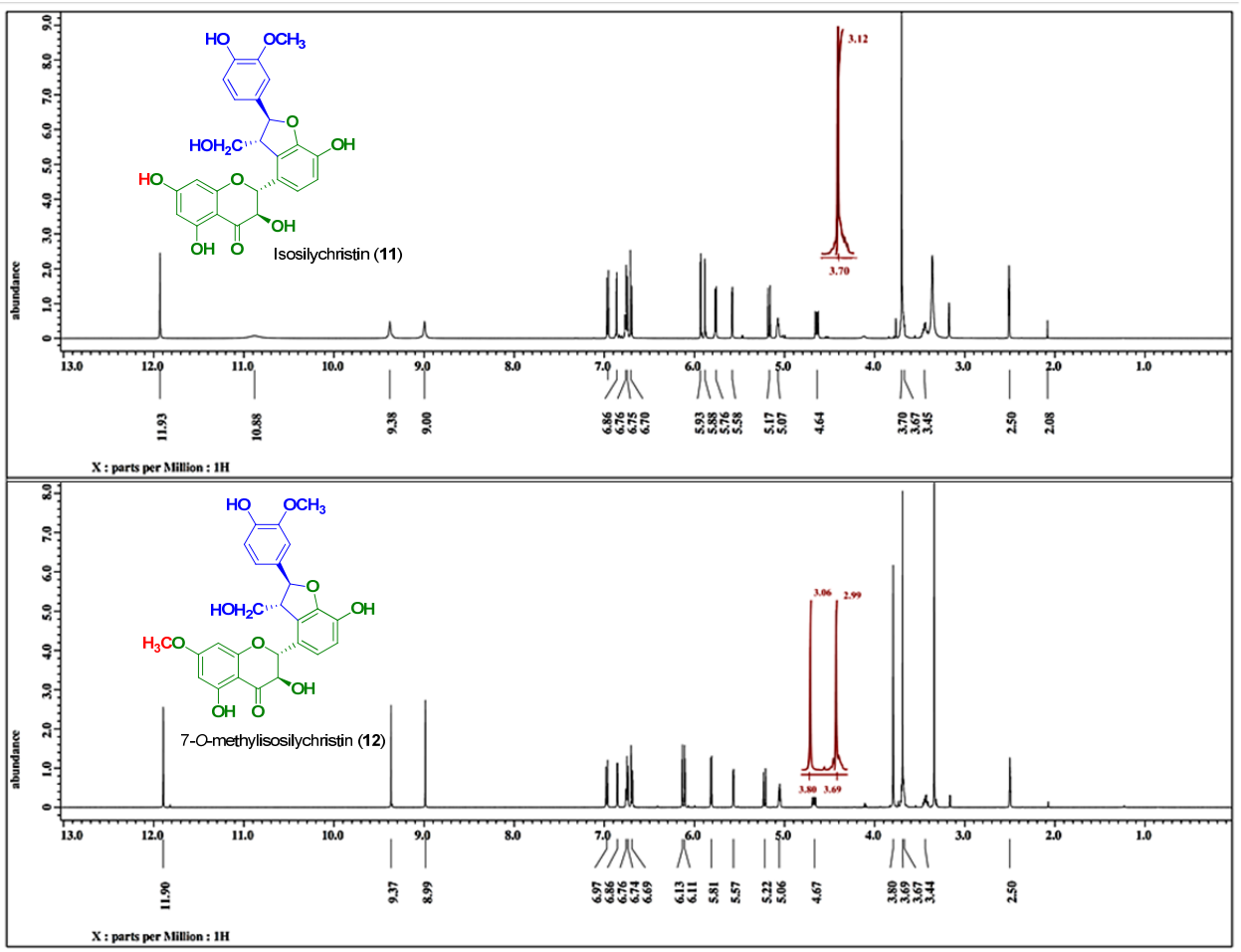

Figure 1.45. ^{1}H NMR spectra (500 MHz, 30 °C) of isosilychristin (**11**) and 7-*O*-methylisosilychristin (**12**) in DMSO-d_6

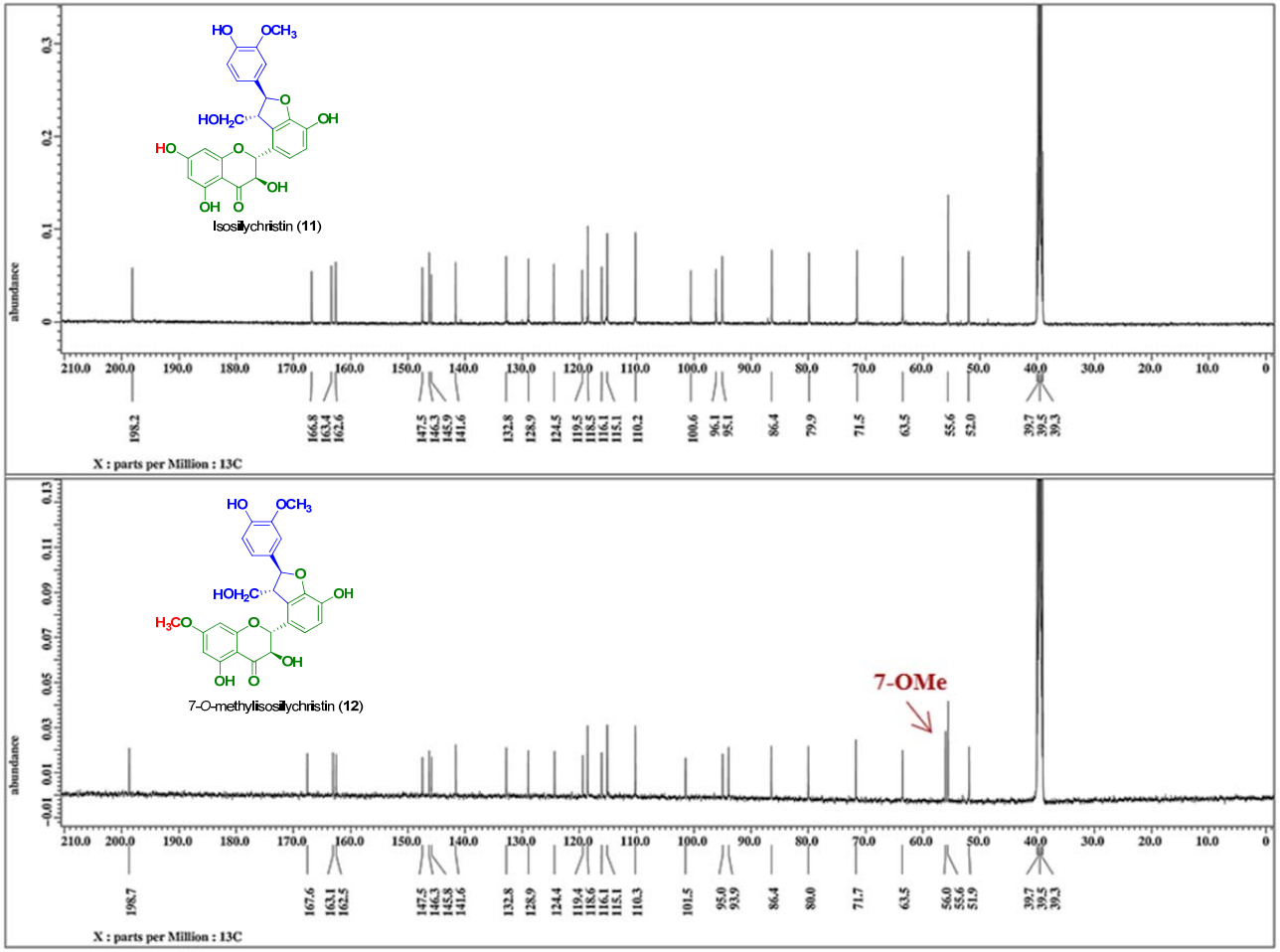

Figure 1.46. ^{13}C NMR spectra (125 MHz, 30°C) of isosilychristin (**11**) and 7-*O*-methylisosilychristin (**12**) in DMSO-d_6

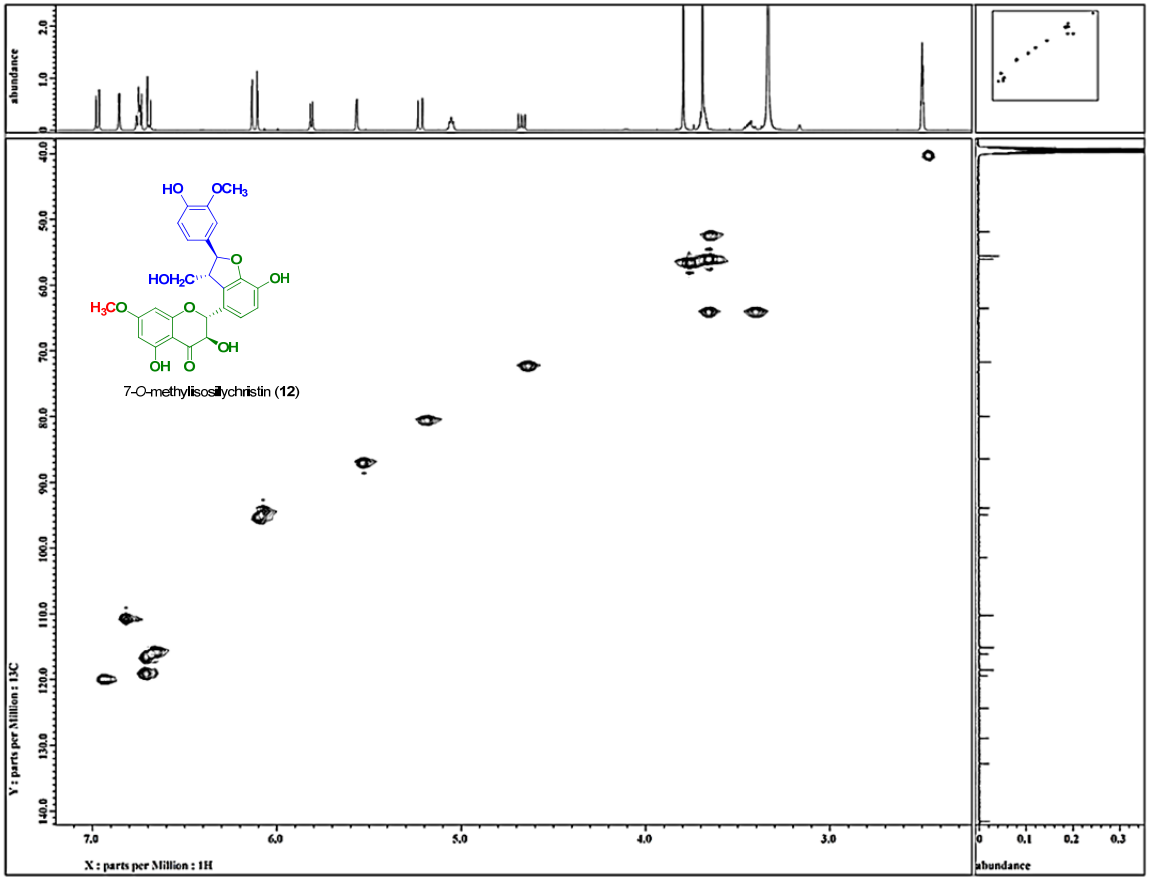

Figure 1.47. HSQC NMR spectrum (DMSO-d_6, 30 °C) of 7-*O*-methylisosilychristin (**12**) showing the key correlation

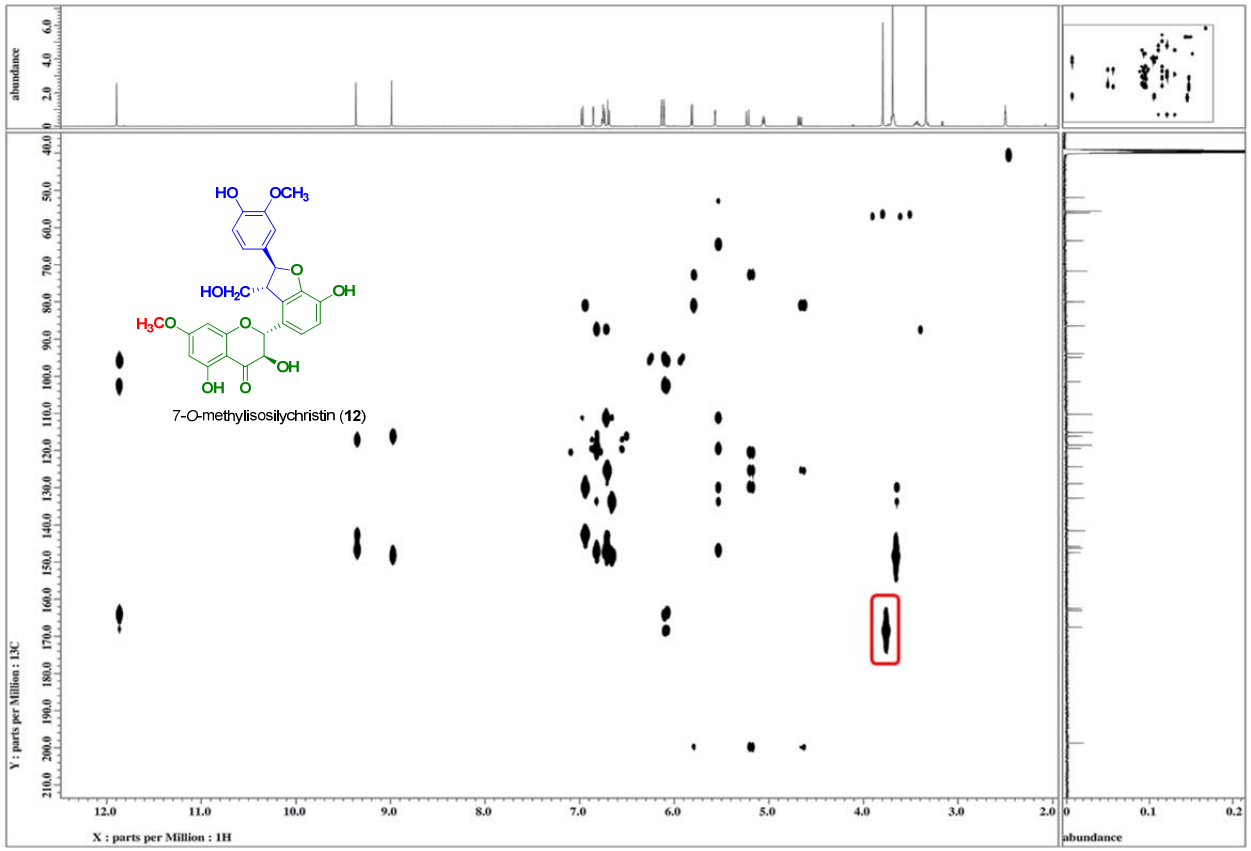

Figure 1.48. HMBC NMR spectrum (DMSO-d_6, 30 °C) of 7-*O*-methylisosilychristin (**12**) showing the key correlation between the methoxy protons and C-7

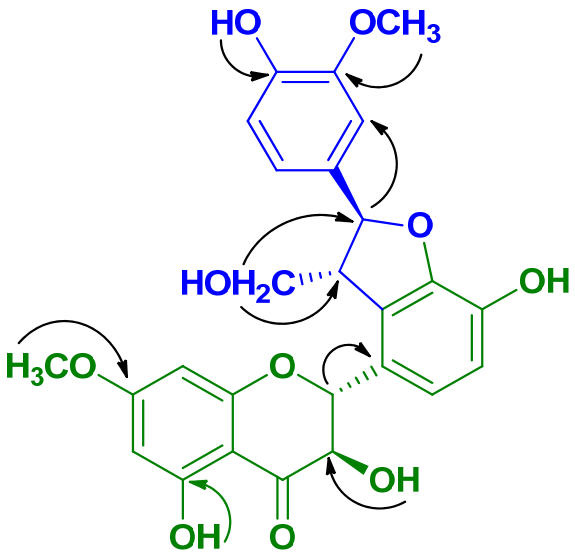

Figure 1.49. Key HMBC correlations of 7-*O*-methylisosilychristin (**12**)

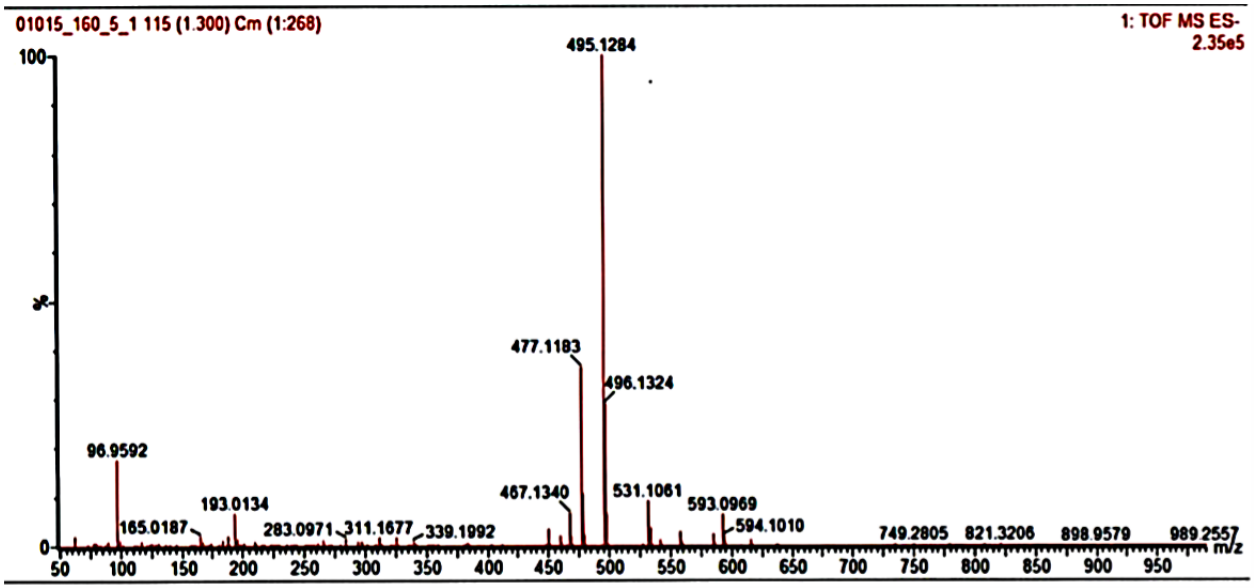

Figure 1.50. HRESIMS m/z 495.1284 $[M-H]^-$ of 7-*O*-methylisosilychristin (**12**)

1.5.2.7. 7-*O*-Methylsilydianin (14)

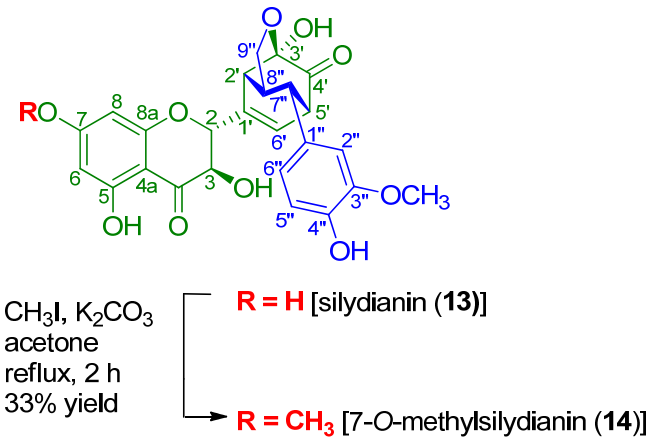

Scheme 1.7. Synthesis of 7-*O*-Methylsilydianin (**14**).

In a manner that was otherwise consistent with the preparation and purification of 2, compound 13 was reacted with 12 equivalents of CH_3I at reflux for 2 h to yield compound 14. The compounds were purified as described in Fig. 1.51.

Yield: 20 mg, 33%; white solid;

$[\alpha]_D^{20}$: +157.9 (*c* 0.06, MeOH);

UV (MeOH) λ_{max} (log ε): 207 (3.9), 288 (3.6) nm.

^{1}H NMR (500 MHz, DMSO-d_6): δ = 2.73 (br s, 1H, H-8"), 3.19 (dd, *J* = 6.9, 3.0 Hz,1H, H-5'), 3.31 (br s, 1H, H-7"), 3.45 (dd, *J* = 4.0, 2.0 Hz, 1H, H-2'), 3.74 (s, 3H, 3"-OCH_3), 3.78 (d, *J* = 8.0 Hz, 1H, H-9"b), 3.79 (s, 3H, 7-OCH_3), 4.13 (dd, *J* = 8.0, 3.0 Hz, 1H, H-9"a), 4.48 (dd, *J* = 10.4, 5.4 Hz, 1H, H-3), 4.91 (dd, *J* = 10.4 Hz, 1H, H-2), 6.01 (d, *J* = 6.9 Hz, 1H, H-6'), 6.04 (d, *J* = 6.3 Hz, OH-3), 6.11 (d, *J* = 1.9 Hz, 1H, H-8), 6.12 (d, *J* = 1.9 Hz, 1H, H-6), 6.56 (dd, *J* = 8.4, 1.9 Hz, 1H, H-6"), 6.64 (d, *J* = 8.4 Hz, 1H, H-

5"), 6.76 (d, *J* = 1.9 Hz, 1H, H-2"), 3.17 (s, , OH-3'), 8.79 (s, , OH-4"), 11.77 (s, OH-5). (see, Tables 1.2 and Fig. 1.52).

^{13}C NMR (125 MHz, DMSO-d_6): δ 44.0 (C-8″), 46.0 (C-7″), 48.7 (C-2′), 53.3 (C-5′), 55.4 (3″-OCH_3), 71.0 (C-3), 72.8 (C-9″), 81.8 (C-2), 93.8 (C-8), 95.2 (C-6), 96.7 (C-3′), 101.2 (C-4a), 112.4 (C-2″), 115.0 (C-5″), 120.3 (C-6″), 124.0 (C-6′), 133.0 (C-1″), 139.4 (C-1′), 145.1(C-4″), 132.4 (C-1″), 147.2 (C-3″), 162.0 (C-8a), 163.0 (C-5), 167.6 (C-7), 197.6 (C-4), 201.9 (C-4′). ^{13}C NMR data, (see, Tables 1.3 and Fig. 1.53).

HSQC data: H-2→C-2; H-3→C-3; H-6→C-6; H-8→C-8; H-2'→C-2'; H-5'→C-5'; H-6'→C-6'; H-2"→C-2"; H-5"→C-5"; H-6"→C-6"; H-7"→C-7"; H-8"→C-8"; H-9"a→C-9"; H-9"b→C-9"; OCH_3-7→C-7; OCH_3-3"→C-3" (see Fig. 1.54).

HMBC data: H-2→C-3, 1'; H-3→C-2; OH-3→C-2, 3; H-6→C-7, 4a, OCH_3-7→C-7; H-8→C-6, 8a; H-2'→C-4'; OH-3'→C-2'; H-5'→C-1', 4', 6'; H-6'→C-2', 4', 5' , H-7"→C-9" , 1", 2", 6"; H-9"→C-7", 8", 3'; H-8"→C-3'; H-2"→C-7", 3", 6", OCH_3-3"→C3"; OH-4"→C-3", 5"; H-5"→C-1", 3", 4"; H-6"→C-7" , 1", 4" (see Figs. 1.55 and 1.56).

HRESIMS *m/z*: 495.1284 $[M-H]^-$ (calcd for $C_{26}H_{23}O_{10}$ 495.1297; see Fig. 1.57).

Analytical method: 20:80 to 36:64 CH_3CN:H_2O (0.1% formic acid) over 24 min.

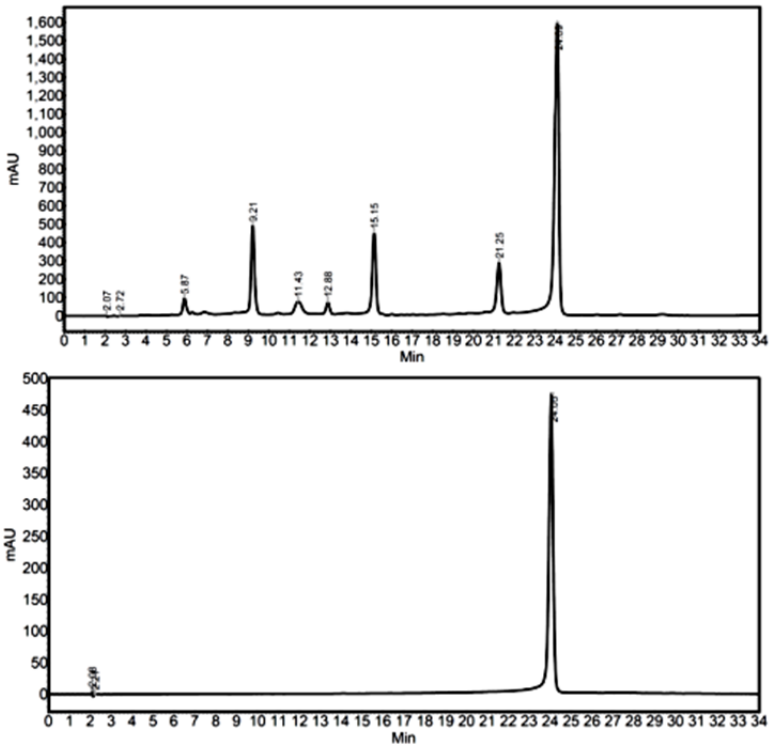

Analytical method: 20:80 to 36:64 CH_3CN:H_2O (0.1% formic acid) over 24 min.

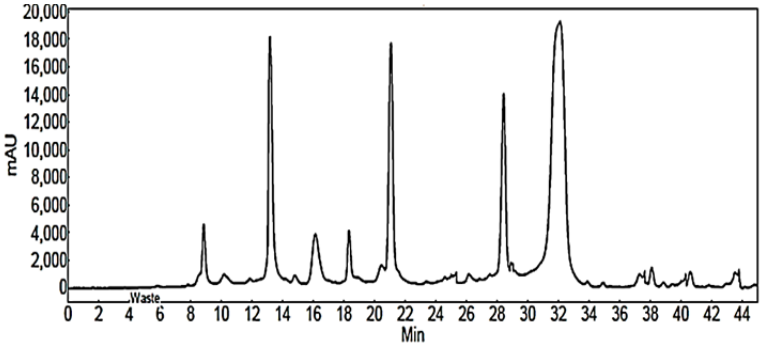

Figure 1.51. HPLC chromatograms of crude reaction mixtures (a), purified 7-*O*-methylsilydianin (b) at 288 nm and preparative HPLC (c).

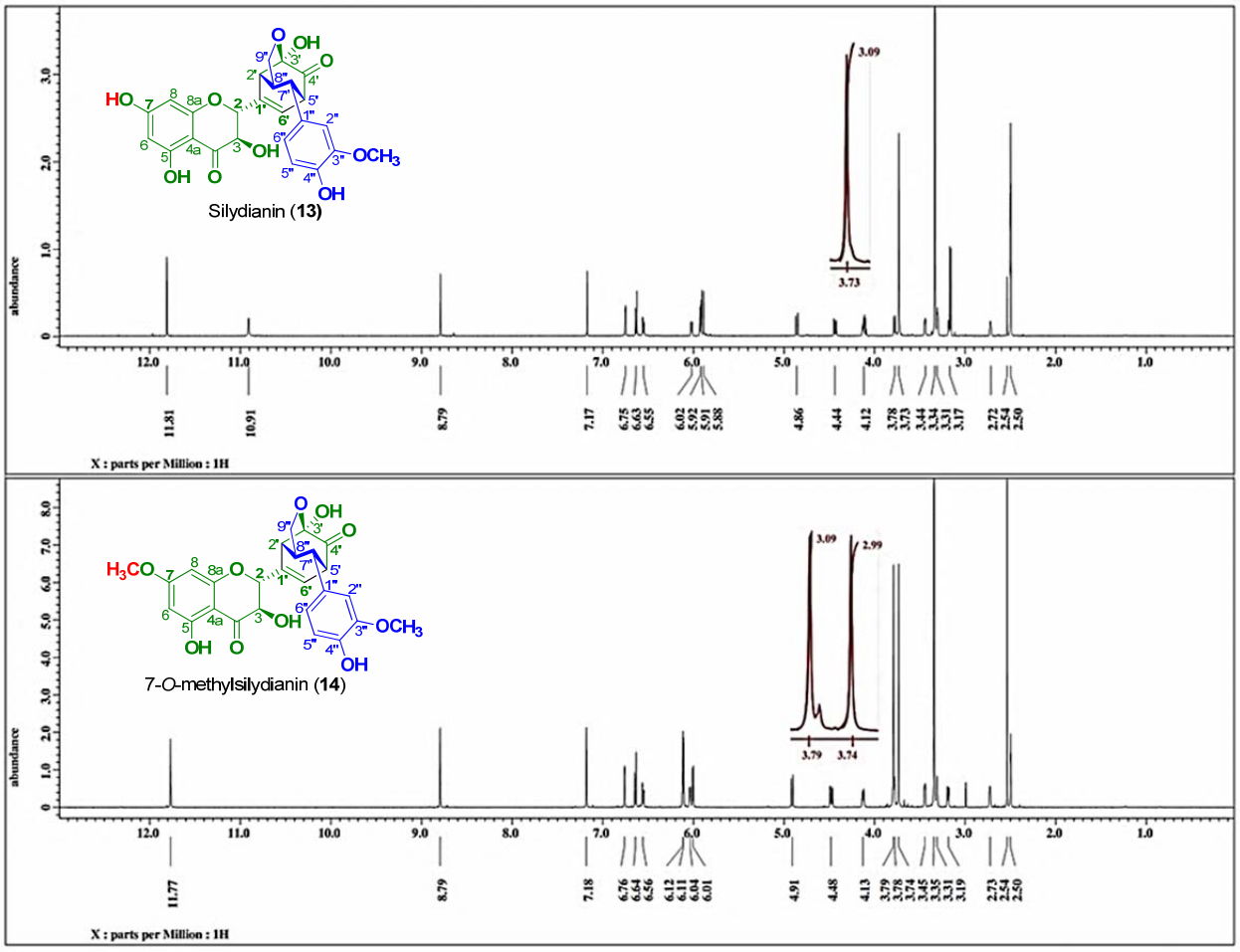

Figure 1.52. ^{1}H NMR spectra (500 MHz, 30 °C) of silydianin (**13**) and 7-*O*-methylsilydianin (**14**) in DMSO-d_6

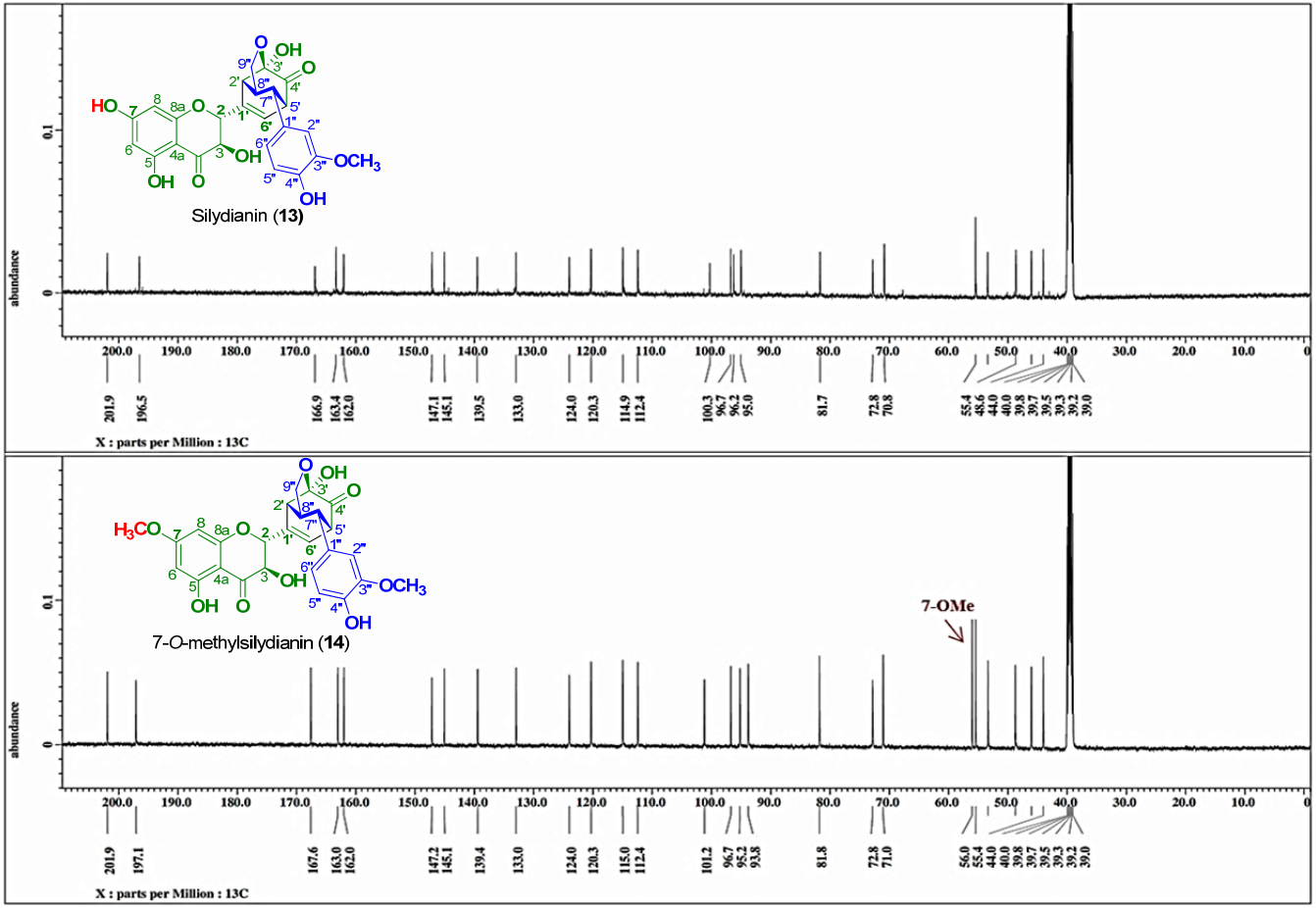

Figure 1.53. ^{13}C NMR spectra (125 MHz, 30 °C) of silydianin (**13**) and 7-*O*-methylsilydianin (**14**) in DMSO-d_6

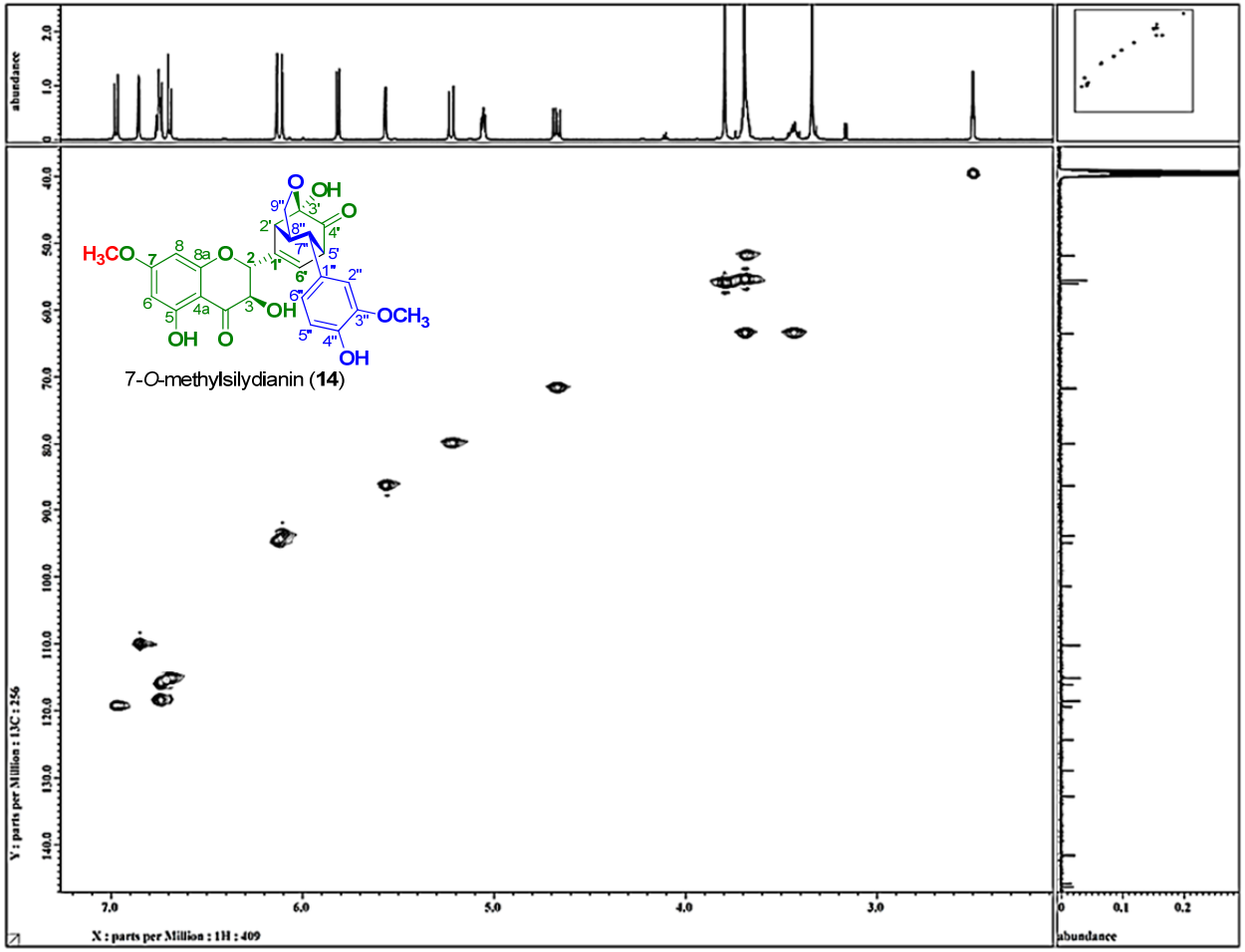

Figure 1.54. HSQC NMR spectrum (DMSO-d_6, 30 °C) of 7-*O*-methylsilydianin (**14**) showing the key correlation

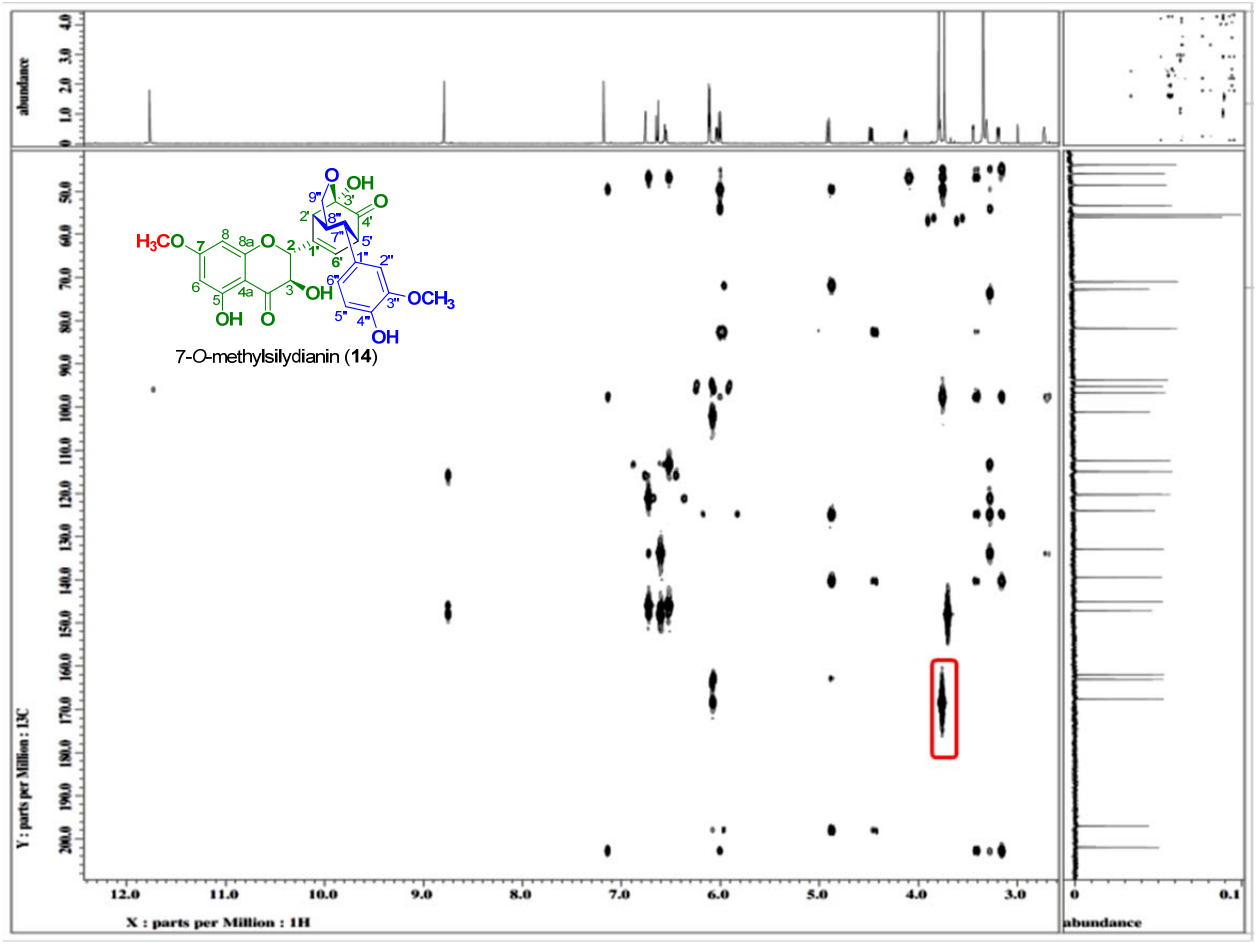

Figure 1.55. HMBC NMR spectrum (DMSO-d_6, 30 °C) of 7-*O*-methylsilydianin (**14**) showing the key correlation between the methoxy protons and C-7

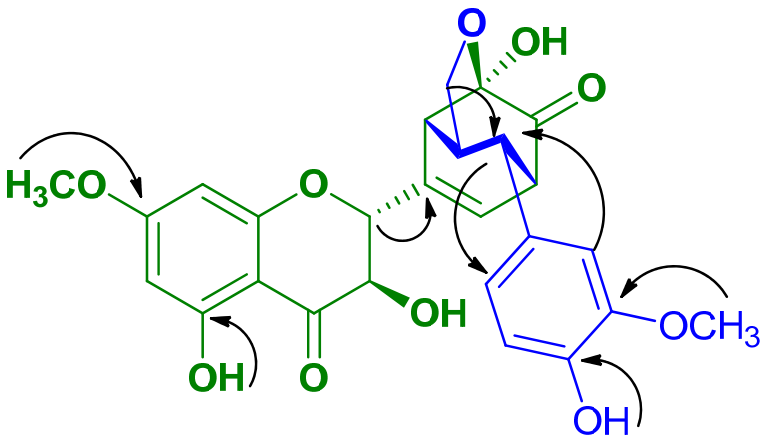

Figure 1.56. Key HMBC correlations of 7-*O*-methylsilydianin (**14**)

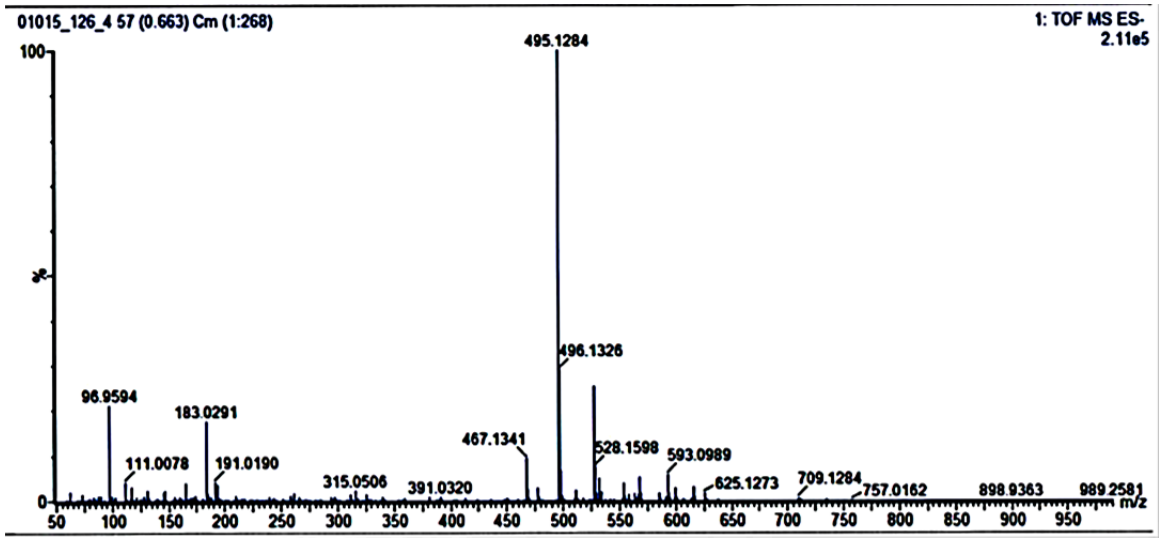

Figure 1.57. HRESIMS m/z 495.1284 $[M-H]^-$ of 7-*O*-methylsilydianin (**14**)

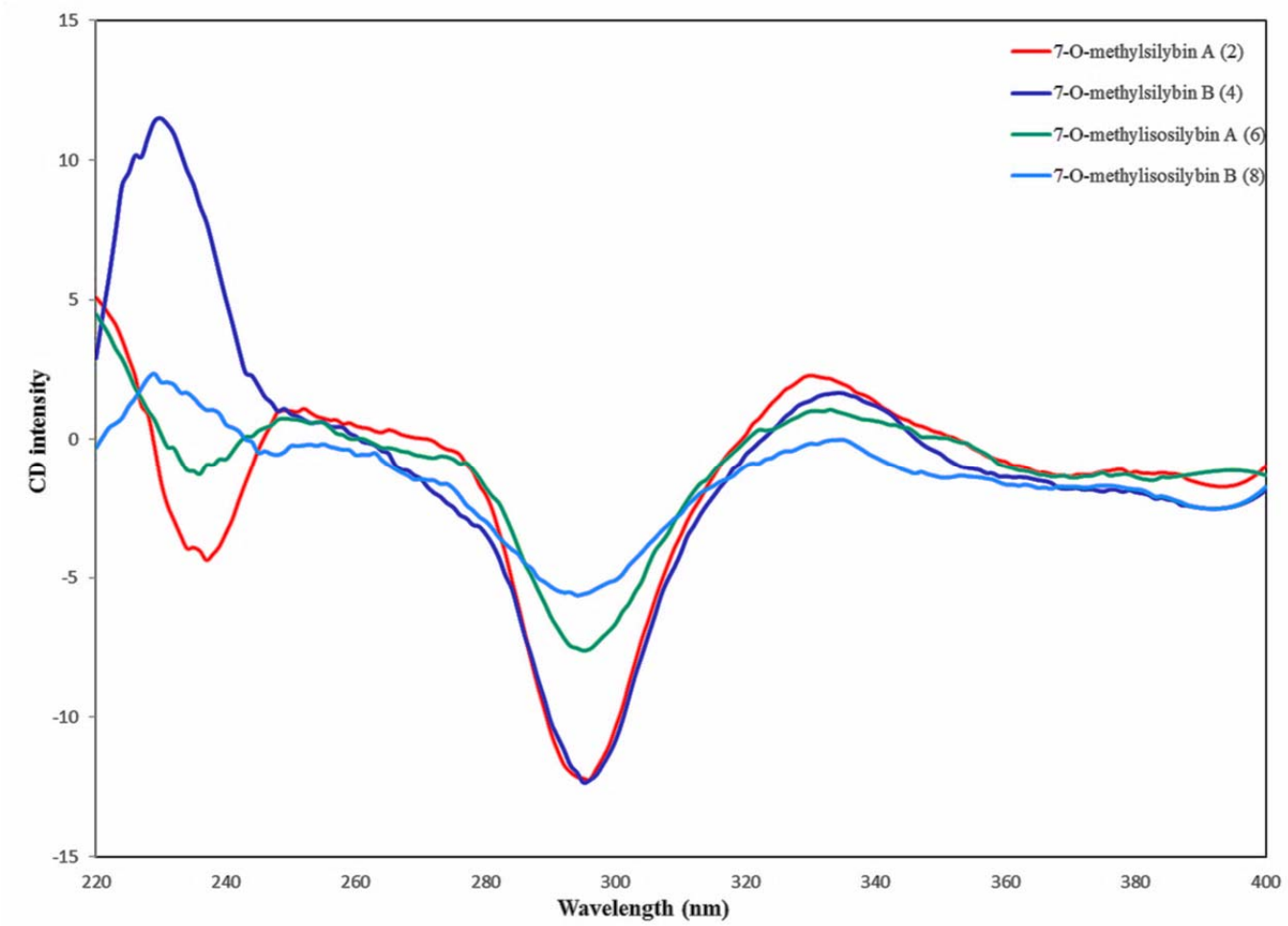

Figure 1.58. Circular Dichroism (CD) spectra of 7-*O*-methylflavonolignans

1.6. Biological Assay

1.6.1. Anti-proliferative assay

The antiproliferative/cytotoxic activities of all compounds were examined against a human hepatoma cell line, Huh7.5.1,[115] as described previously.[116] Briefly, 10,000 cells per well were plated in 96-well plates, and following overnight incubation, were incubated with increasing concentrations of compounds. Cell viability was measured 72 h later using the ATPlite kit, as described previously,[109] and an IC_{50} value was calculated by linear regression using GraphPad Prism.

1.6.2. Anti-viral assay

Cells (150,000) were plated in 12-well plates, and the next day cells were infected with JFH-1, a HCV that grows well in Huh7.5.1 cells, at a multiplicity of infection of 0.05 focus forming units per cell. Virus inocula were removed 5 h post-infection and replaced with fresh medium containing test compounds. Protein lysates were harvested 72 h later, and HCV proteins were detected by Western blot analyses as described previously.[109]

1.6.3. Inhibition of drug metabolizing enzymes

Milk thistle flavonolignans and 7-*O*-methylated analogues were evaluated as inhibitors of CYP2C9, CYP3A, and UGT activity using the probe substrates (*S*)-warfarin,

midazolam, and 4-methylumbelliferone (4-MU), respectively. *Inhibition of CYP2C9 activity*. Incubation mixtures consisted of pooled HLM (0.1 mg/mL microsomal protein), (*S*)-warfarin (4 μM), flavonolignan or 7-*O*-methylated analogue (10 or 100 μM), and potassium phosphate buffer (100 mM, pH 7.4). The CYP2C9 inhibitor sulfaphenazole (1 μM) was used as a positive control. Control incubation mixtures contained 0.75% MeOH (v/v) in place of flavonolignan/7-*O*-methylated flavonolignan or sulfaphenazole. Incubation mixtures were analyzed for 7-hydroxywarfarin by LC/MS-MS as described previously.[117] *Inhibition of CYP3A activity.* Incubation mixtures consisted of pooled HIM (0.05 mg/mL microsomal protein), midazolam (4 μM), flavonolignans or 7-*O*-methylated analogue (10 or 100 μM), and potassium phosphate buffer (100 mM, pH 7.4) supplemented with magnesium chloride (3.3 mM). The CYP3A inhibitor ketoconazole (1 μM) was used as a positive control. Control incubation mixtures contained 0.1% DMSO (v/v) in place of flavonolignan/7-*O*-methylated flavonolignan or ketoconazole. Incubation mixtures were analyzed for 1′-hydroxymidazolam by LC/MS-MS as described previously.[118] *Inhibition of UGT activity*. Incubation mixtures consisted of pooled HLM (0.4 mg/mL microsomal protein), 4-MU (100 μM), flavonolignan or 7-*O*-methylated analogue (10 or 100 μM), bovine serum albumin (BSA, 0.05%), and Tris-HCl buffer (0.1 M, pH 7.5) supplemented with magnesium chloride (5 mM). The UGT inhibitor diclofenac (400 μM) was used as a positive control. Control incubation mixtures contained 0.2% MeOH (v/v) in place of flavonolignan/7-*O*-methylated flavonolignan or diclofenac. Incubation mixtures were analyzed for 4-MU depletion by fluorescence as described previously.[119]

Data were analyzed statistically using SigmaStat (version 3.5; Systat Software, Inc., San Jose, CA) and are presented as means ± SDs of triplicate incubations. Concentration-dependent inhibition of each flavonolignan/7-*O*-methylated analogue and comparisons between flavonolignan and 7-*O*-methylated analogue at 100 μM were evaluated by two-way analysis of variance (ANOVA) with Bonferroni adjustment for multiple comparisons; $p < 0.05$ was considered significant.

1.7. Development of Flavonolignans Separation Using Pentaflurophenyl Propyl (PFP) Column

1.7.1. Introduction

Endcapped octadecyl silica (ODS) C18 column played an important role in the separation of flavonolignans diastereoisomers and it was used for a long time. Separation on the pentafluorophenyl propyl (PFP) column showed good resolution, enhanced the separation and helped to remove some unknown compounds. The PFP column has some properties for solute retention on fluorinated phases including: dipole–dipole interactions; π-π interactions; charge transfer and ion-exchange mechanism.[121] This column helped to remove small impurities that were not separated using YMC C18. It is important to note that there is no separation for diastereoisomers on PFP.

1.7.2. Separation Methods

To purify the compounds, two different reverse-phase columns [ODS-A C18 (5 μm; 250 × 20 mm) and PFP (5 μm; 250 × 21 mm)] were examined. Accordingly, each flavonolignan was purified until >98% pure, as measured by analytical HPLC. Silybin B were purified using a gradient of 20:80 to 40:60 CH_3CN:H_2O (0.1 % formic acid) over 20 min and hold 5 min. Isosilybin B was purified using a gradient of 20:80 to 40:60 CH_3CN:H_2O (0.1 % formic acid) over 45 min. Silychristin and isosilychristin fraction mixture was purified using two methods first, 15:85 to 36:64 CH_3CN:H_2O (0.1 % formic acid) over 40 min. Second method was using a gradient of 20:80 to 42:58 CH_3CN:H_2O (0.1% formic acid) over 35 min.

Analytical method: gradient of 20: 80 to 40:60 $CH_3CN:H_2O$ (0.1% formic acid) over 20 min 40: 60 hold for 5 min, using PFP column

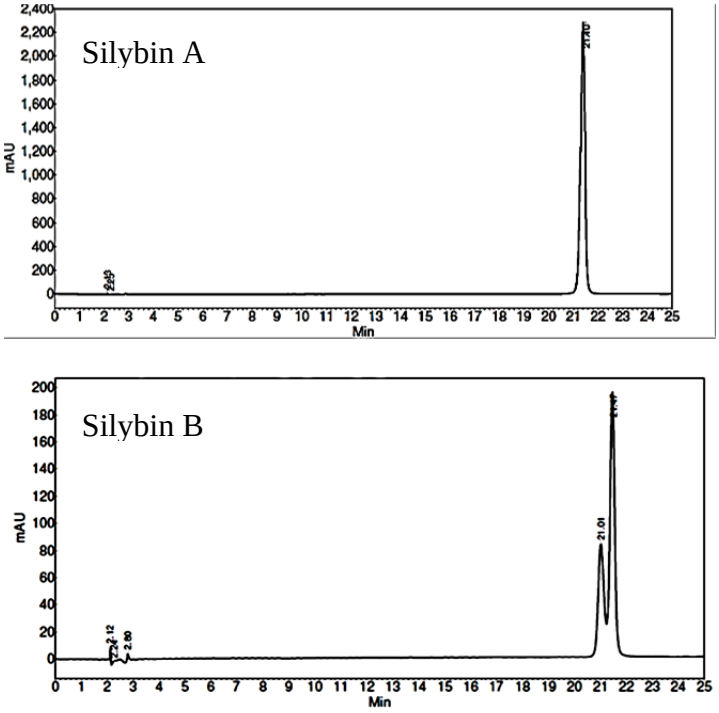

Separation method: gradient of 20: 80 to 40:60 $CH_3OH:H_2O$ over 20 min 40: 60 hold for 5 min, using PFP column

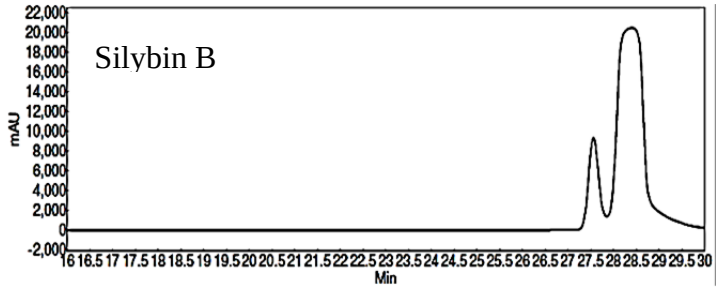

Figure 1.59. HPLC chromatograms analytical and separation of silybin A and silybin B at 288 nm

Analytical method: gradient of 20: 80 to 60:40 $CH_3CN:H_2O$ (0.1% formic acid) over over 30 min using PFP column

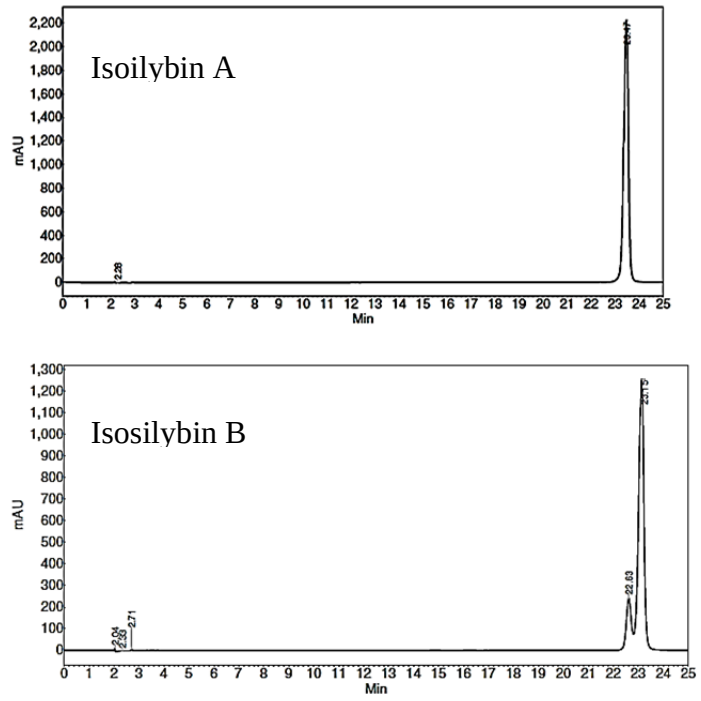

Separation method: gradient of 20: 80 to 60:40 $CH_3CN:H_2O$ (0.1% formic acid) over over 45 min using PFP column

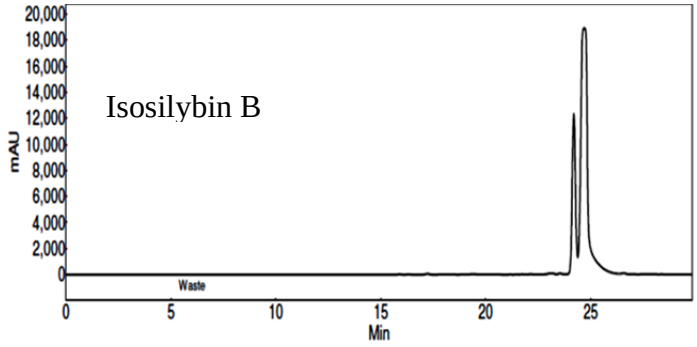

Figure 1.60. HPLC chromatograms analytical and separation of isosilybin A and isosilybin B at 288 nm

Analytical method: gradient of 20: 80 to 60:40 CH_3CN:H_2O (0.1% formic acid) over over 30 min using PFP column

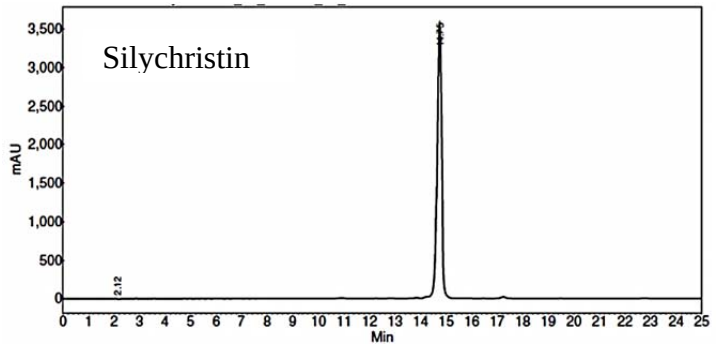

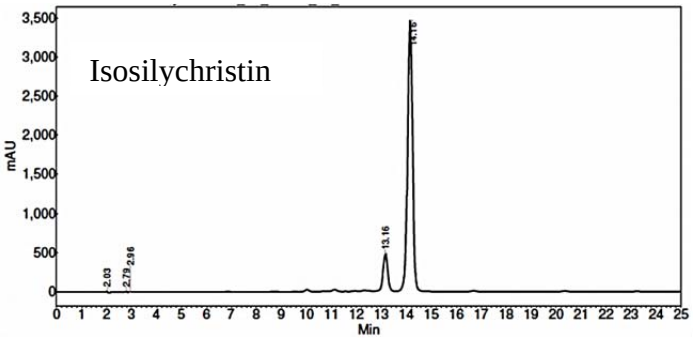

Analytical method: gradient of 5: 90 to 45:55 CH_3CN:H_2O (0.1% formic acid) over over 30 min using PFP column

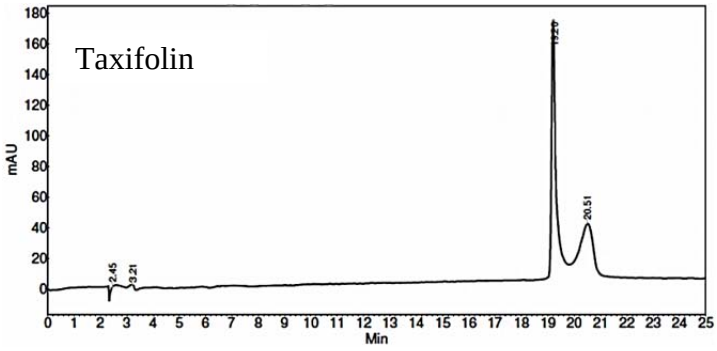

Figure 1.61. HPLC chromatograms analytical of silychristin, isosilychristin and taxifolin at 288 nm

Separation method A: 15: 75 to 36:64 $CH_3CN:H_2O$ (0.1% formic acid) over 40 min using PFP column

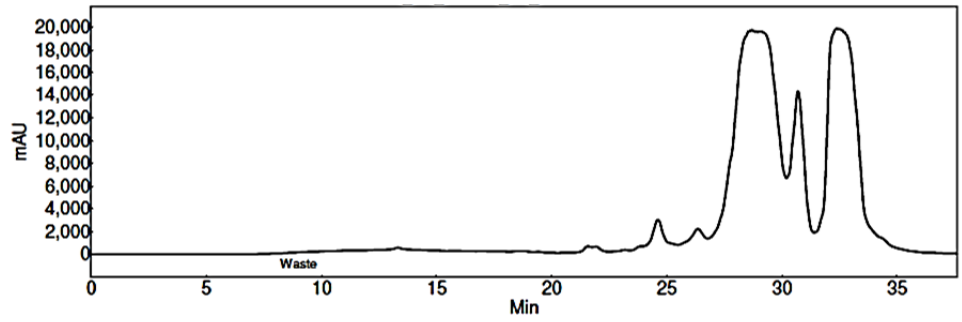

Separation method B: 20: 80 to 42:58 $CH_3CN:H_2O$ (0.1% formic acid) over over 35 min using PFP column.

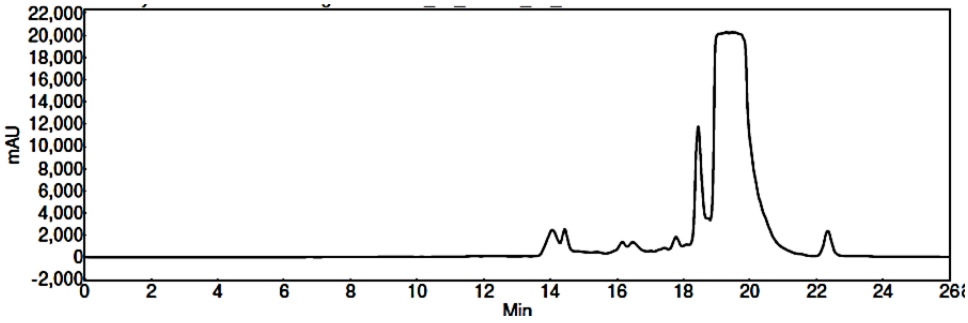

Figure 1.62. HPLC chromatograms separation of silychristin and isosilychristin at 288 nm

CHAPTER II

MECHANISTIC STUDY OF THE BIOMIMETIC SYNTHESIS OF FLAVONOLIGNAN DIASTEREOISOMERS

This project was submitted for publication.

2.1. Introduction

2.1.1. Flavonolignans biosynthetic hypothesis

Flavonolignans (**1-7**, Fig. 2.1) are characterized by the presence of a flavonoid moiety (taxifolin) that is linked to a phenylpropane (coniferyl alcohol).[6,121,122] Within flavonolignans, two pairs of *trans*-disteroisomers have been characterized with respect to the relative configuration at the C-7″ and C-8″ in the 1,4-benzodioxane ring, silybinin (silybin A and silybin B) and isosilybinin (isosilybin A and isosilybin B).[7,20,62] In contrast, silychristin and isosilychristin have dihydrobenzofuran rings and silydianin contains a structurally more complex bicyclo[2.2.2]octenone with a hemiketal (Fig. 2.1)[6] It has been proposed that flavonolignans are biosynthetically derived from an oxidative coupling reaction of coniferyl alcohol and taxifolin (Scheme 2.1).[3,123-126]

The mechanisms presented are typically based on Freudenberg's hypothesis for the synthesis of lignans from coniferyl alcohol. For the flavonoligans, this involves single electron oxidation of both coniferyl alcohol and taxifolin individually and then combination of these two radicals to synthesize silibinin and isosilibinin. Besides free radical coupling reaction, Diels-Alder reaction was proposed as a possible reaction for silydianin formation.[12]

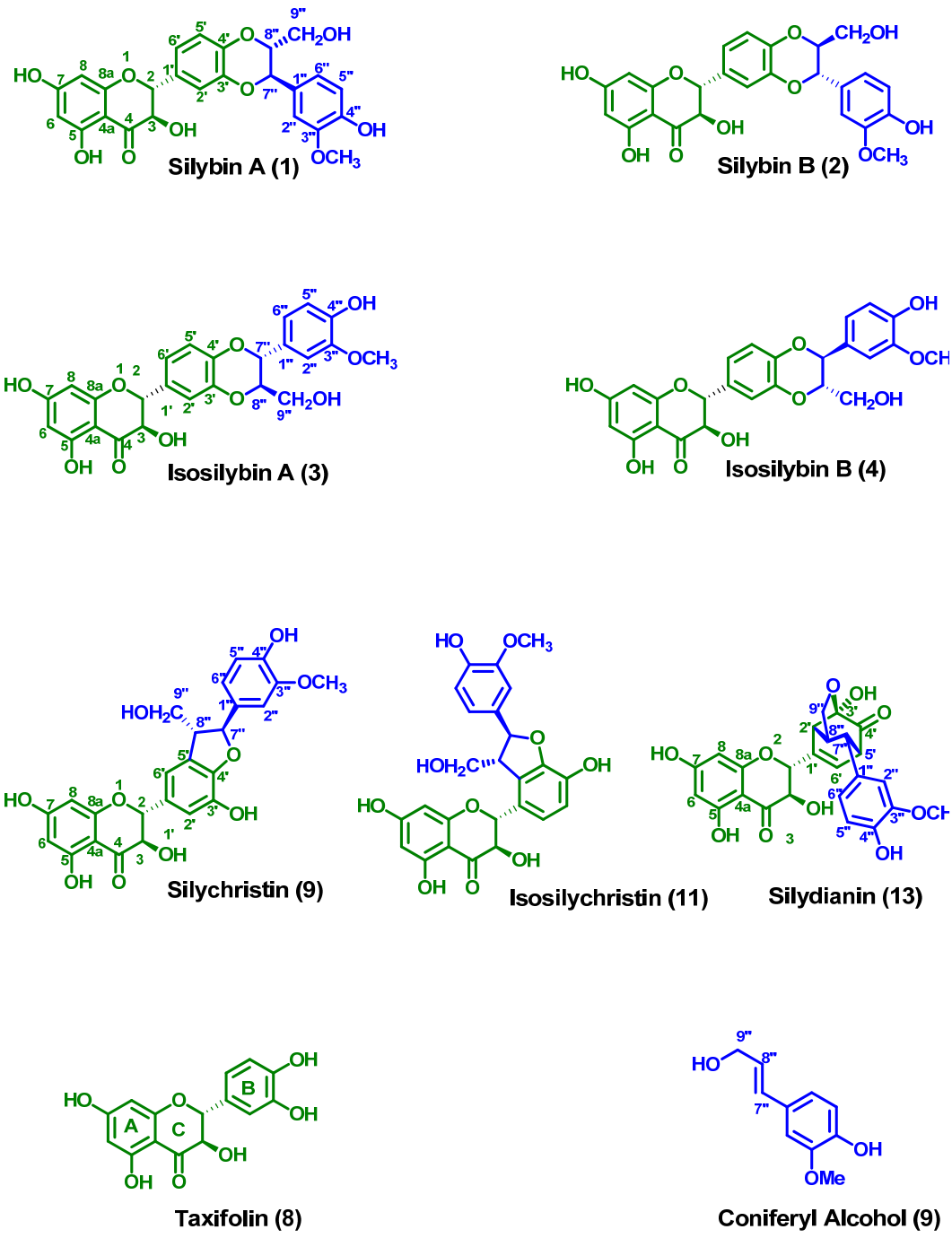

Figure 2.1. Flavonolignans Isolated from Silymarin and their Precursors.

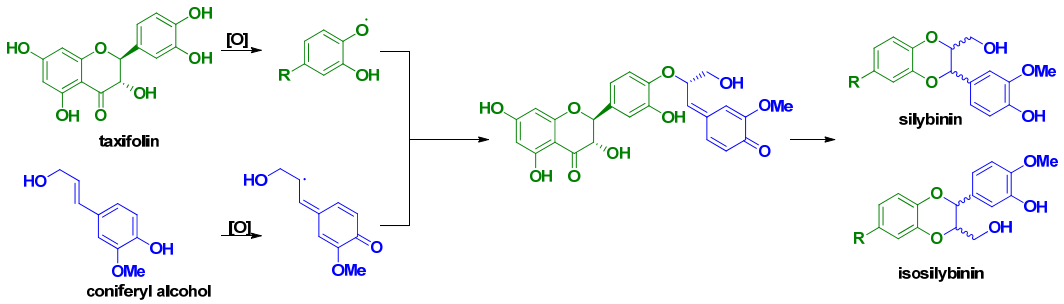

Scheme 2.1. Previously Proposed Flavonolignans Biosynthesis Theory.

2.1.2 Biomimetic synthesis of flavonolignans

The biomimetic synthesis is a reaction or sequence of reactions that mimic the biosynthetic pathway.[127,128] The concept of biomimetic synthesis was firstly introduced in 1917 by Sir Robert Robinson (1886-1975, Nobel Prize 1947) at Oxford University and is still considered.[130] Robinson's synthesis of tropinone, an alkaloid, from succindialdehyde (1), methylamine and acetone dicarboxylic acid (2) under Mannich reaction conditions was the first example of biomimetic synthesis.[128] This biomimetic strategy reduced Willstätter's 1903 seventeen step synthesis starting with suberone into a single step.[127,129]

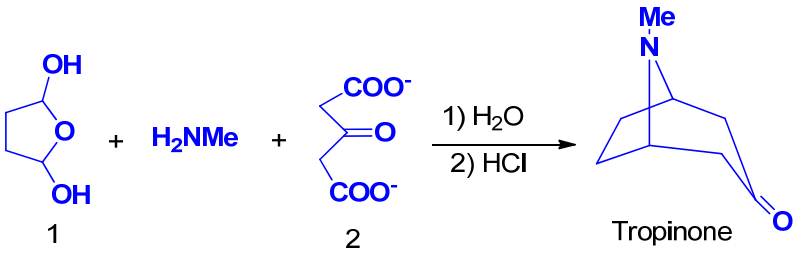

Scheme 2.2. Robinson's Biomimetic Synthes of Tropinone.

In the area of flavonolignans synthesis, the first total synthesis was before the correction of silybin structures in 1971 by Mishima and co-worker and later it was found out this synthesis was of isosilibinin.[130,131] In 1985, Tanaka and co-worker achieved the first total synthesis of silybinin. Soon after, the synthesis of silychristin was reported in 1988, again by the Tanaka group. The biomimetic synthesis of flavonolignans were first reported by Merlini and co-worker in 1979.[131] In this synthesis they used silver oxide to promote the reaction of taxifolin with coniferyl alcohol to yield a 1: 1 mixture of silybinin and isosilybinin. This synthesis was before isolation and structure elucidation of flavonolignans **1-4** (Fig. 2.1).

Recently, Guz, 2000, used Merlini's biomimetic method to synthesize hydnocarpin, structurally related flavonolignans with 1,4-benzodioxane ring system, which isolated from *hydnocarpus wightiana*.[132,133] In addition to using silver carbonate to oxidize the starting materials, they used horseradish peroxidase (HRP) enzyme to promote the reaction of luteolin with coniferyl alcohol to yield a racemic mixture of hydnocarpin and hydnocarpin-D. Reactions under Ag_2CO_3 oxidation yielded a mixture

having the major product hydnocarpin-D and the horseradish peroxidase (HRP) reactions major product hydnocarpin (Scheme 2.3).[133]

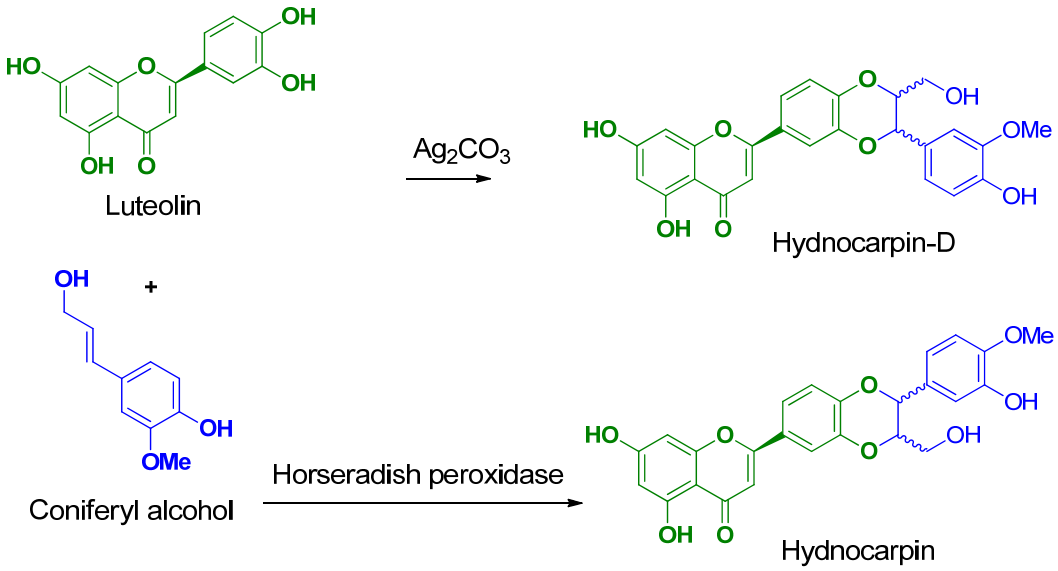

Scheme 2.3. Biomimetic Synthesis of Hydnocarpin and Hydnocarpin-D.

Interestingly, most of the reported mechanisms for this transformation[131,134] involve single electron oxidation of both coniferyl alcohol and taxifolin individually and then combination of these two radicals to synthesize silybinin and isosilybinin (Scheme 2.4, option 1).

While there is a slight possibility that this type of pathway could occur in an enzyme pocket, the probability of two radicals being formed in solution from silver oxide and then combining productively is beyond the realm of possibilities. This is due to the fact that the concentration of each radical will be extremely low, due to the inherent reactivity of the reactive intermediates. Since the rate of the reaction is directly

correlated to the concentration of each radical, the reaction rate will be essentially zero. Given that this unlikely biosynthetic proposal, often cited as Freudberg's proposal even though he did not appear to ever propose such a mechanism, is still referred to in the current literature for these compounds, we decided to perform a more thorough exploration of the biosynthetic options. Herein we report the results of our biosynthetic analysis, which suggests that flavonolignans could be derivative through initial single-electron oxidation of coniferyl alcohol, coupling to taxifolin, and finally an additional oxidation to yield silybinin and isosilybinin.

2.2 Results and Discussion

2.2.1. Mechanistic possibilities for biomimetic synthesis

The conversion of coniferyl alcohol and taxifolin to silybinin and isosilybinin necessarily requires an oxidation. The oxidant for this conversion is an enzyme in the natural environment but it has been shown that silver salts can also efficiently effect this conversion. Since silver oxidations typically occur through a series of single electron transfers, the various mechanistic options were explored (Scheme 2.4). In order to resolve the different mechanistic options, the various logical processes were explored. Specifically, the process necessarily involves three steps: two single electron oxidations and the coupling of taxifolin to coniferyl alcohol (or an oxidized variant of either partner). The five options discussed below cover all of the logical sequences of these three reactions.

As mentioned earlier, the prominent proposal in the literature involves simultaneous oxidation of both coniferyl alcohol and taxifolin and then combination of the resultant radicals to form ether **14** (scheme 2.4) which undergoes rapid addition of the phenol to the electrophilic *p*-quinone methide to yield silybin A (Option 1; Scheme 2.4). The same mechanism with opposite stereoselectivity to create ether **14** results in the formation of silybin B and the analogous reactions where the phenoxide radical of taxifolin is formed would produce the isosilybinin diastereomers. Although this mechanism is commonly invoked in the literature, there was no evidence to support it and is counter to the first principles discussed earlier.

Option 2 involves two sequential oxidations of taxifolin to yield an o-quinone (12). This option seemed much more possible since it is highly precidented to react an o-quinone with an alkene in a Diels-Alder reaction.[135] Additionally, the Diels-Alder reaction conserves the stereochemistry of the dienophile, so the *trans*-stereochemistry at C7" and C8" could result from this concerted cycloaddition.

Options 3 and 4 are similar since they both involve single oxidation of either taxifolin (Option 3) or coniferyl alcohol (Option 4) and then coupling to coniferyl alcohol or taxifolin, respectively. The resultant radicals are further oxidized to yield silybin A. These two options seem possible since both coniferyl alcohol and taxifolin are electron-rich and likely susceptible to oxidation or reaction with a radical.

The final option explored involves two sequential oxidations of coniferyl alcohol and subsequent coupling to taxifolin (Option 5). It is expected that the oxidation reactions

occur to yield coniferyl aldehyde (**16**), however, it is unlikely that the redox reaction of this aldehyde and taxifolin would occur to yield silibin A. For the sake of this study, all 5 of these mechanistic options were considered options while interrogating the mechanism via judicious choices of reaction conditions.

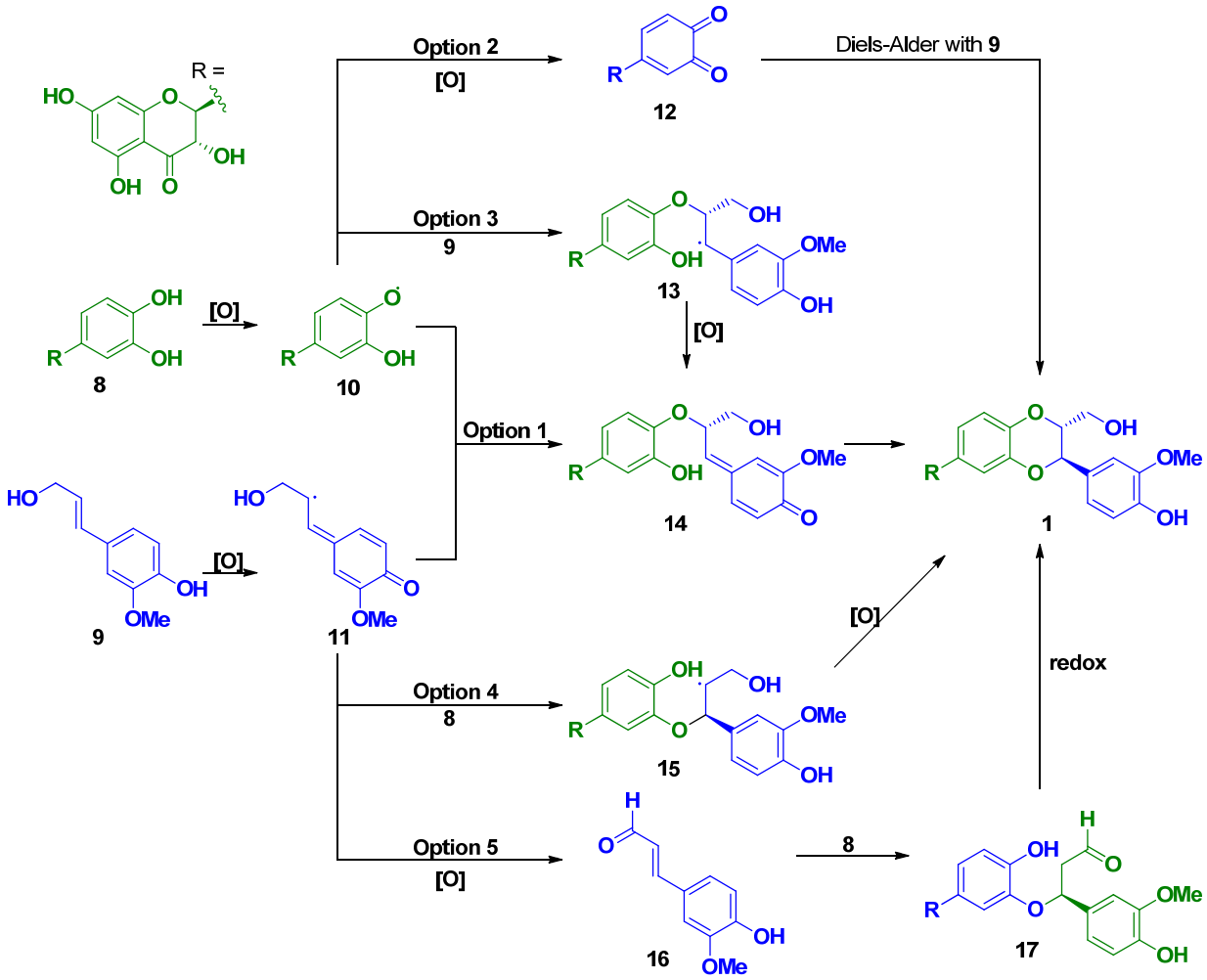

Scheme 2.4 Mechanistic Options for the Biosynthesis of Flavonolignans.

2.2.2. Biomimetic synthesis and optimization

The biomimetic synthesis started with natural taxifolin and commercially available coniferyl alcohol. Taxifolin was isolated from milk thistle extract in >90% purity (see experimental section). Since the starting material is relatively expensive and taxifolin isolated in several purification steps, reactions were initially explored on small scale (~1 mg taxifolin) and monitored by HPLC. The reaction conditions were based upon a procedure described by Merlini *et al.*,[131] with moderate optimizations. Several solvents, oxidizing agents and temperature were tested and the best results were obtained when reacting 1 equivalent of taxifolin with 2 equivalents of coniferyl alcohol in ethyl acetate containing 4 equivalents of Ag_2O at 75 °C for 96 hours. These conditions afforded a mixture of silybin A, silybin B, isosilybin A, and silybin B in 49% yields. The biomimetic synthesis enhanced the yield of flavonolignans, particularly of the highly potent compound, isosilybin B (Scheme 2.4, Fig. 2.2, and 2.3).

Flavonolignans **1**-**4** were separated by HPLC in greater than 99% purity, and their structures were confirmed by NMR (see experimental for more details). In addition to these four flavonolignans, coniferyl aldehyde and neolignin **18** were produced in moderate amounts (Scheme 2.5, Fig.2.3). It is worth noting that trace amounts of flavonolignans **5**-**7** appear to be forming during some of the reactions, but the quantities were never sufficient to verifiably confirm their formation.

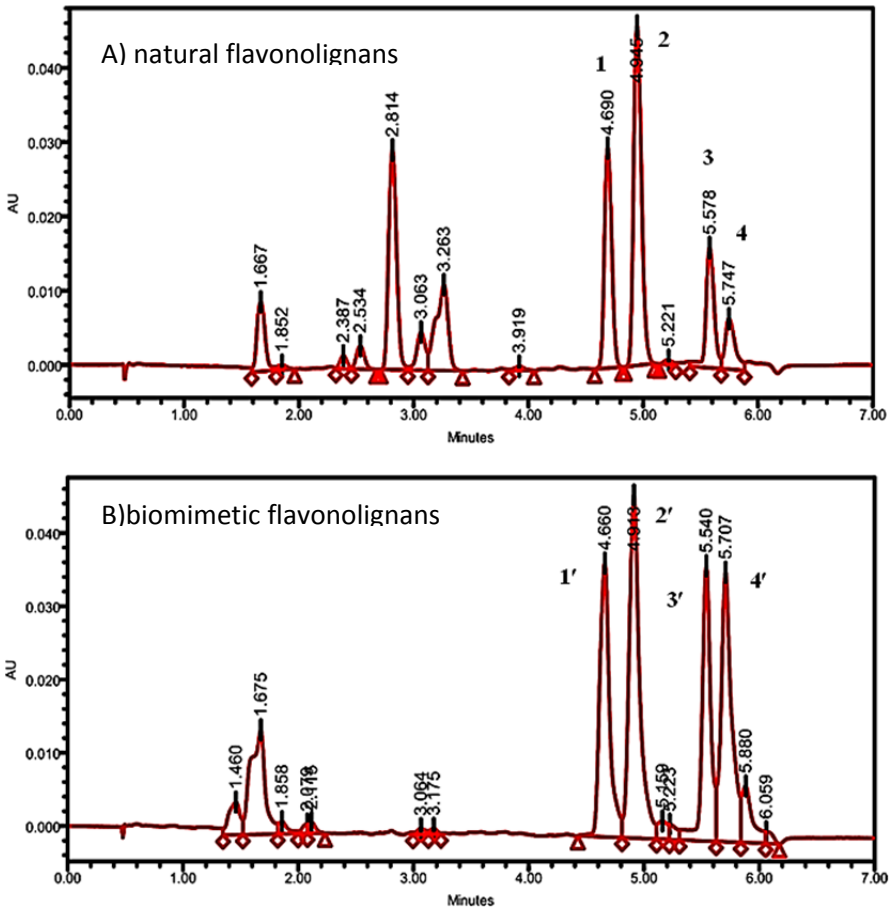

Figure 2.2. UPLC Chromatograms of Biomimetic Flavonolignans Compared with Natural Flavonolignans

Compounds were silybin A (**1**) & (**1′**); silybin B (**2**) & (**2′**); isosilybin A (**3**) & (**3′**); isosilybin B (**4**) & (**4′**).

Method: gradient of 5:95 to 80:20 over 10 min, CH_3OH:H_2O (HSST3 column) at 288 nm.

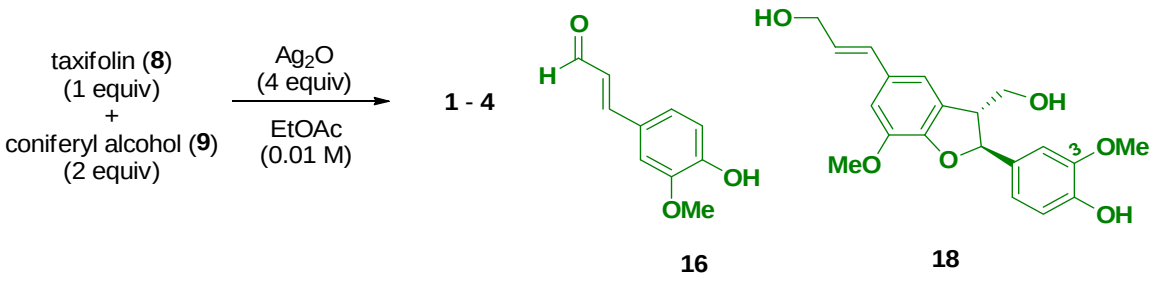

Scheme 2.5. Biomimetic Synthesis of Silybinin and Isosilybinin and Other Byproducts.

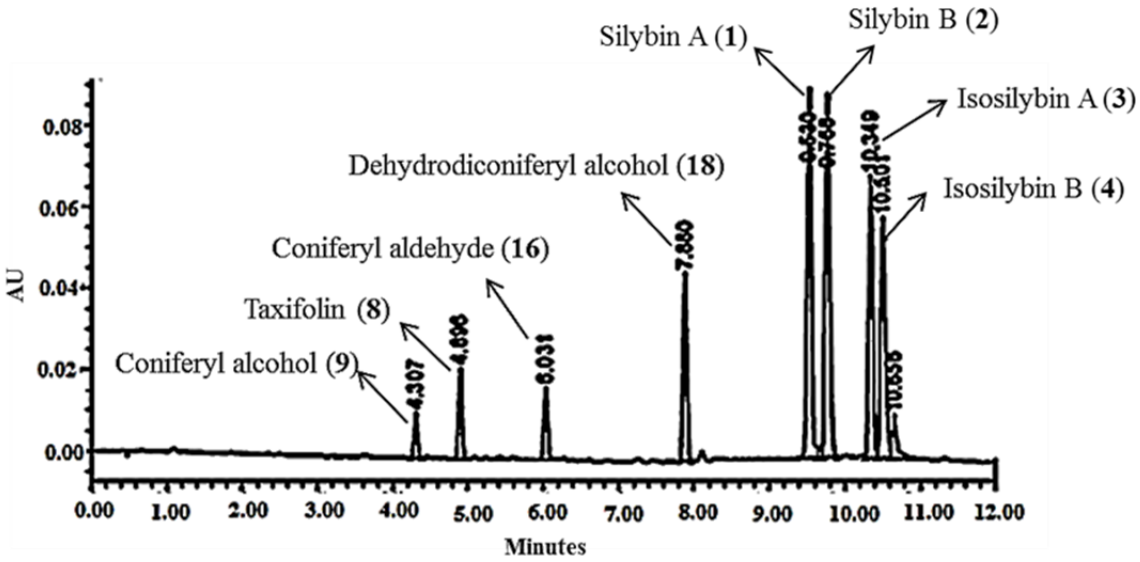

Figure 2.3. UPLC trace of Biomimetic Reaction.

2.2.3. Mechanistic investigation reactions

The initial reaction to explore the mechanistic possibilities involved the reaction of *cis*-coniferyl alcohol with taxifolin using silver oxide. If Option 2 (Scheme 2.4) is occurring, the product would maintain a *cis*-relationship at C7" and C8" since the Diels-Alder reaction maintains the stereochemistry of the dienophile. With all of the other options, the stereochemistry of the initial coniferyl alcohol can be scrambled and presumably a *trans*-relationship would be produced since this is thermodynamically more favorable. Importantly, *cis*-coniferyl alcohol* was found to produce the identical products as *trans*-coniferyl alcohol (Scheme 2.6 ; Fig. 2.4). It is important to note that the *cis*-coniferyl alcohol did isomerize to *trans*-coniferyl alcohol under the conditions of this reaction, however, this isomerization occurred much more slowly than the rate of forming silybinin and isosilybinin. These results removed Option 2 from the list of possible mechanisms.

*this compound synthesized by Dr. Maria Elena Meza-Aviña

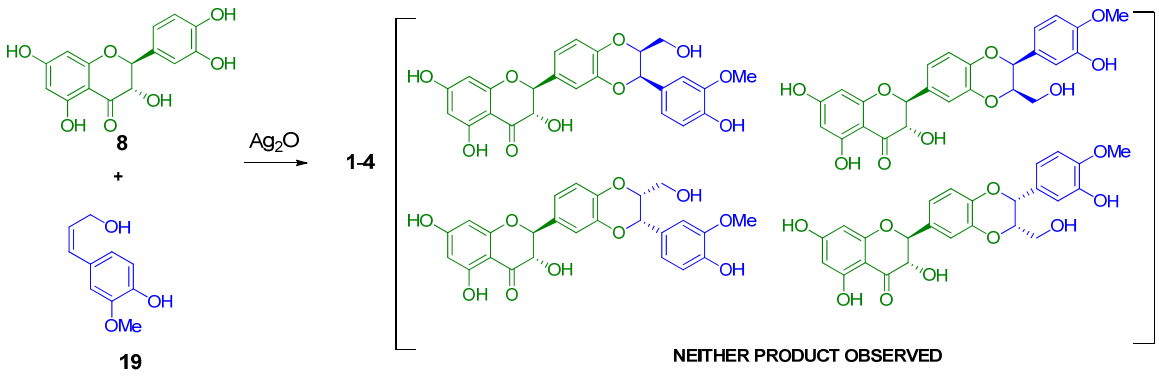

Scheme 2.6**.** Mechanistic Investigation into the Quinone Diels-Alder Possibility

The next key mechanistic reaction explored the oxidation abilities of coniferyl alcohol or taxifolin individually with silver oxide in the absence of the other compound (Scheme 2.7). Interesting, coniferyl alcohol is rapidly oxidized by silver oxide whereas taxifolin is practically inert to those oxidation conditions (Scheme 2.7; Fig. 2.5 and 2.6). The lack of reactivity towards oxidation of taxifolin implies that Options 1-3 in Scheme 2.4 are all not viable mechanisms and simplifies the possibilities to only Option 4 or 5. Importantly, further scrutiny of the oxidation of coniferyl alcohol in the absence of taxifolin revealed two major products were formed, coniferyl aldehyde and neolignan **18 (**Fig. 2.5). This verifies that two oxidations of coniferyl alcohol does yield coniferyl aldehyde, and also that the initial radical from single-electron oxidation is prone to reaction with an electron-rich phenol of a different molecule of coniferyl alcohol. Hypothetically, if taxifolin were in solution with this singly oxidized radical, it could similarly react to give silybinin and isosilybinin. Thus, the experiments by separate oxidations show that Options 1-3 and invalid, and that Options 4 or 5 are potential pathways.

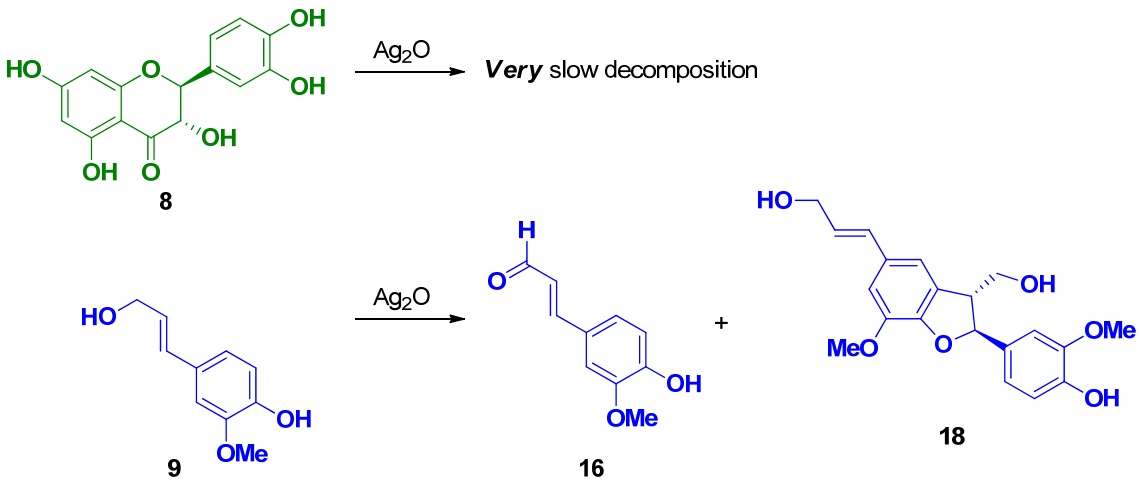

Scheme 2.7. Individual Oxidations of Taxifolin and Coniferyl Alcohol

As mentioned earlier, it did not seem likely that coniferyl aldehyde (16) would react with taxifolin to undergo a redox reaction and yield silybinin and isosilybinin. To test this, we simply examined the reaction of coniferyl aldehyde with taxifolin in the both presence and absence of silver oxide (Scheme 2.8; Fig. 2.7). As anticipated, silybinin and isosilybinin were not observed to be produced with this reaction. Thus, the only remaining mechanism is Option 4 where coniferyl alcohol is oxidized, taxifolin reacts with the radical, and then the compound is oxidized further to yield silybinin.

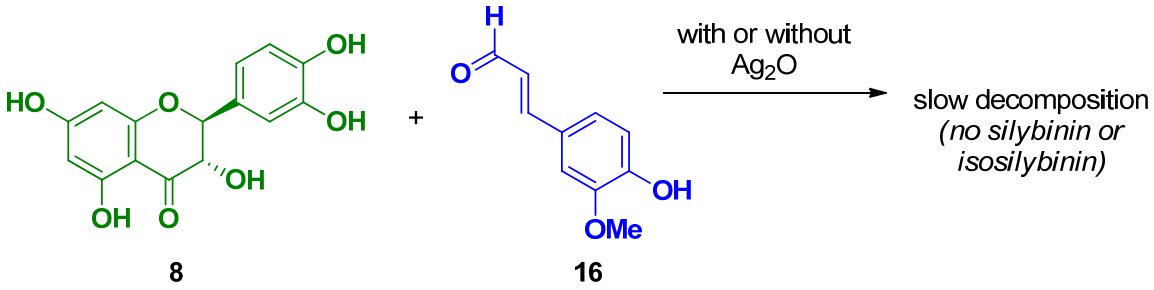

Scheme 2.8. Attempted Coupling of Coniferyl Aldehyde to Taxifolin

Our investigations in this area showed that none of the first three options were viable since taxifolin was not readily oxidized. Experiments showed consumption of coniferyl alcohol and formation of both coniferyl aldehyde and lignin **18** in the absence of taxifolin. Finally, we determined that coniferyl aldehyde and taxifolin do not react together in an isohypsic reaction to yield flavonolignans. Thus, all of the experiments perform only support the oxidation of coniferyl alcohol to generate an intermediate radical of coniferyl alcohol which combines with taxifolin and is subsequently oxidized to silybinin and isosilybinin (Scheme 2.9).

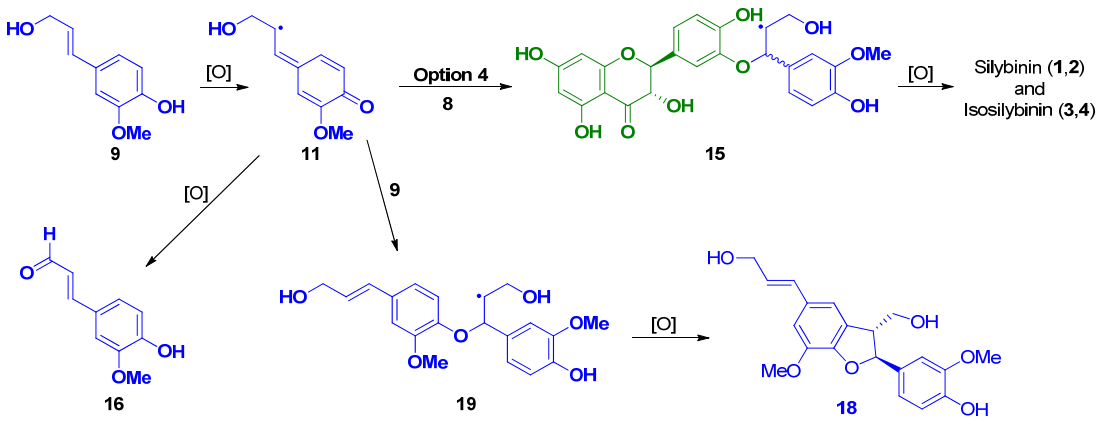

Scheme 2.9. Mechanistically Supported Biosynthesis of Flavonolignans

A) *Cis*-coniferyl

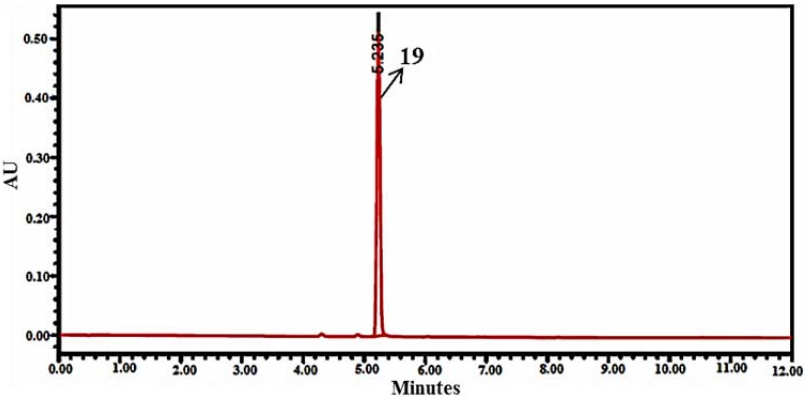

B) Reaction of *Cis* -coniferyl alcohol (2 equiv) with taxifolin (1 equiv) and Ag_2O (4 equiv).

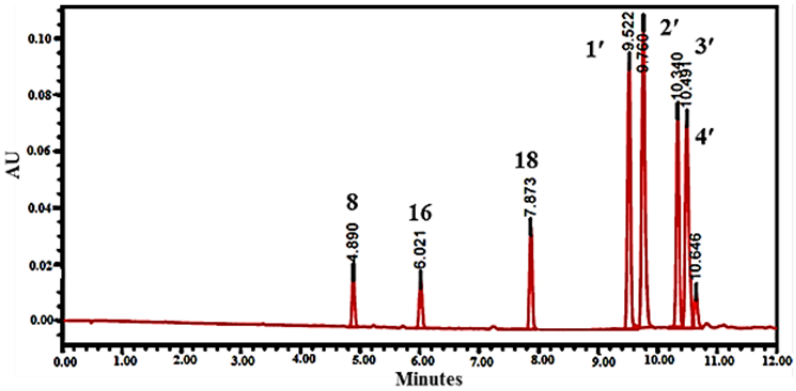

Figure 2.4**.** UPLC chromatograms of biomimetic reaction of Cis-coniferyl alcohol with taxifolin.
Method: gradient of 5:95 to 50:50 over 12 min, CH_3OH:H_2O (0.1% formic acid) (HSST3 column) at 288 nm. Reactions were in ethyl acetate ran for 96 h at 75 °C.

A) *Trans*-coniferyl

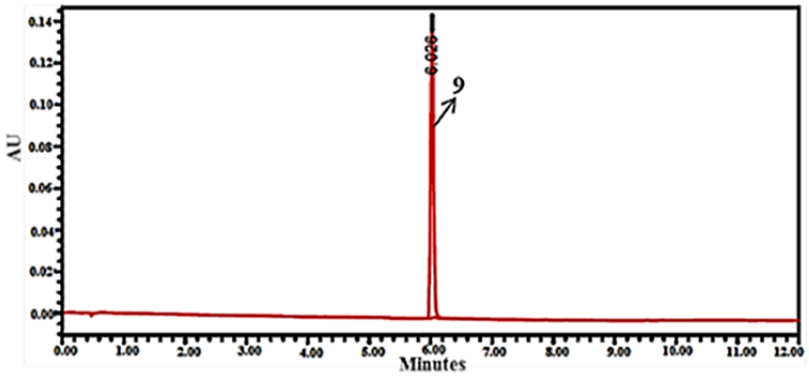

B) Oxidation reaction of *Trans* -coniferyl alcohol (2 equ) with Ag2O (4 equ).

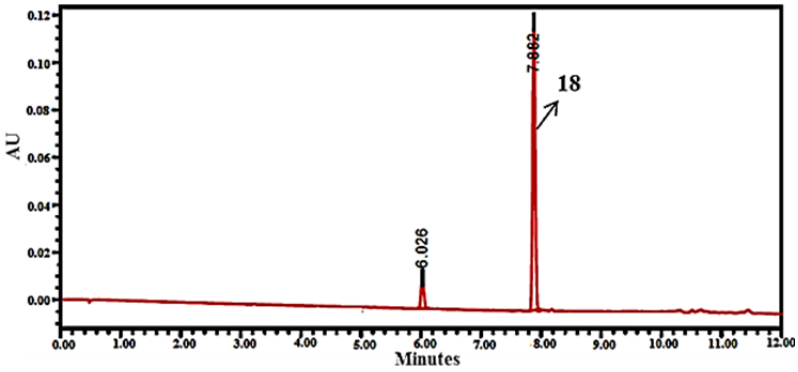

Figure 2.5. UPLC chromatograms of oxidation reaction of trans-coniferyl alcohol in absent of taxifolin.
Method: gradient of 5:95 to 50:50 over 12 min, CH_3OH:H_2O (0.1% formic acid) (HSST3 column) at 288 nm. Reactions were is ethyl acetate ran for 96 h at 75 °C.

A) Taxifolin

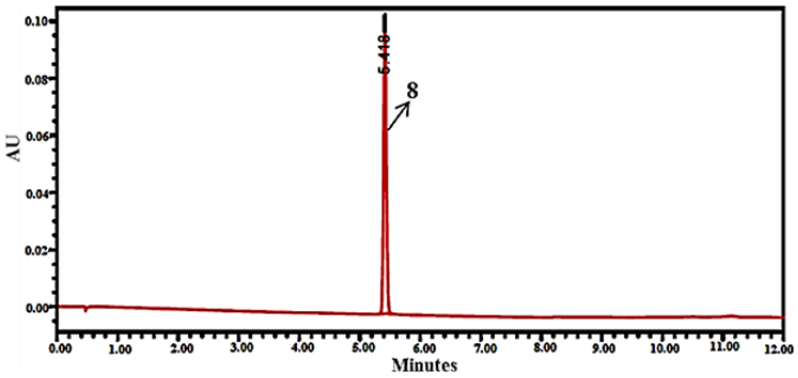

B) Oxidation reaction of taxifolin (1 equiv) with Ag_2O (4 equiv).

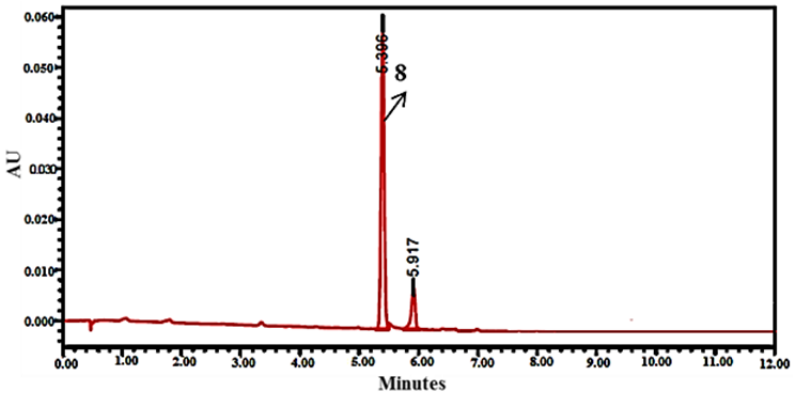

Figure 2.6. UPLC chromatograms of oxidation reaction of taxifolin in absence of coniferyl alcohol.
Method: gradient of 5:95 to 50:50 over 12 min, CH_3OH:H_2O (0.1% formic acid) (HSST3 column) at 288 nm. Reactions were in ethyl acetate ran for 96 h at 75 °C.

A) Coniferyl aldehyde

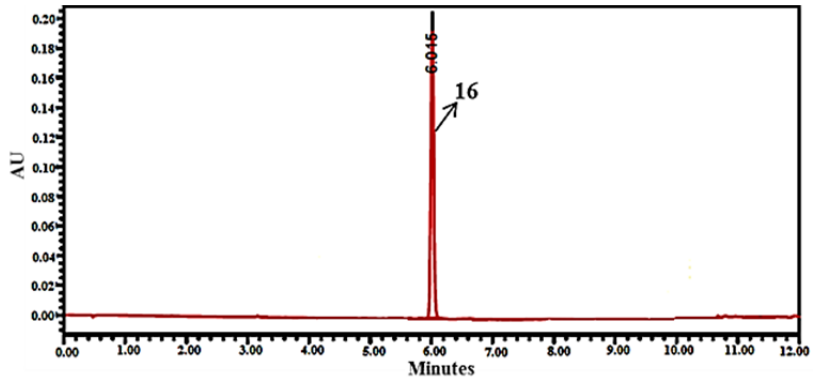

B) Oxidation reaction of coniferyl aldehyde (2 equiv) with taxifolin (1 equiv) and Ag_2O (4 equiv).

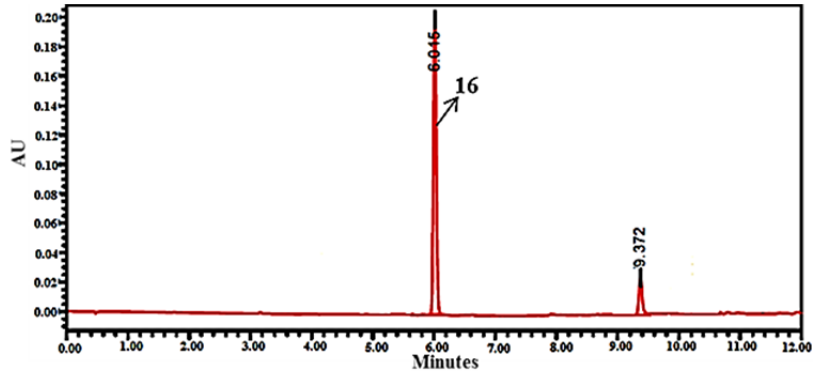

Figure 2.7. UPLC chromatograms of biomimetic reaction of coniferyl aldehyde with taxifolin.
Method: gradient of 5:95 to 50:50 over 12 min, CH_3OH:H_2O (0.1% formic acid) (HSST3 column) at 288 nm. Reactions were in ethyl acetate ran for 96 h at 75 °C.

2.3. Conclusion

In summary, a biomimetic synthesis of four major flavonolignans present in silymarin is reported, accomplished in one step, and careful analysis of the reactions and resulting products were used to support or refute possible mechanisms. From this analysis it is proposed that the biomimetic synthesis of flavonolignans likely proceeds by single electron oxidation of coniferyl alcohol, addition of taxifolin, and finally oxidation to yield silybinin and isosilybinin. This synthesis increases the yield of the most potent and biologically active of the flavonolignans, isosilybin B, and future studies will use this method to produce and study the activity of analogues of flavonolignans.

2.4. Experimental

2.4.1. Taxifolin purification

Taxifolin was isolated in >90% purity from milk thistle extract (silymarin) as described in fig 2.7). To purify taxifolin, two different reverse-phase columns [ODS-A C18 (5 µm; 250 × 20 mm) and PFP (5 µm; 250 × 21 mm)] were examined. taxifolin was purified until >90% pure, as measured by analytical UPLC. First method was 15:85 to 50:50 CH_3OH:H_2O (0.1 % formic acid) over 60 min using C18. Second method was using a gradient of 5:90 to 70:30 CH_3CN:H_2O (0.1% formic acid) over 30 min.

Method 1: Gradient of 15:85 to 50:50 over 60 min $CH_3OH:H_2O$ (YMC C-18 column).

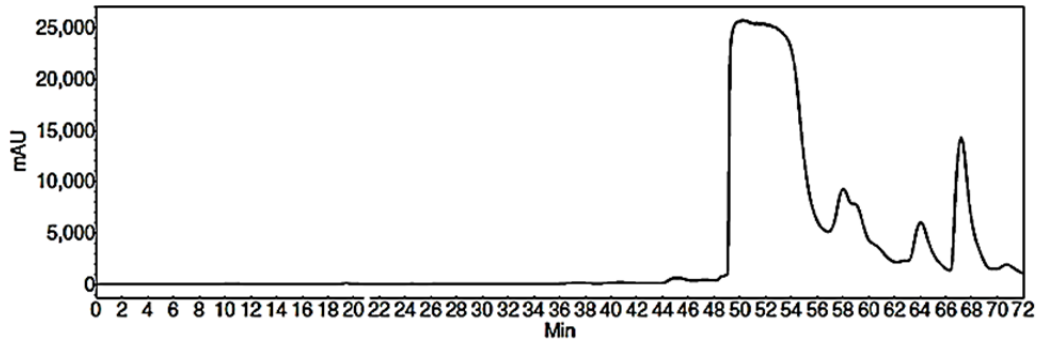

Method 2: Gradient of 5:90 to 70:30 over 30 min $CH_3CN:H_2O$ min PentaFlurophenyl Propyl (PFP) column.

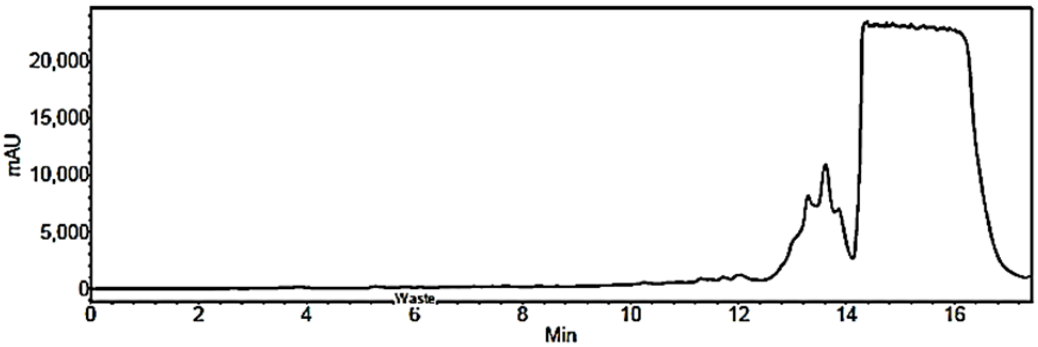

Figure 2.8**.** HPLC chromatograms of taxifolin separation at 288 nm.

2.4.2. Chemistry and Syntheses

To a 100 ml round-bottom flask, were dissolved taxifolin (105.9 mg, 0.348 mmol) and *E*-coniferyl alcohol (125 mg, 0.696 mmol) in ethyl acetate (30 mL, 0.01 M) under an atmosphere of nitrogen gas. After stirring for 10 min, Ag_2O (323 mg, 1.39 mmol) was added and the flask was covered with foil and equipped with a reflux condenser. The solution was stirred and heated to 75 °C for 96 h under an atmosphere of nitrogen gas. The reaction mixture was then cooled to room temperature and filtered through celite (Celite®545, 45µ) meshand washed with ethyl acetate. A yellow filtrate was concentrated under reduced pressure, dissolved in 2-3 ml ethyl acetate and centrifuged through a polypropylene eppendorf tube filter (0.22 µm), to remove any residues of Ag_2O. The crude product (225 mg) was purified by reverse-phase HPLC to afford flavonolignans with a total yield of 82.6 mg, (21.4 mg: 21.1 mg: 20.7 mg: 19.5 mg for **1′**, **2′**, **3′**, and **4′**, respectively), 52% of flavonolignans. In addition to the four major compounds, coniferyl aldehyde (**16**, 2.3 mg) and lignan **18** (13.6 mg) were isolated.

The reaction mixture was first purified via a gradient of 20:80 to 50:50 CH_3OH:H_2O over 90 min and hold for 20 min using YMC C18 (5 µm; 250 × 20 mm) column. The fractions with mixtures of isomers from the first purification were purified via other several rounds of a gradient of 20:80 to 50:50 over 50 min and hold for 40 min using YMC C18. The last purification step was by PFP column via a gradient of 20:80 to 40:60 CH_3CN:H_2O (0.1 % formic acid) over 30 min. (Fig. 2.8-2.11).

Method 1 PREP-HPLC of crude biomimetic reaction mixtures: gradient of 20:80 to 50:50 over 90 min, hold 50:50/ 70 min CH_3OH: H_2O (C18 column) at 288 nm.

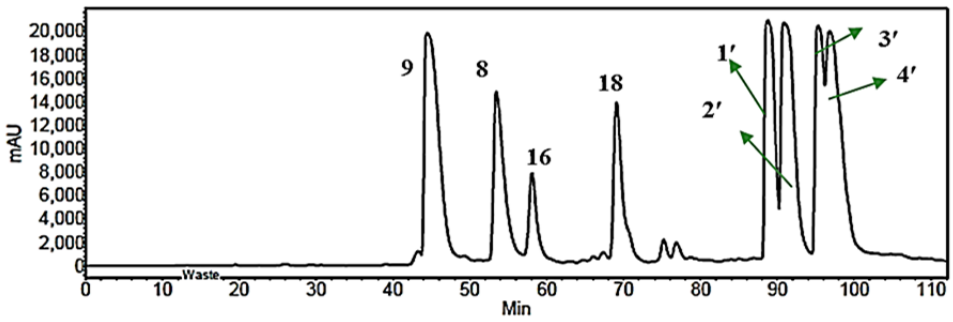

Method 2 Semi-PREP -HPLC of biomimetic silybin A and silybin B: gradient of 20:80 to 50:50 50 min, hold 50:50 over 40 min CH_3OH:H_2O (C18 column) at 288 nm.

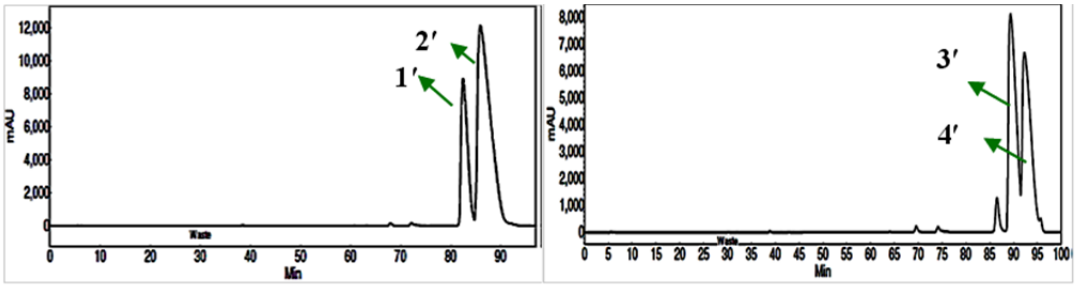

Method 3 PREP-HPLC using pentafluorophenyl propyl (PFP) column: Biomimetic silybin B was purified using a gradient of 20:80 to 40:60 over 30 min, CH_3CN:H_2O (0.1% formic acid) at 288 nm. Biomimetic isosilybin B was purified using a gradient of 20:80 to 60:40 over 45 min, CH_3CN:H_2O (0.1% formic acid) at 288 nm.

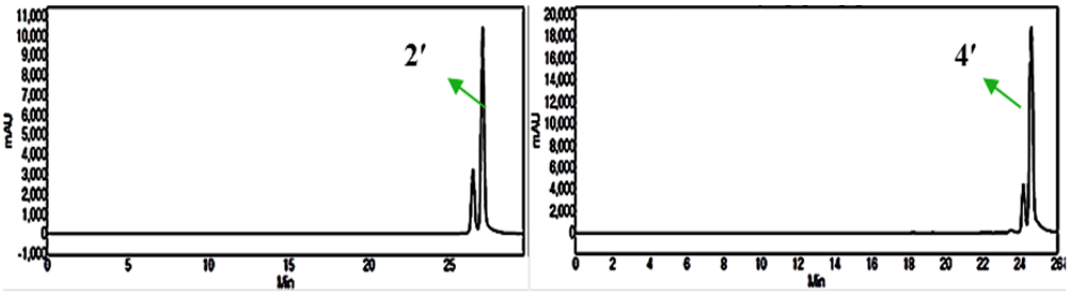

Figure 2.9. HPLC chromatograms example of biomimetic disteroisomers separation at 288 nm.

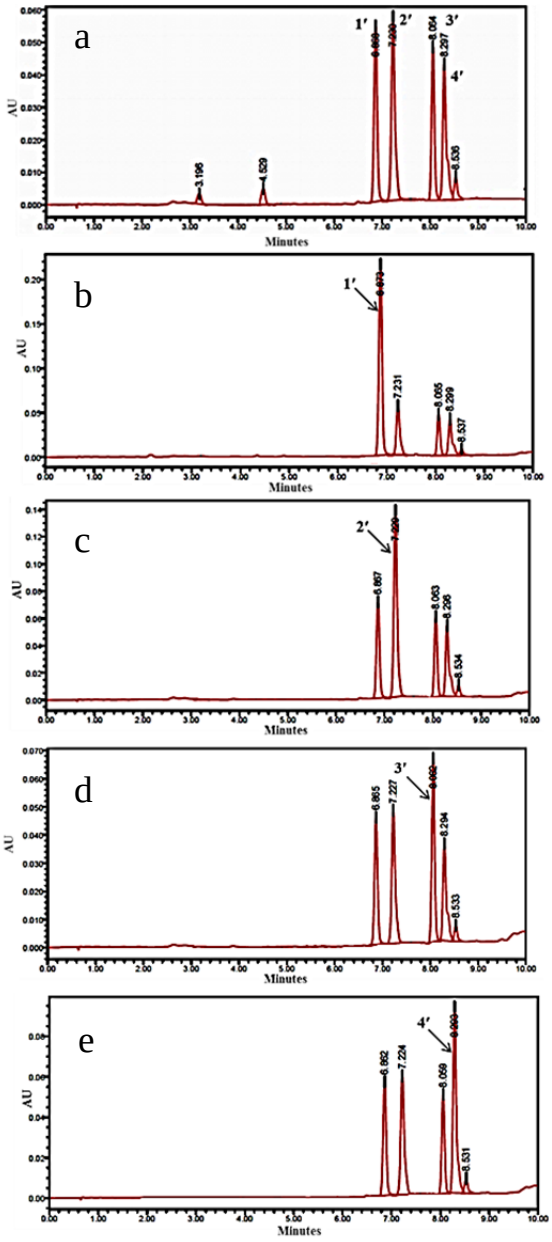

Figure 2.10. HPLC chromatograms of crude reaction mixtures (a) and co-injection of natural flavonolignans (b) silybin A (**1**); (c) silybin B (**2**); (d) isosilybin A (**3**); (e) isosilybin B (**4**) at 288 nm.
Method: gradient of 5:95 to 80:20 over 10 min, CH_3OH:H_2O (HSST3 column).

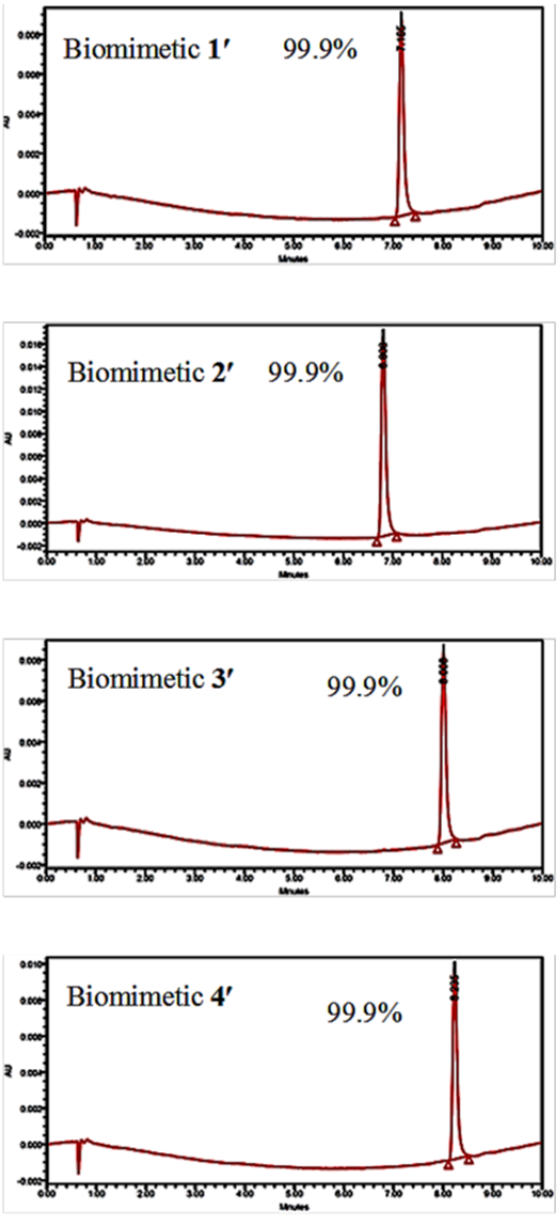

Figure 2.11. UPLC chromatograms of biomimetic flavonolignans.
Method: gradient of 5:95 to 80:20 over 10 min, CH_3OH:H_2O (HSST3 column) at 288 nm.

Flavonolignan **1** and Biomimetic **1′**

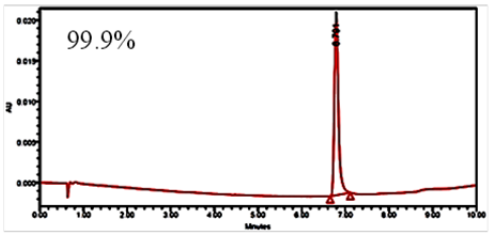

Flavonolignan **2** and Biomimetic **2′**

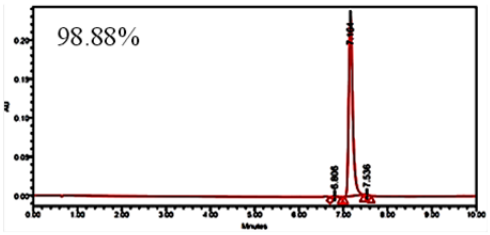

Flavonolignan **3** and Biomimetic **3′**

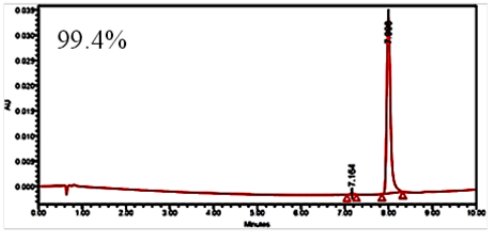

Flavonolignan **4** and Biomimetic **4′**

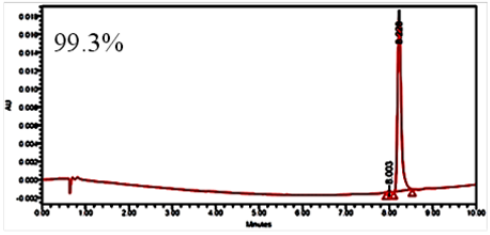

Figure 2.12. UPLC chromatograms of co-injection of biomimetic and natural flavonolignans.
Method: gradient of 5:95 to 80:20 over 10 min, CH_3OH:H_2O (HSST3 column) at 288 nm.

2.4.2.1. 4-(3-Hydroxy-prop-1-ynyl)-2-methoxy-phenol

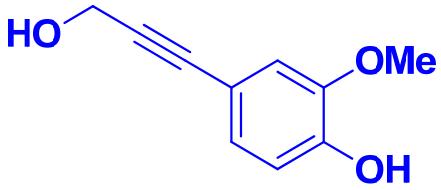

Figure 2.13. 4-(3-Hydroxy-prop-1-ynyl)-2-methoxyphenol.

To a dry flask with a stir bar were added 4-bromo-2-methoxy-phenol (1.00 g, 4.93 mmol), CuI (282 mg, 0.1479 mmol, 3 mol %), bis(triphenylphosphine)palladium(II) dichloride (104 mg, 0.1479 mmol, 3 mol %) and triethyl amine (10 ml). The flask was purged with nitrogen gas and propargyl alcohol was added with stirring. The reaction was heated to 95 °C for 4 hr, cooled to room temperature, filtered through celite, and concentrated under reduced pressure. The crude extract was purified by silica gel column chromatography (85:15, hexanes:ethyl acetate) to yield 80 mg of 4-(3-hydroxyprop-1-ynyl)-2-methoxyphenol (9 % yield) as a clear, colorless oil.

^{1}H NMR (500 MHz, $CDCl_3$) δ = 3.89 (s, 3H), 4.48 (s, 2H), 5.74 (s, 1H), 6.86 (d, J = 8.1 Hz, 1H), 6.95 (d, J = 1.5 Hz, 1H), 7.0 ppm (dd, J = 8.1, 1.7 Hz, 1H) (see, Fig. 2.14)..

^{13}C NMR (125 MHz, $CDCl_3$) δ = 51.9, 56.1, 85.5, 86.1, 114.1, 114.2, 114.7, 125.8, 146.3, and 146.6 (see, Fig. 2.15).

HRMS (APCI) m/z 179.06982 $[M+H]^+$ (calcd for $C_{10}H_{11}O_3$ 179.07137).

*: Compound synthesized by Dr. Maria Elena Meza-Aviña,

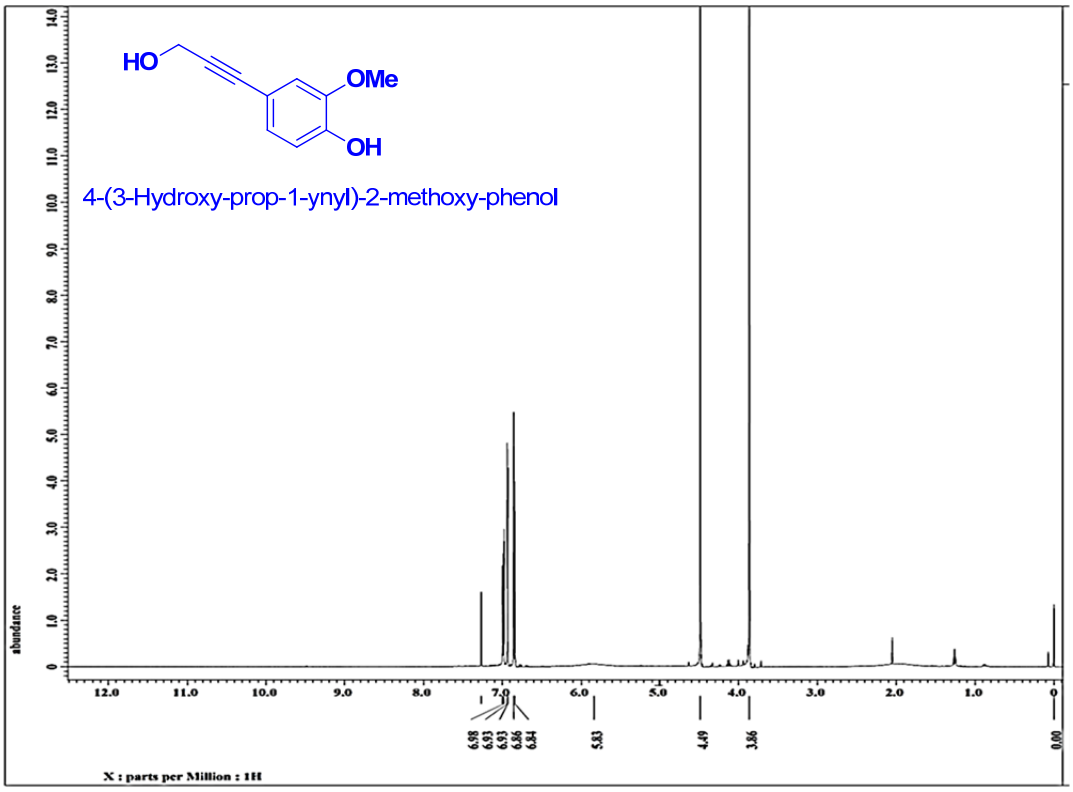

Figure 2.14. [1]H NMR spectra of 4-(3-hydroxyprop-1-ynyl)-2-methoxyphenol

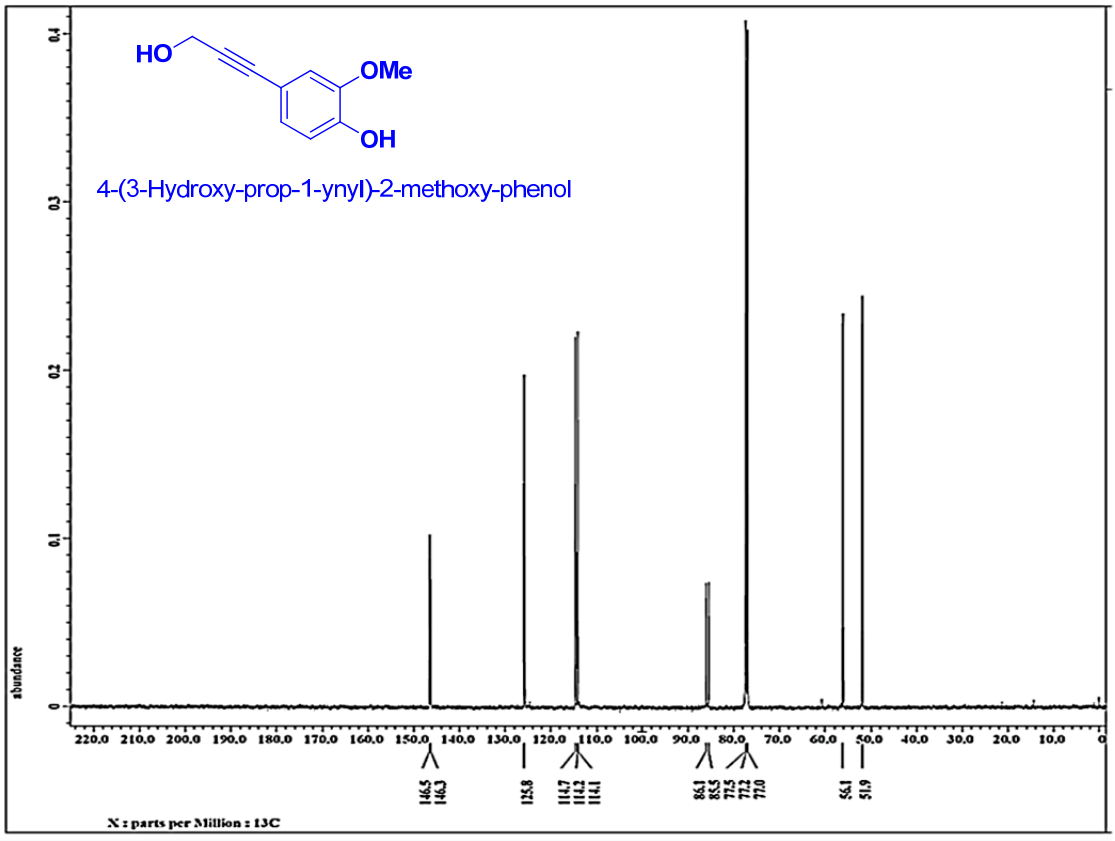

Figure 2.15. ^{13}C NMR spectra of 4-(3-hydroxyprop-1-ynyl)-2-methoxyphenol

2.4.2.2. 4-(3-Hydroxy-propenyl)-2-methoxy-phenol or (Z)-coniferyl alcohol (19)*

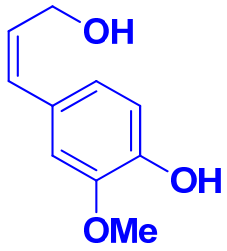

Figure 2.16**.** (Z)-coniferyl alcohol (**19**)

Lindlar's catalyst (0.016 g, 37 mol %) was added to a flask with 4-(3-Hydroxy-prop-1-ynyl)-2-methoxy-phenol (72 mg, 0.402 mmol) in 10 ml of methanol. The reaction mixture was stirred for 1 hr, filtered through celite, concentrated under reduced pressure, and purified by silica gel column chromatography (80:20 hexanes/ethyl acetate) to yield 37 mg of cis-coniferyl alcohol (51% yield) as a clear, colorless oil. The ^{1}H NMR spectrum matched the previously reported data[136] (Fig. 2.17).

*: Compound synthesized by Dr. Maria Elena Meza-Aviña,

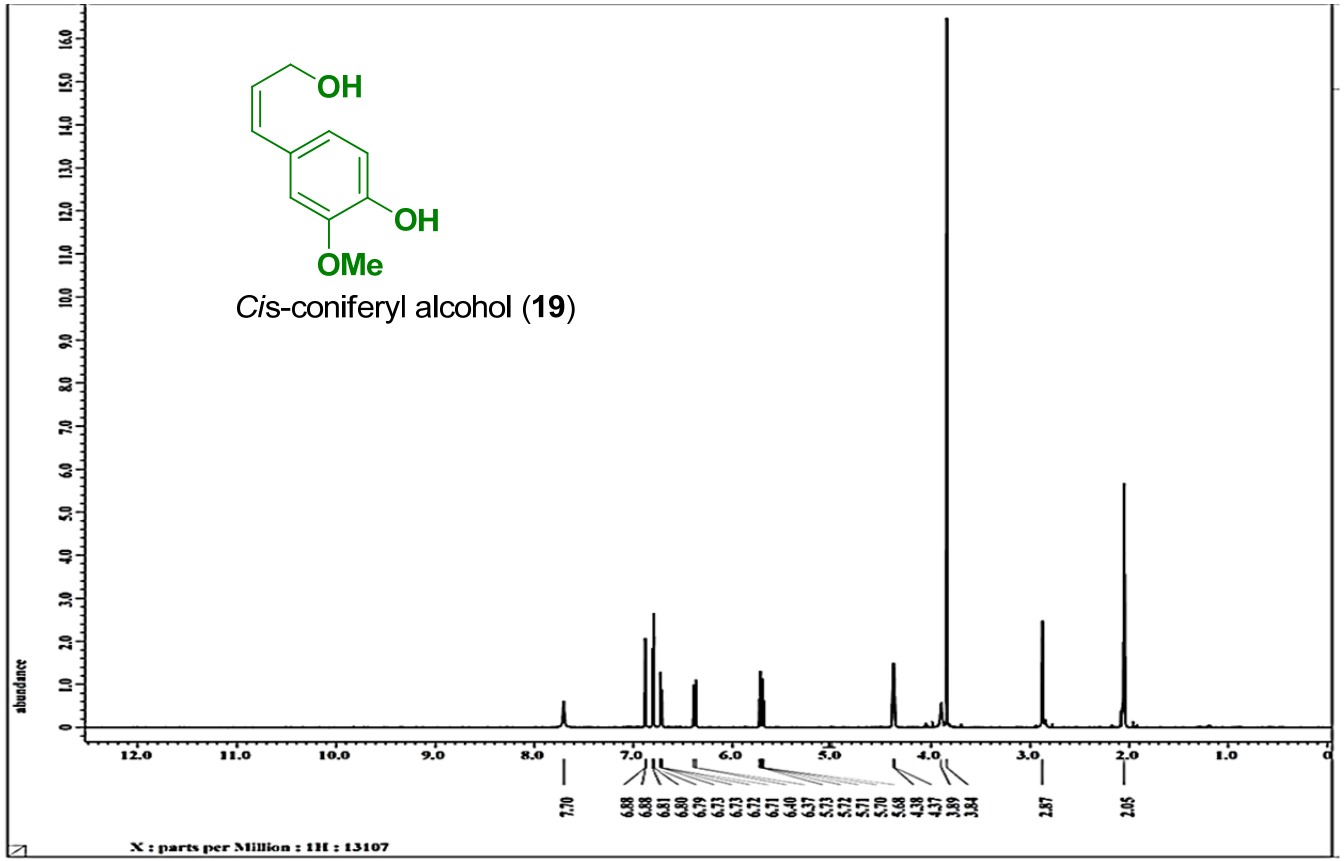

Figure 2.17. ^{1}H NMR spectra (500 MHz) of *cis*-coniferyl alcohol (**19**) standard and isolated from reaction in DMSO-d_6.

2.4.2.3. Biomimetic silybin A (1′)

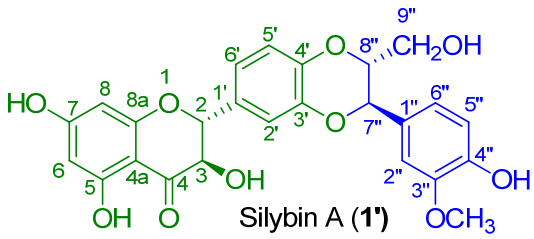

Figure 2.18. Biomimetic silybin A (**1′**)

Yield: 18 mg, 11%; white solid.

$[\alpha]_D^{20}$ = + 19 (*c* 0.07, MeOH);

UV (MeOH) λ_{max} (log ε) = 212 nm (4.3), 288 nm (4.1);

CD (MeOH) λ_{ext} ($\Delta\varepsilon$) = 236 (+10.1) 295 (-33.7), 330 (-7.6), Fig. 2.42.

^{1}H NMR (500 MHz, DMSO-d_6 at 30 °C) δ = 3.32 (m, 1H, H-9"b), 3.53 (ddd, *J* = 10.3, 5.2, 2.3 Hz, 1H, H-9"a), 3.77 (s, 3H, 3"-OCH_3), 4.17 (ddd, *J* = 8.0, 4.6, 2.3 Hz, 1H, H-8"), 4.60 (dd, *J* = 11.5, 6.3 Hz, 1H, 3-H), 4.90 (d, *J* = 8.0 Hz, 1H, H-7"), 4.96 (dd, *J* = 5.7, 5.2 Hz, OH-9"), 5.07 (d, *J* = 11.5 Hz, 1H, 2-H), 5.81 (d, *J* = 6.3 Hz, 3-OH), 6.86 (d, *J* = 1.7 Hz, 1H, H-8), 6.90 (d, *J* = 1.7 Hz, 1H, H-6), 6.80 (d, *J* = 8.0 Hz, 1H, H-5"), 6.85 (dd, *J* = 8.0, 1.7 Hz, 1H, H-6"), 6.97 (d, *J* = 8.0 Hz, 1H, H-5'), 7.00 (dd, *J* = 8.0, 1.7 Hz, 1H, H-6'), 7.01 (d, *J* = 1.8 Hz, 1H, H-2"), 7.09 (d, *J* = 1.7 Hz, 1H, H-2'), 9.18 (s, 4"-OH), 11.90 (s, 5-OH). (Table 2.1, Fig. 2.19);

^{13}C NMR (125 MHz, DMSO-d_6 at 30 °C) = δ 55.7 (3″-OCH_3), 60.2 (C-9″), 71.4 (C-3), 75.9 (C-8″), 78.1 (C-7″), 82.5 (C-2), 95.2 (C-8), 96.2 (C-6), 100.2 (C-4a), 111.6 (C-2″),

115.3 (C-5″), 116.3 (C-5′), 116.6 (C-2′), 120.5 (C-6″), 121.4 (C-6′), 127.5 (C-1″), 130.1 (C-1′), 143.3 (C-3′), 143.7 (C-4′), 147.0 (C-4″), 147.6 (C-3″), 162.5 (C-8a), 163.3 (C-5), 167.5 (C-7), 197.6 (C-4) (Table 2.6, Fig. 2.20);

HSQC data = H-2→C-2; H-3→C-3; H-6→C-6; H-8→C-8; H-2'→C-2'; H-5'→C-5'; H-6'→C-6'; H-2"→C-2"; H-5"→C-5"; H-6"→C-6"; H-7"→C-7"; H-8"→C-8"; H-9"a→C-9"; H-9"b→C-9"; OCH_3-7→C-7; OCH_3-3"→C-3" (see Fig. 2.21).

HMBC data = see Fig. 2.22.

HRESIMS *m/z* = 481.1140 $[M-H]^-$ (calcd for $C_{25}H_{22}O_{10}$ 481.1140; see Fig. 2.23).

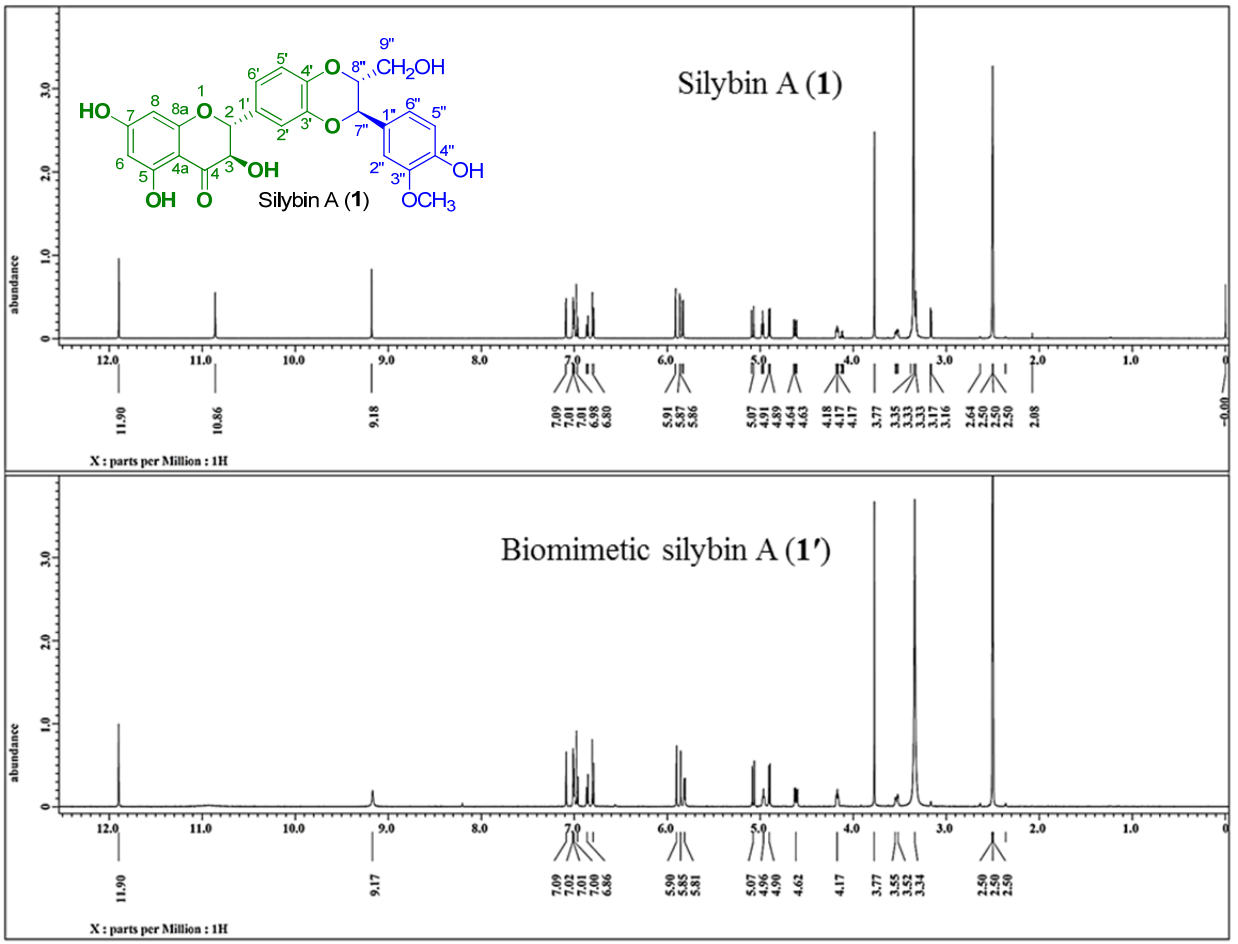

Figure 2.19. ^{1}H NMR spectra (500 MHz, 30 °C) of silybin A (**1**) and biomimetic silybin A (**1′**) in DMSO-d_6.

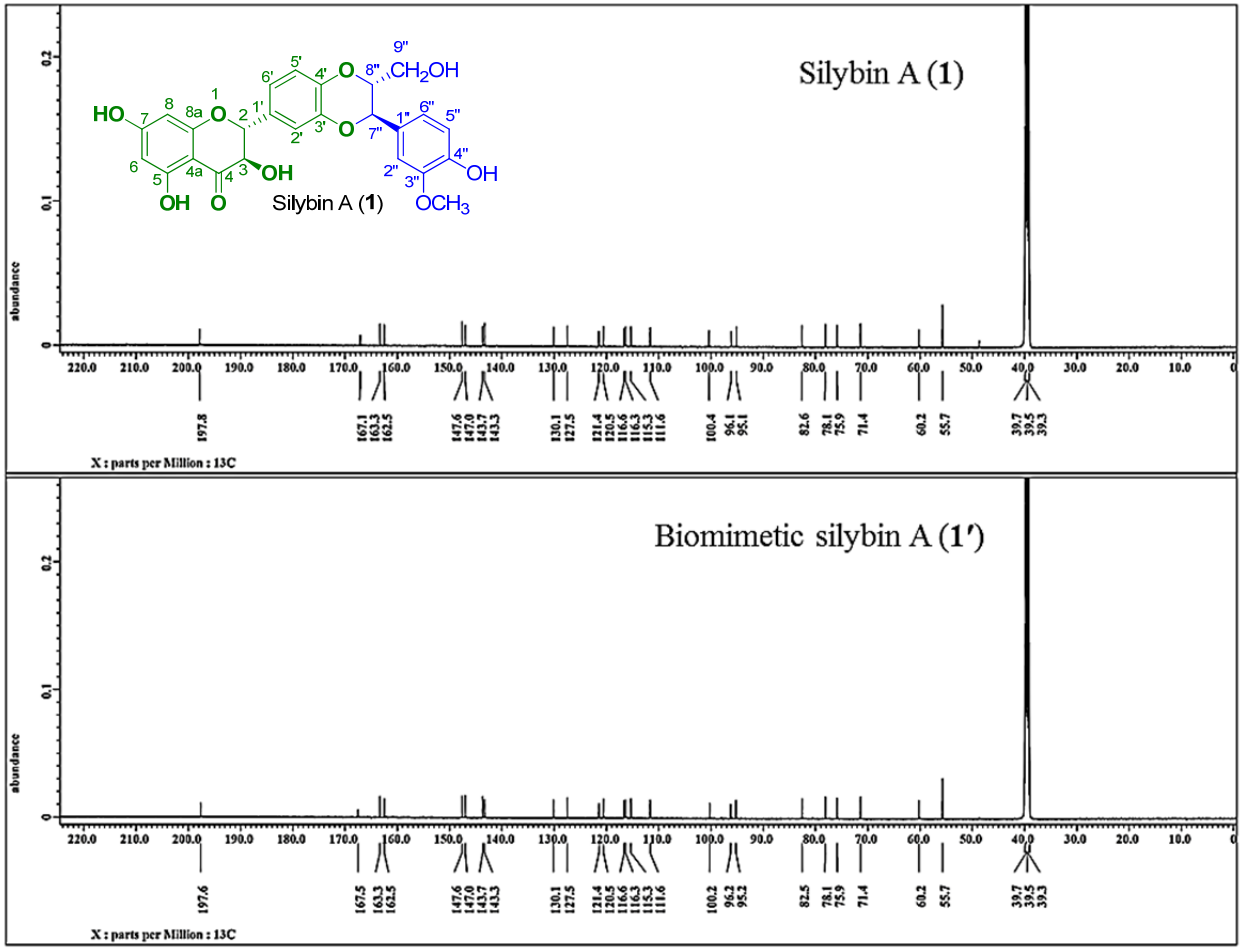

Figure 2.20. ^{13}C NMR spectra (125 MHz, 30 °C) of silybin A (**1**) and biomimetic silybin A (**1′**) in DMSO-d_6 .

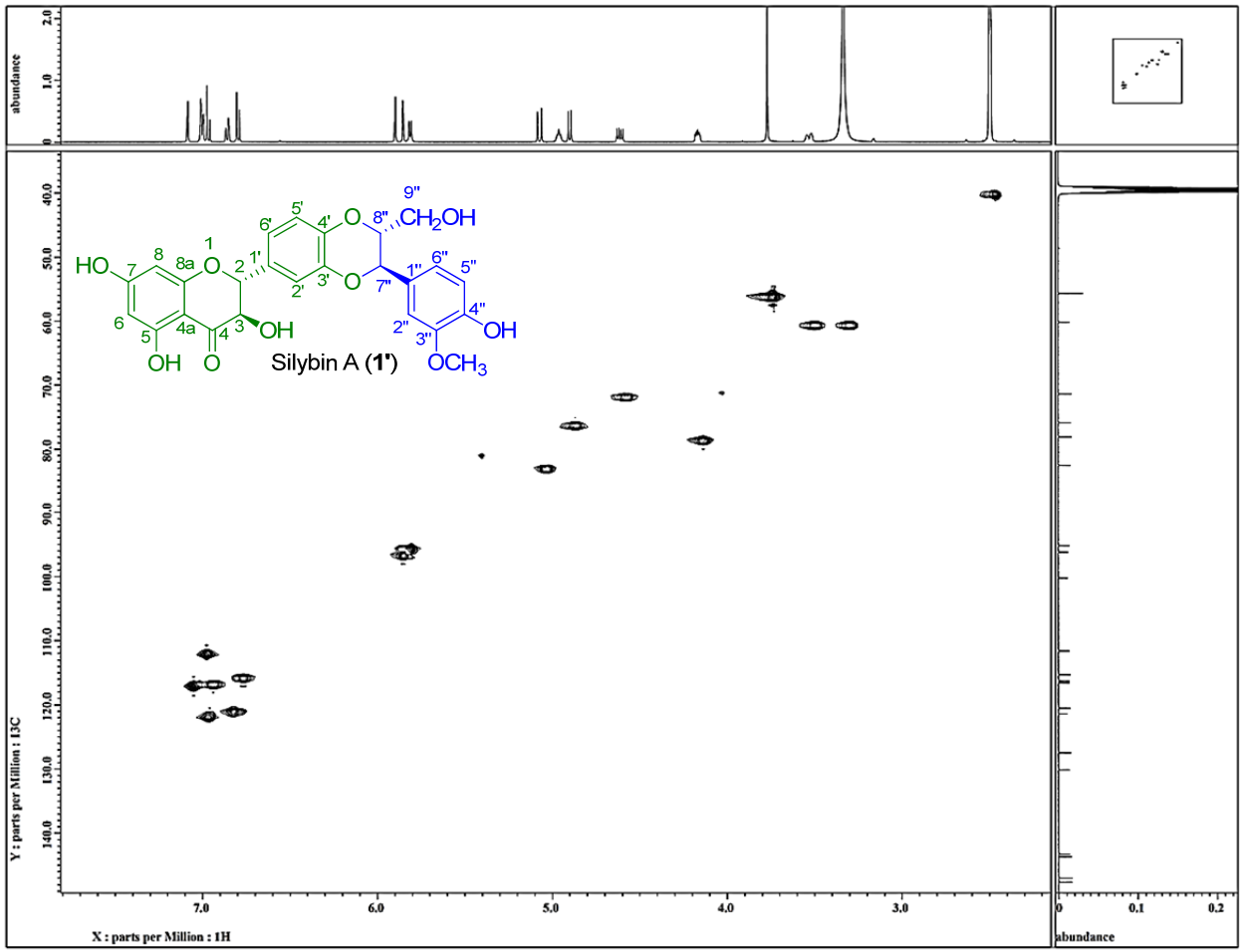

Figure 2.21. HMBC NMR spectrum (DMSO-d_6, 30 °C) of biomimetic silybin A **(1′)**.

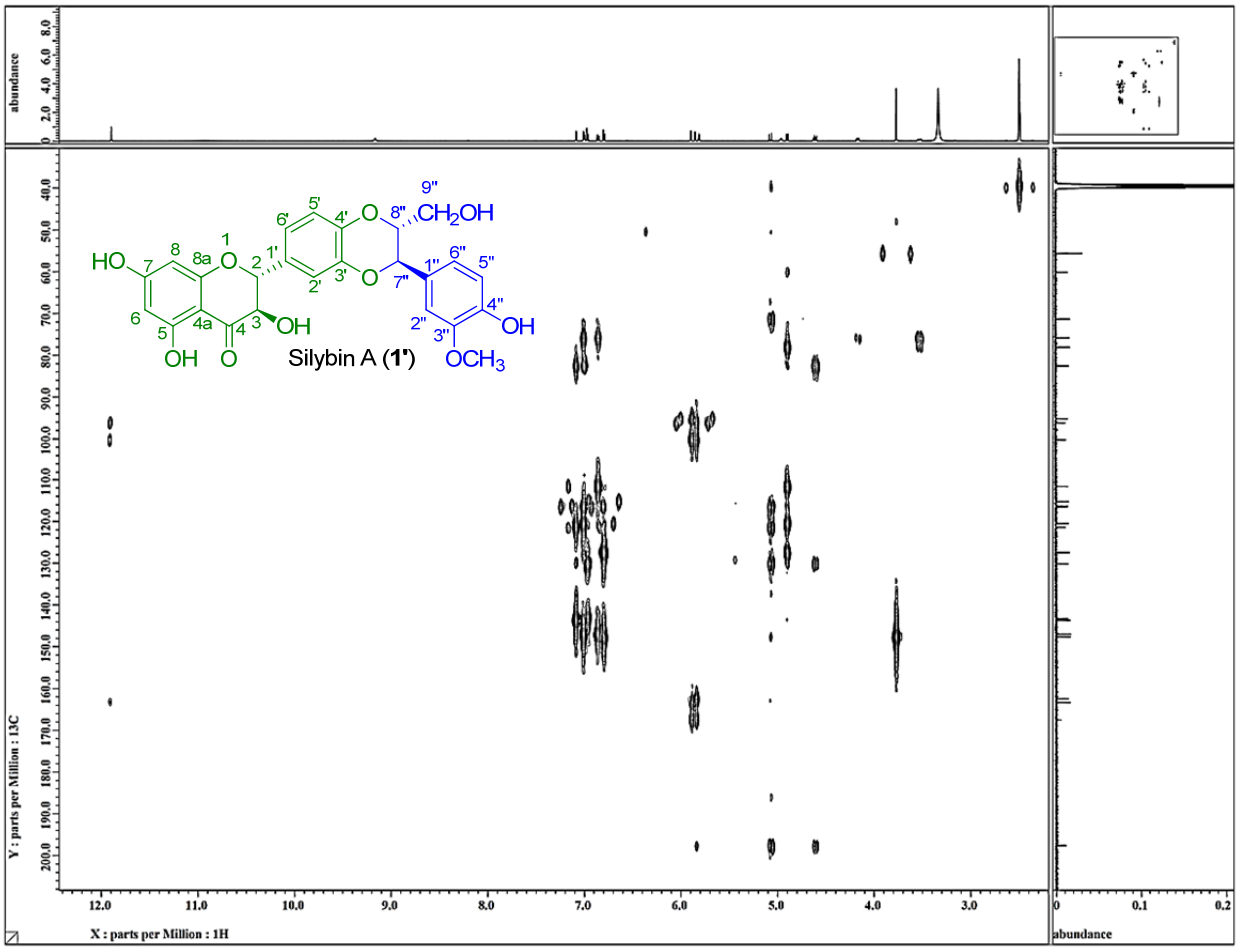

Figure 2.22. HMBC NMR spectrum (DMSO-d_6, 30 °C) of biomimetic silybin A (**1′**).

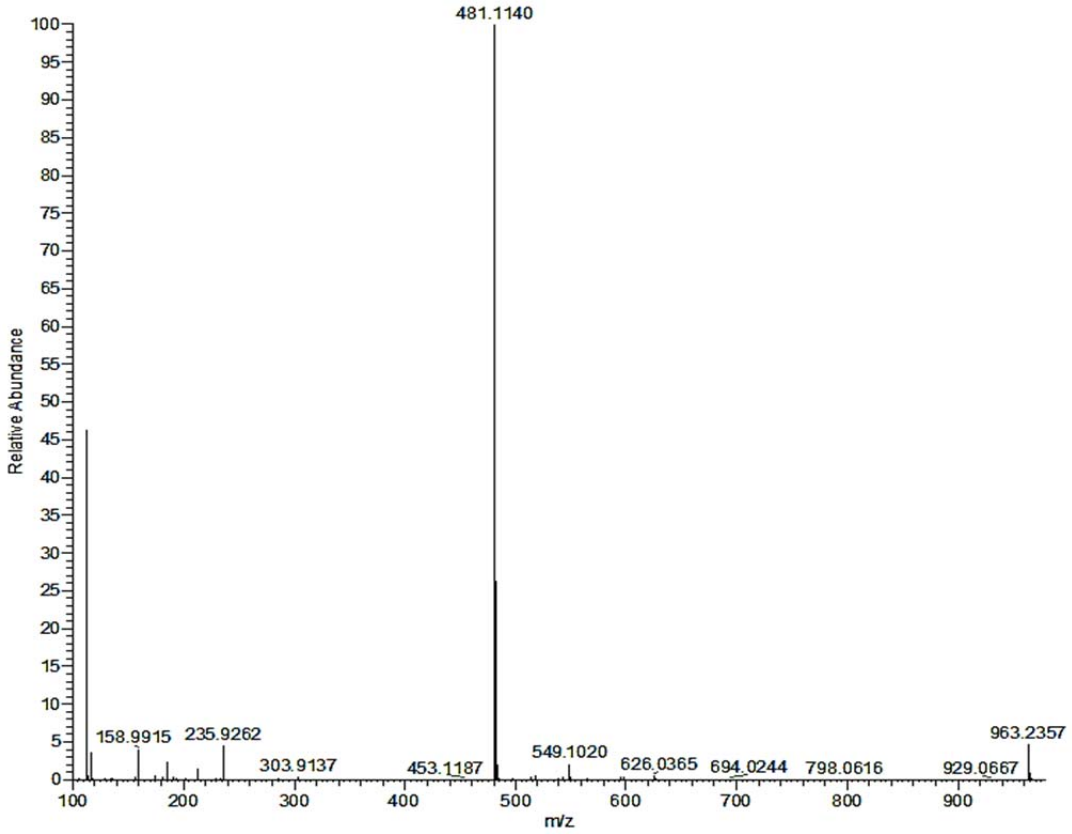

Figure 2.23. HRESIMS m/z 481.1140 $[M-H]^-$ of silybin A (**1′**) .

2.4.2.4. Biomimetic silybin B (2′)

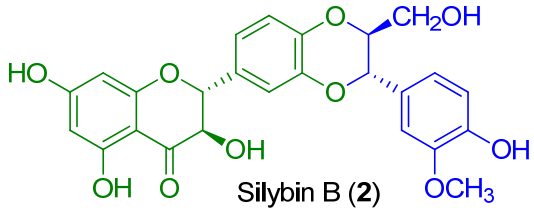

Figure 2.24. Biomimetic silybin B (**2′**).

Yield: 18 mg, 11%; white solid

$[\alpha]_D^{20}$ **:** +6.9 (*c* 0.09, MeOH);

UV (MeOH) λ_{max} **(log** ε**)**: 211 (4.0), 288 (3.7) nm;

CD (MeOH) λ_{ext} **(**$\Delta\varepsilon$**)**: 328 (+6.5), 295 (-33.4), 234 (+34.9) nm, Fig. 2.42.

^{1}H NMR (500 MHz, DMSO-d$_6$ at 30 °C): δ = 3.31 (m, 1H, H-9"b), 3.52 (ddd, *J* = 9.7, 5.2, 2.3 Hz, 1H, H-9"a), 3.77 (s, 3H, 3"-OCH$_3$), 4.17 (ddd, *J* = 8.0, 4.6, 2.3 Hz, 1H, H-8"), 4.59 (dd, *J* = 11.5, 6.3 Hz, 1H, 3-H), 4.90 (d, *J* = 7.5 Hz, 1H, H-7"), 4.99 (dd, *J* = 5.7, 5.2 Hz, OH-9"), 5.06 (d, *J* = 11.5 Hz, 1H, 2-H), 5.80 (d, *J* = 6.3 Hz, 3-OH), 6.82 (d, *J* = 1.7 Hz, 1H, H-8), 6.86 (d, *J* = 1.7 Hz, 1H, H-6), 6.80 (d, *J* = 8.0 Hz, 1H, H-5"), 6.86 (dd, *J* = 8.0, 1.7 Hz, 1H, H-6"), 6.97 (d, *J* = 8.6 Hz, 1H, H-5'), 7.01 (dd, *J* = 8.0, 1.7 Hz, 1H, H-6'), 7.02 (d, *J* = 1.7 Hz, 1H, H-2"), 7.07 (d, *J* = 1.7 Hz, 1H, H-2'), 9.19 (s, 4"-OH), 11.90 (s, 5-OH). (Table 2.1, Fig. 2.25);

^{13}C NMR (125 MHz, DMSO-*d*$_6$ at 30 °C): δ 55.7 (3″-OCH$_3$), 60.2 (C-9″), 71.4 (C-3), 75.9 (C-7″), 78.1 (C-8″), 82.5 (C-2), 95.2 (C-8), 96.2 (C-6), 100.2 (C-4a), 111.6 (C-2″),

115.3 (C-5″), 116.4 (C-5′), 116.7 (C-2′), 120.5 (C-6″), 121.2 (C-6′), 127.5 (C-1″), 130.2 (C-1′), 143.3 (C-3′), 143.6 (C-4′), 147.0 (C-4″), 147.6 (C-3″), 162.5 (C-8a), 163.3 (C-5), 167.6 (C-7), 197.6 (C-4) (Table 2.6, Fig. 2.26);

HSQC data: H-2→C-2; H-3→C-3; H-6→C-6; H-8→C-8; H-2'→C-2'; H-5'→C-5'; H-6'→C-6'; H-2"→C-2"; H-5"→C-5"; H-6"→C-6"; H-7"→C-7"; H-8"→C-8"; H-9"a→C-9"; H-9"b→C-9"; OCH_3-7→C-7; OCH_3-3"→C-3" (see Fig. 2.27).

HMBC data: see Fig. 2.28.

HRESIMS *m/z* : 481.1141$[M-H]^-$ (calcd for $C_{25}H_{22}O_{10}$ 481.1140; see Fig. 2.29).

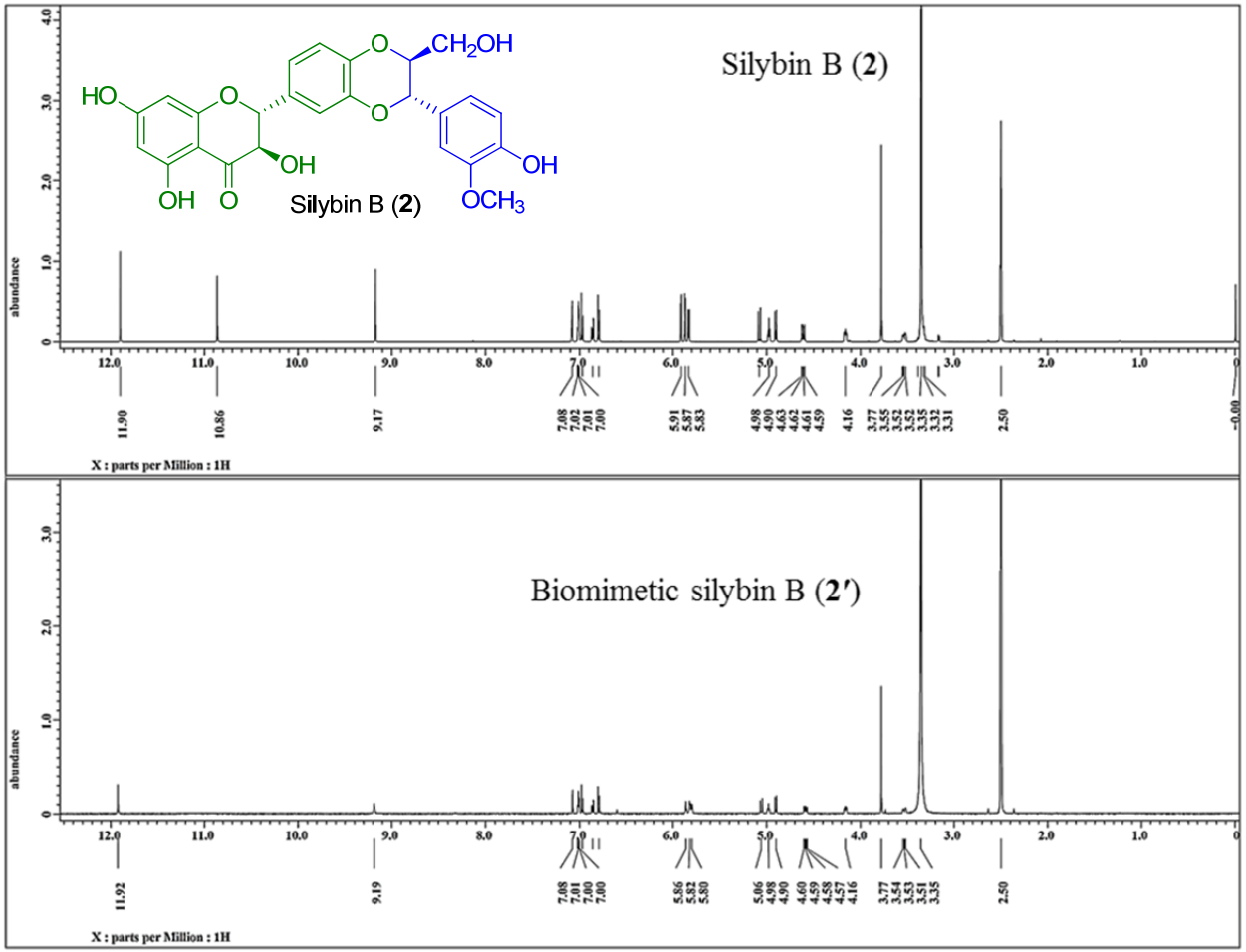

Figure 2.25. ^{1}H NMR spectra (500 MHz, 30 °C) of silybin B (**2**) and biomimetic silybin B (**2′**) in DMSO-d_6.

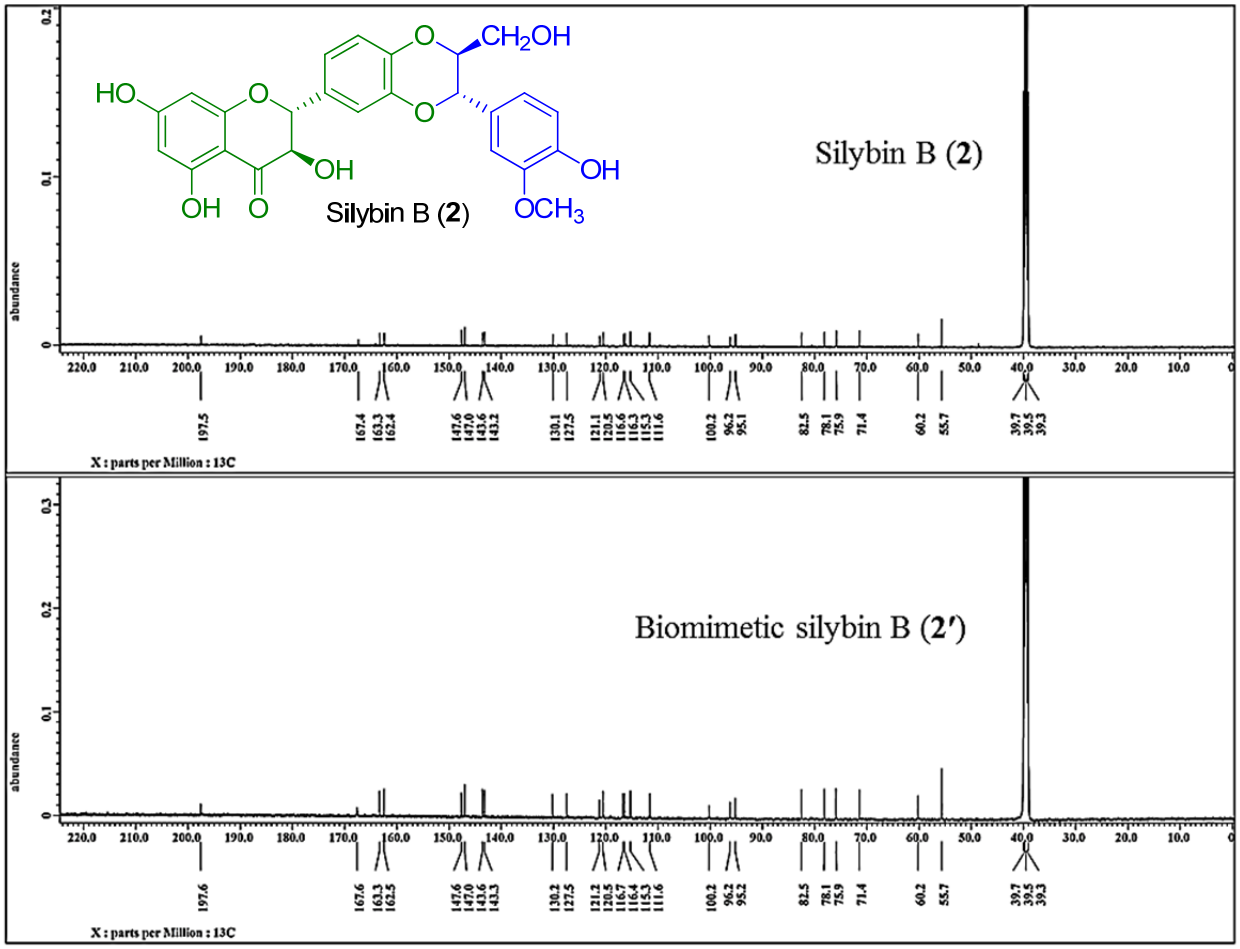

Figure 2.26. ^{13}C NMR spectra (125 MHz, 30 °C) of silybin B (**2**) and biomimetic silybin B (**2′**) in DMSO-d_6.

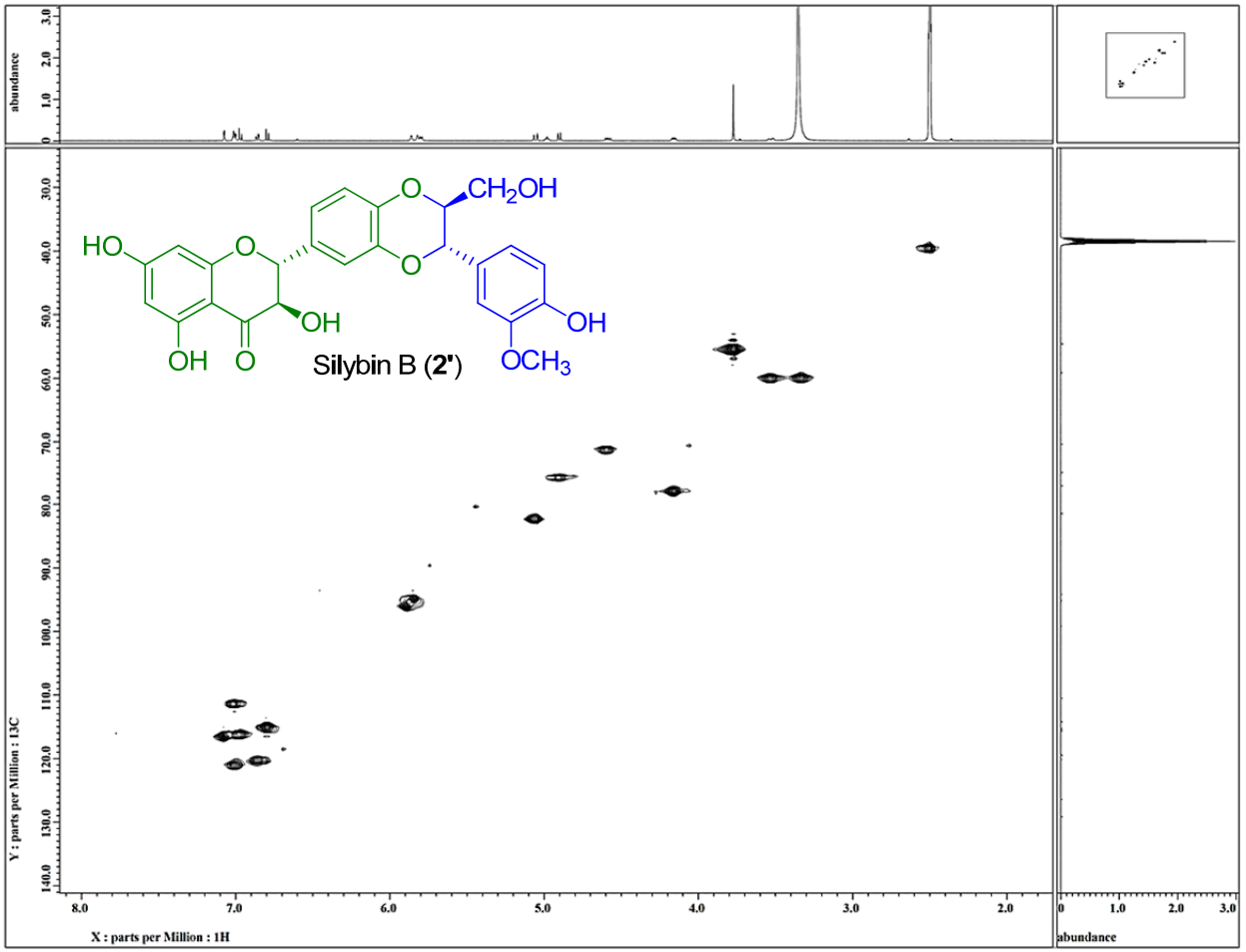

Figure 2.27. HMBC NMR spectrum (DMSO-d_6, 30 °C) of biomimetic silybin B (**2′**).

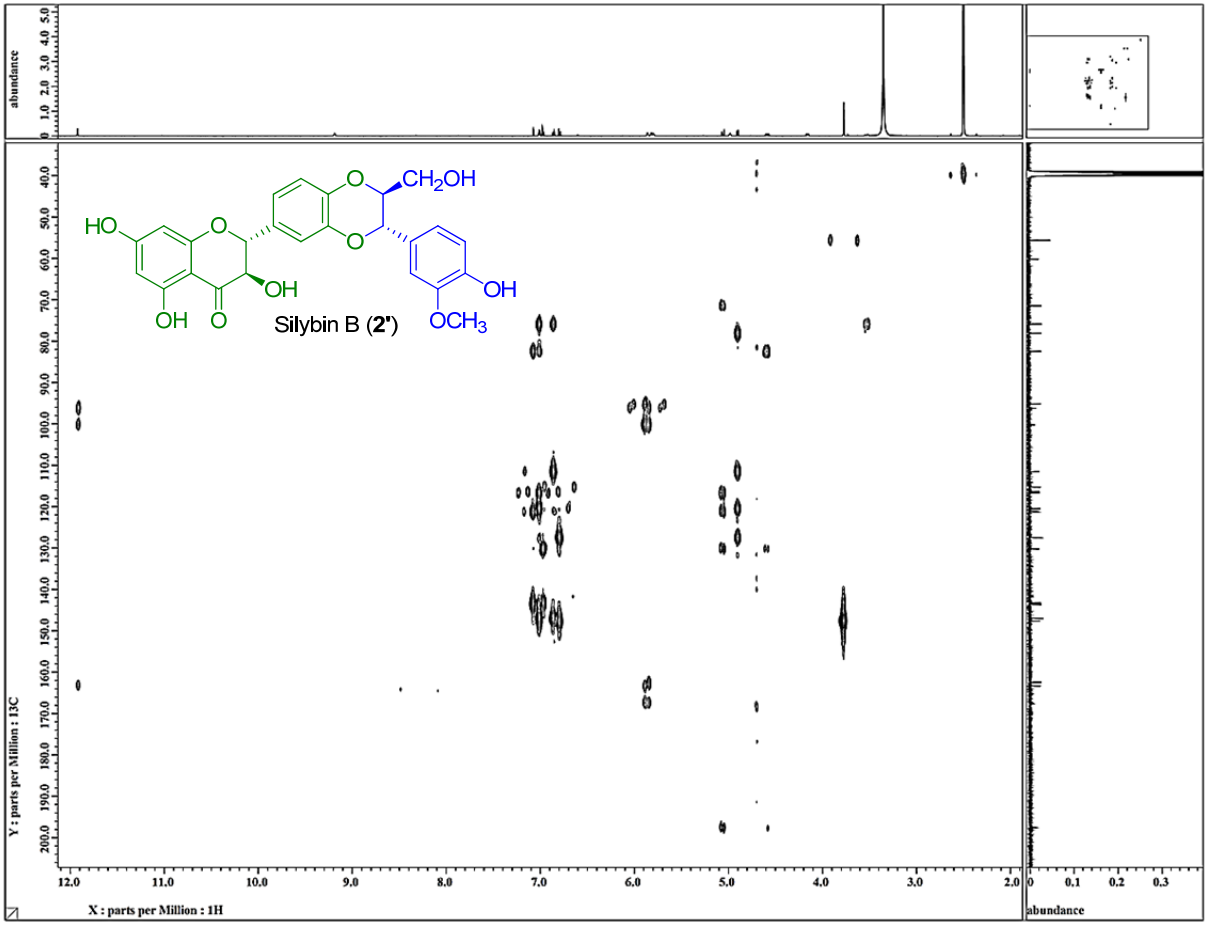

Figure 2.28. HMBC NMR spectrum (DMSO-d_6, 30 °C) of biomimetic silybin B (**2′**).

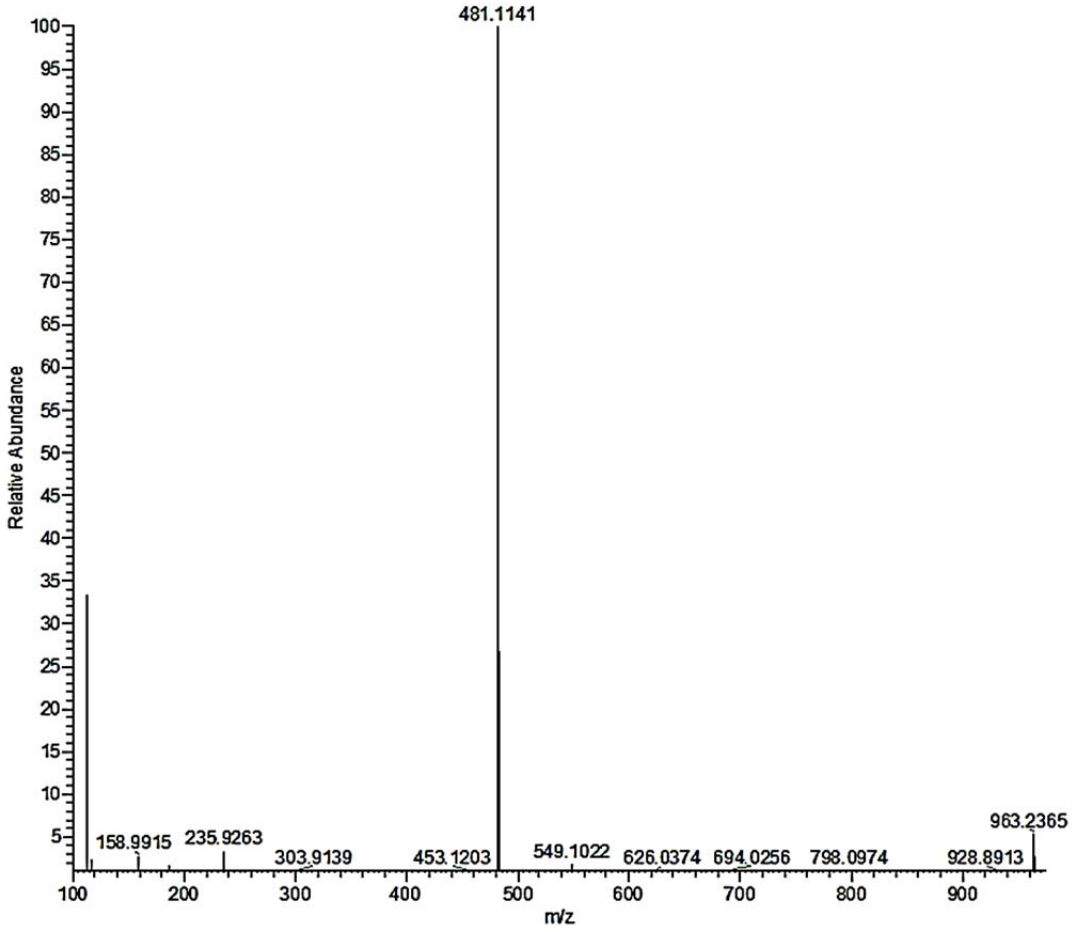

Figure 2.29. HRESIMS m/z 481.1141 $[M-H]^-$ of silybin B (**2′**).

2.4.2.5. Biomimetic isosilybin A (3′)

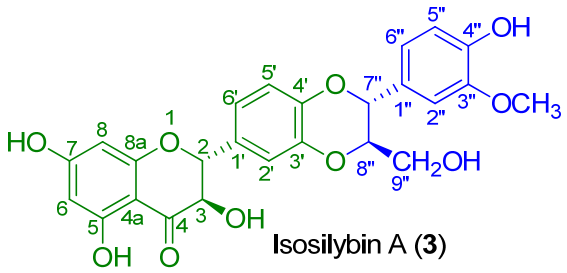

Figure 2.30. Biomimetic isosilybin A (**3′**).

Yield: 15 mg, 9%; white solid.

$[\alpha]_D^{20}$ = +48.1 (*c* 0.1, MeOH);

UV (MeOH) λ_{max} (log ε): 212 (4.3), 288 (4.1) nm;

CD (MeOH) λ_{ext} ($\Delta\varepsilon$): 329 (+3.2), 295 (-15.6), 232 (+1.6) nm, Fig. 2.42.

^{1}H NMR (500 MHz, DMSO-d$_6$ at 30 °C) : δ = 3.33 (m, 1H, H-9"b), 3.53 (ddd, *J* = 12.0, 5.2, 2.3 Hz, 1H, H-9"a), 3.77 (s, 3H, 3"-OCH$_3$), 4.16 (ddd, *J* = 8.0, 4.6, 2.3 Hz, 1H, H-8"), 4.58 (dd, *J* = 10.9, 6.3 Hz, 1H, 3-H), 4.91 (d, *J* = 8.0 Hz, 1H, H-7"), 4.98 (dd, *J* = 5.7, 5.2 Hz, OH-9"), 5.10 (d, *J* = 10.9 Hz, 1H, 2-H), 5.84 (d, *J* = 6.3 Hz, 3-OH), 5.86 (d, *J* = 1.7 Hz, 1H, H-8), 5.89 (d, *J* = 1.7 Hz, 1H, H-6), 6.80 (d, *J* = 8.6 Hz, 1H, H-5"), 6.86 (dd, *J* = 8.0, 1.7 Hz, 1H, H-6"), 6.93 (d, *J* = 8.6 Hz, 1H, H-5'), 6.98 (dd, *J* = 8.6, 2.3 Hz, 1H, H-6'), 7.00 (d, *J* = 1.7 Hz, 1H, H-2"), 7.09 (d, *J* = 2.3 Hz, 1H, H-2'), 9.19 (s, 4"-OH), 11.92 (s, 5-OH). (Table 2.1 , Fig. 2.31);

^{13}C NMR (125 MHz, DMSO-*d$_6$* at 30 °C): δ 55.7 (3″-OCH$_3$), 60.2 (C-9″), 71.5 (C-3),

75.9 (C-7″), 78.0 (C-8″), 82.5 (C-2), 95.3 (C-8), 96.2 (C-6), 100.2 (C-4a), 111.7(C-2″), 115.3 (C-5″), 116.5 (C-5′), 116.5 (C-2′), 120.5 (C-6″), 120.9 (C-6′), 127.5 (C-1″), 130.4 (C-1′), 142.9 (C-3′), 143.9 (C-4′), 147.0 (C-4″), 147.6 (C-3″), 162.5 (C-8a), 163.4 (C-5), 167.7 (C-7), 197.5 (C-4) (Table 2.2 , Fig. 2.32);

HSQC data: H-2→C-2; H-3→C-3; H-6→C-6; H-8→C-8; H-2'→C-2'; H-5'→C-5'; H-6'→C-6'; H-2"→C-2"; H-5"→C-5"; H-6"→C-6"; H-7"→C-7"; H-8"→C-8"; H-9"a→C-9"; H-9"b→C-9"; OCH_3-7→C-7; OCH_3-3"→C-3" (see Fig. 2.33).

HMBC data: see Fig. 2.34.

HRESIMS *m/z* : 481.1139 $[M-H]^-$ (calcd for $C_{25}H_{22}O_{10}$ 481.1140; see Fig. 2.35).

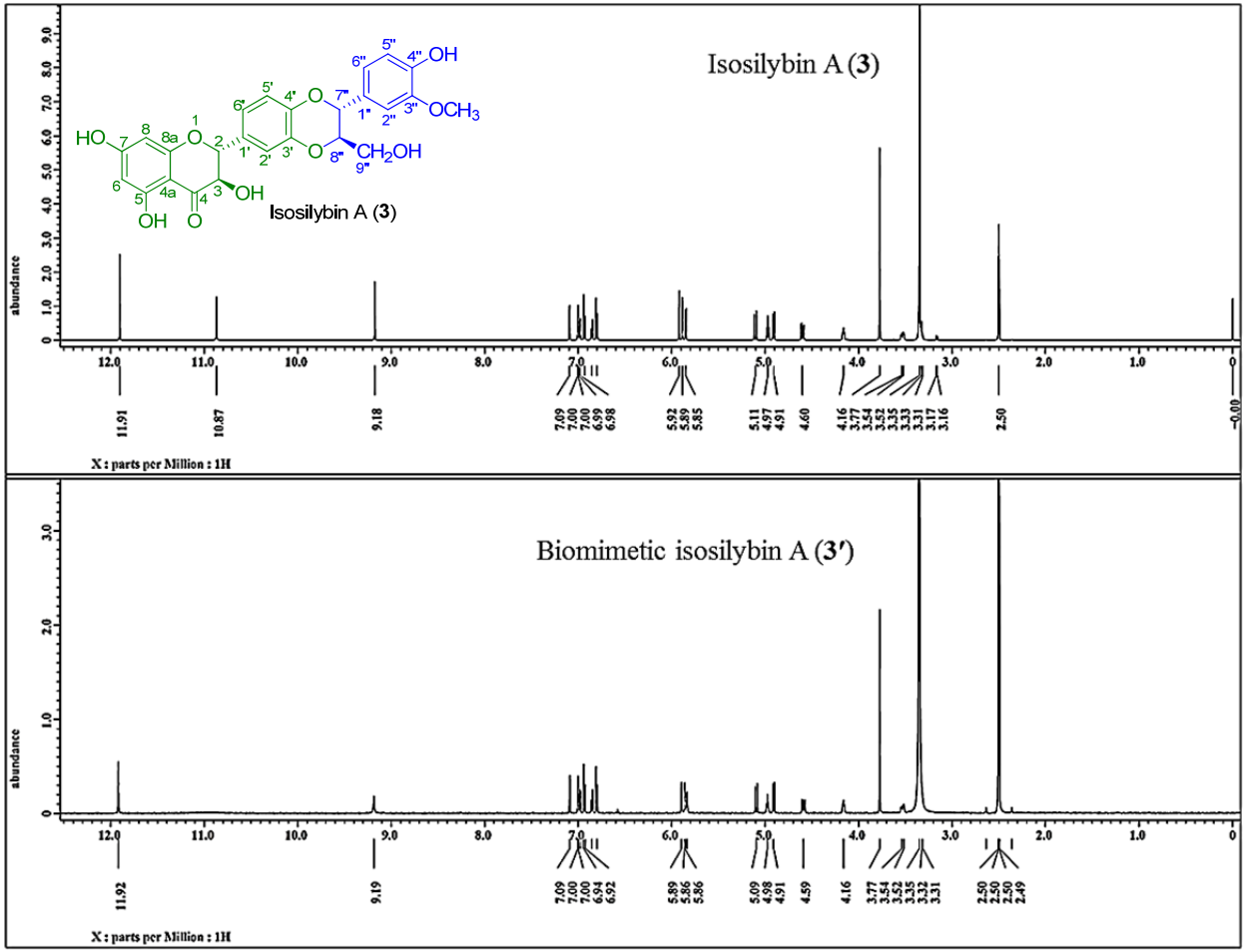

Figure 2.31. ^{1}H NMR spectra (500 MHz, 30 °C) of isosilybin A (**3**) and biomimetic isosilybin A (**3′**) in DMSO-d_6.

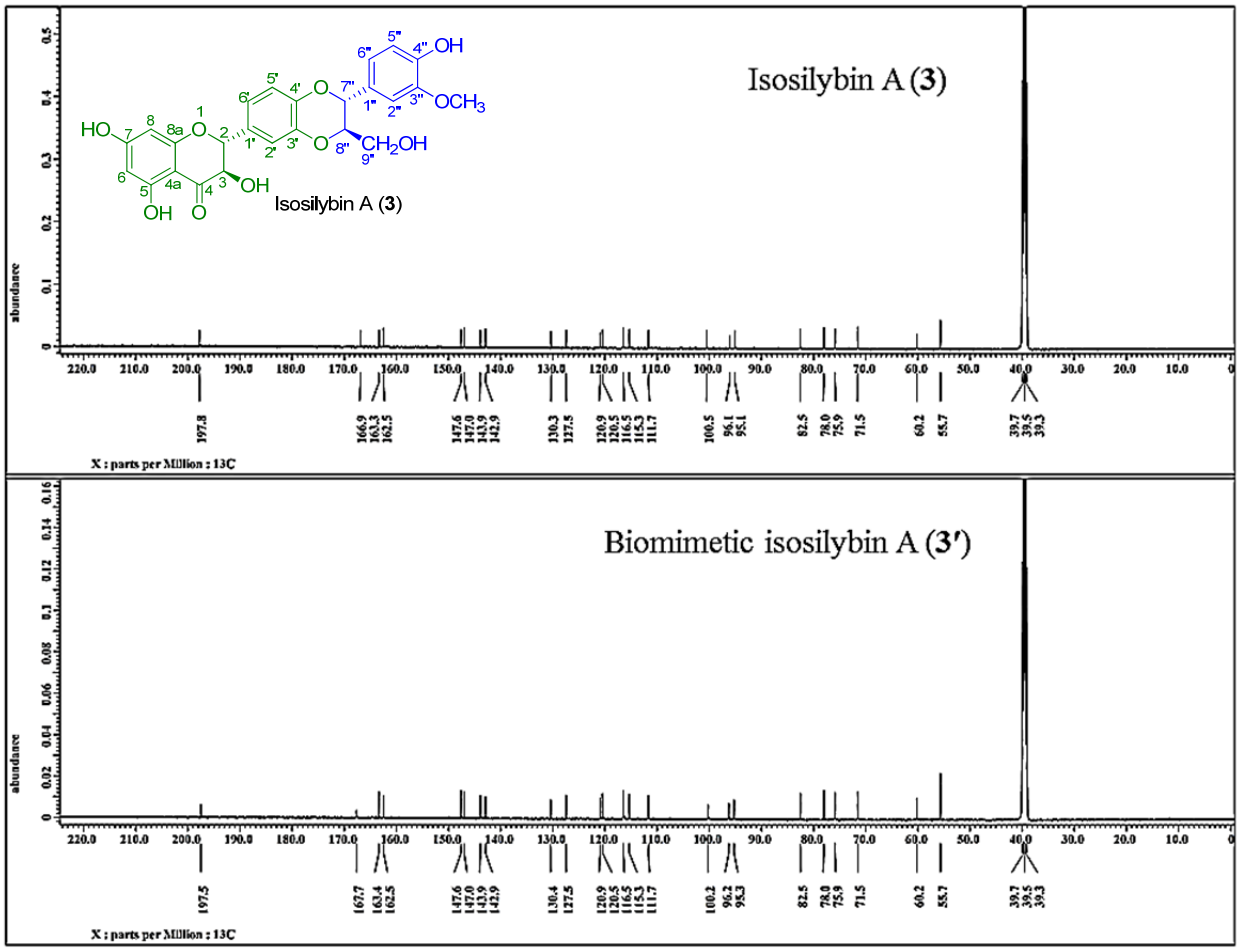

Figure 2.32. ^{13}C NMR spectra (125 MHz, 30 °C) of isosilybin A (**3**) and biomimetic isosilybin A (**3′**) in DMSO-d_6.

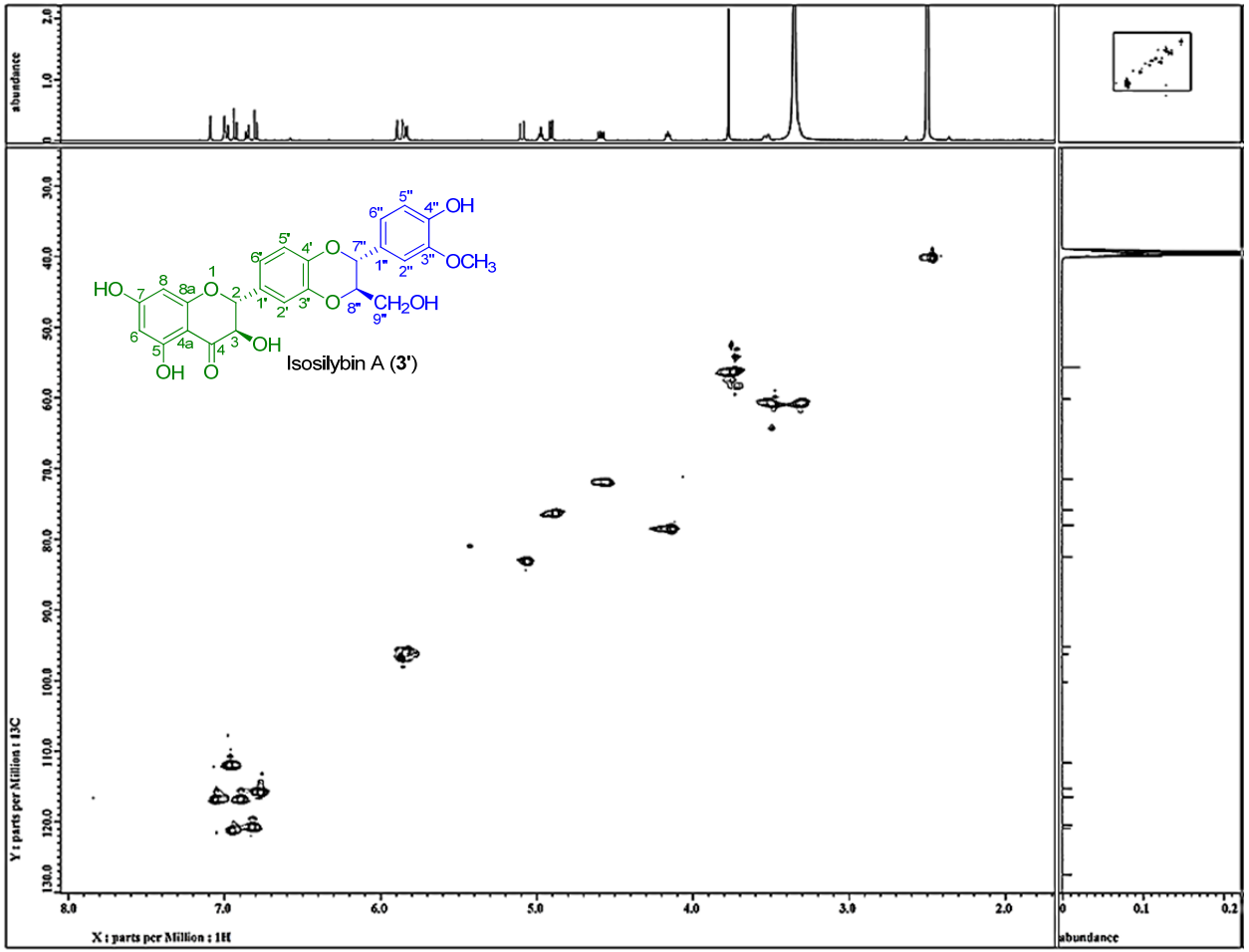

Figure 2.33. HSQC NMR spectrum (DMSO-d_6, 30 °C) of biomimetic isosilybin A (**3′**).

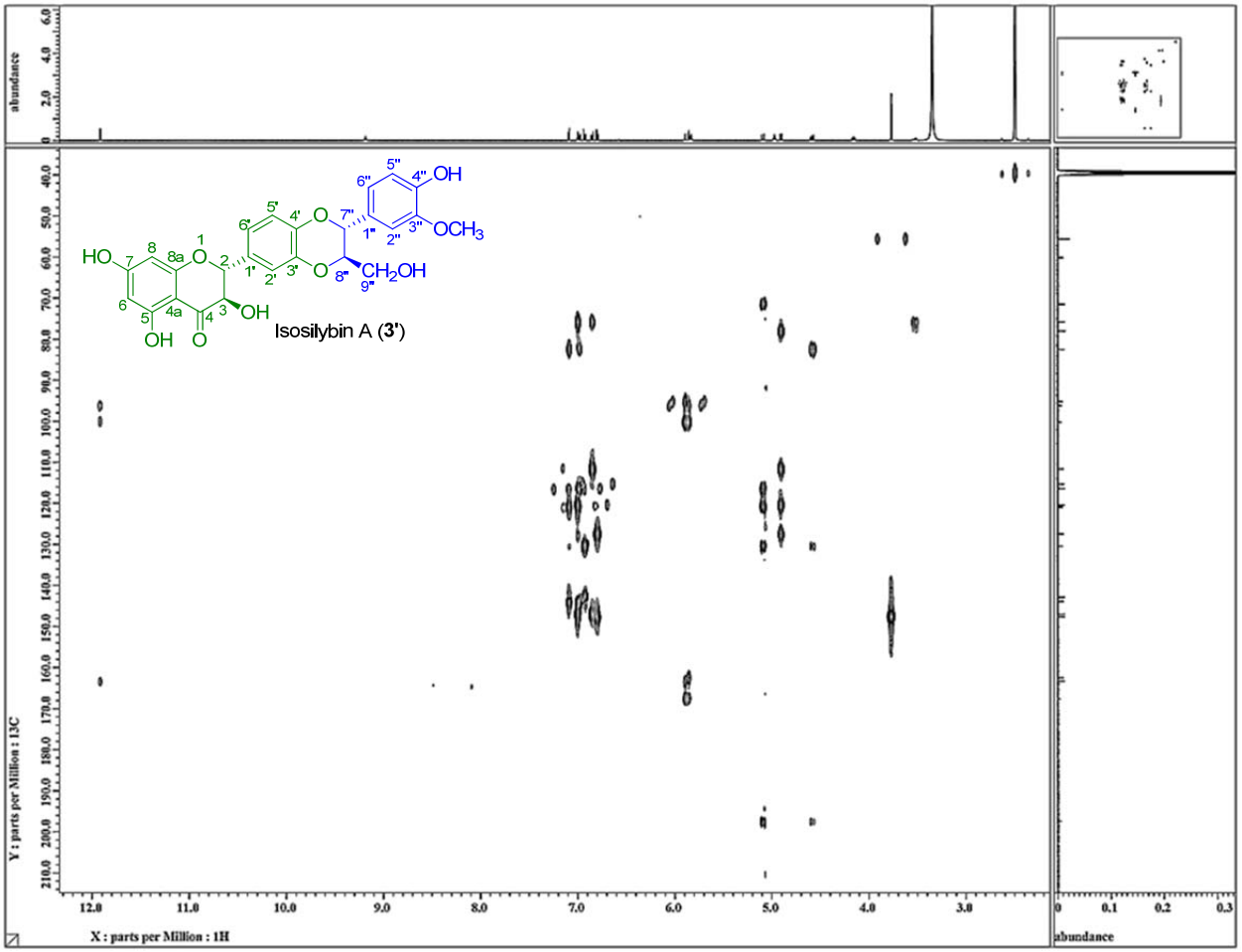

Figure 2.34. HMBC NMR spectrum (DMSO-d_6, 30 °C) of biomimetic isosilybin A (**3′**) .

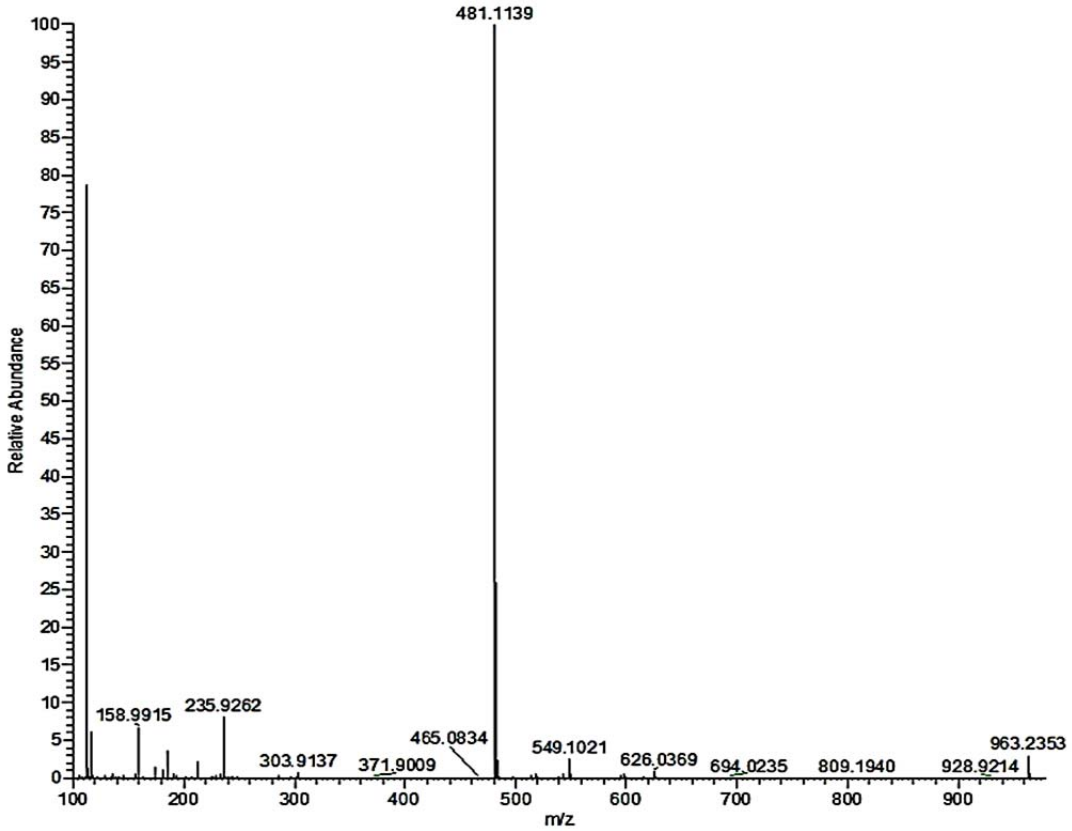

Figure 2.35. HRESIMS m/z 481.1139 $[M-H]^-$ of isosilybin A (**3′**) .

2.4.2.6. Biomimetic isosilybin B (4′)

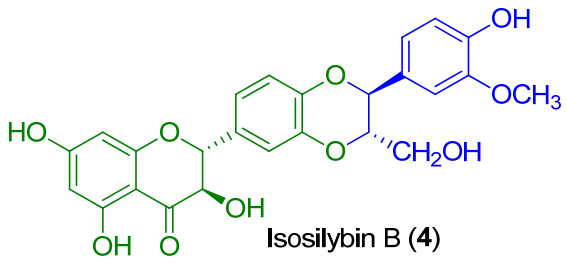

Figure 2.36. Biomimetic isosilybin B (**4′**).

Yield: 14 mg, 8 %; white solid. $[\alpha]_D^{20}$ **:** -20.80 (*c* 0.1, MeOH);

UV (MeOH) λ_{max} (log ε): 213 (4.1), 288 (3.9) nm;

CD (MeOH) λ_{ext} ($\Delta\varepsilon$): 328 (+3.8), 294 (-23.3), 228 (+16.1) nm (see Fig. 2.42).

^{1}H NMR (500 MHz, DMSO-d$_6$ at 30 °C): δ = 3.33 (m, 1H, H-9"b), 3.53 (ddd, *J* = 11.9, 5.2, 2.3 Hz, 1H, H-9"a), 3.77 (s, 3H, 3"-OCH$_3$), 4.17 (ddd, *J* = 8.0, 4.6, 2.3 Hz, 1H, H-8"), 4.58 (dd, *J* = 10.9, 6.3 Hz, 1H, 3-H), 4.91 (d, *J* = 8.0 Hz, 1H, H-7"), 4.97 (dd, *J* = 5.7, 5.2 Hz, OH-9"), 5.08 (d, *J* = 10.9 Hz, 1H, 2-H), 5.81 (d, *J* = 6.3 Hz, 3-OH), 5.83 (d, *J* = 2.3 Hz, 1H, H-8), 5.86 (d, *J* = 2.3 Hz, 1H, H-6), 6.80 (d, *J* = 8.0 Hz, 1H, H-5"), 6.85 (dd, *J* = 8.0, 1.8 Hz, 1H, H-6"), 6.93 (d, *J* = 8.0 Hz, 1H, H-5'), 6.98 (dd, *J* = 8.0, 1.8 Hz, 1H, H-6'), 7.00 (d, *J* = 1.8 Hz, 1H, H-2"), 7.10 (d, *J* = 1.8 Hz, 1H, H-2'), 9.19 (s, 4"-OH), 11.93 (s, 5-OH) (Table 2.1 , Fig. 2.37);

^{13}C NMR (125 MHz, DMSO-d_6 at 30 °C): δ 55.7 (3″-OCH$_3$), 60.2 (C-9″), 71.4 (C-3), 75.8 (C-7″), 78.0 (C-8″), 82.4 (C-2), 95.3 (C-8), 96.3 (C-6), 100.1 (C-4a), 111.6 (C-2″), 115.3 (C-5″), 116.5 (C-5′), 116.5 (C-2′), 120.5 (C-6″), 120.9 (C-6′), 127.5 (C-1″), 130.4

(C-1′), 142.9 (C-3′), 143.9 (C-4′), 147.0 (C-4″), 147.6 (C-3″), 162.4 (C-8a), 163.4 (C-5), 167.0 (C-7), 197.2 (C-4) (Table 2.2, Fig. 2.38);

HSQC data: H-2→C-2; H-3→C-3; H-6→C-6; H-8→C-8; H-2'→C-2'; H-5'→C-5'; H-6'→C-6'; H-2"→C-2"; H-5"→C-5"; H-6"→C-6"; H-7"→C-7"; H-8"→C-8"; H-9"a→C-9"; H-9"b→C-9"; OCH_3-7→C-7; OCH_3-3"→C-3" (see Fig. 2.39).

HMBC data: correlations observed between the protons at δ_H 5.83 and 5.86 to C-7 (δ_C 167.0) confirmed the presence of signal of C-7 in **4′**; see Fig. 2.40).

HRESIMS *m/z*: 481.1141 $[M-H]^-$ (calcd for $C_{25}H_{22}O_{10}$ 481.1140; see Fig. 2.41).

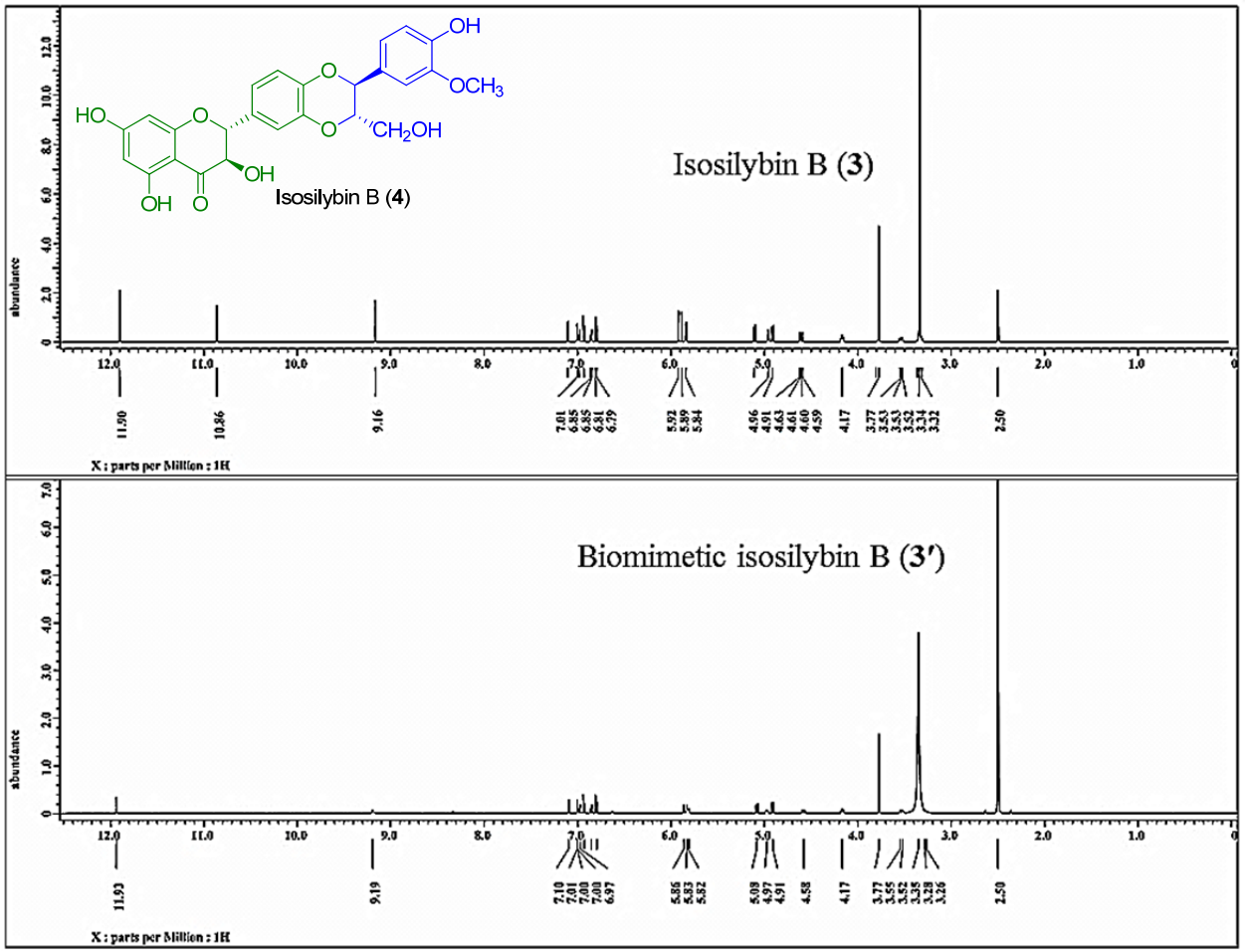

Figure 2.37. ^{1}H NMR spectra (500 MHz, 30 °C) of isosilybin B (**4**) and biomimetic isosilybin B (**4′**) in DMSO-d_6

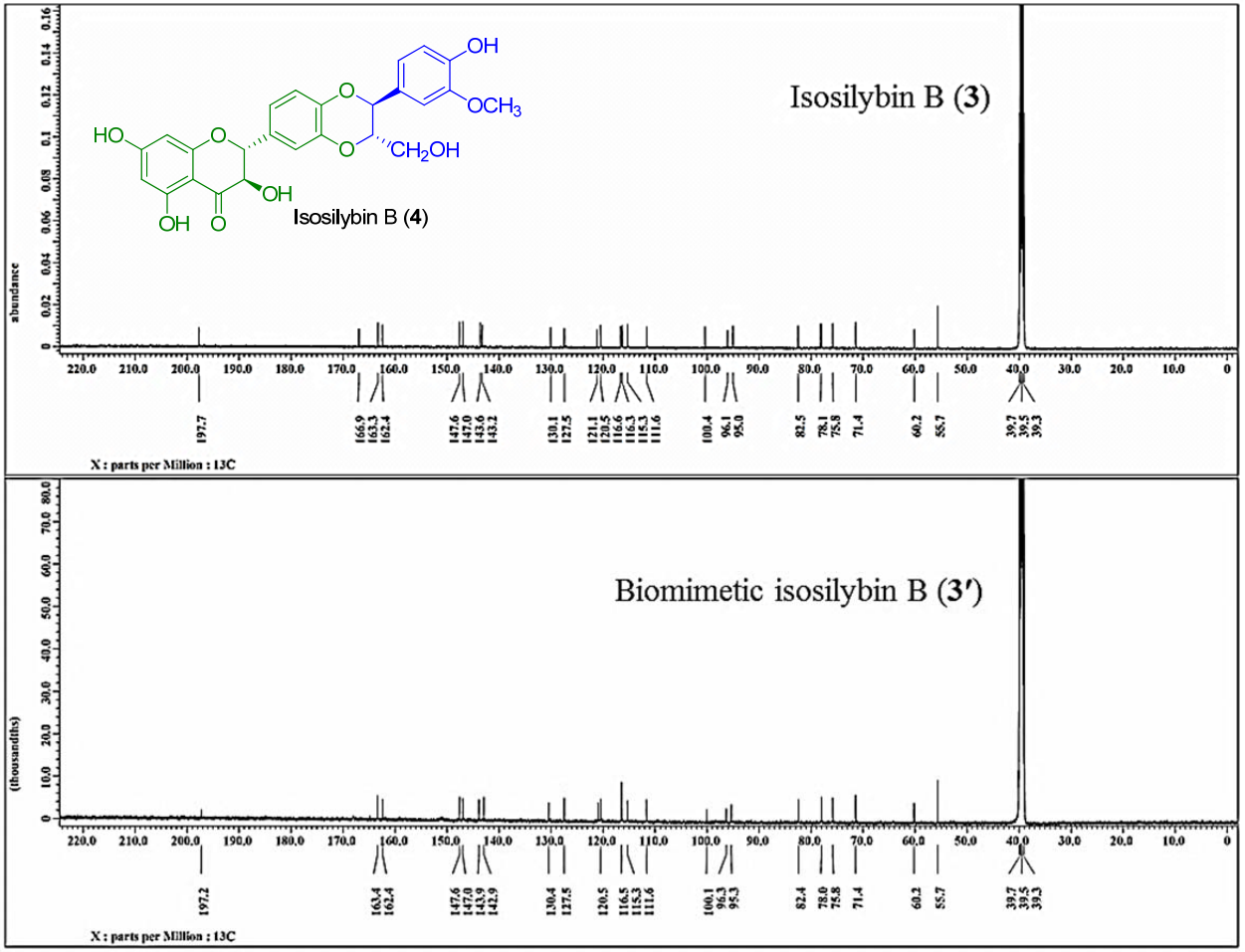

Figure 2.38. ^{13}C NMR spectra (125 MHz, 30 °C) of isosilybin B (**4**) and biomimetic isosilybin B (**4′**) in DMSO-d_6

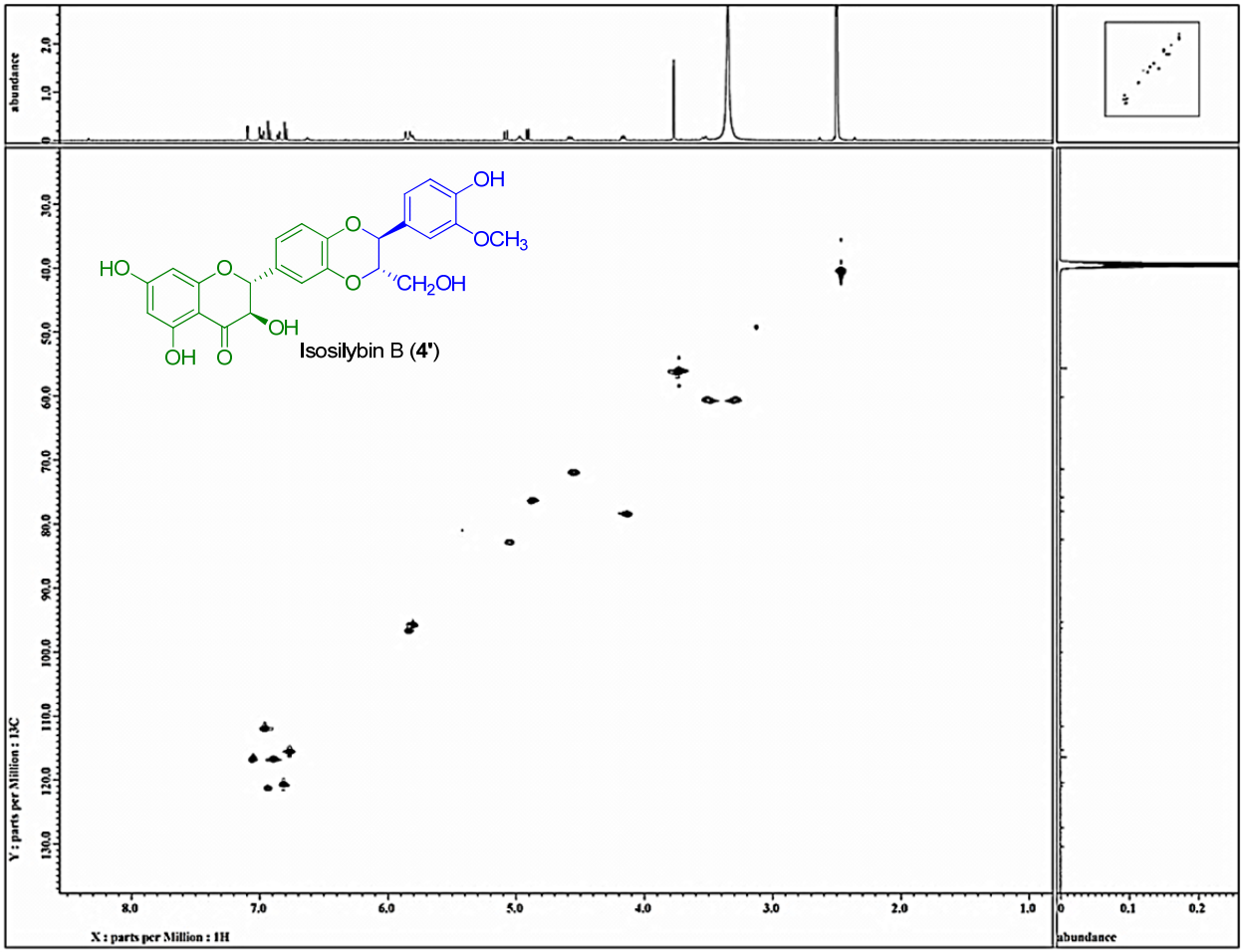

Figure 2.39. HSQC NMR spectrum (DMSO-d_6, 30 °C) of biomimetic isosilybin B (**4′**) correlations

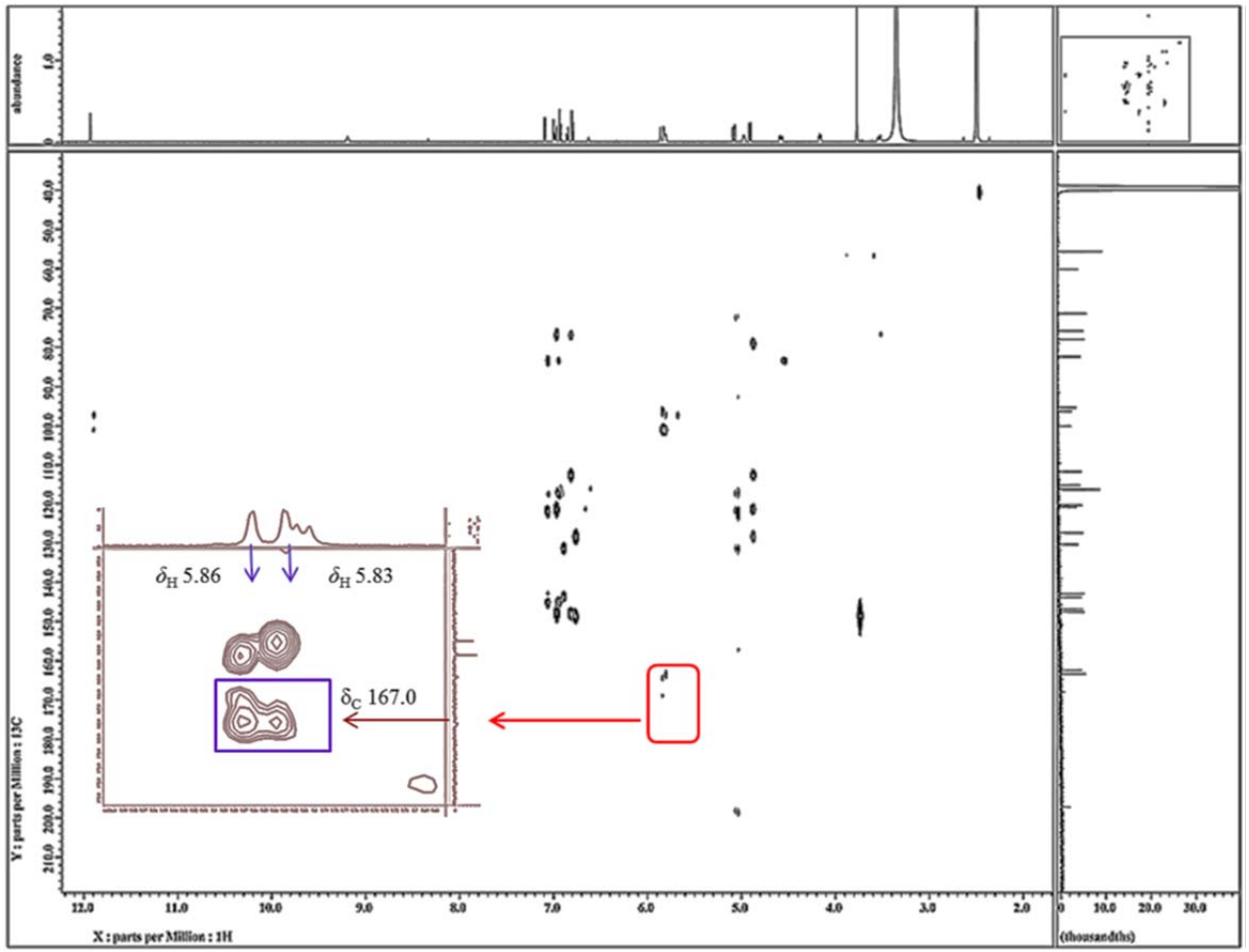

Figure 2.40. HMBC NMR spectrum (DMSO-d_6, 30 °C) of biomimetic isosilybin B (**4′**) correlations between the protons at H-6, H-8 to C-7

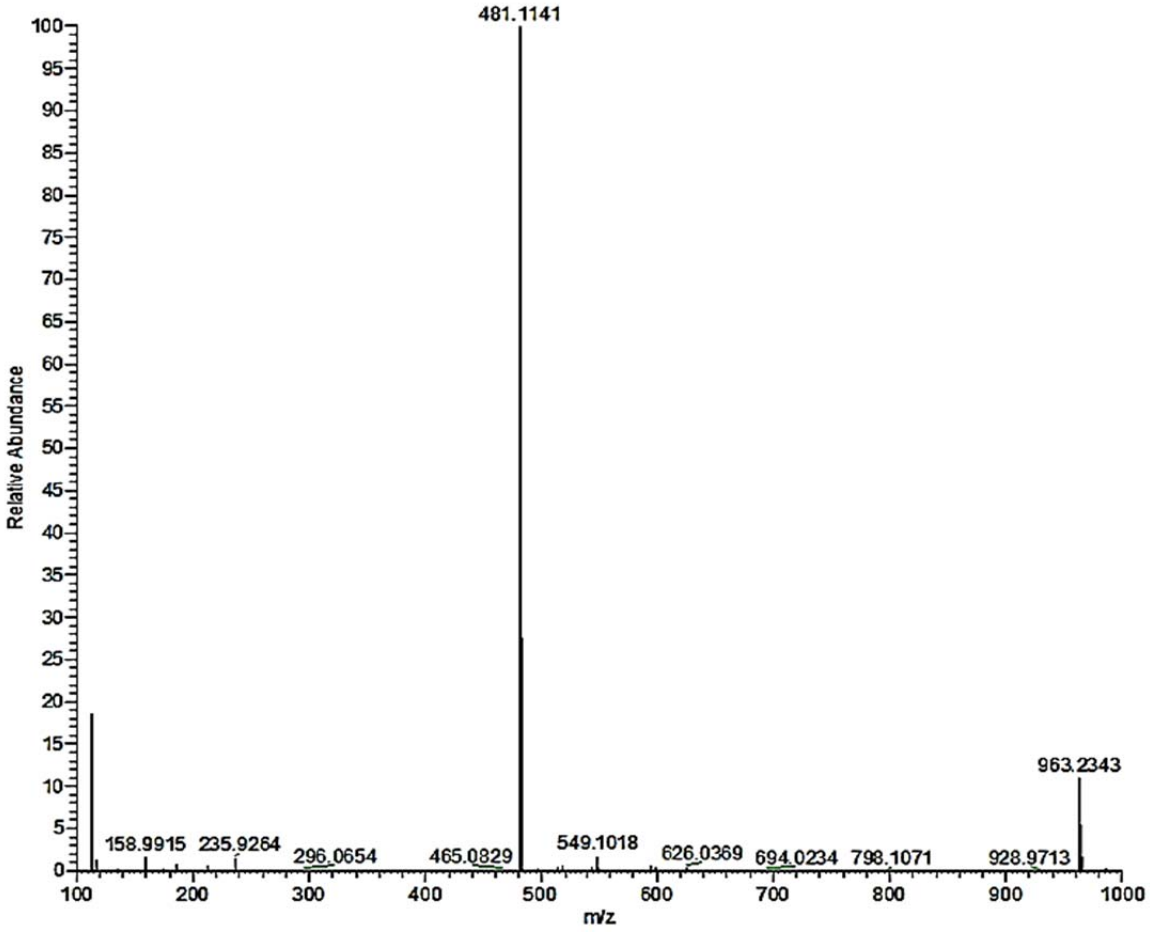

Figure 2.41. HRESIMS m/z 481.1141 $[M-H]^-$ of isosilybin B (**4′**)

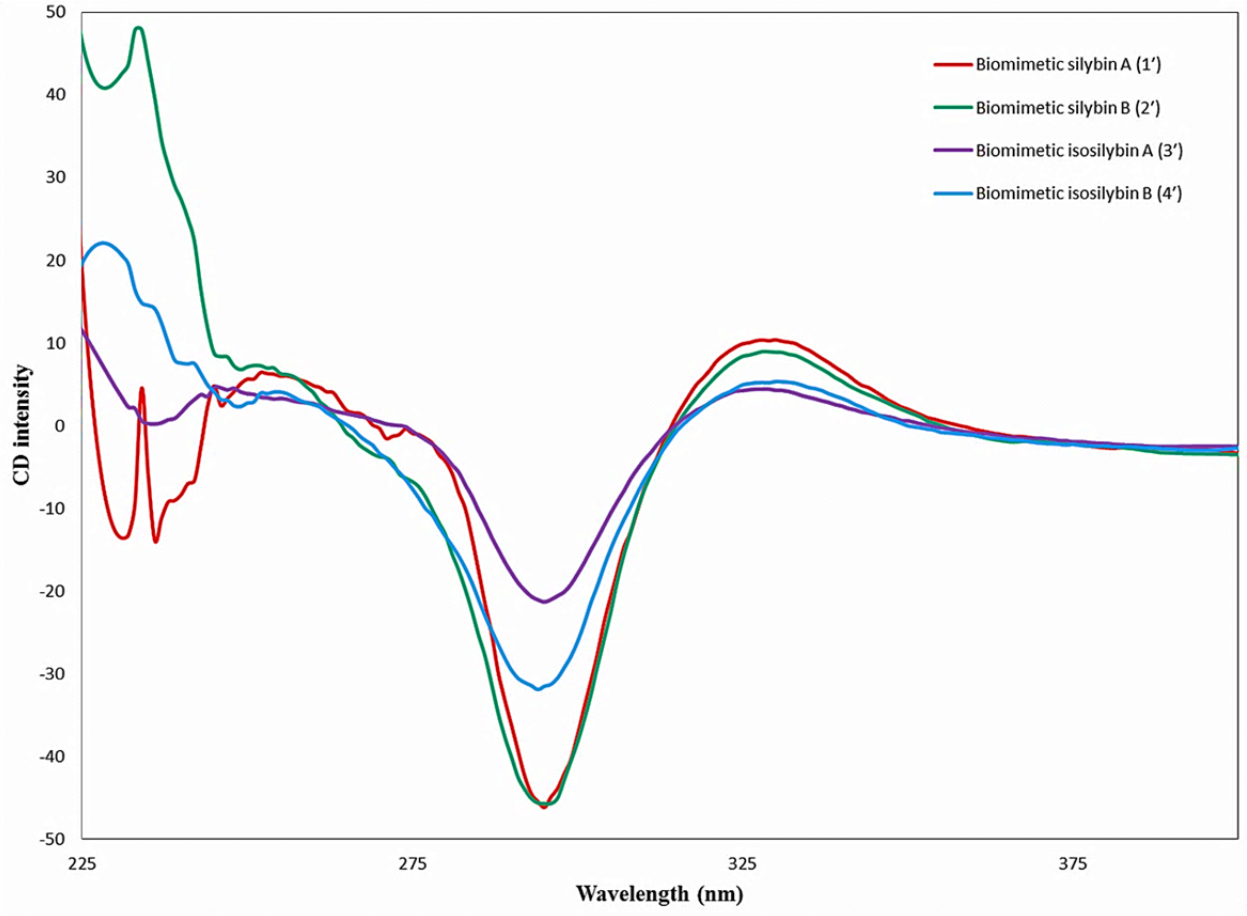

Figure 2.42 Circular Dichroism (CD) spectra of biomimetic flavonolignans

Table 2.1. ^{1}H NMR data of flavonolignans and biomimetic flavonolignans in DMSO-d_6 (500 MHz, 30 °C)

Position	**1**	**1′**	**2**	**2′**	**3**	**3′**	**4**	**4′**
2	5.08, d (11.5)	5.07, d (11.5)	5.08, d (11.5)	5.06, d (11.5)	5.11, d (10.9)	5.10, d (10.9)	5.11, d (11.5)	5.08, d (10.9)
3	4.63, dd (11.5, 6.3)	4.60, dd (11.5, 6.3)	4.61, dd (11.5, 6.3)	4.59, dd (11.5, 6.3)	4.60, dd (10.9, 6.3)	4.58, dd (10.9, 6.3)	4.61, dd (11.5, 5.9)	4.58, dd (10.9, 6.3)
6	5.91, d (1.7)	5.90, d (1.7)	5.91, d (2.3)	5.86, br d (1.7)	5.92, d (2.3)	5.89, d (1.7)	5.92, d (2.0)	5.86, d (2.3)
8	5.86, d (1.7)	5.86, d (1.7)	5.87, d (2.3)	5.82, br d (1.7)	5.89, d (2.3)	5.86, d (1.7)	5.89, d (2.0)	5.83, d (2.3)
2'	7.09, d (1.7)	7.09, d (1.7)	7.08, d (1.8)	7.07, d (1.7)	7.09, d (2.3)	7.09, d (2.3)	7.10, d (1.8)	7.10, d (1.8)
5'	6.97, d (8.0)	6.97, d (8.0)	6.97, d (8.1)	6.97, d (8.6)	6.93, d (8.6)	6.93, d (8.6)	6.93, d (8.0)	6.93, d (8.0)
6'	7.00, dd (8.0, 1.7)	7.00, dd (8.0, 1.7)	7.02, dd (8.1, 1.8)	7.01, dd (8.6, 1.7)	6.98, dd (8.6, 2.3)	6.98, dd (8.6, 2.3)	6.98, dd (8.0, 1.8)	6.98, dd (8.0, 1.8)

chemical shifts in δ, coupling constants in Hz

Table 2.1. ^{1}H NMR (continued)

Position	**1**	**1′**	**2**	**2′**	**3**	**3′**	**4**	**4′**
2"	7.01, d (1.8)	7.01, d (1.8)	7.02, d (1.7)	7.02, d (1.7)	7.00, d (1.7)	7.00, d (1.7)	7.00, d (2.3)	7.00, d (1.8)
5"	6.80, d (8.6)	6.80, d (8.0)	6.79, d (8.6)	6.79, d (8.0)	6.80, d (8.6)	6.80, d (8.0)	6.80, d (8.6)	6.80, d (8.0)
6"	6.86, dd (8.6, 1.8)	6.85, dd (8.0, 1.7)	6.86, dd (8.6, 1.7)	6.86, dd (8.0, 1.7)	6.86, dd (8.6, 1.7)	6.86, dd (8.0, 1.7)	6.86, dd (8.6, 2.3)	6.85, dd (8.0, 1.8)
7"	4.90, d (7.5)	4.90, d (8.0)	4.90, d (7.5)	4.90, d (7.5)	4.91, d (8.1)	4.91, d (8.0)	4.91, d (7.5)	4.91, d (8.0)
8"	4.17, ddd (7.5, 4.6, 2.3)	4.17, ddd (8.0, 4.6, 2.3)	4.16, ddd (7.5, 4.1, 2.3)	4.16, ddd (7.5, 4.1, 2.3)	4.16, ddd (8.1, 4.6, 2.3)	4.16, ddd (8.0, 4.6, 2.3)	4.17, ddd (7.5, 4.6, 2.3)	4.17, ddd (8.0, 4.6, 2.3)
9"a	3.53, ddd (10.3, 5.2, 2.3)	3.53, ddd (10.3, 5.2, 2.3)	3.53, ddd (9.8, 4.6, 2.3)	3.52, ddd (9.7, 5.2, 2.3)	3.53, ddd (12.0, 4.6, 2.3)	3.53, ddd (12.0, 5.2, 2.3)	3.54, ddd (11.9, 5.2, 2.3)	3.53, ddd (11.9, 5.2, 2.3)
9"b	3.33, m	3.32, m	3.33, m	3.31, m	3.33, m	3.33, m	3.33, m	3.33, m

chemical shifts in δ, coupling constants in Hz

Table 2.1. ^{1}H NMR (continued)

Position	**1**	**1′**	**2**	**2′**	**3**	**3′**	**4**	**4′**
3"-OCH_3	3.77, s	3.77, s	3.77, s	3.77, s	3.78, s	3.77, s	3.77, s	3.77, s
3-OH	5.83, d (6.3)	5.81, d (6.3)	5.83, d (6.3)	5.80, d (6.3)	5.83, d (6.3)	5.84, d (6.3)	5.84, d (5.9)	5.81, d (6.3)
5-OH	11.90, s	11.90, s	11.90, s	11.90, s	11.90, s	11.92, s	11.90, s	11.93, s
7-OH	10.86, s	-	10.86, s	-	10.85, s	-	10.86 s	-
4"-OH	9.18, s	9.18, s	9.17, s	9.19, s	9.15, s	9.19, s	9.16, s	9.19, s
9"-OH	4.97, dd	4.96, dd	4.98, dd	4.99, dd	4.95, dd	4.98, dd	4.96, dd	4.97, dd
	(5.7, 5.2)	(5.7, 5.2)	(5.7, 4.6)	(5.7, 5.2)	(5.7, 4.6)	(5.7, 5.2)	(5.5, 5.0)	(5.7, 5.2)

chemical shifts in δ, coupling constants in Hz

Table 2.2. ^{13}C NMR data of flavonolignans and biomimetic flavonolignans in DMSO-d_6 (125 MHz, 30 °C)

Position	**type**	**1**	**1′**	**2**	**2′**	**3**	**3′**	**4**	**4′**
2	CH	82.6	82.5	82.5	82.5	82.5	82.5	82. 5	82. 4
3	CH	71.4	71.4	71.4	71.4	71.5	71.5	71.5	71.4
4	C	197.8	197.6	197.7	197.6	197.8	197.5	197.8	197.2
4a	C	100.4	100.2	100.4	100.2	100.5	100.2	100.5	100.1
5	C	163.3	163.3	163.3	163.3	163.3	163.4	163.3	163.4
6	CH	96.1	96.2	96.1	96.2	96.1	96.2	96.1	96.3
7	C	167.1	167.5	166.9	167.6	166.9	167.7	166.9	167.0
8	CH	95.1	95.2	95.0	95.2	95.1	95.3	95.1	95.3
8a	C	162.5	162.5	162.4	162.5	162.5	162.5	162.5	162.4
1'	C	130.1	130.1	130.1	130.2	130.3	130.4	130.3	130.4
2'	CH	116.6	116.6	116.6	116.7	116.5	116.5	116.5	116.5
3'	C	143.3	143.3	143.2	143.3	142.9	142.9	142.9	142.9
4'	C	143.7	143.7	143.6	143.6	143.9	143.9	143.9	143.9

chemical shifts in δ

Table 2.2. ^{13}C NMR (continued)

Position	**type**	**1**	**1′**	**2**	**2′**	**3**	**3′**	**4**	**4′**
5'	CH	116.3	116.3	116.3	116.4	116.4	116.5	116.5	116.5
6'	CH	121.4	121.4	121.4	121.2	120.9	120.9	120.9	120.9
1"	C	127.5	127.5	127.5	127.5	127.5	127.5	127.5	127.5
5'	CH	116.3	116.3	116.3	116.4	116.4	116.5	116.5	116.5
6'	CH	121.4	121.4	121.4	121.2	120.9	120.9	120.9	120.9
1"	C	127.5	127.5	127.5	127.5	127.5	127.5	127.5	127.5
2"	CH	111.6	111.6	111.6	111.6	111.7	111.7	111.7	111.6
3"	C	147.6	147.6	147.6	147.6	147.6	147.6	147.6	147.6
4"	C	147.0	147.0	147.0	147.0	147.0	147.0	147.0	147.0
5"	CH	115.3	115.3	115.3	115.3	115.3	115.3	115.3	115.3
6"	CH	120.5	120.5	120.5	120.5	120.5	120.5	120.5	120.5
7"	CH	75.9	75.9	75.8	75.9	75.9	75.9	75.9	75.8

chemical shifts in δ

Table 2.2. ^{13}C NMR (continued)

Position	**type**	**1**	**1′**	**2**	**2′**	**3**	**3′**	**4**	**4′**
7"	CH	75.9	75.9	75.8	75.9	75.9	75.9	75.9	75.8
9"	CH_2	60.2	60.2	60.2	60.2	60.2	60.2	60.2	60.2
3"-OCH_3	CH_3	55.7	55.7	55.7	55.7	55.7	55.7	55.7	55.7

chemical shifts in δ

2.4.2.7. Coniferyl aldehyde (16)

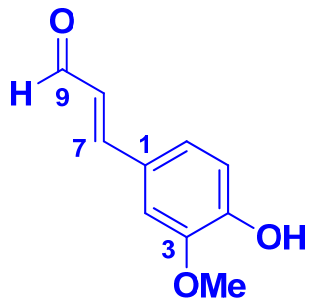

Figure 2.43**.** Coniferyl aldehyde

Yield: 2.3 mg, 2%; this compound was isolated from the biomimetic reaction and oxidation reaction of coniferyl alcohol. The ^{1}H NMR data matched literature values and that from coniferyl aldehyde purchased from Aldrich [135]

^{1}H NMR (500 MHz, acetone-d_6) δ = 3.93 (s, 3H, 3-OCH_3), 6.68 (dd, J = 15.6, 7.8 Hz, 1H, H-8), 6.91 (d, J = 7.8 Hz, 1H, H-5), 7.22 (dd, J = 7.8, 1.8 Hz, 1H, H-6), 7.39 (d, J = 15.6 Hz, 1H, H-2), 7.58 (d, J = 15.6 Hz, 1H, H-7), 9.64 (d, J = 7.8, Hz, 1H, H-9). (Fig. 2.44).

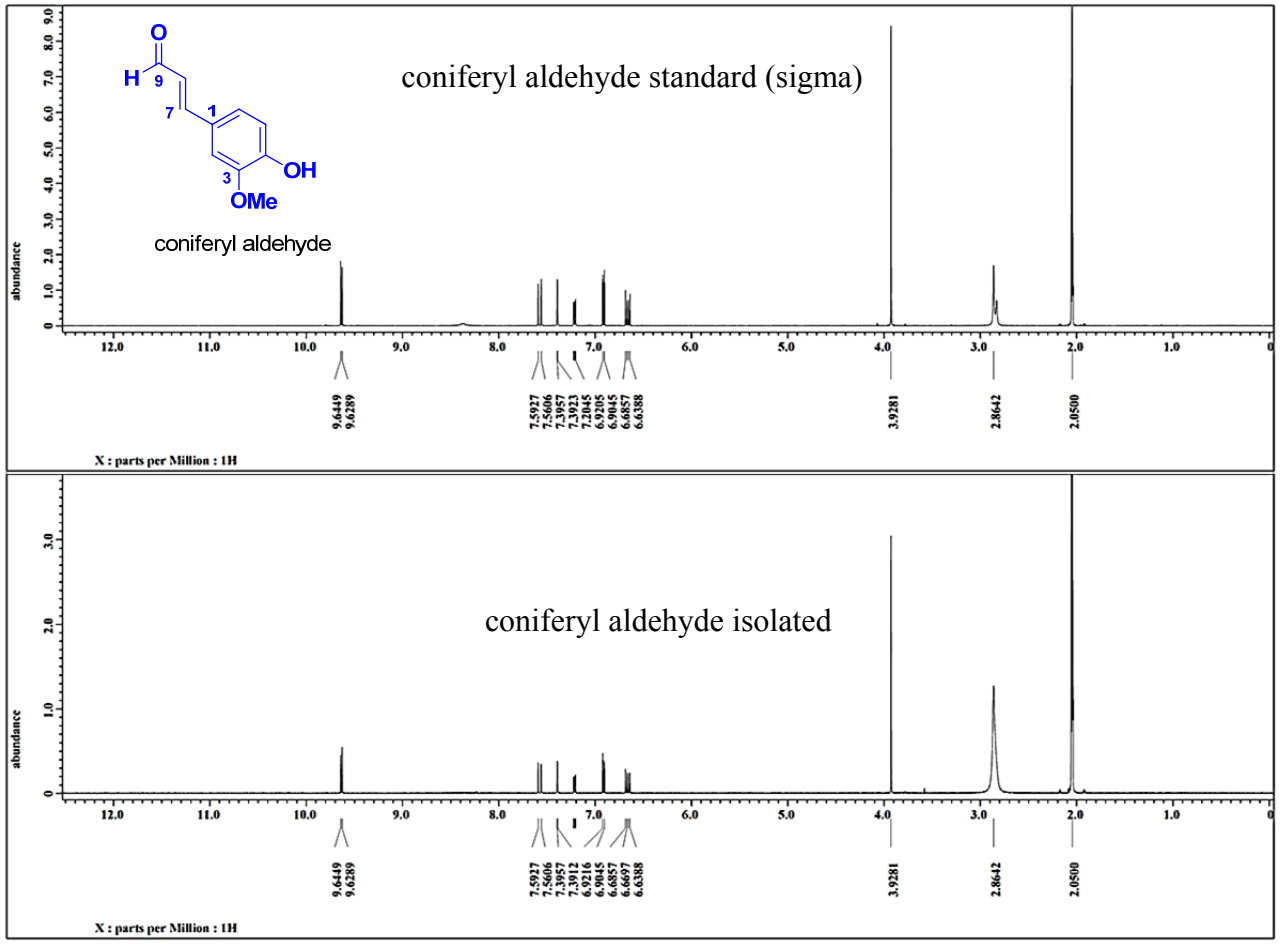

Figure 2.44. ^{1}H NMR spectra (500 MHz) of coniferyl aldehyde (**16**) standard and isolated from reaction in acetone-d_6.

2.4.2.8. Dehydrodiconiferyl Alcohol (18)

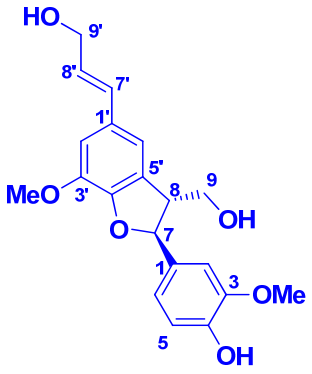

Figure 2.45. Dehydrodiconiferyl Alcohol

Yield: 13.6 mg, 6%; this lignin was isolated from the biomimetic reaction and oxidation reaction of coniferyl alcohol. The ^{1}H and ^{13}C NMR data matched literature values.[136]

^{1}H NMR (500 MHz, acetone-*d*$_6$) δ = 3.53 (q, J = 6.3 Hz, 1H, H-8), 3.82 (s, 3H, 3-OCH_3), 3.83 (dd, J = 10.3, 6.9 Hz, 1H, Ha-9), 3.86 (s, 3H, 3′-OCH_3), 3.88 (dd, J = 10.3, 5.2 Hz, 1H, Hb-9), 4.20 (dd, J = 5.7, 1.8 Hz, 1H, H-9′), 5.56 (br d, J = 6.3 Hz, 1H, H-7), 6.24 (dt, J = 16.0, 5.2 Hz, 1H, H-8′), 6.52 (dt, J = 16, 1.7 Hz, 1H, H-7′), 6.81 (d, J = 8.0 Hz, 1H, H-5),6.88 (dd, J = 8.0, 1.7 Hz, 1H, H-6), 6.95 (d, J = 1.7 Hz, 1H, H-2′), 6.98 (br s, 1H, H-6′), 7.04 (d, J = 2.3 Hz, 1H, H-2) (Table 2.3, Fig. 2.46).

^{13}C NMR (125 MHz, acetone-*d*$_6$) δ 54.8 (C-8), 56.3 (C-3-OCH_3), 56.4 (C-3′-OCH_3), 63.5 (C-9′), 64.6 (C-9), 88.6 (C-7), 110.5 (C-2), 111.6 (C-2′), 115.7 (C-5), 116.1 (C-6′), 119.6 (C-6), 128.4 (C-8′), 130.4 (C-5′), 130.5 (C-7′), 132.0 (C-1′), 134.4 (C-1), 145.2 (C-3′), 147.4 (C-4), 148.4 (C-3), 149.0 (C-4′) (Table 2.4, Fig 2.47).

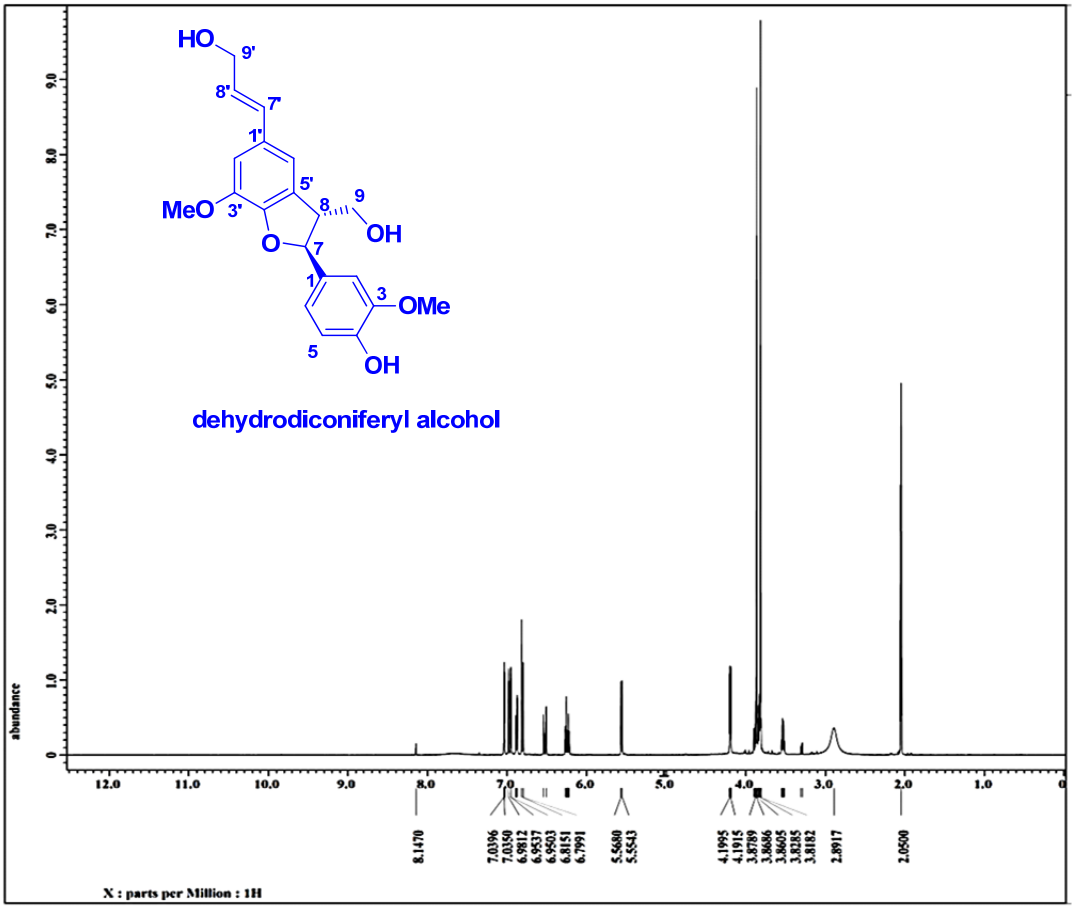

Figure 2.46. ^{1}H NMR spectra (500 MHz) of dehyderodiconiferyl alcohol (**18**) isolated from reaction in acetone-d_6

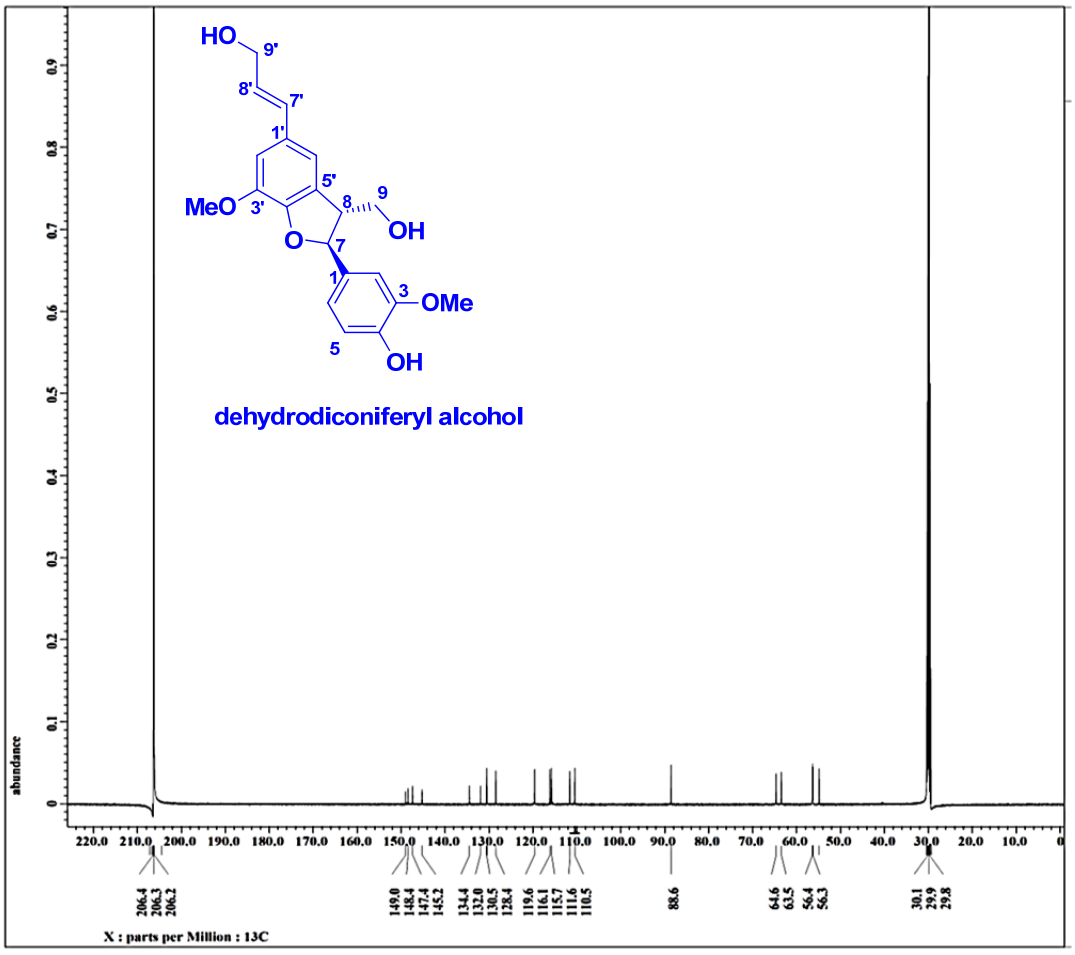

Figure 2.47. ^{13}C NMR spectra (125 MHz) of dehyderodiconiferyl alcohol (**18**) isolated from reaction in acetone-d_6

Table 2.3. ^{1}H NMR spectra comparison of dehyderodiconiferyl alcohol (**18**) with literature values in acetone-d_6

Position	**Type**	**Experimental** (shift, multiplicity, coupling)	**Literature**[a] (shift, multiplicity, coupling)
2	CH	7.04, d (2.3)	7.03, d (2.0)
5	CH	6.81, d (8.0)	6.80, d (8.1)
6	CH	6.88, dd (8.0, 1.7)	6.87, ddd (8.1, 2.0 and 0.5)
7	CH	5.56, br d (6.3)	5.56, dt (6.3, not given)
8	CH	3.53, q (6.3)	3.53 br q (not given)
9a	CH_2	3.83, dd (10.3, 6.9)	3.78 m
9b	CH_2	3.88, dd (10.3, 5.2)	3.88 m
OCH_3	CH_3	3.82, s	3.81, s
2′	CH	6.95, d (1.7)	6.94, br s
6′	CH	6.98, br s	6.97, br s
7′	CH	6.52, dt (16.0, 1.7)	6.52, dt (15.8, 1.5)
8′	CH	6.23, dt (16.0, 5.2)	6.23, dt (15.8, 5.5)
9′	CH_2	4.20, dd (5.7, 1.8)	4.19, td (5.2, 1.5)
OCH_3	CH_3	3.86, s	3.85, s

chemical shifts in δ, coupling constants in Hz

[a]Quideau, S.; John, R. *Holzforschung* , **1994**, *48*, 12-22.

Table 2.4. ^{13}C NMR data of dehyderodiconiferyl alcohol (**18**) with literature values in acetone-d_6

Position	**type**	**Experimental**	**Literature**[a]
1	C	134.4	134.4
2	CH	110.5	110.5
3	C	148.4	148.4
4	C	147.4	147.3
5	CH	115.7	115.7
6	CH	119.6	119.6
7	CH	88.6	88.5
8	CH	54.8	54.7
9	CH_2	64.6	64.6
OCH_3	CH_3	56.3	56.3
1	C	132.0	131.9
2	CH	111.6	111.7
3	C	145.2	145.1
4	C	149.0	148.8
5	C	130.5	130.4
6	CH	116.1	116.1
7	CH	130.5	130.5

chemical shifts in δ

Table 2.4. ^{13}C NMR (continued)

Position	**type**	**Experimental**	**Literaturea**
8	CH	128.4	128.3
9	CH_2	63.5	63.4
OCH_3	CH_3	56.4	56.4

chemical shifts in δ

[a]Quideau, S.; John, R. *Holzforschung* , **1994**, *48*, 12-22.

REFERENCES

1. Pradhan, S. C.; Girish, C. *Indian Journal of Medical Research* **2006,** *124*, 491-504.

2. Karkanis, A.; Bilalis, D.; Efthimiadou, A. *Industrial Crops and Products* **2011,** *34*, 825-830.

3. Nyiredy, S.; Samu, Z.; Szucs, Z.; Gulacsi, K.; Kurtan, T.; Antus, S. *Journal of Chromatographic Science* **2008,** *46*, 93-96.

4. Wagner, H.; Horhamme.L; Munster, R. *Arzneimittel-Forschung* **1968,** *18*, 688-&.

5. Wagoner, J.; Morishima, C.; Graf, T. N.; Oberlies, N. H.; Teissier, E.; Pecheur, E. I.; Tavis, J. E.; Polyak, S. J. *Plos One* **2011,** *6*, 9.

6. Kurkin, V. A.; Zapesochnaya, G. G. *Khimiya Prirodnykh Soedinenii* **1987**, 11-35.

7. Kroll, D. J.; Shaw, H. S.; Oberlies, N. H. *Integrative Cancer Therapies* **2007,** *6*, 110-119.

8. Kren, V.; Walterova, D. *Biomedical papers of the Medical Faculty of the University Palacky, Olomouc, Czechoslovakia* **2005,** *149*, 29-41.

9. Simanek, V.; Kren, V.; Ulrichova, J.; Vicar, J.; Cvak, L. *Hepatology* **2000,** *32*, 442-443.

10. Gazak, R.; Sedmera, P.; Vrbacky, M.; Vostalova, J.; Drahota, Z.; Marhol, P.; Walterova, D.; Kren, V. *Free Radical Biology and Medicine* **2009,** *46*, 745-758.

11. Pelter, A.; Hänsel, R. *Tetrahedron Letters* **1968,** *9*, 2911–2916.

12. Abraham, D. J.; Takagi, S.; Rosenstein, R. D.; Shiono, R.; Wagner, H.; Hoerhammer, L.; Seligmann, O.; Farnsworth, N. R. *Tetrahedron Letters* **1970,** *11*, 2675-2678.

13. Hänsel, R.; Schulz, J.; Pelter, A.; *Journal of the Chemical Society, Chemical Communications*, **1972**, *3*,195-196.

14. Arnone, A.; Merlini, L.; Zanarotti, A. *Journal of the Chemical Society-Chemical Communications* **1979**, 696-697.

15. Hänsel, R.; Schulz, J.; Pelter, A.; Rimpler, H.; Rizk, A. F. *Tetrahedron Letters*, **1969**; *51*, 4417-4420.

16. Pelter, A.; Hänsel, R. *Chemische Berichte* **1975**;*108*. 790-802.

17. Hänsel, R.; Schulz, J.; Pelter, A. *Chemische Berichte-Recueil* **1975,** *108*, 1482-1501.

18. Hänsel, R.; Schopflin, G.; *Tetrahedron Letters* **1967**; *37*, 3645-3648.

19. Pelter, A.; Hänsel, R.; Kaloga, M. *Tetrahedron Letters*, **1977**; *18*, *4547-4548*.

20. Kim, N. C.; Graf, T. N.; Sparacino, C. M.; Wani, M. C.; Wall, M. E. *Organic & Biomolecular Chemistry* **2003,** *1*, 1684-1689.

21. Lee, D. Y. W.; Liu, Y. Z. *Journal of Natural Products* **2003,** *66*, 1171-1174.

22. Saller, R.; Meier, R.; Brignoli, R. *Drugs* **2001,** *61*, 2035-2063.

23. Vuda, M.; D'Souza, R.; Upadhya, S.; Kumar, V.; Rao, N.; Boillat, C.; Mungli, P. *Experimental and Toxicologic Pathology* **2012,** *64*, 855-859.

24. Polyak, S. J.; Morishima, C.; Lohmann, V.; Pal, S.; Lee, D. Y. W.; Liu, Y. Z.; Graf, T. N.; Oberlies, N. H. *Proceedings of the National Academy of Sciences of the United States of America* **2010,** *107*, 5995-5999.

25. Ferenci, P. *Jama-Journal of the American Medical Association* **2012,** *308*, 1856-1857.

26. Reyes, D.; Mangubat, C. M.; Patal, P. *Journal of Gastroenterology and Hepatology* **2012,** *27*, 270-270.

27. Vogel, G.; Temme, I. *Arzneimittel-Forschung* **1969,** *19*, 613-615.

28. Choppin, J.; Desplaces, A. *Arzneimittel-Forschung/Drug Research* **1978,** *28-1*, 636-641.

29. Brandon-Warner, E.; Eheim, A. L.; Foureau, D. M.; Walling, T. L.; Schrum, L. W.; McKillop, I. H. *Cancer Letters* **2012,** *326*, 88-95.

30. Chen, I. S.; Chen, Y. C.; Chou, C. H.; Chuang, R. F.; Sheen, L. Y.; Chiu, C. H. *Journal of the Science of Food and Agriculture* **2012,** *92*, 1441-1447.

31. Abenavoli, L.; Capasso, R.; Milic, N.; Capasso, F. *Phytotherapy Research* **2010,** *24*, 1423-1432.

32. Salama, S. M.; Bilgen, M.; Al Rashdi, A. S.; Abdulla, M. A. *Evidence-Based Complementary and Alternative Medicine* **2012**, 12.

33. Li, P. C.; Chiu, Y. W.; Lin, Y. M.; Day, C. H.; Hwang, G. Y.; Pai, P. Y.; Tsai, F. J.; Tsai, C. H.; Kuo, Y. C.; Chang, H. C.; Liu, J. Y.; Huang, C. Y. *Evidence-Based Complementary and Alternative Medicine* **2012**, 9.

34. Muriel, P.; Moreno, M. G.; Hernandez, M. D.; Chavez, E.; Alcantar, L. K. *Basic & Clinical Pharmacology & Toxicology* **2005,** *96*, 375-380.

35. Au, A. Y.; Hasenwinkel, J. M.; Frondoza, C. G. *Journal of Veterinary Pharmacology and Therapeutics* **2011,** *34*, 120-129.

36. Souza, C. O. d.; Peracoli, M. T. S.; Weel, I. C.; Bannwart, C. F.; Romao, M.; Nakaira-Takahagi, E.; Medeiros, L. T. L. d.; Silva, M. G. d.; Peracoli, J. C. *Life Sciences* **2012,** *91*, 159-65.

37. Flaig, T. W.; Gustafson, D. L.; Su, L. J.; Zirrolli, J. A.; Crighton, F.; Harrison, G. S.; Pierson, A. S.; Agarwal, R.; Glode, L. M. *Investigational New Drugs* **2007,** *25*, 139-146.

38. Tyagi, A.; Agarwal, C.; Dwyer-Nield, L. D.; Singh, R. P.; Malkinson, A. M.; Agarwal, R. *Molecular Carcinogenesis* **2012,** *51*, 832-842.

39. Agarwal, R.; Agarwal, C.; Ichikawa, H.; Singh, R. P.; Aggarwal, B. B. *Anticancer Research* **2006,** *26*, 4457-4498.

40. Singh, R. P.; Dhanalakshmi, S.; Agarwal, C.; Agarwal, R. *Oncogene* **2005,** *24*, 1188-1202.

41. Flora, K.; Hahn, M.; Rosen, H.; Benner, K. *American Journal of Gastroenterology* **1998,** *93*, 139-143.

42. Sonnenbichler, J.; Mattersberger, J.; Hanser, G. *Hoppe-Seylers Zeitschrift Fur Physiologische Chemie* **1980,** *361*, 1751-1756.

43. Schnabel, R.; Sonnenbichler, J.; Zillig, W. *Febs Letters* **1982,** *150*, 400-402.

44. Marouf, B. H.; Zalzala, M. H.; Al-Khalifa, II; Aziz, T. A.; Hussain, S. A. *Saudi Pharmaceutical Journal* **2011,** *19*, 177-183.

45. Moulisova, V.; Srbova, M.; Jedlickova, O.; Sebestian, J.; Jegorov, A. *Biochemistry-Moscow* **2006,** *71*, 1110-U20.

46. Podder, B.; Kim, Y. S.; Zerin, T.; Song, H. Y. *Food and Chemical Toxicology* **2012,** *50*, 3206-3214.

47. Gupta, O. P.; Sing, S.; Bani, S.; Sharma, N.; Malhotra, S.; Gupta, B. D.; Banerjee, S. K.; Handa, S. S. *Phytomedicine* **2000,** *7*, 21-24.

48. Fiebrich, F.; Koch, H. *Experientia* **1979,** *35*, 1548-1550.

49. Roberti, R.; Mozzi, R.; Demedio, G. E.; Francesc.E; Porcella.G. *Pharmacological Research Communications* **1973,** *5*, 249-257.

50. Fiebrich, F.; Koch, H. *Experientia* **1979,** *35*, 1550-1552.

51. Li, L.; Zeng, J.; Gao, Y.; He, D. L. *Expert Opinion on Investigational Drugs* **2010,** *19*, 243-255.

52. Deep, G.; Agarwal, R. *Integrative Cancer Therapies* **2007,** *6*, 130-145.

53. Singh, R. P.; Agarwal, R. *Mutation Research-Fundamental and Molecular Mechanisms of Mutagenesis* **2004,** *555*, 21-32.

54. Li, W. H.; Mu, D. G.; Song, L. Q.; Zhang, J.; Liang, J.; Wang, C. M.; Liu, N. N.; Tian, F.; Li, X. F.; Zhang, W.; Wang, X. P. *Cancer Biotherapy and Radiopharmaceuticals* **2011,** *26*, 317-324.

55. Kaur, M.; Agarwal, R. *Toxicology and Applied Pharmacology* **2007,** *224*, 350-359.

56. Chittezhath, M.; Deep, G.; Singh, R. P.; Agarwal, C.; Agarwal, R. *Molecular Cancer Therapeutics* **2008,** *7*, 1817-1826.

57. Sharma, G.; Singh, R. P.; Chan, D. C. F.; Agarwal, R. *Anticancer Research* **2003,** *23*, 2649-2655.

58. Faezizadeh, Z.; Mesbah-Namin, S. A. R.; Allameh, A. *Planta Medica* **2012,** *78*, 899-902.

59. Li, L.; Gao, Y.; Zhang, L. L.; Zeng, J.; He, D. L.; Sun, Y. *Cancer Letters* **2008,** *272*, 61-69.

60. Liang, L.; Li, L.; Zeng, J.; Gao, Y.; Chen, Y. L.; Wang, Z. Q.; Wang, X. Y.; Chang, L. S.; He, D. L. *Oncology Reports* **2012,** *28*, 999-1005.

61. Wang, H. J.; Tashiro, S. I.; Onodera, S.; Ikejima, T. *Journal of Pharmacological Sciences* **2008,** *107*, 260-269.

62. Lee, S. O.; Jeong, Y. J.; Im, H. G.; Kim, C. H.; Chang, Y. C.; Lee, I. S. *Biochemical and Biophysical Research Communications* **2007,** *354*, 165-171.

63. Kaur, M.; Velmurugan, B.; Tyagi, A.; Deep, G.; Katiyar, S.; Agarwal, C.; Agarwal, R. *Molecular Cancer Therapeutics* **2009,** *8*, 2366-2374.

64. Yang, S. H.; Lin, J. K.; Chen, W. S.; Chiu, J. H. *Journal of Surgical Research* **2003,** *113*, 133-138.

65. Agarwal, C.; Singh, R. P.; Dhanalakshmi, S.; Tyagi, A. K.; Tecklenburg, M.; Sclafani, R. A.; Agarwal, R. *Oncogene* **2003,** *22*, 8271-8282.

66. Sy-Cordero, A. A.; Graf, T. N.; Runyon, S. P.; Wani, M. C.; Kroll, D. J.; Agarwal, R.; Brantley, S. J.; Paine, M. F.; Polyak, S. J.; Oberlies, N. H. *Bioorganic & Medicinal Chemistry* **2013,** *21*, 742-747.

67. Singh, R. R.; Raina, K.; Deep, G.; Chan, D.; Agarwal, R. *Clinical Cancer Research* **2009,** *15*, 613-621.

68. Agarwal, C.; Tyagi, A.; Kaur, M.; Agarwal, R. *Carcinogenesis* **2007,** *28*, 1463-1470.

69. Deep, G.; OberlieS, N. H.; Kro, D. J.; Agarwal, R. *International Journal of Cancer* **2008,** *123*, 41-50.

70. Zi, X. L.; Zhang, J. C.; Agarwal, R.; Pollak, M. *Cancer Research* **2000,** *60*, 5617-5620.

71. Singh, R. P.; Agarwal, R. *Molecular Carcinogenesis* **2006,** *45*, 436-442.

72. Davis-Searles, P. R.; Nakanishi, Y.; Kim, N. C.; Graf, T. N.; Oberlies, N. H.; Wani, M. C.; Wall, M. E.; Agarwal, R.; Kroll, D. J. *Cancer Research* **2005,** *65*, 4448-4457.

73. Deep, G.; Gangar, S. C.; Rajamanickam, S.; Raina, K.; Gu, M.; Agarwal, C.; Oberlies, N. H.; Agarwal, R. *PloS one* **2012,** *7*, e34630.

74. Deep, G.; Singh, R. P.; Agarwal, C.; Kroll, D. J.; Agarwal, R. *Oncogene* **2006,** *25*, 1053-1069.

75. Roy, S.; Kaur, M.; Agarwal, C.; Tecklenburg, M.; Sclafani, R. A.; Agarwal, R. *Molecular Cancer Therapeutics* **2007,** *6*, 2696-2707.

76. Meroni, P. L.; Barcellini, W.; Borghi, M. O.; Vismara, A.; Ferraro, G.; Ciani, D.; Zanussi, C. *International Journal of Tissue Reactions-Experimental and Clinical Aspects* **1988,** *10*, 177-181.

77. Singh, R. P.; Sharma, G.; Dhanalakshmi, S.; Agarwal, C.; Agarwal, R. *Cancer Epidemiology Biomarkers & Prevention* **2003,** *12*, 933-939.

78. Bhatia, N.; Agarwal, C.; Agarwal, R. *Nutrition and Cancer-An International Journal* **2001,** *39*, 292-299.

79. Deep, G.; Oberlies, N. H.; Kroll, D. J.; Agarwal, R. *Carcinogenesis* **2007,** *28*, 1533-1542.

80. Deep, G.; Raina, K.; Singh, R. P.; Oberlies, N. H.; Kroll, D. J.; Agarwal, R. *International Journal of Cancer* **2008,** *123*, 2750-2758.

81. Wu, J. W.; Lin, L. C.; Tsai, T. H. *Journal of Ethnopharmacology* **2009,** *121*, 185-193.

82. Halbach, G.; Trost, W. *Arzneimittel-Forschung/Drug Research* **1974,** *24*, 866-868.

83. Lecomte, J. *Revue medicale de Liege* **1975,** *30*, 110-4.

84. Jancova, P.; Siller, M.; Anzenbacherova, E.; Kren, V.; Anzenbacher, P.; Simanek, V. *Xenobiotica* **2011,** *41*, 743-751.

85. Kren, V.; Ulrichova, J.; Kosina, P.; Stevenson, D.; Sedmera, P.; Prikrylova, V.; Halada, P.; Simanek, V. *Drug Metabolism and Disposition* **2000,** *28*, 1513-1517.

86. Calani, L.; Brighenti, F.; Bruni, R.; Del Rio, D. *Phytomedicine* **2013,** *20*, 40-46.

87. Beckmann-Knopp, S.; Rietbrock, S.; Weyhenmeyer, R.; Bocker, R. H.; Beckurts, K. T.; Lang, W.; Hunz, M.; Fuhr, U. *Pharmacology & Toxicology* **2000,** *86*, 250-256.

88. Zuber, R.; Modriansky, M.; Dvorak, Z.; Rohovsky, P.; Ulrichova, J.; Simanek, V.; Anzenbacher, P. *Phytotherapy Research* **2002,** *16*, 632-638.

89. Sridar, C.; Goosen, T. C.; Kent, U. M.; Williams, J. A.; Hollenberg, P. F. *Drug Metabolism and Disposition* **2004,** *32*, 587-594.

90. Brantley, S. J.; Oberlies, N. H.; Kroll, D. J.; Paine, M. F. *Journal of Pharmacology and Experimental Therapeutics* **2010,** *332*, 1081-1087.

91. D'Andrea, V.; Perez, L. M.; Pozzi, E. J. S. *Life Sciences* **2005,** *77*, 683-692.

92. Doehmer, J.; Tewes, B.; Klein, K. U.; Gritzko, K.; Muschick, H.; Mengs, U. *Toxicology in Vitro* **2008,** *22*, 610-617.

93. Lee, C. K.; Choi, J. S. *Pharmacology* **2010,** *85*, 350-356.

94. Jancova, P.; Anzenbacherova, E.; Papouskova, B.; Lemr, K.; Luzna, P.; Veinlichova, A.; Anzenbacher, P.; Simanek, V. *Drug Metabolism and Disposition* **2007,** *35*, 2035-2039.

95. Han, Y. H.; Lou, H. X.; Ren, D. M.; Sun, L. R.; Ma, B.; Ji, M. *Journal of Pharmaceutical and Biomedical Analysis* **2004,** *34*, 1071-1078.

96. Dzubak, P.; Hajduch, M.; Gazak, R.; Svobodova, A.; Psotova, J.; Walterova, D.; Sedmera, P.; Kren, V. *Bioorganic & Medicinal Chemistry* **2006,** *14*, 3793-3810.

97. Pifferi, G.; Pace, R.; Conti, M. *Farmaco* **1994,** *49*, 75-76.

98. Kren, V.; Kubisch, J.; Sedmera, P.; Halada, P.; Prikrylova, V.; Jegorov, A.; Cvak, L.; Gebhardt, R.; Ulrichova, J.; Simanek, V. *Journal of the Chemical Society-Perkin Transactions 1* **1997**, 2467-2474.

99. Loguercio, C.; Andreone, P.; Brisc, C.; Brisc, M. C.; Bugianesi, E.; Chiaramonte, M.; Cursaro, C.; Danila, M.; de Sio, I.; Floreani, A.; Freni, M. A.; Grieco, A.; Groppo, M.; Lazzari, R.; Lobello, S.; Lorefice, E.; Margotti, M.; Miele, L.; Milani, S.; Okolicsanyi, L.; Palasciano, G.; Portincasa, P.; Saltarelli, P.; Smedile, A.; Somalvico, F.; Spadaro, A.; Sporea, I.; Sorrentino, P.; Vecchione, R.; Tuccillo, C.; Blanco, C. D.; Federico, A. *Free Radical Biology and Medicine* **2012,** *52*, 1658-1665.

100. Kidd, P.; Head, K. *Alternative Medicine Review* **2005,** *10*, 193-203.

101. Barzaghi, N.; Crema, F.; Gatti, G.; Pifferi, G.; Perucca, E. *European Journal of Drug Metabolism and Pharmacokinetics* **1990,** *15*, 333-338.

104. Gazak, R.; Purchartova, K.; Marhol, P.; Zivna, L.; Sedmera, P.; Valentova, K.; Kato, N.; Matsumura, H.; Kaihatsu, K.; Kren, V. *European Journal of Medicinal Chemistry* **2010,** *45*, 1059-1067.

105. Wang, F.; Huang, K. X.; Yang, L. X.; Gong, J. X.; Tao, Q. F.; Li, H. B.; Zhao, Y.; Zeng, S.; Wu, X. M.; Stockigt, J.; Li, X. K.; Qu, J. *Bioorganic & Medicinal Chemistry* **2009,** *17*, 6380-6389.

106. Gazak, R.; Svobodova, A.; Psotova, J.; Sedmera, P.; Prikrylova, V.; Walterova, D.; Kren, V. *Bioorganic & Medicinal Chemistry* **2004,** *12*, 5677-5687.

107. Theodosiou, E.; Loutrari, H.; Stamatis, H.; Roussos, C.; Kolisis, F. N. *New Biotechnology* **2011,** *28*, 342-348.

108. Gazak, R.; Valentova, K.; Fuksova, K.; Marhol, P.; Kuzma, M.; Medina, M. A.; Oborna, I.; Ulrichova, J.; Kren, V. *Journal of Medicinal Chemistry* **2011,** *54*, 7397-7407.

109. Graf, T. N.; Wani, M. C.; Agarwal, R.; Kroll, D.; Oberlies, N. H. *Planta Medica* **2007,** *73*, 1495-1501.

110. Polyak, S. J.; Morishima, C.; Lohmann, V.; Pal, S.; Lee, D. Y.; Liu, Y.; Graf, T. N.; Oberlies, N. H. *Proceedings of the National Academy of Sciences USA* **2010,** *107*, 5995-5999.

111. Davis-Searles, P. R.; Nakanishi, Y.; Kim, N. C.; Graf, T. N.; Oberlies, N. H.; Wani, M. C.; Wall, M. E.; Agarwal, R.; Kroll, D. J. *Cancer Research* **2005,** *65*, 4448-4457.

112. Deep, G.; Oberlies, N. H.; Kroll, D. J.; Agarwal, R. *Carcinogenesis* **2007,** *28*, 1533-1542.

113. Deep, G.; Oberlies, N. H.; Kroll, D. J.; Agarwal, R. *Oncogene* **2008,** *27*, 3986-3998.

114. Deep, G.; Oberlies, N. H.; Kroll, D. J.; Agarwal, R. *International Journal of Cancer* **2008,** *123*, 41-50.

115. Paine, M. F.; Hart, H. L.; Ludington, S. S.; Haining, R. L.; Rettie, A. E.; Zeldin, D. C. *Drug Metab. Dispos*, **2006**; *34*, 880-886.

116. Zhong, J.; Gastaminza, P.; Cheng, G.; Kapadia, S.; Kato, T.; Burton, D. R.; Wieland, S. F.; Uprichard, S. L.; Wakita, T.; Chisari, F. V. *Proceedings of the National Academy of Sciences USA* **2005,** *102*, 9294-9299.

117. Sy-Cordero, A. A.; Graf, T. N.; Runyon, S. P.; Wani, M. C.; Kroll, D. J.; Agarwal, R.; Brantley, S. J.; Paine, M. F.; Polyak, S. J.; Oberlies, N. H. *Bioorganic and Medicinal Chemsitry* **2013,** *21*, 742-747.

118. Brantley, S. J.; Oberlies, N. H.; Kroll, D. J.; Paine, M. F. *Journal of Pharmacology and Experimental Therapeutics* **2010,** *332*, 1081-1087.

119. Wang, M. Z.; Wu, J. Q.; Bridges, A. S.; Zeldin, D. C.; Kornbluth, S.; Tidwell, R. R.; Hall, J. E.; Paine, M. F. *Drug Metabolism and Disposition* **2007,** *35*, 2067-2075.

120. Collier, A. C.; Tingle, M. D.; Keelan, J. A.; Paxton, J. W.; Mitchell, M. D. *Drug Metabolism and Disposition* **2000,** *28*, 1184-1186.

121. Ashu-Arrah, B. A.; Glennon, J. D.; Albert, K. *Journal of Chromatography A* **2013,** *1273*, 34-43.

122. Kurkin, V. A. *Chemistry of Natural Compounds* **2003,** *39*, 123-153.

123. Elwekeel, A.; Elfishway, A.; AbouZid, S. *Phytochemistry Letters* **2012,** *5*, 393-396.

124. Tanaka H, S. M., Ohira K, Ito K. *Chem. Pharm. Bull*. **1985**; *33*, 1419-1423.

125. Merlini, L.; Zanarotti, A.; Pelter, A.; Rochefort, M. P.; Hansel, R. *J. Chem. Soc., Chem. Commun.* **1979**,*0*, 695-695.

126. Merlini, L.; Zanarotti, A.; Pelter, A.; Rochefort, M. P.; Hansel, R. *Journal of the Chemical Society-Perkin Transactions* **1980**, *1*, 775-778.

127. de la Torre, M. C.; Sierra, M. A. *Angewandte Chemie-International Edition* **2004,** *43*, 160-181.

128. Mondal, N.; Mandal, S. C.; Das, G. K.; Mukherjee, S. *Journal of Chemical Research-S* **2003**, 580-583.

129. Nakanishi, K.; *Comprehensive Natural Products Chemistry*, **1999**; 1-31.

130. Mishima, H.; Kurabayashi, M.; Hirai, K.; *Sankyo Kenkyusho Nenpo* **1971**; *23*, 70-88.

131. Guz, N. R.; Stermitz, F. R. *Journal of Natural Products* **2000,** *63*, 1140-1145.

132. Guz, N. R.; Stermitz, F. R.; Johnson, J. B.; Beeson, T. D.; Willen, S.; Hsiang, J. F.; Lewis, K. *Journal of Medicinal Chemistry* **2001,** *44*, 261-268.

133. Nair, V.; Menon, R. S.; Biju, A. T.; Abhilash, K. G. *Chemical Society Reviews* **2012,** *41*, 1050-1059.

134 Ralph, J.; Zhang, Y. S. *Tetrahedron* **1998**, 54, 1349.

135 Jiang, A. L.; Wang, C. H. *Process Biochemistry* **2006**, *41*, 1111-1116

136. Quideau, S.; Ralph, J. *Holzforschung* **1994**, *48*, 12-22.